5X01

C83

DIVISION OF STRUCTURES AND ENGINEERING SERVICES
TRANSPORTATION LABORATORY
RESEARCH REPORT

Improved Nuclear Gage Development Phase I And II

76-45

INTERIM REPORT
CA-DOT-TL-2857-1-76-45
SEPT. 1976

Prepared in Cooperation with the U.S. Department of Transportation,
Federal Highway Administration

Caltrans
CALIFORNIA DEPARTMENT OF TRANSPORTATION

STATE OF CALIFORNIA
DEPARTMENT OF TRANSPORTATION
DIVISION OF STRUCTURES & ENGINEERING SERVICES
OFFICE OF TRANSPORTATION LABORATORY

September 1976

TL No. 632857
Item No. F-4-8

Mr. C. E. Forbes
Chief Engineer

Dear Sir:

I have approved and now submit for your information this interim research project report titled:

IMPROVED NUCLEAR GAGE DEVELOPMENT -

PHASE I AND II

Study made by . . . . . Geotechnical Branch

Under the Supervision of . . . . . Raymond A. Forsyth, P.E.

Principal Investigators . . . . . Joseph B. Hannon, P. E.
Jerry C. Chang, P. E.

Co-Investigator . . . . . Ellsworth L. Chan

Assisted by . . . . . Frank C. Champion
David R. Castanon

Very truly yours,

George A. Hill

GEORGE A. HILL
Chief, Office of Transportation Laboratory

Attachment
RAF:bjs

ACKNOWLEDGEMENTS

The individuals involved in this research project wish to express their gratitude to the Federal Highway Administration for the financial support and encouragement, which made this work possible.

The contents of this report reflect the views of the Transportation Laboratory which is responsible for the facts and the accuracy of the data presented herein. The contents do not necessarily reflect the official views or policies of the State of California or the Federal Highway Administration. This report does not constitute a standard, specification, or regulation.

The authors gratefully acknowledge the initiative and dedication of Frank C. Champion and David R. Castanon who conducted the laboratory experiments, participated in the analysis and interpretation of data, fabricated and assembled the Autoprobe backscatter gage, and assisted in the preparation of this report.

We wish to thank Mr. D. L. Durr and Mr. R. E. Smith for the comments and suggestions given during their review of this work.

TABLE OF CONTENTS

	Page
ACKNOWLEDGEMENTS	i
LIST OF FIGURES	iii
LIST OF TABLES	vii
LIST OF PHOTOGRAPHS	ix
INTRODUCTION	1
CONCLUSIONS	3
RECOMMENDATIONS	7
IMPLEMENTATION	10
STATEMENT OF THE PROBLEM	12
DISCUSSION	14
BASIC FACTORS	23
GAMMA SOURCE EVALUATION	25
NEUTRON SOURCE EVALUATION	36
GAMMA DETECTOR EVALUATION	42
NEUTRON DETECTOR EVALUATION	50
PRIMARY SHIELDING OF GAMMA EMISSIONS	69
CHEMICAL COMPOSITION ERROR	77
OPTIMUM GAGE PARAMETERS	83
PROTOTYPE NUCLEAR MOISTURE-DENSITY GAGE	94
Present Autoprobe Specifications	97
Present Autoprobe Performance Specifications	98
Field Density Test Procedures	99
BACKSCATTER GAGE-TEST SURFACE CONTACT AREA	103
ANALYSIS OF FIELD DATA	108
REFERENCES	115
FIGURES	117
TABLES	176
PHOTOGRAPHS	197
APPENDIX	200
California Department of Transportation Specifications for Nuclear Density-Moisture Gage	

LIST OF FIGURES

Figure

1 Gamma Spectrum of Radium 226 and Daughters

2 Gamma Spectrum of Cesium 137

3 Gamma Spectrum of Cobalt 60

4 Determination of Chemical Composition Error Magnitude from Density Calibration Curve

5 Backscatter Apparatus

6 Transmission Apparatus

7 Depth of Influence of Cobalt Emission Penetration in a Sandy-Silt Standard

8 Depth of Influence of Cesium Emission Penetration in a Sandy-Silt Standard

9 Depth of Influence of Cobalt Emission Penetration in a Magnesium Standard

10 Depth of Influence on Cesium Emission Penetration in a Magnesium Standard

11 Depth of Influence of Cobalt Emission Penetration in a Magnesium Standard Versus Gage Indicated Density

12 Depth of Influence of Cesium Emission Penetration in a Magnesium Standard Versus Gage Indicated Density

13 Calibration Curve for the Experimental Cesium 137 Backscatter Gage

14 Calibration Curve for the Experimental Cobalt 60 Backscatter Gage

15 Calibration Curve for the Experimental Cobalt 60 Backscatter Gage

16 Neutron Spectrum From a BF_3 Proportional Counter

17 Neutron Spectrum From a He-3 Proportional Counter

18 Reduction of Neutron Absorption Effects Obtained by Boron Trifloride (BF_3) Detector Discrimation

Figure

19 Reduction of Neutron Absorption Effects Obtained by Helium (He-3) Detector Discrimation

20 Reduction of Neutron Absorption Effects Obtained by Lithium-Iodide Detector Discrimination

21 Experimental Backscatter Gage Employing a Geiger-Mueller Detector

22 Experimental Transmission Gage Employing a Geiger-Mueller Detector

23 Experimental Backscatter Moisture Gage Employing a Lithium-Iodide Scintillation Detector

24 1 1/2" x 33mm Lithium-Iodide Detector Spectrum

25 Lithium-Iodide Detector Moisture Gage Calibration Curves

26 Boron Trifloride Detector Moisture Gage Calibration Curves

27 Boron Trifloride Proportional Counter Moisture Gage Curves

28 8 Inch Helium Three (He-3) Proportional Counter Moisture Gage Calibration Curves

29 Comparison of Thermal Neutron Detectors By Moisture Gage Calibration Curves

30 He-3 Detector Count Rate Plateau Intervals Obtained by Applied Detector Voltage and Amplification Variations

31 Two Inch Diameter Boron Trifloride Detector Count Rate Plateau Intervals Obtained by Applied Detector Voltage and Amplification Variation

32 One Inch Diameter Boron Trifloride Detector Count Rate Plateau Intervals Obtained By Applied Detector Voltage and Amplification Variation

33 He-3 Detector Count Rate Variations Due to Operating Temperature Influences

34 Two Inch Diameter Boron Trifloride Detector Count Rate Variation Due to Operating Temperature Influences

Figure

35 Lithium-Iodide Detector Count Rate Variation Due to Operating Temperature Influence and Discriminator Threshold Setting Variation

36 Lithium-Iodide Detector Count Rate Variation Due to Temperature Variation and Discriminator Interval

37 Backscatter Density Gage Primary Shielding

38 Variation of Backscatter Density Gage Calibration Curve Due to Primary Shielding Thickness

39 Observed Density Standard Count Rate Change Due to Primary Shielding Thickness

40 Average Percent Count Rate Reduction Due to Primary Shielding Recorded on the California Density Calibration Standards

41 Backscatter Density Gage Chemical Composition Error Due to Primary Shielding Thickness

42 Gamma Ray Absorption Using Lead (Pb)

43 Geiger-Mueller Backscatter Density Gage Primary Shielding Test Apparatus

44 Observed Percent Count Rate Reduction Due to Primary Shielding Thickness and Detected Gamma Energies

45 Transmission Gage Test Apparatus to Determine Primary Shielding Influence on Count Rate

46 Primary Shielding Influence on Transmission Gage Count Rate

47 Determination of Chemical Composition Error Magnitude From Density Calibration Curve

48 The Effect of Neutron Energy Discrimination on Moisture Gage Chemical Composition Error

49 Effectiveness of a 0.01" Cadmium Discriminator on Moisture Gage Chemical Composition Error

Figure

50 Effectiveness of a 0.2188" Polyethylene Filter Discriminator on Moisture Gage Chemical Composition Error

51 Effectiveness of a 0.01" Cadmium and 0.2188" Polyethylene Discriminator on Moisture Gage Chemical Composition Error

52 Optimum Observed Calibration Curves for The Cobalt 60 Backscatter Gage

53 The Variation of Chemical Composition Error, Due to Discriminator Selection - Cobalt 60, 13" Source-Detector Separation

54 The Variation of Chemical Composition Error Due to Discriminator Selection - Cobalt 60, 11 3/8" Source-Detector Separation

55 The Variation of Chemical Composition Error Due to Discriminator Selection - Cesium 137, 6" Primary Shielding, 11" Source-Detector Separation

56 The Variation of Chemical Composition Error Due to Discriminator Selection - Cesium 137, 2" Primary Shielding, 10" Source-Detector Separation

57 Sources of Air-Gap Error

58 Calibration Curves Resulting From Changes in Source Collimator Cavity Shape and Protrusion Pad Thickness

59 Comparison of Nuclear Density Gage Measurement Statistics

60 Regression Analysis of the Absolute Difference Between Standard Deviations of the Commercial and Autoprobe Backscatter Gages with Transmission Gage and Core Samples Relative to Soil Type Grouping

61 Regression Analysis of the Absolute Differences Between Mean Indicated Density of the Commercial and Autoprobe Backscatter Gage with Transmission Gage and Core Samples Relative to Soil Type Grouping

LIST OF TABLES

Table

1 Backscatter Gage Air-Gap Error Obtained By Laboratory Experiments

2 Gamma Detector Specifications

3 Summary of Detector Test Results Obtained in the Backscatter Gage Configuration

4 Summary of Detector Test Results Obtained in the Transmission Gage Configuration

5 Summary of Sodium-Iodide Scintillation Detector Test Results in the Backscatter and Transmission Gage Configuration

6 Proportional Counter (Neutron Detector) Specifications

7 Lithium-Iodide Scintillation Detector Specifications

8 Gamma Events Recorded by Proportional Neutron Detectors

9 Summary of Proportional Counter Test Results

10 Variation of Percent Chemical Composition Error in the Calibration Curve Due to Primary Shielding Thickness Placed in the Backscatter Gage

11 Primary Shielding Effect on Count Rate

12 Summary of Chemical Composition Error and Geiger-Mueller Detector Sensitivity Due to Backscatter Gage Configuration

13 The Effects of Electronic Energy Discrimination on Chemical Composition Error and Sensitivity Response Ratio in the Backscatter Mode

14 The Effects of Energy Discrimination on Chemical Composition Error in the Transmission Mode

Table

15 Energy Discrimination Effects on Moisture Gage Chemical Composition Error and Sensitivity

16 Cobalt 60 Backscatter Gage Configurations Which Exceed 1.90 Sensitivity Ratio

17 Cesium 137 Backscatter Gage Configurations Which Exceed 1.90 Sensitivity Ratio

18 Mean Density and Standard Deviation of Gage Measurements

19 Percent Probability of Coincident Density Measurements Between Backscatter and Transmission Gages

20 Average Absolute Difference Between Nuclear Density Measurements and Average Percent Probability of Identical Nuclear Density Measurements

21 Average Absolute Difference Between Nuclear Density Measurements Based on Material or Soil Type

LIST OF PHOTOGRAPHS

Photo

1 Autoprobe in Contact with Soil

2 Field Test: Clayey Silty Sand with Aggregate

3 Field Test: Portland Cement Concrete Pavement

4 Field Test: Silty Sand and Aggregate Subbase

5 Electronic Instrument Module

INTRODUCTION

The use of nuclear moisture-density gages for determination of in-situ soil moisture and density values has been adopted by many Federal, state, county and city agencies as well as commercial firms because this method is accurate and more rapid than former methods. The degree of acceptance in the past was limited due to questions as to the reliability of the equipment and an unwillingness of some agencies to change from an established method of testing. However a recent survey of the 50 State Highway Departments in the U. S., conducted by the Transportation Reseach Board(1), indicated that by 1973 all were engaged in nuclear gage testing on either a research basis or as a field control, or both. This contrasts with the year, 1962, when only about one half of these agencies were so involved.

Numerous Highway Departments have conducted research and concluded that the design of a gage has a direct influence on its reliability. For example, nuclear gage density measurements can vary depending upon the chemical composition of the material or soil being tested. A gage's performance is also influenced by its internal characteristics, such as the amount of lead shielding between the radioactive source and radiation detector, or the geometric relationship between the source and detector.

In an attempt to increase nuclear gage reliability the Transportation Laboratory of the California Department of Transportation in 1969 initiated a research program to investigate the parameters affecting the operation of the basic "backscatter" nuclear moisture-density gage. The term "backscatter" denotes that both the radioactive source and detector are placed on the test soil surface, and defines the detection of attenuated radiation which has traveled from the source through the soil to the detector.

The research project was divided into three phases. Phase one consisted of laboratory testing of the basic nuclear gage in the

"backscatter" and "transmission" modes. The transmission mode defines the detection of attenuated radiation transmitted through the soil. In this case the radioactive source is placed at a specific depth in the soil while the detector remains at the surface. Several gage parameters such as geometry, gage materials and electronic components were investigated. The selection of proper parameters has produced an efficient and accurate gage. In phase two the optimum gage parameters were incorporated into the construction of a prototype nuclear gage. This prototype, which incorporates an improved backscatter gage unit, an electronic monitoring system, and a vehicle-hydraulic system, will be used for field evaluation of the gage improvements revealed by phase one experiments. In the third phase the prototype gage was used to conduct field tests. These test results were compared with those obtained with the presently employed portable gage. A statistical analysis was performed to evaluate the field data. Additional modifications of the prototype may be required to correct difficulties encountered during field operations.

The ultimate goal is to improve the backscatter gage and make it comparable in accuracy to the transmission gage. This research was conducted based on nuclear gage specifications which were in use prior to September 1973. The present state-of-the-art is reflected in the specifications which are presented in the Appendix of this report. This research has developed the basic facts which have been applied to these improved nuclear gage specifications and the initiation of new avenues of investigation.

CONCLUSIONS

General

1. Initial field investigation of the Autoprobe nuclear moisture-density gage which was constructed using optimum backscatter gage parameters furnished evidence that this device is superior to the commercial backscatter gage, and is nearly equivalent to the commercial transmission gage selected for the field comparison.

2. Initial test data indicate that the commercial and Autoprobe moisture gages yield practically identical moisture content measurements. However the average Autoprobe moisture gage error (due to small quantities of neutron capturing minerals such as iron and boron and large quantities of bentonite or kaolinite), was approximately 1.1 pcf water content. A commercial moisture gage tested under identical conditions produced an average 1.6 pcf error.

3. The Autoprobe moisture gage appears to be about 45 percent less sensitive to mineral absorbers than the commercial model. The outstanding quality of the Autoprobe moisture gage is the count rate sensitivity to changes in moisture content. Under normal operating conditions, the count rate change for one pound per cubic foot change in water content was found to be 121 percent better than the commercial moisture gage.

4. The Autoprobe moisture gage is less sensitive to test surface irregularities because of the high efficiency of its lithium-iodide scintillation detector.

5. The Autoprobe has provided to be an efficient, expeditious, and relatively accurate device for compaction control operations.

6. The Autoprobe Vehicle-gage unit is especially suited for

compaction control of roadway subgrade, subbase, and base materials. Asphalt and portland cement concrete pavements can also be surveyed by this form of backscatter unit.

7. Autoprobe backscatter tests on relatively smooth uniform roadway surfaces can be performed rapidly with minimum disturbance of the materials being tested.

8. Simultaneous measurement of in-situ moisture content and density plus the shorter count period required for a statistically reliable count permit moisture density determinations in a much shorter period of time than that required with todays commercially available equipment.

Source Selection

1. A Radium-226 source possesses a large quantity of low initial gamma energies which may render a gage overly sensitive to the mineral composition of the soil.

2. Evaluation of Cesium-137 and Cobalt-60 revealed that both sources provide similar density gage sensitivity, count rates and amounts of chemical composition error, when appropriate adjustments are made in each gage apparatus.

3. When shielding, gage size requirements, and backscatter surface errors were evaluated, Cesium was found most suitable for density gage use.

4. Americium-beryllium appeared to be a suitable source from both the moisture and density standpoint.

5. Cesium-137 and Americium-beryllium can coexist within the same gage apparatus without conflict of their respective radioactive functions, therefore they were selected for use in the Autoprobe.

Detector Selection

1. Examination of three Geiger-Mueller detectors and a sodium-iodide scintillation detector indicated that the scintillation detector is the most desirable for gamma detection and use in a nuclear density gage in both "backscatter" and "transmission" configurations.

2. Selection of an efficient gamma detector, such as the scintillation crystal, is important to the accuracy of the density gage. The ability of the detector to discriminate gamma energies between 0.14 and 0.34 mev is highly desirable and it appears to be independent of the gamma sources used.

3. Moisture gage performance with a lithium-iodide scintillation detector proved superior to that with a proportional counter detector. The large count rates, electronically adjustable energy discrimination, and greater sensitivity to epithermal neutron energies are the qualities that make the lithium-iodide scintillation detector more desirable for moisture gage use. Ambient temperature effects were encountered but count rate variations were not overwhelming and easily corrected by slight adjustment of the applied voltage.

Shielding and Source-Detector Separation

1. The most important aspect of shielding involves protection of the gamma and neutron detectors from detrimental detection of the gamma emissions being attenuated within the moisture-density gage apparatus.

2. Lack of adequate shielding between gamma source and detector will render a gage virtually insensitive to density.

3. Protection of the neutron detector from excessive gamma bombardment is an important factor when considering the gamma-

neutron pulse height ratio and strength of gamma source being used.

4. The small neutron source-detector separation required for moisture gage sensitivity excludes space for lead shielding when a duplex source is employed.

5. Shielding of the neutron detectors from attenuated neutron energies created within the gage apparatus was not a major problem. The close physical location of the neutron source and detector precludes most fast neutron attenuation to thermal neutron energies by the time the emissions penetrate the detector.

6. Experiments conducted with the density gage indicate that gage sensitivity increases with increasing source-detector separation. The backscatter density gage sensitivity, as defined by the California 1969 criteria, can be increased by approximately 54 percent in the presence of adequate shielding. Ultimate sensitivity, however, cannot be utilized because of other performance considerations.

7. Moisture gage sensitivity increases with decreasing source-detector separation. Best sensitivity results were obtained with the detector located directly adjacent to the neutron source housing.

8. Laboratory experiments confirmed that specific amounts of collimation were beneficial to density gage sensitivity. The laboratory apparatus, under adequate shielding conditions, showed that source and detector collimation equal to one inch or less could improve sensitivity by approximately 4 percent. A 1-inch source and 1/2-inch detector collimation produced this slight rise in performance. The amount of collimation applied also depends on the collimator shape, source size, and count rate. Excessive collimation degrades count rate and increases chemical composition error.

RECOMMENDATIONS

The use of the vehicle-Autoprobe unit under field conditions during the evaluation phase of the project disclosed that certain modifications might improve performance. The operation of the vehicle unit and the hydraulic system which positions the Autoprobe on the test surface can be repositioned to remove the visual barrier between gage operator and the Autoprobe. Presently, the operator is unable to see the Autoprobe as it is being lowered to the test surface; he must leave the passenger compartment to ascertain that the Autoprobe is properly seated on the test surface. To correct this deficiency, the Autoprobe could feasibly be stored, and operate, from a location directly behind the vehicle-gage operator. A shielded storage compartment could be constructed below the vehicle bed, directly behind the operator's compartment. An automated system, either hydraulic or electric, would remove the Autoprobe from the storage area horizontally, and lower the gage vertically to the test surface. The Autoprobe would thus appear as an outrigger, on the driver's side of the vehicle. A mirror, installed on the vehicle, would permit the driver-operator to check the seating of the gage without leaving the controls of the vehicle or Autoprobe monitoring equipment.

Some type of guide mechanism to orient the vehicle-gage to use on inclined embankments is also needed. Presently, the gage is limited to vertical positioning, due to gravity. Some degree of latitude is permitted with the present guide system; sufficient only to accommodate minor test surface irregularities. The new guide design should be capable of permitting Autoprobe operation on slopes equal to, or greater than, six percent.

The Autoprobe gage can be completely rearranged to reduce gage size and to ensure satisfactory performance. Original design and assembly of the Autoprobe was based, to a certain degree, on

versatility and flexibility, to accommmodate gage modifications as research progressed. The experience obtained with the Autoprobe now warrants a design with permanent gage component fixity. The duplex gamma-neutron source can be relocated so that the gamma detector and neutron detector could be positioned on opposite sides of the source.

The bulk of the Autoprobe body, or housing, can also be reduced by eliminating the box channel construction of the gage frame that formerly housed a series of thermal neutron proportional counters. These counters have now been superseded by the lithium-iodide scintillation detector.

An important matter remains unresolved. This concerns the performance characteristic changes of the scintillation detector as a function of temperature. Testing of the scintillation detector in a laboratory environmental chamber should clarify this aspect of performance. Some inquiry must be made to determine the durability of the crystal under such dynamic impacts as are occasionally sustained during field operations. Also, the long-term drift should be investigated.

Several changes can also be made within the Autoprobe. Important items to be considered are the source and possibly the detector collimator design. A beneficial change of the source collimator was achieved following the initial field trials of the Autoprobe. This design modification reduced gage error caused by irregular surface conditions. Additional investigation of collimator principles should lead to further improvements.

Two inter-related gage components; the source size, and scintillation crystal size, might be varied to obtain a maximum count rate in a count period less than the 40-second interval now employed. An increase in the scintillation crystal thickness or diameter can increase the number of emissions being detected.

On the other hand, enlargement of the source size, (number of millicuries employed) would also increase the count rate. Source size, however, is limited by shielding and health safety requirements. Therefore, enlargement of the crystal would seem to be the approach to pursue. Cost may also be a governing factor. The expense of large photomultiplier tubes must be considered. The goal to be achieved is to shorten the time required to conduct the backscatter test. Possibly a period of thirty seconds or less can be realized.

Reducing the test period may lead to the development of a continuous moisture-density logging apparatus, similar to the device now available commercially. The Autoprobe could easily be adapted to this technique. This form of nuclear gage testing is particularly ideal for all types of roadway compaction activities. The Autoprobe could be lowered from the vehicle storage compartment and fastened to a carriage mounting frame, which maintains a constant vertical air-gap dimension between the test surface and the gage bottom during the logging. The Autoprobe's ability to perform static as well as dynamic backscatter testing would certainly enhance the vehicle-gage versatility.

Finally, as was mentioned briefly in the conclusions, many of the gage parameters discovered through the research can be adapted to the nuclear gage specifications required of the commercial vendors competing for nuclear gage contracts with the Department of Transportation. The experience gained with the vehicle-Autoprobe unit should be closely examined and the feasibility of constructing several production line vehicle-gage units for use by each Transportation District should be pursued.

IMPLEMENTATION

Further improvements of the Autoprobe density gage have been initiated and laboratory modifications will be evaluated by field testing. Hopefully, such modifications will reduce backscatter gage deficiencies caused by rough surface conditions encountered during field test operations.

Presently, the time required to seat the Autoprobe on the test surface, record four separate count rates for moisture and density, determine the in-situ parameters, and retrieve the gage, is approximately five minutes. The use of a portable electronic calculator enables the recorded counts to be converted to moisture and density values during the test period. A completely automated system is being considered, which requires the acquisition of a printer-recorder and mini computer. Count rates can then be processed by the computer and printed on paper tape for the operator's review. Test results can be made available to the resident engineer and compaction contractor in a very short period of time, thus reducing construction delays. Time, an important commodity to both the engineer and the contractor, can be utilized more effectively by employing a unit similar to the Autoprobe. The economic implications of this time factor are self-evident. Compaction operations can continue within minutes after the tests are finished and the nuclear gage unit can proceed to other test areas.

The conclusions derived from the Autoprobe's development and testing raise a question concerning the choice of nuclear test method (either transmission or backscatter) used for a particular compaction operation: In other words which nuclear test method would yield a more representative measurement of the compaction achieved by the contractor? The improved backscatter gage (Autoprobe) in addition to the transmission gage techniques would certainly give the resident engineer an opportunity to exercise greater authority and judgment over compaction operations. Availability

of both test methods would also enable the gage operator to select the test procedure best suited for the materials or compaction conditions encountered in the field.

STATEMENT OF THE PROBLEM

Previous analyses of the parameters affecting nuclear moisture-density gage measurements have been limited to investigations of the difficulties encountered under field conditions. Factors such as surface roughness, air gaps, and gage calibration methods, were among the items investigated. This project involved evaluation of the nuclear gage itself, together with the basic gage principles related to the "backscatter" and the "transmission" modes of operation.

This study encompassed interrelated parameters that have significant effect on gage performance. These include: the geometric relationships between the radioactive source; the test material; and the radiation detector. The "backscatter" mode, which relies on the number of attenuated emission deflected to the test medium surface, depends on the distance separating the radioactive source and the radiation detector. In the "transmission" mode the radioactive source is lowered into the test medium while the detector remains at the surface. Therefore the intervening thickness of test material between the source and detector becomes an important variable. Thus, source-detector separation and source depth were explored.

Secondly, the detection of particular attenuated emission energies may have a marked effect on gage performance. The available radioactive sources produce a wide range of emission energies. Each source has its own characteristic energy spectrum. Attenuation of the spectrum by the test medium produces a wider variation of low energy emissions than originally emitted by the source. Detection of low energies are undesirable because of absorption effects within the test materials. Thus this gage parameter must be carefully examined to minimize or eliminate the chemical composition error generated by various test materials.

An important consideration in gage design is proper shielding between the source and detector. Inadequate shielding permits nondensity sensitive radiation to activate the detector, which results in degraded gage performance. This occurrence is particularly true for "backscatter" gages.

Lastly, detector collimation and source collimation are possible tools for improving gage performance and reducing gage error. Collimation restricts the direction and number of emissions entering the detector as well as restricting the direction and number of emissions projected into the test material. An investigation of various combination and amount of collimation may prove beneficial to gage accuracy.

This test program examined these and other areas of investigation.

DISCUSSION

Radioactive Sources

Radium-226, Cesium-137, and Cobalt-60 were evaluated to determine their suitability as a gamma source for a nuclear density gage. A survey of existing data indicated that Radium-226 possesses a large quantity of low initial gamma energies, which would be extremely susceptible to photoelectric absorption after minimal density attenuation. Since a large number of photoelectric events result in inaccurate density gage measurement laboratory experiments proposed for radium were cancelled. Most commercial nuclear gage manufacturers have also excluded radium in selecting their gamma source.

The evaluation of Cesium-137 and Cobalt-60 disclosed that both gamma sources will yield about the same density gage results. Each provides comparable density gage sensitivity, count rate, and amount of chemical composition error when gage apparatus are properly adjusted. Other source differences reltative to shielding, gage size, and backscatter surface errors must be considered. These latter criteria favor selection of cesium as the primary choice. Cobalt requires a greater source-detector separation to achieve the same gage sensitivity as the Cesium gage which affects gage size. Gage weight is also affected, since Cobalt requires approximately twice the amount of lead to properly shield against health hazards and ensure gage sensitivity. Cesium was thoroughly evaluated and found suitable for density gage use.

Two fast neutron sources, Radium-beryllium and Americium-beryllium, were tested in the laboratory to determine the advantages and disadvantages of each as a possible source in a density-moisture gage. These experiments indicated that Radium-beryllium would be unsuitable as a neutron source for several reasons. The major disadvantage is the high energy gamma output of radium and its influence on the adjacent neutron detector. Due to the small neutron source-detector separation (necessary for best moisture gage

energy discrimination ability of the electronic components associated with the scintillation crystal. Selecting the gamma energies to be monitored can easily be accomplished thereby eliminating most of the detected energies which cause density gage error.

Laboratory tests indicate that the scintillation detector count rate is influenced by changes in ambient temperature. Count rate variations can be effectively controlled by slight adjustment of the voltage supplied to the photomultiplier tube. Count rate variation due to temperatures from 32 to 120 degrees Fahrenheit was not extremely large and could be corrected by relatively small changes of the applied voltage.

Neutron Detectors: A comparison of proportional counter detectors and a lithium-iodide scintillation detector resulted in conclusions similar to those mentioned above for the sodium-iodide scintillation detector. Moisture gage performance is definitely superior with a scintillation detector than with a proportional counter detector. The large count rates, electronically adjustable energy discrimination, and greater sensitivity to epithermal neutron energies, are the qualities which make the lithium-iodide scintillation detector most desirable for moisture gage use. Ambient temperature effects were again encountered, but the count rate variations were not overwhelming, and are easily corrected by slight adjustment of the applied voltage.

Effect of Chemical Composition of Soil

The chemical composition of soil can induce density gage error as evidenced by the relative discrepancy of the calibration curve produced from the silicous and calcareous density standards. The maximum discrepancy in density occurs in the ranges between 100 pcf and 140 pcf and varies with the amount of chemical composition and the sensitivity of a particular detector. Chemical composition error is a function of the photoelectric photons produced by the

sensitivity) the radium gamma emissions saturate the neutron detector, yielding extremely high count rates in the energy region normally reserved for detecting neutrons. Another adverse factor is the low neutron (less than 0.7 mev) energies resulting from the (γ,n) reactions. This source of low energy neutrons would be subject to rapid attenuation, which can result in moisture gage error. These considerations, plus the fact that radium was not considered desirable for the density gage, eliminated Radium-beryllium as a practical choice.

Most of the laboratory research centered around the use of Americium-beryllium. Americium 241 emits a series of low gamma energies (below 0.37 mev.) which are well below the gamma energies required to produce the (γ,n) reactions mentioned above. This precludes the production of photoneutrons and excessive detection of gamma event by the thermal neutron detector. The principle gamma energy of .060 mev emitted by Americium will not affect the performance of the density gage if removed by electronic discrimination. Thus, Americium-beryllium appeared to be a suitable source from both the moisture and density standpoints.

The coexistance of Cesium-137 and Americium-beryllium in the same gage apparatus does not alter respective individual radioactive functions.

Detectors

Gamma Detectors: Examination of three Geiger-Mueller detectors and a sodium-iodide scintillation detector indicated that the scintillation detector is the most desirable for use in a nuclear density gage. Scintillation crystal efficiency in the detection of gamma emissions is much greater than that of the Geiger-Mueller detector; therefore, the gamma count during any unit time is much larger when using the scintillation detector. Large count rates are essential to statistical reliability. Another outstanding advantage of the scintillation detector is the incremental

chemical constituents of the test material. A thin lead sheet or a combination of lead and brass sheets placed beneath a Geiger-Mueller detector proved very effective in reducing chemical composition error. This mechanical filtration of gamma energies reduced chemical error to approximately 1.0 pcf., but count rates were also severely reduced. The mechanical filtration was extremely effective in reducing error while providing adequate count rates, and was typical of the performance displayed by the sodium-iodide scintilaltion detector. The exclusion of gamma energies below approximately 0.15 mev and above approximately 0.8 mev provided favorable results.

Detection of low thermal neutron energies that are subject to capture by interactions with test soil minerals will lead to varying amounts of moisture gage error. Experiments with a lithium-iodide scintillation detector indicate that mechanical discrimination, in the form of polyethylene and cadmium, and energy discrimination, accomplished by electronic means, are effective tools for minimizing moisture gage errors due to soil constituents. A number of thin polyethylene disks and/or a thin cadmium foil placed beneath the scintillation crystal reduced chemical error considerably; however, other moisture gage parameters, such as gage sensitivity, preclude their use. Possibly, the polyethylene-cadmium discrimination technique can be applied when proportional counters are employed.

Shielding

The most important aspect of shielding is the protection of the gamma and neutron detectors from detrimental detection of the gamma emissions being attenuated within the moisture-density gage apparatus. Approximately 4.5 inches of lead, placed directly between a cesium source and gamma detector will absorb at least 99.5 percent of all the undesirable emissions directed toward the detector from within the gage. Cobalt requires approximately 50 percent more lead (6.5 inches) provide the same degree

of protection. Lack of adequate shielding between gamma source and detector will produce a backscatter mode gage that is insensitive to density.

Protection of the neutron detector from excessive gamma bombardment is an important factor when considering the gamma-neutron pulse height ratio and strength of gamma source being used. The small neutron source-detector separation required for moisture gage sensitivity precludes space for lead shielding when a duplex source is employed. Tungsten could be used in place of lead when shielding thicknesses are restricted. Another alternative would be selection of a gamma source possessing gamma emission energies below those which seriously affect the neutron detector count rate. Minimal shielding, in this case, would satisfy the gamma absorption requirements. If adequate neutron detector shielding cannot be achieved, separate location of the gamma and neutron source together with appropriate location of their respective detectors, would be required. This condition, however, would increase gage size and weight.

Shielding of the neutron detector from attenuated neutron energies created within the gage apparatus was not a major problem. The close physical location of the neutron source and detector precludes most fast neutron attenuation to thermal neutron energies by the time the emissions penetrate the detector. The moisture gage neutron detector is relatively insensitive to high energy neutrons, therefore, these emissions pass through the detector unnoticed. Moisture gage sensitivity is not impaired by fast neutron penetration.

Source-Detector Separation

Source-detector separation directly affects both moisture and density gage sensitivities. Experiments conducted with the density gage indicate that gage sensitivity increases with increasing source-detector separation. Ultimate sensitivity,

however, cannot be utilized because of other performance considerations. Count rates decline sharply, and chemical composition error, (denoted by the separation of the gage calibration curves), is increased drastically with wider source-detector separations. The optimum separation for 10 mc of Cesium-137 is about 11 inches. The optimum separation for 3 mc of Cobalt-60 is approximately 13 inches.

An investigation of the transmission technique showed that density gage sensitivity is primarily governed by the minimum path length between gamma source and detector. Longer path lengths produce greater density gage sensitivity. Certain energy bands, however, tend to maintain a given gage sensitivity regardless of the minimum path length employed. Compromise is again necessary to satisfy count rate and chemical composition criteria.

Moisture gage sensitivity, as indicated by these experiments increases with decreasing source-detector separation. Best sensitivity results were obtained with the detector located directly adjacent to the neutron source housing. Apparatus limitations should be eased through redesign of the neutron source-detector housing to permit minimal separation. Moisture gage sensitivity (defined as the change in count rate per pound change in water content), varied considerably with separation distance. In most cases, the neutron detectors examined exhibited an increased sensitivity from 50 to 400 percent with one-half reduction of the original separation distance. The prototype moisture gage constructed following the research work employed a 3.3 inch source-detector separation.

Collimation

Source and detector collimations were explored to determine their potential benefit to backscatter gage performance. Prime emphasis was placed on gamma source and detector collimation. Laboratory experiments confirmed that specific amounts of collimation were beneficial to density gage sensitivity. The laboratory apparatus, under adequate shielding conditions, showed that source and detector collimation amounting to one inch or less could improve sensitivity by approximately 4 percent. A 1-inch source and 1/2-inch detector collimation produced this slight rise in performance. The amount of collimation applied also depends on the collimator shape, source size, and count rate. Excessive collimation degrades count rate and increases chemical composition error. The optimum collimation derived from the laboratory cesium backscatter gage was 0.65-inch source and 0.25-inch detector collimation.

Collimator shape significantly influenced backscatter gage reaction to test soil surface conditions. A 0.2-inch air-gap between the backscatter gage bottom and the test surface simulated the error induced by an improperly seated gage. A modified wedge-shaped collimator reduced air-gap error by approximately 20 percent. Gage sensitivity appeared unaffected by the collimation shape, but source orientation and collimation height within the collimator governs sensitivity values.

Further experimentation with the moisture will be required to determine the amount of collimation needed for optimum gage operation. Data obtained during the density gage air-gap study clearly indicated a loss of moisture gage sensitivity and count rate with increasing height above the test surface. Fortunately, chemical composition error remained relatively unchanged with this form of collimation.

Autoprobe Design and Analysis

Optimum backscatter gage parameters established by this investigation were utilized in the construction of a hybrid nuclear moisture-density gage. The hybrid gage (also referred to as Autoprobe in this report) was so constructed that the individual components could be modified if required to accommodate future improvements. Analysis of the results of initial field investigation of the Autoprobe indicated that it is superior to the commercial backscatter gage and nearly equivalent to the commercial transmission gage selected for the field comparison.

The mean indicated density, standard deviation, and percent probability of the indicated densities were calculated statistically for all gages and their respective differences determined. The Autoprobe showed a significant reduction in the backscatter standard deviation when compared to the commercial backscatter gage. However, significant differences in standard deviation between the Autoprobe and the commercial transmission gage were not found.

Assuming that the commercial transmission gage used in this study provided acceptable measurements, the Autoprobe provides 7 to 18 percent greater probability of indicating the mean transmission gage density than the commercial backscatter gage. Based on relative differences between the Autoprobe and the commercial backscatter gage, the Autoprobe shows a 21 percent improvement in the backscatter technique.

Efforts to further improve the Autoprobe density gage have been initiated and laboratory modifications will be evaluated by field testing. Hopefully, the modifications will improve the backscatter gage efficiency when used on rough surface conditions often encountered during field test operations.

Sufficient field data has not as yet been compiled to adequately evaluate the Autoprobe moisture gage. Initial test data, however, indicate that the commercial and Autoprobe moisture gages yield practically identical moisture content measurements. Laboratory tests showed that the average Autoprobe moisture gage error is approximately 1.1 lbs per cubic foot water content due to small quantities of neutron capturing minerals such as iron and boron and large quantities of bentonite or kaolinite. A commercial moisture gage tested under identical conditions produced an average 1.6 lbs per cubic foot error.

The Autoprobe appears to be about 45 percent less sensitive to mineral absorbers. The outstanding quality of the Autoprobe moisture gage is the count rate sensitivity to changes in moisture content. Under normal operating conditions, the count rate change for one pound per cubic foot change in water content was found to be 121 percent better than the commercial moisture gage. Under a 0.2 inch air-gap, the Autoprobe lost 7 percent of its count rate sensitivity, compared to a 25 percent loss for the commercial gage. This fact implies that the Autoprobe moisture gage would be less sensitive to test surface irregularities. The major factor contributing to this performance is the high efficiency of the lithium-iodide scintillation detector installed in the Autoprobe. The proportional counter detectors found in most commercial back-scatter gages possess only a fraction of this efficiency.

BASIC FACTORS

Discussed in this report are several factors common to both backscatter and transmission modes of gage operation and others peculiar to one mode only.

One factor in common is the depth or material thickness that a particular radioactive emission will penetrate. This penetration depth is dependent upon the initial energy emitted by the radioactive source, which governs the size of the test volume being examined by the nuclear gage. Other common factors are radiation detector type, and electronic monitoring equipment. In both gage operating modes under consideration, the radiation detector is located at the surface of the test material and the electronic monitoring equipment attached to the detector requires no component changes for each operating mode. Beyond these three, all other basic factors depend on the mode of gage operation.

The differences in basic factors between the "transmission" and the "backscatter" mode are dependent upon the physical position of the radioactive source and its geometric relationship with the radiation detector. For instance, a given radioactive source will penetrate a particular test material to a depth that is governed by the source, but the volume of test material being bombarded by radioactive emissions is considerably different, due to the mode of testing.

Source-detector separation, or the geometric relationship between source and detector, has a basic mode difference. Test material completely separates the source and detector in the "transmission" mode. In this case, a large majority of attenuated emission entering the radiation detector are those emerging from the test material. In the "backscatter" mode, soil attenuated emissions as well as non-soil attenuated emissions enter the detector. These non-soil attenuated emissions are independent of the test

material and are the result of the emission flux surrounding the source at the surface of the test medium. The presence of this flux field, if not properly controlled, may prevent the "backscatter" gage from yielding accurate test measurements. Adequate shielding between the source and detector can eliminate a large portion of the nonattenuated emissions.

Collimation of nonattenuated emissions entering the test material (or attenuated emissions emerging from the test material) is an effective tool that can be used to promote "backscatter" gage accuracy. Source collimation, as stated previously, restricts the number and direction of emissions entering the test material. The attenuated emissions emerging from the test material in the immediate vicinity of the radiation detector restrict the number and direction of emissions that can activate the detector. Collimation is therefore a geometric factor, and is most applicable to the "backscatter" mode.

Other basic factors relative to each operating mode are the electronic monitoring system settings, which are an integral part of the detector. These settings concern the magnitude of the signals received from the detector and the emission energy which can be detected.

These basic gage factors are all significant in considering the efficiency, accuracy, physical size, and operating mode of a nuclear moisture-density gage.

GAMMA SOURCE EVALUATION

Discussion

A radioactive source is identified by the type of radiation emitted and by the energies the emissions possesses. Sources under consideration must emit an adequate quantity of gamma photons. Gamma photons are defined as amounts of pure electromagnetic radiation, similar to light or X-ray, ejected from the interior of an unstable nucleus. Gamma photons or rays, being pure energy with no mass, posses the ability to pass through materials to a considerable depth. As the gamma photon proceeds through a material, it collides with the atoms of the material, losing a portion of its initial energy. The number of collisions that occur and the amount of energy lost are functions of the material density. Therefore, by monitoring the number of gamma photons, of a given energy emerging from a test material, a relationship between the material density and the number of photons detected can be established. This relationship is the basic principle governing the nuclear density gage.

The evaluation of any gamma source involves determination of the initial gamma energies emitted by the source and the attenuated gamma energies detected. One method of examining the attenuating process is to examine the gamma photon energy spectrum before and after passing through a test material. The spectrum, which is the relationship between photon energy and number of photons detected, will indicate how many gamma photons of a given energy have been attenuated to a lower energy.

Attenuation is a photon energy absorption process which may occur in one of three ways, depending upon the photon energy state before collision. Energy is absorbed by pair production, Compton scattering, or photoelectric absorption. Pair production occurs when a high energy photon transforms itself into a positron and electron pair, independent of any collision with an atom of the test material. The positron will combine with another

available electron and emit a low energy gamma photon. This photon is commonly known as annihilation radiation. When a gamma photon collides with an atom the reaction takes place between the photon and an orbiting electron. Energy is expended by the gamma photon to dislodge the electron producing an ion pair. Compton scattering thus occurs when a portion of the initial gamma energy is absorbed due to ion pair production and the remaining photon energy is deflected to a different direction. Photoelectric absorption occurs when a low gamma energy is completely absorbed by the gamma-electron collision. The photon in this case is completely annihilated(2).

Since pair production is an independent gamma property and photoelectric absorption completely annihilates the photon, Compton scattering is the primary reaction which describes the attenuation process that enables determination of the relationship between gamma energy and material density.

The preceding exposition strongly suggests that radio-isotopes possessing initially low gamma energies would be undesirable due to the dominance of photoelectric absorption. In the research being reported, three commonly used radioisotopes were selected for evaluation and comparison; a 10 mc Cesium-137, a 3 mc Cobalt-60 and a 4.5 mc Radium 226-beryllium source. The initial step towards evaluation was to examine the initial gamma spectrums of the three isotopes. Figure 1 indicates that radium emits a large quantity of low energy photon; thus photo-electric absorption may be a predominant reaction. Cesium (Figure 2) shows a characteristic energy of 0.662 mev whereas cobalt (Figure 3) shows a range of high energy peaks(3).

This spectrum evaluation provided background information on the manner in which each source would perform. As a consequence, the test program for radium-beryllium was shortened. Also indicated was that cobalt would probably require a moderate amount of lead shielding for health safety reasons as well as detector shielding.

Another characteristic to be considered is the half-life or change in the rate of radioactive decay. The half-life is the time required by a radioisotope to reduce the number of radioactive emissions to one-half its initial number. This factor would affect the calibration requirements of the nuclear density gage. A short half-life would require several gage calibration adjustments during the life of the gage. Cobalt-60 has a 5.27 year half-life whereas Cesium-137 has a 33 year half-life. Radium 226 half-life is 1622 years. Recalibration of a density gage with a radium source would be unnecessary(4).

The evaluation of these three radioactive sources was accomplished by comparing the gage sensitivity ratio, chemical composition error and count-rate obtained with each source. The "SENSITIVITY RATIO" is defined as the ratio between the detector count rate obtained from the gage calibration for 110 pcf density to the count rate obtained for 140 pcf density. A large ratio, say 1.9, indicates that the gage possesses a greater sensitivity to small density changes than a gage having a smaller ratio of say 1.3. The two reference densities (110 pcf and 140 pcf) were chosen because they represent the wide range of materials densities found under field conditions. To examine the gage error introduced by chemical composition, the horizontal separation in pcf between the gage calibration curves (see Figure 4) is obtained from the standard density blocks. Thus the source sensitivity to the compositional differences between the calcium and the silicon standards can be determined.

The count rate quality of the sources can be determined from the density calibration curve. The required count rates are governed from statistical consideration and are available in the "Specifications for Nuclear Density-Moisture Gage" included in the Appendix.

Each gamma source was examined in a backscatter gage arrangement. A 1 1/2 inch x 1 1/2 inch sodium iodide scintillation crystal served as the gamma detector for all three gamma sources. Other experimental adjustments were made relative to source-detector separation, source collimation, and lead shielding between source and detector. The term lead shielding, referred to as "PRIMARY SHIELDING", refers to the additional lead thickness placed between the source and detector and does not include the 3/4 inch thick lead cylinder housing, the detector, or the 1.75 inch lead cylinder containing the gamma source. A typical experimental arrangement of the gage apparatus showing the positioning of the primary shielding is illustrated in Figure 5. During the initial series of tests no additional primary shielding was placed between source and detector. Following analysis of the initial test results, the effects of increasing the source collimation and adding primary shielding were explored.

The three gamma sources were also evaluated in the "transmission" mode. Calibration curves were obtained for each source by employing six standard density blocks. Transmission tests were conducted at 6 and 12 inch depths below the surface of the standard block. Figure 6 illustrates the arrangement of the "transmission" apparatus. Horizontal source-detector separation was varied to explore its relationship to "transmission" depth. The sensitivity ratio, chemical composition error, and count rate obtained with each source was examined and compared in a manner similar to the "backscatter" analysis.

Among the various physical parameters of gages used during the laboratory testing was lead (primary) shielding. As mentioned previously, shielding is required to decrease the detection of the gamma flux surrounding the source and improves overall gage sensitivity to changes in density. The source mechanism was designed to shield 10 mc of Cesium -137. This limited the size of the radium and cobalt source that could be used from a health safety standpoint.

The test results indicated that additional shielding is most beneficial for cobalt increasing the sensitivity ratio by as much as 50 percent. Cesium test results showed only minimal benefits: in this case, the ratio increased by about 10 percent. The small improvement for the cesium gage is probably due to the fact that the major portion of the flux is eliminated by the lead source mechanism housing and the lead detector housing.

The amount of shielding required for each source is a function of the initial gamma energies being emitted. High initial photon energies require greater lead thicknesses; hence the amount of lead used in a gage will govern the weight and dimensions of the apparatus. With this criterion in mind, it was verified by experiment that cobalt requires about twice as much shielding as cesium. The shielding needs of radium were not explored during this investigation.

Source-detector separation is another factor governing gage size. The primary factor governing source-detector separation is also a function of the initial gamma energies being emitted by the source. High energies require a greater separation to obtain optimum sensitivity than low energies. This hypothesis relates to the path length taken by a photon to attain a given moderate energy. Test results showed that the high energy cobalt source required approximately 15 inches to optimize the gage whereas the lower energy cesium gage optimum was 11 inches.

The path length taken by a gamma photon also indicates the material thickness required to reduce an initial photon energy to a photoelectric absorption energy. This thickness or depth of penetration is also related to the volume of test material being sampled by the density gage. A series of tests were conducted to determine the depth of penetration attained by the cobalt and cesium sources.

The penetration depth was determined by noting the change in count rate due to a change in the test material thickness. Two test materials were employed. A sandy-silt compacted in 1-inch lifts with an average density of approximately 112 pcf and a series of one-half-inch thick magnesium plates, having a 112 pcf density, served as the test materials.

A plot of "backscatter" count rates versus material thickness indicated the thicknesses where the change in count rate was statistically unchanged. This count rate defines the penetration depth. The test materials were supported on wood, concrete, or steel bases. A frame was also constructed to provide a 1-inch air gap beneath the test materials to determine its influence. The changes in count rates were due to the combined influence of the test material and the base support.

Test results obtained with cobalt and cesium, respectively are depicted in Figures 7 and 8. The maximum penetrations on the sandy-silt material were approximately 8.0 inches for cobalt and 7.2 inches for cesium. A much greater penetration depth with cobalt had been anticipated. The magnesium plates data supported that obtained with the sandy-silt. Cobalt and cesium penetration depths were approximately 6 1/2 inches. Data employing a magnesium standard are presented on Figures 9 and 10. The difference in penetration depths between the sandy-silt and magnesium is attributed to irregularities of, and nonuniformity within, the compacted soil. In each case the cobalt source appeared to have greater penetration.

The relationships between material thickness and gage indicated density for the cobalt and cesium source are representated by Figures 11 and 12. Inspection of Figure 7 shows that 90 percent of the cobalt gage-indicated density was obtained from the top 5.3 inches of the sandy-silt while Figure 8 shows that 90 percent of the cesium gage-indicated density came from 4.4 inches of the sandy-silt. The approximately one inch difference between the 90 percent indicated densities was confirmed on the magnesium plates (see Figure 11 and Figure 12).

In summation these experiments indicated no significant difference between the photon penetration depths of cobalt and cesium. The indicated density from the cobalt source appears to originate from emissions from a slightly greater depth than cesium possibly due to the greater source detector separation of the cobalt gage.

Another parameter which may be related to penetration depth is surface error. Surface error is defined as the density error induced by irregular surface texture of the test material. In many cases, surface texture can result in air gaps between the bottom of the "backscatter" gage and the test material. Gamma emissions reflected from the air gap area may stream along the gage test material interface toward the detector. The lack of uniform contact with the material results in gage error.

Two procedures can reduce or eliminate such gage error. The test surface can be carefully prepared to remove surface irregularities before the gage is placed on the test material, or the gage can be constructed to minimize these surface influences. As surface preparation is time-consuming, various gage electronics (gage configurations) were introduced to offset surface effects. The gage configurations pertain to the collimation of the gamma source and/or gamma detector. Source collimation reduces the number, and restricts the direction, of gamma photons entering the test material. Detector collimation applies similar limitations on the moderated gamma photons emerging from the test material beneath the detector. A 10 mc cesium gage was employed in this test series.

An irregular surface texture condition was simulated by creating an air gap beneath various components of the density gage. A 0.051 inch air gap, produced by one inch wide aluminum strips, elevated the gage components above the test surface. Test data indicate that an air gap extending beneath the entire gage produces the greatest error. Source and detector collimation generally reduced but did not totally eliminate surface error. The error was

reduced as the amount of collimation increased. The optimum collimation distances were not determined. Table 1 summarizes the errors encountered under the various gage conditions examined. Gage error was most evident when the air gap was beneath the gamma source. This condition induced about twice the error recorded for an air gap beneath the detector. Additional source collimation (from 0.25 to 0.65 inches) appeared to equalize the error due to source or detector air gap.

The results tabulated in Part III (Table I) show the combined effect of both source and detector collimation. The average error under Part III (Table I) conditions, for an air gap under the entire gage, was approximately 24 percent below the average error reduced by source collimation alone. It therefore appears that surface or air gap errors can be reduced by some combination of source-detector collimation. Air gap experimentation involving the cobalt gage was not attempted during the course of this study.

The utility of a "backscatter" gage depends on three calibration qualities: sensitivity ratio, chemical composition error, and count ratio. Prior to 1972 the California Department of Transportation minimum criterion for an acceptable "backscatter" gage sensitivity ratio was 1.3. This criterion is the basis for this study.

The chemical composition effect is defined as the separation in lbs/cu ft between the calibration curves obtained from a series of calcium and silicon density standards. The maximum chemical error acceptable is 4.0 pcf for "backscatter" gage densities ranging between 100 and 160 pcf based on the criterion established prior to 1972. The count rate is defined as the number of detected events recorded in one minute indicated at 140 pcf on the gage calibration curve. The minimum acceptable "backscatter" count rate criterion is 10,000 counts per minute.

This study has indicated that both sensitivity ratio and chemical composition criteria can be significantly improved. For example, the "backscatter" sensitivity ratio can be upgraded from 1.3 to approximately 2.0. Chemical error can also be reduced from 4.0 pcf error to about 2.0 pcf error.

Under optimum gage condition cesium appears to be slightly superior to cobalt. Cesium sensitivity ratios were generally greater than 2.0, whereas the cobalt ratios were slightly less. Cesium also showed less chemical error than cobalt. Average error over the specified density range was approximately 1.5 pcf compared to 2.0 pcf for cobalt. Typical calibration curves with the associated sensitivity ratio, chemical composition error, and count rate, are presented on Figure 13 and Figure 14. Additional laboratory work with the cobalt gage disclosed that when properly adjusted the detector discriminator interval can reduce chemical error to about 0.5 pcf (see Figure 15). Discriminator adjustments for the cesium gage have not been performed; however, beneficial results can be anticipated with appropriate adjustments. Hence, from a calibration curve standpoint, the test data indicate that cobalt and cesium are nearly equal.

Summary

To summarize this discussion of gamma source; three commonly used radioisotopes (Cesium-137, Cobalt-60, and Radium 226-beryllium) were evaluated. Following inspection of available data radium was eliminated from further consideration in this laboratory test program. The predominantly low initial photon energies emitted by radium are susceptible to photoelectric absorption. Therefore, in consideration of the time and economic limitations of this project, experimental efforts were confined to cesium and cobalt.

Several nuclear density gage parameters were investigated to evaluate and select the most appropriate gamma source for the prototype nuclear density gage. The prime selection criterion was which gamma source would provide the best sensitivity to density changes and reduce chemical composition error. Test results indicated that cobalt and cesium possess comparable sensitivity and compositional qualities. The degree of equality with regard to these two gage parameters hinges upon the gage geometry; detector type; amount of primary shielding, and the electronic discriminator capabilities associated with the gage.

In considering a suitable gamma source it was recognized that employment of cobalt, as opposed to cesium, would require a gage of greater overall dimensions and weight due to lead shielding requirements. Cesium was initially chosen as the preferable gamma source to use in the prototype gage. The design construction and operation of the prototype gage will not, however, be severely restricted in terms of size or weight. A final decision on the gamma source will be made only after field evaluation of a cobalt source prototype gage.

The photon penetration depth, which relates to the test material volume being sampled by the gage was considered. Generally speaking, cobalt and cesium penetration depths are comparable, however, the cobalt "backscatter" gage obtains 90 percent of its indicated density from a 5.3 inch thick volume of test material beneath the gage. The cesium gage obtains the same percent indicated density from approximately 4.4 inches of test material. Therefore, the effective depth of test desired should be a consideration in the selection of the gamma source.

Surface error induced by the surface texture of test material or minor air gaps may equal about 3 pcf from indicated gage density f4r the cesium "backscatter" gage. Source and detector collimation can reduce this form of gage error, but may not totally eliminate surface effect. The amount of surface error associated with the cobalt gage was not determined.

Chemical composition error was found to be approximately 2 pcf for both the cesium and cobalt gages under optimum configuration conditions. Additional work with the cobalt gage showed that fine adjustments of the detector's discrimination interval can reduce chemical composition to a nearly insignificant amount. Experiments with the discriminator interval has reduced gage error from about 2 pcf to 0.5 pcf.

The prototype nuclear density gage will have the capability of field evaluating either the cobalt or cesium source. Interchangeable gage components and adjustable gage geometry will allow acceptance of either source. The field evaluation of the prototype gage will begin under Phase III of this project with a 10 mc cesium source. If time and funds permit, the cesium will be replaced with cobalt and a field evaluation program conducted similar to the cesium study. The final selection of the gamma source will be made after a thorough field test analysis has been completed.

NEUTRON SOURCE EVALUATION

Two commonly used neutron sources were selected for the evaluation of the moisture gage. Several commercial gages employ either Radium 226-beryllium or Americium-241 beryllium. The advantages and disadvantages of each source were evaluated.

The first consideration is directed towards the characteristics of each neutron source. A brief description of the neutron producing reactions encountered is here presented.

The alpha-neutron (α,n) reaction and the gamma-neutron (γ,n) reaction are considered herein. The (α,n) reactions are common to both radium-beryllium and americium-beryllium. Alpha particles, emitted by both radium and americium, collide with the beryllium nucleus and release a neutron possessing considerable energy. A similar reaction between various gamma emissions and the beryllium nucleus also occurs. Neutrons produced by the (γ,n) reactions possess relatively low initial energies. Alpha produced neutrons possess high initial energies. A tabulation compiled by the National Bureau of Standards indicates that radium-beryllium will yield 15×10^6 neutrons per second per curie. The maximum neutron energy produced is 13.08 mev with an average neutron energy of 3.9 mev. The (γ,n) reaction yield is 1.3×10^6 neutrons per second per curie. The gamma produced neutron possesses energies up to 0.7 mev(5). The americium-beryllium (α,n) reaction process yields 2.2×10^6 neutrons per second per curie.

The advantage of radium-beryllium is greater neutron yield. The yield is over seven times the americium-beryllium yield. The main disadvantage of radium-beryllium is the strong gamma background emissions accompanying the neutron output. Statistics indicate 6,500 gamma emissions accompany one neutron emission. Strong gamma fields detrimentally affect neutron detectors; thus moisture gage sensitivity is impaired. Another disadvantage is

the number of low energy neutron emissions produced by gamma (γ,n) reactions. Moderation of low initial neutron energies yields neutron energies that are susceptible to rapid thermalization and subject to chemical absorption. Absorption of thermal neutrons by nonhydrogen moderators produce moisture gage errors.

The following is a review of the mechanics of neutron moderation. Several possible reactions may occur once a fast neutron enters the moderating material. Hydrogen and nonhydrogen elements will moderate neutrons to thermal energies. Two reactions are possible, depending upon the initial neutron energy prior to the collision. Elastic scattering of the neutron reduces neutron energy and imparts kinetic energy to the nucleus it collides with. Inelastic scattering produces increased changes in nucleus-neutron kinetic energy and neutron path, as well as nucleus excitation which causes the emission of a gamma photon. Neutron absorption is the other possible reaction to consider. A moderator element may capture the neutron and react in several ways. The by-products of neutron absorption are gamma radiation, proton or alpha emissions, or the release of a neutron by the absorbing nucleus(6).

The probability that a particular neutron energy will be absorbed by a particular moderating element is expressed by the probable cross-sectional target area of the element. The units associated with this probability are known as "Barns" or "Fermi" and are expressed in multiples of 10^{-24} cm^2(5). Low neutron energies in and below thermal levels have high absorption probabilities. An intuitive evaluation of these facts seems to indicate that a neutron source producing high neutron energies will yield higher moderate energies after emerging from the moderating material. These higher moderated energies are less susceptible to absorbing elements. Thus, moisture gage error could be reduced by detecting the intermediate neutrons above the thermal range. At the present time, the moisture gage is solely dependent upon detecting thermal neutrons.

The following describes the ways in which neutrons can be used to identify the moisture in a test material. Fast neutrons are rapidly moderated by a small number of collisions with any hydrogen atom. Therefore water or any other hydrogen-bearing mineral in the test material will drastically reduce fast neutron energies to the thermal neutron state. A fast neutron must collide with approximately 18 hydrogen atoms before reaching a thermal neutron energy. The number of scattering collisions with nonhydrogen elements required to achieve a thermal state is relatively large compared to hydrogen. For example, an average of 262 collisions with numerous silicon atoms results in thermalization(7). The thermalizing ability of hydrogen is attributed to the mass of the hydrogen atom and the neutron mass. Both have approximately the same mass, therefore a large amount of kinetic energy is transferred from the neutron to the hydrogen nucleus during a collision. Once a neutron has been reduced to the thermal stage, it is subject to absorption by elements such as boron, lithium, cadmium, iron, chlorine, silver, gold and other rare earths. Sufficient quantities of these elements in the test material removes a portion of the thermal neutrons from possible detection.

Two sources of moisture gage error require examination. First, the thermal neutrons being detected may be a function of the test material mineralogy instead of the actual water content of the material. Secondly, thermal neutron absorbers may cause the moisture gage to indicate a lower water content than the true amount.

Consideration must then be given to selection of the moderated neutron energies which should be detected and which are less susceptible to absorption and more sensitive to changes in moisture content.

Radium-beryllium may be preferred to americium-beryllium from a "backscatter" moderated neutron standpoint. The high initial neutron energies produced by radium seems desirable. However, the low photoneutrons and thermal neutrons output accompanying the high energies may be detrimental to gage accuracy.

A rather important aspect of the nuclear moisture-density gage involves the gamma photon energies being emitted by the neutron source. Radium-beryllium emits both gamma photons and fast neutrons. Thus, this source can accommodate both gage functions. The intense gamma output accompanying the neutrons affect the efficiency of most thermal neutron detectors. Americium emits relatively low gamma energies (.060 mev.) and would be less troublesome in this respect.

The preliminary evaluation of radium-beryllium eliminated this particular neutron source from further consideration.

Next, the americium-beryllium source was evaluated by examining the energy spectrum obtained with various neutron detectors, the moisture gage sensitivity, and the absorption error. To realistically evaluate the neutron source, the americium-beryllium was placed on top of a 10 mc cesium gamma source. This would simulate present commercial gage configurations. Test results with and without cesium present are compared.

First to be discussed is the neutron spectrum results in the absence of cesium. A moderated neutron spectrum was obtained with two individual thermal neutron detectors. The fast neutrons emitted by a 50 mc americium-beryllium source passed through a one-inch thick polyethylene plate. A "BF_3" proportional counter produced the spectrum presented on Figure 16. As this figure indicates, the largest number of detected neutrons are in the low thermal energy range. The spectrum portion near the upper limits of the detector are of particular interest. These are the epithermal neutron energies below the 0.5 mev. level. The change in this predominant peak was monitored as changes in test material

moisture content and gamma intensity varied. A similar spectrum was obtained with a "He-3" proportional counter (see Figure 17). The difference in spectrum shapes are due to the operational characteristics and the electronic settings used with each detector.

Now that the general sectrum shape has been defined, how did the 10 mc cesium gamma source affect the spectrum? Actually, the gamma photons coming from the cesium will not cause (γ,n) reactions since initial gamma energies being emitted are below 1 mev. Therefore, any change in the detected spectrum is due to the gamma flux activating the detector. A large number of gamma events were recorded by the detectors in the low thermal energy region. Therefore, under actual field conditions, monitoring this region of the spectrum would give erroneous moisture content results. The increased count rate near the upper energy limits of the detector were not as severe. Approximately 418,000 gamma counts were experienced with 10 mc cesium present, as recorded with the BF_3 detector in the low thermal energy region of the spectrum. The He-3 recorded 115,000 to 200,000 gamma events. Thus a thermal neutron detector that is sensitive to lower thermal energies is not desirable in the presence of a gamma flux.

The experimental findings suggest two possible alternatives that could improve gage performance. First, a neutron detector capable of refined energy discrimination would minimize gamma influence. Secondly, water content may best be determined by monitoring epithermal or intermediate neutron energies. The first hypothesis will be discussed later in this report.

The argument favoring epithermal neutrons and intermediate neutrons concerns the resistance to capture by various elements found in some soil types. Thermal neutron capture produces gage error. Figure 18 represents the various moisture calibration curves

obtained from our moisture standards, using the cesium plus americium-beryllium source and a BF_3 detector. These calibration curves indicate the error produced by a moisture standard containing a thermal neutron absorber element (iron). A basilite material, rich in iron, served as the absorber. The data points, resulting from the basilite, showed a sharp departure from the linear calibration line obtained with the nonbasilite standards. Detector discrimination can be a useful tool in eliminating this absorption departure. Various energy segments of the detector spectrum appears to be less sensitive to absorber error. Figure 19, obtained with the He-3 detection and Figure 18, obtained with the BF_3 detector show similar results. A similar trend was also noted with a lithium-iodide scintillation crystal detector, see Figure 20. In each case, the detection of higher energies tends to minimize absorption error. These results warrant a detailed investigation in the area of detecting nonthermal neutrons.

To summarize this discussion, work to date has been limited to an evaluation of americium-beryllium. The neutron spectrums obtained by three different thermal neutron detectors indicate a single high energy peak which could be monitored as a function of moisture content. Selecting a neutron detector with the ability to discriminate and chosing the energies found in the high energy region will eliminate or minimize absorption and gamma influence errors.

Americium-beryllium, due to the absence of (γ,n) reactions appears to be the most desirable neutron source to incorporate into a moisture-density gage. If epithermal and intermediate neutrons can be detected by some other experimental technique, the ;articular neutron source then becomes of less importance.

GAMMA DETECTOR EVALUATION

The two gamma detectors considered here are the Geiger-Mueller (G.M.) detector and the scintillation crystal detector. The Geiger-Mueller detector is a cylindrical cathode tube filled with an inert gas. A thin wire anode is fastened to the center of the tube. A gamma ray penetrating the tube and colliding with a gas atom will cause ionization. The freed electron then migrates to the wire anode producing an output signal. The G.M. tube is thus activated and the gamma ray is detected. A small amount of a quenching gas is added to the ionizable gas to discontinue ionization during the signal pulse output. The time interval required to return the gas to its unionized state is commonly referred to as "dead time". During the dead-time interval ionization events will not produce a signal pulse; therefore, the efficiency of a G.M. detector is a function of its "dead-time" characteristic(8).

A scintillation crystal detector also functions as an ionization medium. When a gamma ray ionizes a sodium atom, a minute quantity of light is emitted. The scintillation event occurs in approximately one microsecond, which is about one-one hundredth of the "dead time" required by a G.M. detector. The probability of a gamma ray ionizing an atom of the crystal is much greater than the ionization probability of the G.M. detector. Therefore, the scintillation crystal will record a significantly larger quantity of gamma rays per given time than the G.M. detector.

The amount of light emitted by the scintillation event is proportional to the gamma energy causing the ionization. Thus detection of various gamma energies can be accomplished by proper calibration and adjustment of the electronic detector components. The detection of various selected gamma energies is referred to as "energy discrimination".

Three Geiger-Mueller detectors were evaluated on the calcareous and silicious density standards. These detectors were tested to determine the chemical composition error, due to gamma absorption by the test media, the minimum one-minute detector count (cpm), and the sensitivity ratio.

Each detector was evaluated in the backscatter mode with the 10 mc Cesium-137 as the gamma source. Each individually tested G.M. detector was fastened to a lead channel with exposed ends and detector surface adjacent to the test media. The cesium source was contained in a 1.75-inch thick cylindrical lead housing, (see Figure 21).

Various source-detector separations and metallic filters of the type employed between the detector and test material were examined. These filters serve as low energy discriminators. Certain low gamma energies are virtually eliminated from the detector spectrum by this method(9). Although a considerable reduction in the count rate can be anticipated with filtration, a beneficial decrease in chemical composition error may be expected. Severe count rate reduction can be overcome by using multiple detectors. Source-detector separation governs gage sensitivity to changes in density. Sensitivity increases with increase in separation.

Another important gage factor evaluated through experimentation was primary shielding. Primary shielding reduces or eliminates the detectable radiation surrounding the gamma source, which is independent of the moderated gamma radiation emerging from the test material. Ideally, all detected radiation should consist of moderated gamma emission emerging from the test material (see Figure 21).

The following is a discussion of each G.M. detector and the test results obtained by the "backscatter" mode. The G.M. Detector

I is of the stainless steel halogen-quenched type. The manufacturer's specifications for this equipment are listed in Table 2. Two source-detector geometrics were used for this detector and 6.5 inch and 10 inch separations were employed. Various lead filters ranging up to 0.042-inch thick were used with 6.5-inch separation. Two inches of primary shielding was a constant gage component for the 6.5-inch configuration.

The maximum count as determined for 140 pcf density from the calibration curve was approximately 1000 cpm, far below the 10,000 cpm required for statistical reliability. Such a low count rate would require multiple detectors in an operational gage.

The chemical composition error could not be maintained below present "backscatter" specification limits (± 4 pcf) without a lead filter. The error was within the acceptable range when the 0.042-inch thick filter was placed beneath Detector I.

The sensitivity ratios under all filter conditions and both separation configurations ranged from 1.32 to 1.43; above the minimum 1.3 value presently acceptable for "backscatter" gage performance.

At the 10-inch source-detector configuration, the same filter thicknesses were employed. Primary shielding was maintained at four inches. The tests showed no improvement in gage performance. Chemical error and count rates worsened, while the sensitivity ratio fell below acceptable values. A 0.0045-inch lead filter elevated the sensitivity ratio to 1.97; but count rate and chemical error were not within acceptable limits. In this instance, a 200 cpm count rate and 12 pcf chemical error were recorded.

A summary of all detector test results is presented in Table 3.

Geiger-Mueller Detector II is a tantalum-lined detector. Complete equipment specifications were not available and the detector is no longer in production. Detector II was examined by the same test procedures used for Detector I; the 6.5-inch separation, however, was changed to 9 inches. Lead, brass, and a combination of both were examined for filter properties. The brass thickness of 0.033 inches was not varied throughout the test. Primary shielding remained at four inches for all tests.

The test results showed that the single tantalum-lined detector could not satisfy our minimum count rate requirement at either 9 inch or 10 inch gage configuration. As might be expected, the count rates were smaller at 10 inch separation than at 9 inch separation. Chemical composition error showed a considerable reduction with approximately 0.024 inch of lead filter and the chemical error was reduced by approximately 50 percent. A lead-brass combination was not effective with 9 inch separation but proved slightly superior to the lead filters, with 10 inch source-detector separation. A 0.0045 inch lead filter plus the 0.033 inch brass filter suppressed chemical error by approximately 70 percent.

All sensitivity ratios were exceptionally high and equivalent to present "transmission" standards. The 10 inch configuration produced ratios at the 1.9 level and the 9 inch configuration resulted in ratios of about 1.7. As was noted with Detector I, source-detector separation appears to govern the sensitivity ratio.

G.M. Detector III is a platinum-lined detector. Specifications are listed in Table 3.

The test results for Detector I and Detector II indicated that the 9-inch "backscatter" configuration was sufficient for testing Detector III. Lead filters and 4 inch primary shielding was provided in all tests.

As noted with the other detectors, acceptable count rates could not be obtained with a single detector. Chemical composition error exceeded allowable limits in all cases, with one exception. Using a 0.042 inch lead filter reduced chemical error to 1.8 pcf, or 21 percent of the initial "no-filter" condition. Sensitivity ratios were comparable to those obtained with Detector II at the 9 inch configuration.

The "transmission" configuration used with Detector III is illustrated in Figure 22. A vertical and a horizontal dimension are used to describe the "transmission" geometry. The horizontal distance between the source and detector plus the vertical depth of the cesium source below the surface of the test standard identifies the "transmission" gage configuration. Two configurations were examined; 10 inch horizontal separation with 10 inch depth and 12 inch horizontal separation with 12 inch depth. Lead filters were exclusively used beneath the detector and four inches of primary shielding remained adjacent to the detector, on the surface and between the detector and source. In this configuration the primary shielding absorbed moderated gamma emissions emerging from the density standard.

Transmission test results showed that no one-minute count rates met minimum count specifications. Sensitivity ratios equalled or exceeded 2.3 in all transmission configurations. Ratios as high as 3.7 were attained, but the adverse affect produced on the other gage parameters lead to rejection of many of these high ratio configurations.

These findings indicate that present ratio specification might be up-graded should deeper transmission depths or greater source-detector separations prove feasible. In general terms, the sensitivity ratio increases with increasing transmission depth.

A lead filter beneath the surface detector proved of value in the control of chemical composition error. The degree of effectiveness was found to be a function of the filter thickness and of transmission depth. For example, at 10 inch horizontal separation and 10 inch depth a 0.068 inch filter reduced the chemical error of the non-filtered configuration by approximately 60 percent. The error was reduced from 6 pcf to about 2 pcf. By increasing the transmission depth to 12 inches, the chemical error appeared to have been influenced by filter thickness. A 0.056 inch filter held chemical error to about 1 pcf. The 0.068 inch filter showed 2.5 pcf error for the 12 inch source depth. Therefore, the optimum filter thickness seems to decrease with increasing source depth. Chemical error control proved to be effective with lead filtration of the Geiger-Mueller detector.

The 12 inch horizontal separation with 12 inch depth configuration proved unacceptable from a count-rate chemical-composition standpoint. The low count rates can be explained by the increased path length and amount of energy moderation required to reach the detector. Chemical error to a magnitude of 6 pcf was also encountered. This again is a function of the larger quantity of lower gamma energies reaching the detector. It is conjectured that use of much thinner filters would have reduced chemical error.

The transmission data leads to the conclusion that sensitivity can be greatly enhanced by proper source depth and horizontal separation selection. Secondly, chemical error can be minimized by appropriate filter thickness. Also, multiple detectors of the platinum type could be used to satisfy the statistical count rate required. Transmission test results are summarized in Table 4.

For the limited number of tests and Geiger-Mueller detectors examined, the Tantalum-lined Geiger-Mueller detector proved to be the most desirable, from comparison of "backscatter" performance. The count rates and controlled chemical error were acceptable from a single G.M. detector standpoint. Several detectors would be required to attain statistical count stability. The sensitivity ratio obtained from this particular detector and gage configuration showed that improvement of portable backscatter gages sensitivity can be effected by proper gage construction.

A sodium-iodide scintillation crystal was the fourth and final gamma detector to be examined. A summary of manufacturers' specifications are listed in Table 5. Both "backscatter" and "transmission" modes were used to evaluate this detector. An 11 inch source-detector separation was used exclusively for all "backscatter" tests. The 12 inch horizontal separation with 6 inch and 12 inch source depth explored the "transmission" mode.

The experimental results indicate that both gage modes appeared desirable and far superior to the Geiger-Mueller detectors. The major advantage of the scintillation detector is its ability to detect a larger quantity of gamma emissions in a given time interval. Electronic filtering (energy discrimination) is also an advantage and convenience. Sensitivity ratios and chemical errors were generally superior to the values obtained with the Geiger-Mueller detectors, for both "backscatter" and "transmission" configurations.

The cesium-scintillation "backscatter" gage configuration had an 11 inch source-detector separation, 2 inches of primary shielding, no lead filtration and discriminators set to count two ranges of

gamma energies 0.15 mev to 0.275 and 0.15 mev to 0.42 mev. The transmission configuration used a 12 inch horizontal separation and either a 6 inch or 12 inch source depth. The detector discriminator interval was set for 0.42 mev to 2.1 mev emissions. Primary shielding and lead filters were not used.

"Backscatter" performance at each energy interval was examined with and without two inches of primary shielding. Shielding improved the sensitivity ratio by about 5 percent; held chemical error to 1.6 pcf; and caused peculiar results in count rates. Normally count rates decrease with primary shielding for all discriminator intervals. The 0.15 to 0.275 mev interval produced a higher count rate with primary shielding than without shielding. This anomaly may be attributable to operational error. All "backscatter" results met or exceeded every gage parameter desired (see Table 5).

Under the two "transmission" conditions and constant discriminator interval all experimental results exceeded all performance criteria for "transmission" gages, and was far superior to the transmission-G.M. detector performance. The sensitivity ratio increased from 2.4 to 3.2 by changing the gamma source depth from 6 to 12 inches. Chemical composition error, however, increased slightly from 1.5 pcf to 2.5 pcf at the deeper depth. As expected, the count rate dropped significantly with increased source depth. An interpolation of count rates recorded at 6 inch and 12 inch depths showed that the probable count rate at 8 inch depth (required at 140 pcf density by this Department's "transmission" specifications) is approximately 17,000 cpm. Such a count rate would exceed the study criteria by 54 percent.

NEUTRON DETECTOR EVALUATION

Laboratory experimentation procedures entailed evaluating two basic types of detector: the proportional counter, and the scintillator crystal. The scintillation crystal detector produces a small burst of light energy when a thermal neutron is captured. This event is amplified by a photomultiplier tube and recorded. The basic reaction mentioned above is commonly known as the (n,α) reaction. A thermal neutron, when captured will release an alpha particle or positive charged particle. The alpha particle is thus the primary factor in thermal neutron detection. In the presence of the alpha particle the proportional counter releases an avalanche of electrons to neutralize the positive charge. This discharge of electrons activates the detector and the neutron event is recorded. The proportional counter is comprised of a tube lined or filled with a thermal neutron-capturing material such as helium or boron.

Three proportional counter types were used in the evaluation program; two of the boron-trifloride type, and the third a helium type. Although each boron detector employs the same (n,α) reaction, the boron states differ. One is filled with a highly purified boron-trifloride gas, the other detector has an inner lining of boron. The helium (He-3) detector contains an amount of extremely purified helium gas mixed with a quenching gas to prevent continuous detector discharge.

The manufacturer's literature provided valuable information concerning each detector's sensitivity to neutrons. A thermal neutron detector could thus be classified or rated according to various parameters. A review of this information permitted pre-test evaluation of the detectors.

The The boron type detector can be rated according to a number of variables, including neutron sensitivity, gas fill pressure, gamma sensitivity, voltage plateau, count rate, resolution, pulse height and activation time.

The boron-trifloride detector would appear to be the most sensitive to thermal neutrons. Gas fill pressure governs the efficiency of thermal neutron detection and an increase in fill pressure will increase thermal neutron sensitivity. Although such increase is desirable, higher gamma flux sensitivity, higher operating voltage, and higher resolution values may offset the major advantage. The recommended maximum fill pressures are 1.185 atmospheres for a two-inch diameter detector and 2.10 atmospheres for a one-inch diameter detector. The one-inch diameter detector used in the experiments was represented as having boron-trifloride gas at 0.527 atmospheres. This low pressure is the probable cause of the low count rates recorded during the experiments. A low pressure detector, however, has such advantages as less resolution and lower voltage requirements. This detector's specifications and those of the other detectors evaluated are summarized in Table 6.

The boron-lined detector, by comparison, possesses less sensitivity to thermal neutron energies, yet produces a high pulse or signal output when activated. This detector is also less sensitive to gamma emissions and operates at lower voltages. One apparent disadvantage of this detector is the relatively short operating voltage plateau. Voltage plateau length will be discussed in another section of this report.

Detector sensitivity is a function of the boron-10 concentration on the inner wall. The boron-lined detector evaluated as a 0.2 mg/cm^2 layer of boron-10 on the inner cathod wall of the detector. Since optimum neutron sensitivity, according to one manufacturer, requires 0.4 mg/cm^2 the detector used for the evaluation probably did not have optimum capability.

The neutron-alpha (n,α) reaction occurring in the boron ionizes the argon-carbon dioxide gas in the detector which produces a signal pulse proportional to the ionizing energy. The main advantage of this detector is the strong signal pulses produced by the fill gas at low detector voltage. The boron-lined detector is also capable of operating at temperatures to 200 degrees centigrade without change in output characteristics. A further advantage is its capability of operating in the presence of high gamma fields, up to approximately 10^5 roentgens per hour. By contrast a boron-trifloride detector is limited to gamma fields below 10^2 roentgens per hour.

Literature describing the helium (He-3) detector indicates that it would be the most desirable tube type detector to use in a nuclear moisture gage. All parameters mentioned in the boron discussion appear to be a function of the helium gas fill pressure. Overall detector performance apparently increases with increasing pressure. It was also noted that gas fill pressures equal to, or greater than four atmospheres will capture all thermal neutrons entering the detector.

The He-3 detector has the capacity to detect thermal (0.025 ev.), epithermal (0.1 to 100 ev.), and intermediate (1000 to 500,000 ev.) neutron energies. The efficiency of detecting each neutron class depends upon the fill pressure. The detector used has a two atmosphere pressure, which is relatively low. According to published data, such pressure will permit a detector efficiency of from 40 percent for thermal neutrons to less than one percent for intermediate neutrons. Therefore, detection of nonthermal neutrons is possible, if desired. All other detector parameters appear to be similar to these of the boron lined detector.

The basic neutron-helium molecule reaction produces a single helium atom, a single hydrogen atom, and a release of energy. The energy released produces the output pulse of the detector.

A europium activated lithium-iodide scintillation crystal detector was also evaluated. This detector's efficiency in detecting thermal neutrons is claimed by the manufacturer to exceed 90 percent. The basic reaction is: ${}_3Li^6 + {}_0n^1 — {}_2He^4 + H^3 + Q$ The lithium capture of a thermal neutron produces an alpha particle, a triton atom, plus a reaction energy of 4.78 mev, which is shared by the two reaction particles. Nonthermal neutrons will also produce alpha and triton particles, but will impart higher energy. These reactions, however, depend upon the lithium enrichment and temperature of the crystal.

The principal advantage of using a lithium-iodide detector lies in the increased probability of detecting epithermal and intermediate neutrons, as well as fast neutrons between 0.5 to 1.0 mev. The probability of detecting a fast neutron in this range is about one percent. Detection of fast neutrons greater than 1.0 mev. can be accomplished by lowering the crystal temperature to extremely low values. For example, a 7.5 mev. neutron can be detected by lowering the crystal temperature to -200°C. However, this is not practical at the present time. The lithium-iodide crystal has a particular affinity for intermediate neutrons in the vicinity of 0.3 mev at normal operating temperatures. The probability of detecting this energy is approximately 12 percent.

Another major advantage of this detector is low energy gamma production. The reaction between the lithium molecule and the colliding neutron will not result in gamma radiation. Only iodine-neutron and europium-neutron reaction will produce gamma emissions. The number of neutron capturing reactions occurring due to the iodine and europium is estimated to be from one to 11 percent of the total capture capacity of the crystal. Reduction of iodine and europium capture is accomplished by greater lithium enrichment.

A summary of the lithium iodide crystal specifications used in this study is presented in Table 7.

The literature survey has provided a basis for selection of the most desirable moisture detector. This pre-evaluation favors the scintillation detector. The tube, or gas filled type detector appears least desirable. Comparison of the tube detectors shows that He-3 and BF_3 detectors would perform equally well, on the basis of their gas fill pressures. The boron lined detector, on the other hand, possess desirable electronic consideration.

With these facts in mind, an evaluation of these detectors on an experimental basis was begun. A 33 mc americium-beryllium neutron source combined in tandem with a 10 mc cessium gamma source was used to determine each detectors capabilities.

Gamma Sensitivity can be defined as the ratio between the gamma pulse heights and the neutron pulse heights. The magnitude of gamma sensitivity determines a detector's ability to discriminate between neutron and gamma events. Activation of the detector by a gamma flux adversely affects its ability to measure moisture content. Elimination of gamma activated events can be accomplished by mechanically filtering or shielding the detector from gamma emissions. Each of the neutron detectors tested had sensitivity to gamma radiation to some degree.

An experimental procedure was formulated to determine the number of gamma events being recorded by the neutron detector at various gamma energies. A "background" count was first obtained to determine the number of gamma events. Then a 100 mc cesium source, a 10 mc cesium source, and a 3 mc cobalt source were in turn placed near the detector and the respective count rates recorded. The number of gamma events detected versus the energy interval selected for detection are shown in Table 8 for the cesium sources only. The results are quite conclusive. A large number of gamma events were recorded by the He-3, BF_3, and the boron lined detector. The gamma events in the low energy region

are extremely vulnerable to detection. Unfortunately, the lower energy region also contains the thermal neutron region. The count rates in Table 8 result from extreme conditions which would normally be prevented or reduced by proper detector shielding. Another possible way to alleviate gamma influence is to set electronic discrimination levels as high as possible.

It was unnecessary to illustrate the use of cobalt since the gamma photons vary only as to the amount of energy they possess. All other characteristics are the same.

The least sensitive tube-type detector was the boron-trifloride detector. In the presence of 100 mc of cesium, the BF_3 detector can eliminate approximately 99.8 percent of the gamma counts by a slight upward adjustment of the threshold discrimination setting. The boron lined detector possesses about the same reduction character, but the percent reduction appears to be smaller. The He-3 detector, most sensitive to gamma fields required a considerable change in discriminator setting to reduce the gamma influence.

The relative sensitivity of the detectors was not measured since different electronic amplification settings were employed for each detector. The primary purpose of this study was to show the relative magnitude of the detected gamma pulse height compared to the detected (n,α) reaction pulse height. This was accomplished by viewing the detector signal output on an oscilloscope. Each detector was ranked according to the ratio between the maximum pulse height and the maximum gamma pulse height. This particular ratio will give an indication of how successful the neutron detector is in segregating neutron and gamma events. On this basis, the oscilloscope showed that the He-3 detector possessed the lowest pulse height ratio (10:1). The Be BF_3 gas detector provided the best results, showing (30:1) ratio. The boron lined

detector possessed an intermediate ratio of (20:1). Therefore, the boron trifloride reveals the best separation between neutron and gamma generated pulse heights, of the tube detectors examined. The lithium-iodide crystal, (as stated in the literature review) is probably the least sensitive to gamma emissions and probably possesses a larger pulse height ratio than the boron-trifloride detector. It is planned to confirm this assumption through experimentation at a later date.

A further means used to compare detectors involved examination of the calibration curves obtained from Department moisture standards, and resulting energy spectrums. A description of the proportional counters used to obtain the calibration curve is listed in Table 6. The moisture standards consist of compacted Ottawa sand with a specific water content. A 10 mc cesium gamma source and a 33 mc americium-beryllium neutron source were placed on the surface of the moisture standard adjacent to the thermal neutron detector, see Figure 23.

The lithium-iodide detector will be discussed first. The neutron spectrum obtained from the three moisture standards indicate the change in the number of recorded events for any given neutron energy within the detector's limits. Figure 24 shows a plot of the recorded data with the increase in the number of neutrons being detected as the water content increases. Most noticeably is the number of recorded events between the 6.5 to 7.5 volt interval of the single channel analyzer. Although there is an increase in the number of low energy and thermal energy events, the marked change in the higher energy region appears more significant. Therefore, it may be desirable to monitor this particular high energy interval instead of the thermal neutrons conventionally accepted as a function of moisture content.

The calibration curve also reflects the desirability of monitoring the higher energy region of the spectrum. High energy detection provides less gage sensitivity to changes in moisture content than the detection of a broad band of energy including low energies, but selecting narrow bands of high energy will reduce or eliminate chemical absorption error. Figure 25 represents the calibration curves obtained with the lithium iodide detector. One moisture standard contains an amount of Basolite, an iron rich material which will absorb thermal neutrons. The location of the basolite data points on the calibration curves indicate the amount of error induced by neutron absorption. The amount of error was found to be a function of selected energy interval. The precise energy band for eliminating all chemical effects has not been found, but energies detected between 6.0 and 10 volts are being considered for additional testing.

A similar review of the calibration curves obtained with the He-3, BF_3 and B-10 lined detector also indicated the possible elimination of chemical absorption effects by electronic discrimination. The BF_3 detector showed that energies slightly above and adjacent to the thermal neutron region provides desirable results, see Figure 26. The B-10 and He-3 detectors seems to favor higher energies for absorption elimination. Both detectors displayed similar calibration curves.

The calibration curves obtained from the boron and the helium detectors show considerable flucuation in the thermal energy and the high energy regions. Monitoring the high energy region did not reduce the absorption effect, Figure 27 and Figure 28.

Another comparable parameter, mentioned previously, is the detector's sensitivity to changes in water content. Moisture sensitivity, as defined by values taken from the calibration curve, is the ratio between the recorded count rate taken

at 20 pcf and 5 pcf moisture. The Departments nuclear moisture gage specifications require a ratio equal to three or more. On this basis comparison can be made of the ratios and calibration curves obtained with each detector. In Figure 29 the best fit calibration curve for each detector is presented. The lithium-iodide detector is obviously superior to the helium and boron detectors from a count rate standpoint. The count ratio was 3.32 which exceeds the Departments specification requirement. The He-3, BF_3, and B-10 lined detectors were inferior to the scintillation detector with respect to count rate but did exceed the lithium-iodide detector in count ratio. Test results show ratios of 3.60, 3.45 and 3.50 for the He-3, BF_3, and B-10 lined detectors, respectively. Hence, the count ratio may not be a true indicator of moisture gage performance.

Statistically, the scintillation detector is much more reliable for determining moisture content than the other detectors. A high count rate will tend to mask or override the random errors inherent in all gages.

Another method for defining detector sensitivity involves calculating increase or decrease in count rate per pcf water content. This definition indicates that lithium-iodide possesses a sensitivity of 80 counts per pcf water content. Sensitivity is approximately 10 counts per pcf for the He-3 and B-10 detectors and 5 counts per pcf for the BF_3 detector. The scintillation detector is therefore the most desirable from this standpoint.

Low count rate and low counts per pcf water content are principally due to detector efficiency. For example, many of the neutrons which penetrate a tube type detector will not collide with a capturing nuclei, and pass through the detector unnoticed. This condition is particularly true for higher energy neutrons. Gas fill pressure, as mentioned previously, is one method of controlling

high energy neutron detection. According to one detector manufacturer, the efficiency is defined by the equation: $1-e^{-\Sigma ad}$, where Σ = capture element density, a = Avogadro's number (3840×10^{-24} cm^2), and d = path length taken by the neutron through the detector. Gas filled pressure controls density and governs efficiency. Another method of increasing efficiency would be to return undetected neutrons to the detector for a second chance of being captured. A reflector material redirects the neutron towards the detector, giving it another opportunity to enter and collide with the capture element.

Polyethylene is currently being used by one manufacturer to achieve this process. An optimum amount of polyethylene surrounding the detector can increase its efficiency by approximately two percent, according to the manufacturer.

A question arises concerning such employment of polyethylene. The investigators feel that, although initially undetected thermal neutrons are returned to the detector, a number of non-thermal neutrons are moderated in polyethylene and also returned. These neutrons will not represent the moisture content of the test material. Although the thermal neutrons produced by the polyethylene increases the number of detected events, they are not a function of the moisture content of the test material, but rather a function of the thickness and placement of polyethylene surrounding the detector. The benefits of polyethylene will require additional study.

The detector stability parameter involves the change in count rate caused by changes in detector voltage and ambient temperature. The variation produced by the change in voltage is a direct result of the voltage plateau characteristics of each gas-filled detector.

The relationship between the applied detector voltage and the count rate is shown in Figures 30, 31, and 32. Before discussing test results, a number of experimental parameters require definition. These concern the selection of various electronic adjustments. For example, the detectors signal output can be governed by two specific components; the detector's preamplifier, and linear amplifier. These two component adjustments, in concert with the applied detector voltage and selected energy interval, will determine the number of events recorded in a given time interval. Varying applied voltage, while holding other parameters constant, produces the plateau characteristic curve.

With these parameters in mind, it is possible to evaluate each detector's plateau curve. Figure 30 shows the various plateau curves obtained with the He-3 detector. Starting with H.V. Curve A, (at the left side of Figure 30), the energy interval or discriminator interval, was set to record a very wide range of neutron energies. As the applied voltage was increased, no major change in the count rate occurred until the voltage exceeded 800 volts. Above 800 volts the count rate rose sharply with increasing voltage. At 1000 volts, the count rate rises more slowly resembling a step plateau region. At 1200 volts, the count rate again increases dramatically. The major cause for the long flat plateau between 0 and 800 volts is probably electronic "noise" being generated within the electronic system. The He-3 detector is not activated until the applied voltage exceeds 800 volts, therefore, the detector's operating plateau is defined between 1000 and 1200 volts.

The two curves designated "B", immediately below this plateau (again referring to Figure 30) were obtained by increasing the preamplifier voltage gain, increasing the linear amplifier coarse gain, and decreasing the count interval to 30 seconds. The lower limit of the discriminator interval was also raised to

a higher threshold energy. The voltage plateau appears to have shifted to a slightly lower voltage range and lengthened its plateau from 200 volts to about 300 volts. A further increase in the threshold energy had no additional effect in lengthening the voltage plateau. Increasing the threshold energy lowered the count rate in the plateau region. The vertical separation between the first curve and second set of curves is primarily due to the change in discriminator setting. A wide discriminator interval, which includes extremely low energies, detects the electronic "system noise" as well as gamma events.

It was interesting to note the drastic shift of the plateau location when the lower threshold energy was changed by a large factor. Note the relationship between Curve A and Curve C on Figure 30. The general shape of the plateau curve did not change, but the plateau location changed from the 1000 to 1200 applied voltage vicinity to 1400 to 1600 volt range. Curve C indicates that the applied voltage must be greater than 1150 volts before the electronic apparatus begins recording detectable events.

Finally, a reduction in the preamplifier voltage gain and the linear amplifier fine gain had the dual effect of shifting the plateau to a higher voltage interval and of increasing the count rate. This was established by inspecting Curve C and Curve D. As noted before in the discussion of the B Curves, the adjustment of the lower threshold energy produced a decrease in the plateau count rate and slightly displaced the plateau to a higher voltage range.

The plateau length for all practical considerations is nearly nonexistent. The experimental results indicate that the 8-inch long He-3 detector possesses a noticeably steep and extremely short plateau. The plateau slope (defined as the total change

in count rate within the plateau, divided by the plateau voltage length,) is approximately 75 counts per volt.

Figure 31 represents the plateau characteristics of the 2-inch diameter boron-trifloride detector. Of note is the relatively horizontal plateau at a count rate between 2000 and 2500. Curves A and B show the effect of varying the linear amplifier setting, while the other electronic adjustments remain constant. The discriminator interval for both curves reflected a wide range of energies, including system noise. The slight vertical and lateral displacement between Curve A and Curve B is the direct result of a decrease in coarse and fine gain settings of the linear amplifier. The plateau length was increased by the lower gain settings by approximately 150 volts. This elongated plateau occurred between 900 and 1150 volts.

Curve C and Curve E indicate the change in the plateau curve due to changes in preamplifier and discriminator settings. The preamplifier charge sensitivity and bias resistance were reduced by a factor of 10 and the voltage gain reduced by a factor of 4. The lower discriminator threshold was also raised to reduce "system noise". Threshold changes did not noticeably change the count rate. Reduction of the preamplifier adjustments caused the plateau to shift to a higher voltage interval and the plateau length to shorten. The plateau was displaced by approximately 50 volts. Curve C is similar to Curve B. Lateral plateau displacement was the result of the reduction in the linear amplifier coarse gain setting. The plateau displacement is about 200 volts. No change of the plateau length was recorded. The slight decrease in the count rate was attributed to a small change in discriminator settings.

Curve D can be compared with Curve E on the basis of preamplifier change sensitivity. Increasing the sensitivity by a factor of 10 displaced the plateau to a higher range, by 150 volts, and shortened its length by approximately 50 volts.

In summation, it was shown that changes in either preamplifier or linear amplifier gain will alter the count rate in the vicinity of the plateau. Decreasing the linear amplifier coarse gain and fine gain will displace the location of the plateau to a higher voltage interval. Increasing the preamplifier charge sensitivity shifts the plateau to a lower voltage interval. In both cases, plateau lengths will vary by approximately 50 volts. The most desirable operating voltage appears to be between 900 and 1150 volts. In this interval, the plateau length is 250 volts and the plateau slope is approximately two counts per volt.

The one-inch diameter boron-trifloride detector plateau curves are presented on Figure 32. This detector appears to be the most desirable from plateau and operating voltage considerations. Preamplifier and linear amplifier settings were not evaluated. From the two preliminary tests made, the significant parameter to be considered is the discriminator interval. The governing factor was the lower threshold setting. Increasing the threshold energy reduced noise and increased plateau length. Curve B was selected as the optimum plateau curve.

Thus, the detector will perform between 150 and 1300 volts without any significant change in count rate. The plateau is exceptionally flat and has a slope equal to 0.65 counts per volt.

The plateau evaluation of the three detectors has indicated the boron-trifloride detector to be the most desirable from an operating voltage-plateau length standpoint. The helium detector was considered unacceptable due to the extremely short and steep plateau characteristics. The boron-lined detector would appear to be acceptable granted that provisions are made to control and guarantee the applied operating voltage.

The remaining parameter to be discussed which affects the plateau is operating temperature. The detector's sensitivity to temperature was determined by placing the detector in an oven and recording the count rate at various ambient temperatures. The voltages applied to the detectors were the midplateau voltages as determined by previous tests.

The boron-trifloride detector operated at 900 volts was found to maintain a relatively constant count rate up to 300 degrees Fahrenheit. Count rates for temperatures exceeding 300 degrees were not recorded due to the failure of the detector cables under these high temperatures. The cable insulating material melted shorting the shield to the conductor producing erratic count rates. The actual change in the count rate at 300 degrees was about five percent greater than the rate at room temperature, which was slightly above the expected statistical variation of the neutron emissions.

Variation of the applied voltage did not affect the count rate as temperatures increased. A 50 volt decrease or increase in the applied voltage resulted in only ± 3 percent change in count rate recorded at 250 degrees Fahrenheit, probably due to the statistical randomness of the neutron source.

The He-3 detector was subjected to similar temperature conditions imposed upon the 2 inch diameter BF_3 detector. The He-3 performed quite differently than the BF_3. The applied voltage used, according to the plateau curve, was 1500 volts.

The experimental relationships established between temperature, count rate and voltage are presented in Figure 33. The He-3 detector possesses a fairly stable count rate between ambient

room temperature and 200 degrees Fahrenheit. Beyond 200 degrees, the count rate rises sharply. For example, at 270 degrees the count rate is 22 percent higher than the count rate for 200 degrees. Changes also occur with changes in applied voltage. At 270 degrees increasing the voltage to 1550 volts produced a 10 percent increase in count rate above the rate recorded at 1500 volts. A 50 volt decrease at the same temperature reduced the count rate by approximately 15 percent. Thus, temperature stability cannot be maintained at temperatures above 200 degrees Fahrenheit.

An inspection of Figure 34 shows how temperature influences the boron trifloride 2 inch detector. The temperature test was conducted with 1350 volts applied to the detector. The figure indicates that count rate remains relatively constant from 100 to approximately 250 degrees Fahrenheit. Temperatures in excess of 250 degrees induce a tremendous jump in the count rate. A 20 degree increase to 270 degrees increased the count rate by 70 percent.

A 50 volt increase in applied voltage did not effect the count rate significantly for temperatures between 100 and 250 degrees. A 50 volt decrease in applied voltage decreased the count rate by 11 percent at 110 degrees. Thus, voltage drop appears to have the greater influence on the count rate.

This investigation of detector count rate stability with changes in temperature has shown conclusively that the boron-trifloride $B(BF_3)$ detector will remain relatively unaffected by high temperatures. Both boron-lined and helium detectors are limited to a particular range of temepratures and become subject to variations of applied voltage due to plateau characteristics. Therefore the BF_3 detector appears supperior to the other detectors from a temperature standpoint.

Up to this point the investigators have presented data concerning conventional tube type thermal neutron detectors. Table 9 summarizes the experimental findings. These indicate that the boron-trifloride detector embodies the most desirable overall qualities. No valid comparison between this detector and the lithium-iodide scintilaltion crystal can be made since the crystal will out-perform the BF_3 in every parameter, with possible exception of temperature. Data concerning temperature stability of the crystal has not been obtained through experimentation as permanent damage might have resulted from extreme temperatures. More information from scintillation phosphor manufacturers must be secured before proceeding with laboratory experiments.

There are several other advantages and disadvantages which should be considered in evaluating a the lithium-iodide detector. The noncrystal components of the detector, such as the photomultiplier tube and preamplifier should be considered. Such detector characteristics as count rate drift and pulse height resolution should also be investigated.

An experiment to explore count rate variation of the lithium-iodide detector resulting from temperature fluctuation was performed in a small drying oven. The lithium-iodide detector consisting of the scintillation crystal and attached photomultiplier tube was positioned in the oven and aligned with a 33 mc americium-beryllium -10 mc cesium source and a 4-inch thick polyethylene block was placed in contact with the exterior oven wall.

Fast neutrons moderated by the polyethylene block, were initially monitored by the detector at room temperature (75 degrees Fahrenheit). A count rate spectrum was then obtained by leaving the upper discriminator at the maximum setting and incrementally raising the lower discriminator threshold to higher settings. The oven temperature was then elevated to 140 degrees Fahrenheit and allowed to stabilize for approximately 1/2 hour before the count rate spectrum was again obtained.

The data, plotted on Figure 35, indicate a relatively stable count rate can be obtained throughout the 75 to 140 degree temperature range by setting the lower threshold discriminator midway between zero and the upper limit. This particular discriminator region registered count rate variations which were within or slightly greater than the expected variation due to random nuclear events.

The greatest count rate fluctuation occurred when the lower threshold was set above the mid-point mentioned above. A count rate reduction amounting to approximately 65 percent of the ambient (75 degrees) count rate, appeared to be the maximum variation.

Another count rate spectrum, obtained by monitoring narrow incremental discriminator intervals, disclosed the region of maximum count rate alteration. In Figure 36, it can be observed that the 65 degree rise in temperature actually increased the count rate by about 150 percent for a narrow discriminator interval, slightly greater than the mid-point discriminator setting. As the discriminator interval proceeds upward, the count rate fell approximately 20 percent.

The spectrum shape of Figure 35 and the conclusion derived from Figure 36 appear to indicate that a discriminator setting that includes the upper limit and half of the total spectrum will provide count rate stability for temperatures between 75 to 140 degrees Fahrenheit. The rise and fall of count rates within this region must compensate in some degree for the temperature effects.

The upper half of the discriminator range was, therefore, selected for use by the Autoprobe moisture gage. Other parameters, such as chemical composition error and count rate sensitivity, were considered acceptable for the discriminator limits chosen.

From all indications, the lithium-iodide detector would appear to be the preferable component for the Autoprobe moisture gage. Field evaluation of this detector will establish its operational potential. Provision for field testing both proportional counters and the scintillation detectors is afforded by the basic design of the prototype moisture-density gage. The versatile features of the prototype gage will be discussed in another section of this report.

PRIMARY SHIELDING OF GAMMA EMISSIONS

The backscatter density gage configuration permits detection of gamma emissions traversing the distance between the source and detector within the gage (Figure 37). These emissions are independent of the backscatter emissions attenuated by the material under test. Various lead thicknesses were placed between the source and the detector to attenuate and absorb the undesired emissions and permit evaluation of the number of non-density attenuated emissions.

The detection of nondensity attenuated emissions affects backscatter gage performance by reducing gage sensitivity to changes in density; by increasing the standard count rate; and by affecting the chemical composition error of the gage. To investigate the influence of these three factors, a 10 mc cesium source, contained in a 1 1/2 inch thick lead housing, and a 1 1/2 inch x 1 1/2 inch sodium iodide scintillation detector, housed in a 3/4 inch thick lead housing, were employed as basic backscatter apparatus. Lead thicknesses, placed between the source and detector housings, consisted of either thin lead sheets and/or 8 inch x 4 inch x 2 inch lead blocks. The total thickness of sheets and/or blocks is defined as that of the "primary shielding" used during any given shielding experiment. Evaluation of primary shielding effects was determined by placing the cesium backscatter gage on the six California Standard Density blocks.

The backscatter experimental data indicated that 2 inches of primary shielding increased the gage sensitivity ratio by approximately 9 percent. In other words, the gage's sensitivity to changes in density improved. Gage calibration curves showing the change in sensitivity are plotted on Figure 38. A 2.6 percent ratio increase was noted with 0.25 inches of primary shielding. Doubling the thickness from 0.25 inches to 0.50 inches produced an additional 1.5 percent ratio change. The effect of primary shielding, under the gage configuration employed, is apparently maximized with 2 inches of primary shielding. Lead thicknesses,

in excess of 2 inches resulted in negligible benefits. For example, 2.25 inches produced less than 0.1 percent ratio increase. Therefore, 2 inches appeared to provide optimum benefits.

The position of the primary shielding between the gamma source and detector may have been a decisive factor in the shielding effectiveness. In the backscatter gage experiments the primary shielding was placed in contact with the source housing. Since the source-detector separation used was 11 inches, an air space of approximately 5 inches between the primary shielding and detector housing may have some influence on detector count rates. No attempt was made to determine the influence of positioning the primary shielding equally between the source and detector, or in contact with the detector housing. Recent research has indicated that shielding placement will affect detector counts.

Figure 39 illustrates the average decrease in detector count rate with increasing amounts of primary shielding for the density standards ranging from 95.7 to 173 pcf. These data indicate that primary shielding exerted a greater influence on the three calcareous density standards than did the siliceous standards. The probable cause of the differences in primary shielding effects is the gamma absorption properties of calcium. Since calcium has approximately four times the gamma absorbing capacity of silicon, a lower count rate might be expected from the calcareous standards.

The average percent count rate reduction as a result of primary shielding when using the California density standards is shown on Figure 40. The optimum influence of primary shielding is fairly well defined near the 2-inch mark.

The trend noted with reference to the effects of primary shielding on chemical composition error, was toward a slight enlargement of the error. The cause of the increased error is due, in part,

to the subsequent reduction in the count rate. In the absence of primary shielding, the detection of the undesirable source emissions compensates to some degree, for the loss in detector count rate due to chemical absorption within the test material.

The calibration curves presented on Figure 41 indicate the maximum chemical composition error without primary shielding is 1.5 pcf, at 100 pcf density. The chemical error, between the siliceous and calcareous calibration curves (110 pcf to 140 pcf density), was about 1 pcf or less. This amount of error is relatively slight as the allowable commercial backscatter gage is 4 pcf for densities from 100 pcf to 160 pcf. It, however, increases with the introduction of primary shielding. One-fourth inch of primary shielding appeared to intensify the separation between the calibration curves. Approximately 54 percent of the calibration curve, from 100 to 170 pcf, displayed more than 1 pcf chemical error. Compared to the results without primary shielding, the percentage of the calibration curve displaying more than 1 pcf error increased by approximately 3.5 times. A summary of error percentages is presented in Table 10. With the exception of the 2.25 inch primary shielding condition, primary shielding thicknesses resulted in 42 to 64 percent of the calibration curve displaying chemical error greater than or equal to 1 pcf. The maximum chemical error also changed notably; especially near the 170 pcf density region. The error at 170 pcf changed from 0, without primary shielding, to approximately 2.5 pcf error with 2 inches of primary shielding. The error near the 100 pcf density region stayed relatively constant at about 1.5 pcf. The primary reason for the error fluctuation near the high density region is due to the high degree of gamma attenuation and gamma absorption that occurs.

The cause of the chemical errors encountered with 2.25 inches of primary shielding has not been determined.

Considerations given to the count rates and sensitivity ratio with 2.25 inches of primary shielding appear to follow an experimental trend. Possibly the random effects of the radiation, in addition to possible experimental errors, caused the deviation from the apparent trend in the relationship between primary shielding and chemical composition error.

The backscatter gage-primary shielding experiments indicate that gage sensitivity to changes in density is definitely affected by the presence or absence of primary shielding. The data revealed that a 9 percent increase in sensitivity ratio occurred with the addition of 2 inches of primary shielding. The total lead shielding (source and detector housing thickness plus the primary shielding present during the 2-inch primary condition) amounted to approximately 3.7 inches. This amount absorbed approximately 6000 counts per minute under the test configuration used. According to the gamma absorption chart (Figure 42) for Cesium 137, 3.7 inches or 9.43 cm of lead should absorb 99.996 percent of the undesired source emissions directed towards the detector. This was apparently confirmed by the experiments with primary shielding greater than 2 inches. Chemical composition error, however, seems to increase with the presence of primary shielding. The separation between siliceous and calcareous calibration curves intensified sharply with only 1/4 inch of primary shielding. Additional increments of primary shielding did not appear to widen the separation noticeably. As may be noted in Table 10, the separation occurred over approximately 50 to 64 percent of the calibration curve density range. The optimum change in count rate occurs with approximately 2 inches of primary shielding. Approximately 13 percent of the count rate is eliminated by the 2-inch shielding.

The effects of primary shielding on a backscatter gage consisting of the 10 mc Cesium 137 source and a Geiger-Mueller detector were obtained under laboratory cconditions. For these experiments,

a gamma filter was employed beneath the detector. Therefore, both shielding and filter thicknesses were the experimental variables. A detailed illustration of the test apparatus is shown in Figure 43. The C-3 standard density block was used for this test series.

The test results again indicate that a 2 inch thickness of primary shielding appears to be optimum for both filtered and unfiltered detector conditions. The filtration effect was most noticeable in the count rate when primary shielding was less than 2 inches. Shielding greater than 2 inches dominated the reduction of the count rate, thus filter effectiveness was less noticeable.

A comparison between primary shielding and filter conditions showed a count rate reduction of 83 to 95 counts per minute resulted from filtration alone. The use of filtration plus 2-inch shielding reduced the initial unfiltered and unshielded count rate by 88 percent. Shielding is responsible for approximately 67 percent of the reduction, and 21 percent is attributed to the filter. The filter used for this test series was a 0.042-inch lead sheet placed beneath the Geiger-Mueller detector. Filtration is therefore effective in reducing count rate. This topic will be further discussed where chemical composition error is considered.

Experiments with the Geiger-Mueller-cesium backscatter gage verified primary shielding results obtained with the sodium-iodide scintillation detector. Two inches of primary shielding appeared to be optimum thickness for both the filtered and unfiltered Geiger-Mueller detector. As a rule, diminishing returns resulted from shielding in excess of 2 inches. Only 1 and 5 percent count rate reductions occurred under filtered and unfiltered conditions respectively when the primary shielding was increased to 4 inches.

The importance of primary shielding was clearly indicated by comparing the percent count rate reduction of the Geiger-Mueller and sodium-iodide detectors. As indicated in Table 11, the optimum count rate reduction for the sodium-iodide detector is about 13 percent, whereas the reduction for the Geiger-Mueller detector is nearly 80 percent. These percentages indicate that shielding influence is critical when initial detector count rates are relatively low, as experienced with the Geiger-Mueller detector. The direct radiation being detected is therefore a major portion of the total count rate registered by the Geiger-Mueller detector. On the other hand, the sodium-iodide detector's initial count rate is about 100 times that of the Geiger-Mueller count; thus, the direct radiation detected is a much smaller portion of the total count rate. In this case, the sodium-iodide gage is much less effected by shielding deficiency than the Geiger-Mueller gage. Therefore, count rate and gage sensitivity to changes in density are opposing performance criteria in the Geiger-Mueller gage. For example, if large statistical count rates are desired, gage sensitivity experiences degradation. On the other hand, if sensitivity is desired, count rate statistics must suffer. Thus, primary shielding, in addition to controlling the detection of certain backscattered emissions, has a serious effect on Geiger-Mueller backscatter gages.

The next phase of the primary shielding study sought lead thickness requirements for a 3 mc Cobalt 60 source. The sodium iodide detector was employed for this test series. A need for shielding was quite obvious from the initial unshielded count rate. The multiple energies of cobalt produced extremely high count rates. Two-inch increments of primary shielding were placed between the source and detector. A significant count rate reduction was again noted with 2 inches of primary shielding. Additional shielding, in

excess of 2 inches, produced only minor count rate reduction. The percent count rate reduction experienced during the experiment is contained in Figure 44. Two inches of primary shielding produced approximately 79 percent count rate reduction at 0.230 to 4.53 mev. The 4 and 6-inch thicknesses produced 83 and 84 percent, respectively. Test results suggest that approximately 80 to 85 percent of the count rate is primarily due to the gamma emission traversing the distance between the source and detector. Therefore, 4 inches of primary shielding was selected as the optimum thickness for the cobalt-sodium iodide gage.

In summation, comparison of the cobalt and the cesium-sodium iodide gages has shown that the cobalt source requires about twice the amount of shielding as the cesium source. Two inches of primary shielding reduces the cobalt count rate by 50 percent; 67 percent for cesium. Cobalt's greater range of gamma energies, especially the two predominant energies above 1.0 mev, requires a greater thickness of primary shielding. According to the gamma absorption chart, (Figure 42) 8.1 inches (20.57 cm) of lead will absorb virtually all cobalt emissions. The shielded count rate "I" can be determined by the equation $I = I_o e^{-yx}$ where x is the lead thickness, I_o is the unshielded count rate, and y is the linear absorption coefficient. Figure 42 indicates that the 2-inch (5.08 cm) optimum lead thickness assumed for cesium should absorb approximately 99.5 percent of the gamma emission, whereas the 4-inch (10.16 cm) assumed optimum lead thickness for cobalt should absorb approximately 99.6 percent. Therefore, twice the primary shielding is required to protect the gamma detector when cobalt is used.

The primary shielding effects associated with the cobalt gage's sensitivity and chemical composition were not determined. From the results obtained from the cesium-gage, it was assumed that similar relationships and percentages would exist for the cobalt gage.

The placement of primary shielding adjacent to the surface detector of the transmission gage was also explored. Gage configuration and components used in the transmission experiments are illustrated in Figure 45. Results indicate only a slight reduction in the count rate due to primary shielding, generally less than one percent. Statistically, the reductions fall within the expected variation of the nuclear events. Therefore, the results appear to be inconclusive. The reliability of data was probably biased by the fact that a single Geiger-Mueller detector, possessing limited efficiency, was used as the surface detector. The sodium-iodide detector might have provided larger, statistically reliable, count rates.

These experiments indicated that the primary shielding does not appreciably influence transmission gage performance. A trend noted in the recorded data indicates that primary shielding in excess of 1/2 inch will slightly surpress the count rate. The shielding-count rate relationship is depicted in Figure 46.

The primary shielding experiments have very clearly defined how lead shielding effects the quality of backscatter gage performance. Properly designed gage housing can provide for adequate absorption of undesired emissions. Shielding within the transmission gage was found to be unwarranted. In conclusion, minimums of 2 inches, or 4 inches, of primary shielding will be incorporated in the prototype backscatter gage, to eliminate negative aspects of the particular gamma source selected for use.

CHEMICAL COMPOSITION ERROR

Density gage error induced by chemical composition of the material tested is evidenced by the relative displacement of the calibration curves produced from the siliceous and calcareous density standards. The maximum separation between the two curves for densities ranging from 100 pcf to 140 pcf defines the amount of chemical composition sensitivity of a particular detector. How chemical error was determined is illustrated in Figure 47.

Chemical composition error is a function of the photoelectric photons produced by the chemical constituents of the tested material. A gamma detector that is sensitive to a wide range of low gamma energies in the photoelectric region will infer large separation between the calibration curves.

The elimination of these low energy events recorded by detectors was attempted by mechanical filtration. A series of lead strips of various thicknesses were individually placed between the detector and the test material. These served as filtering devices, preventing the low photoelectric energies from reaching the detector.

The density gage configuration and filter thicknesses were varied to induce optimum gage results. A guide to the various test configurations is provided by Figure 43 and a brief summary of test results is presented in Table 12.

Experiments with a 10 mc Cesium source in the backscatter mode were performed using four different detector types. Those examined included a halogen quenched tube; a tantalum lined tube; a platinum lined tube; and a sodium-iodide scintillation crystal. Source-detector separation and filter thickness were varied in experiments with the Geiger-Mueller tube type detectors. Lead filters were not used in the scintillation crystal tests but low photon energies were controlled by electronic discrimination.

The resultant data did not favor the halogen quenched detector. The one-minute count rate under the shielding and source-detector conditions for the entire test series was below the minimum 10,000 cpm required at 140 pcf density. Negative results with respect to chemical composition error were obtained also. Of seven tests, six showed compositional error in excess of 6 pcf separation between calibration curves. The maximum error recorded equalled 15 pcf.

Sensitivity ratios were above the minimum 1.3 value required by our present backscatter gage specifications. Two test configurations failed to meet this requirement.

Lead filters were found ineffective as a chemical composition control. Large count rate reductions were noted as filter thicknesses were increased.

The tantalum lined Geiger-Mueller tube performed well in 19 separate tests. Sensitivity ratios met or exceeded our backscatter criteria. Count rates were below 10,000 cpm, but the majority were above 1000 cpm, hence superior to the Halogen quenched Geiger-Mueller tube. With the exception of the Halogen quenched detector, all tests performed with a lead filter succeeded in reducing chemical error below the maximum 6 pcf acceptance level. Chemical error was reduced to approximately 1.0 pcf. A combination lead and trass filter lowered chemical error to about 0.5 pcf. These results proved that low gamma energies can be effectively controlled by mechanical filtration.

A like conclusion was drawn from experiments with the platinum lined Geiger-Mueller detector. A 0.042-inch lead filter reduced

chemical error from 8.5 pcf (no filter) to 1.0 pcf. Sensitivity ratios obtained with the platinum lined tube were above the acceptable minimum and count rates exceeded 1000 cpm.

This investigation disclosed that both tantalum and platinum Geiger-Mueller detectors can employ filters to control compositional effects. The count rates show that rare earth metals moderate higher photon energies than a halogen quenched detector.

The sodium-iodide detector was consistently superior to the Geiger-Mueller detectors in controlling compositional error. Two discriminator intervals selected for the backscatter tests limited chemical error to approximately 1.5 pcf. The sensitivity ratios and count rates surpassed all values attained by the Geiger-Mueller detectors. Additional adjustment of the electronic (discriminator interval) filtration might possibly reduce the error to a negligible amount (see Table 13).

The sodium-iodide crystal and the platinum lined detector were examined with the cesium source in the transmission mode. Test results (Table 14) showed that both detectors produced a sensitivity ratio above California's 1.9 minimum requirement for transmission gages. Count rates achieved with the scintillation detector were much higher than those achieved by the platinum lined detector. Comparison of chemical composition errors indicate that both detectors provide error control to approximately the same degree. Under optimum transmission configurations, the platinum lined detector showed 1.0 pcf error. Only two transmission test series were conducted with the scintillation detector. Chemical error was approximately 2 pcf. No attempt was made to adjust the electronic filtration to reduce the chemical effect.

The experiments indicated that control of chemical error can be achieved by adequate mechanical filtering in the case of Geiger-Mueller detectors and by selective adjustment of the electronic discriminator interval for the scintillation detector. Appropriate filtration can reduce chemical error to a minimum in either the backscatter or transmission configuration.

Chemical composition error inherent to moisture gage measurements was explored using a lithium-iodide moisture gage. A 83 mc Americium 241-beryllium neutron source with a 3.68 and 2.50 inch source-detector separation provided the chemical composition data.

Three soil specimens were prepared in the laboratory to represent examples of error prone media that might be encountered in the field. Each was proportioned to contain a thermal neutron absorber or hydrogen rich material. An air-dry quantity of bentonite drilling mud was used as representative of hydrogen rich soils; while a basilite soil, containing 5 percent iron, and a sandy soil, with 2 percent boron were selected as moisture gage error indicators. The basilite soil was in a saturated condition at 17.7 pcf water content.

The initial approach to error control involved selection of the desirable electronic discriminator interval. The upper discriminator was set at the maximum upper limit. Minimum chemical error occurred with the threshold discriminator set near 3.5 volts. The boron rich soil, which absorbs thermal neutrons, produced errors that appeared uncontrollable by the discrimination method. The basilite and bentonite errors appeared to fluctuate with the threshold level. Selection of the discriminator threshold at 3.5 volts provided, therefore, the optimal chemical error control while maintaining an acceptable gage sensitivity to changes in moisture content. The effects of threshold discriminator movement are shown in Figure 48.

Results of these discriminator experiments suggest that the detector of higher neutron energies could possibly further reduce chemical composition errors. A second approach was implemented by mechanical filtration of the attenuated neutrons immediately prior to entry into the lithium-iodide crystal. A cadmium foil 0.01 inches thick was placed beneath the crystal, which in principle should absorb a quantity of the thermal neutrons normally penetrating the crystal. This severely reduced moisture gage sensitivity while slightly increasing composition error values (see Figure 49).

Layers of polyethylene were next experimented with. In this case, layers of polyethylene were placed beneath the crystal. Intermediate neutrons, scattered back to the detector are initially intercepted by the polyethylene. Further neutron attenuation occurs within the polyethylene, (a CH_2 structure), resulting in an increased number of thermal neutrons penetrating the detector. The polyethylene improves intermediate neutron energy detection by attenuating a portion of it to thermal energy, and passing it to the lithium-iodide crystal, which possesses a reaction affinity for thermal neutrons.

Data from this test series indicates a definite reduction of chemical composition error and a substantial increase in moisture sensitivity, as compared to that obtained with the cadmium filter. Under optimum discriminator conditions the boron influence was reduced from 2.4 pcf to 1.8 pcf. Basilite and bentonite errors were also reduced, to none and 0.2 pcf, respectively, (Figure 50). These results occurred with a 0.2188 inch polyethylene layer. A doubling of the layer thickness did not improve performance; on the contrary, a slight decline in performance was noted.

Varied thicknesses of polyethylene in combination with a 0.01 inch cadmium foil proved to be inferior to the 0.2188 inch polyethylene filter alone. Chemical composition error equal to that recorded with the single cadmium filter. The only advantage of the combined filter noted was a 20 percent increase in moisture sensitivity. The polyethylene-cadmium data is depicted in Figure 51.

The moisture gage experiments clearly indicate that the overall performance of the lithium-iodide moisture gage is not enhanced by employing mechanical filters. Electronic energy discrimination appears to adequately control chemical composition error. The mechanical filters employed significantly reduced moisture gage sensitivity while contributing little to the suppression of chemical composition error. The errors and sensitivity of the various energy discriminator methods explored are summarized in Table 15.

Calibration of the lithium-iodide scintilaltion crystal was attempted to permit identification of the neutron energies being detected. Unfortunately, such calibration procedures proved too complex for the laboratory facilities and technology at the investigators disposal. The moisture gage test results reported herein, therefore, are simply statements of where the single-channel analyzer interval was located for the amplification levels held constant by the electronic apparatus.

OPTIMUM GAGE PARAMETERS

This discourse on optimum gage parameters will be divided into two major sections: optimum density gage parameters, and the moisture gage parameters. The density gage section will involve separate reviews of experimental cobalt and cesium gage findings, followed by a comparison and conclusion. A similar review will be presented for the americium-beryllium moisture gage.

The basic criteria employed in evaluating moisture and density gage parameters are derived from Departmental nuclear gage specifications, a complete volume of which are attached as an Appendix. The gage parameters examined were: sensitivity ratio, chemical composition error, and count rate.

The specifications employed at the time of this study require a "backscatter" density gage sensitivity ratio of 1.3 and a transmission gage ratio of 1.9. An improved "backscatter" gage sensitivity ratio that would exceed that standard (1.9) "transmission" sensitivity was a goal of this project. The "transmission" mode has been generally accepted as the more reliable method of determining density with nuclear gages. This method, however, requires disturbance of the in situ material by a well or shaft excavated for the insertion of the gamma source. This disturbance and the time expended in opening a suitable shaft are negative aspects of the "transmision" mode. Therefore, if a "backscatter" gage can provide equivalent sensitivity, the need for "transmission" procedures could be reduced, and possibly eliminated. Accuracy, as well as speed of measurement under field conditions, should be considered as prime requisites in nuclear gage measurements.

Reduction of chemical composition error, defined as the separation in pcf between standard calibration curves, was another goal of this research program. Specifications at the time of this study permitted composition errors of 3 pcf and 4 pcf in the "transmission" and "backscatter" modes, respectively, as specified by six Departmental calibration standards. These limits must apply to gage-indicated densities between 100 pcf and 160 pcf. Reduction of chemical error is desirable.

The detector count rate requirement specifies a minimum 10,000 counts per minute for materials having a density of 140 pcf. The count requirement is based on nuclear emission statistics and on a common soil density encountered in the field. This project's goal in this case was to maintain and extend this count requirement to densities greater than 140 pcf, while improving gage sensitivity ratio and reducing chemical composition error.

Consideration of an optimum backscatter density gage is prefaced with a review of the experimental results involving the 3 mc Cobalt-60 equipment. Primary shielding was a major factor governing the backscatter accuracy. The high initial gamma energies required a minimum of four inches of additional lead shielding to protect the sodium-iodide detector from the influence of the gamma flux surrounding the cobalt source. To ensure essentially total detector shielding, it was found necessary to use six inches of lead, in addition to the lead housings of the source and the detector to eliminate the detection of the nondensity sensitive gamma flux.

The optimum parameters were obtained by varying the source-detector separation; adjusting the detector discriminator interval; and by changing the amount of source collimation. Table 16 summarizes

cobalt gage configurations which met or exceeded the "transmission" gage criteria of a 1.90 sensitivity response ratio.

Three source collimation settings were tested. The center of the cobalt source was collimated to 0.65 inch, 1.0 inch and 2.0 inches above the surface of the test material. The test results indicated that increased collimation up to approximately one inch produced a higher sensitivity ratio but reduced the count rates, and appeared to increase compositional error. At two inches source collimation composition error was increased significantly and the sensitivity response ratio decreased sharply with somewhat inconclusive results. Selection of optimum collimation depends upon the order of parameter priority desired. In this case, minimum chemical composition and count rate were preferred over sensitivity ratio therefore, a slight decrease in sensitivity was accepted in order to attain the other two parameters. Sixty-five hundredths of an inch collimation produced minimum chemical error (0.4 pcf) and provided a maximum count rate (34,800 cpm). One inch collimation increased the sensitivity ratio by approximately five percent above the ratio of 0.65 inches. In each case sensitivity ratios was 1.9, or greater. Chemical error observed at one-inch collimation was 3.5 pcf, and count rate fell to 13,600 cpm. Although both values are within present "backscatter" criteria they fall far behind the values obtained with 0.65 inch source collimation. A test at 2-inch collimation confirmed the conclusions reached by comparing the 0.65 inch and 1.0 inch collimation results. Chemical error continued to increase while the count rate continued to decline.

Various source-detector separation distances were examined. The cobalt gage apparatus with source detector separations in excess of 13 inches produced sensitivity response ratios exceeding the specified transmission mode minimum of 1.90. Increasing the source-detector separation produced higher sensitivity ratios but decreased count rates and enlarged chemical composition error. Composition error however, appears to vary and can be partially controlled by selecting an optimum detector discriminator interval.

The test data show that 13 inches approximates an optimum separation distance for the 3 mc cobalt gage. Fifteen-inch separation gave high sensitivity ratios in excess of 2.0, but chemical errors ranging from 5 to 10 pcf were recorded. The best calibration curves for both separation distances are shown in Figure 52.

The discriminator interval is the most critical gage adjustment made for the backscatter gage. It controls the chemical error magnitude, setting the lower threshold and upper limit of the discriminator. This also influences the sensitivity ratio and count rate, but to a lesser degree than that upon composition error. The minor changes in the sensitivity ratio, at the higher values achieved by the cobalt gage, is less significant than the changes in chemical error reduced by discrimination. However, count rate can be drastically altered by minute discriminator changes.

In general, electronic adjustment of the detector's lower gamma threshold energy and upper energy limit will change the gage parameter as both limits are raised to higher energy values. The cobalt gage sensitivity ratio tends to decrease slightly. The count rate also falls due to the reduction of the higher photon energies by attenuation. Chemical composition error, noted by inspection of the calibration curves, appears to increase due to the detection of higher gamma energies.

The relationship between detector discrimination interval and chemical composition error for the cobalt gage is presented on Figure 53. The significant portion of this relationship concerns the energy interval between 0.14 mev and 0.675 mev. Composition error evidently decreases as the upper discriminator limit is

adjusted to detect higher photon energies (see Case I, Figure 53). The critical adjustment appears to be the lower threshold energy. A slight increase in the lower threshold limit sharply widens the separation between the calibration curves. A change in the threshold from 0.14 mev to 0.16 mev increased the chemical composition error 3.5 times. Lowering the threshold limit was not attempted, since the inclusion of extremely low energies in the photoelectric region would have probably increased composition error.

The higher discriminator limit induces various effects that decrease or increase chemical error, depending upon the lower threshold energy. At the 0.14 mev threshold, increasing the upper limit from 0.435 mev to 0.675 mev reduced chemical error (see Case II, Figure 53). Further extension of the upper limit, (from 0.675 mev to 0.90 mev) increased chemical error by approximately 5 times.

Case III, Figure 53, indicates the upper limit effects error with a change in threshold from 0.14 mev to 0.16 mev. Error remained relatively stable as the upper limit was raised from 0.435 mev to 0.90 mev, ranging from 1.8 pcf to 2.5 pcf.

Under another gage configuration (presented in Figure 54), the relationship between chemical error and discriminator limit denotes the crucial effect that the threshold energy has on the amount of error resulting from a change in the upper limit.

It is evident that proper discriminator interval selection is vital when considering composition error. The limited data suggests that the 0.14 mev threshold energy is the most desirable for minimizing gage error when a wide discriminator interval is employed.

In summation, the optimum cobalt gage parameters determined were: 1.9 sensitivity ratio; 0.4 pcf chemical composition error; and 34,800 cpm at 140 pcf density. These values surpass the established "backscatter" gage specifications as well as most "transmission" gage criteria. The cobalt gage, under the optimum configuration

achieved in the laboratory, improved present "backscatter" gage standards by 47 percent in sensitivity ratio, by 90 percent in chemical composition, and secured 3.5 times the count rate required from a 140 pcf test material.

This study has indicated that the combined interaction of source-detector separation, collimation, and detector discrimination produces beneficial changes in all three governing gage parameters. Thus, the optimum cobalt "backscatter" gage configuration derived in the laboratory requires 6 inches of primary shielding; a 13 inch separation between source and detector; 0.65 inch source collimation; and detector discrimination between 0.14 mev and 0.675 mev.

The investigator's experience with the 10 mc Cesium-137 gage indicated that at least two inches of additional lead shielding between source and detector was required to eliminate the detrimental detection of the gamma flux surrounding the source. The laboratory test procedures and objectives for the cesium gage were identical to the program conducted with the cobalt gage. As stated previously, the objective was to exceed present back-scatter gage specifications, therefore several cesium gage geometries were investigated. Gage configurations having 10 and 11-inch source-detector separation, and source collimations, varying from 0.25 to 0.65 inches were examined. Threshold and upper discriminator settings were also varied between 0.127 to 0.738 mev.

Cesium test results revealed that the gage geometry and discrimination criteria closely resembled those developed from the cobalt gage studies. Individual adjustment of gage geometry or of a component will not improve all the gage parameters simultaneously. A combination of gage adjustments is required for optimum gage performance. Those cesium gage configurations that met or exceeded the backscatter specifications are summarized in Table 17.

Quite clearly, the 11-inch source-detector separation produced the highest sensitivity ratios. Values exceeding 2.0 were recorded. Sensitivity ratios slightly greater than 1.9 were obtained with 10-inch separation. The detector discriminator interval controlled chemical composition error. Error fluctuations resulting from varying the threshold and upper discriminator limits for the 11-inch source-detector separation are shown on Figure 55.

There would appear to be two threshold energies that minimize error as the upper limit was adjusted to a higher energy. Setting the threshold energy at 0.127 mev and adjusting the upper discriminator from 0.233 to 0.338 mev reduced chemical composition error from 2.4 pcf to 1.9 pcf. Further adjustment of the upper limit (from 0.338 mev to 0.420 mev) did not reduce error.

The second threshold energy worthy of note is 0.170 mev. Changing the upper limit from 0.215 to 0.355 reduced the chemical error from 2.5 pcf to 1.5 pcf, or 40 percent. Adjusting the upper limit to 0.630 mev slightly increased chemical error. When the upper limit was set to 0.738 mev, which includes all initial cesium energies, chemical error at approximately 1.7 pcf was apparent. Therefore, both threshold energies appear factors in chemical composition error magnitude when the discriminator interval widens to include initial or slightly moderated cesium energies. Minimum chemical error was associated with two additional threshold energies yet placed restrictions on the upper discriminator energy. A 0.150 mev threshold and 0.420 mev upper limit showed a minimum chemical error of 1.5 pcf. Adjusting the upper limit to include the highest initial cesium energy (0.662 mev), doubled chemical error (3 pcf). An exceptionally high threshold energy (0.215 mev) also displayed the 1.5 pcf minimum error, but placed strict limitations on the upper discriminator setting. In this case, the upper limit was restricted to 0.420 mev. Figure 55 shows the resulting 0.5 pcf error increase.

A similar inspection of the discriminator interval and chemical error relationship was conducted with the cesium gage at 10-inch source-detector separation. The results are plotted on Figure 56. Again the detector threshold energy appears to be the basic controller of chemical composition error. As was discovered for the 11-inch source-detector separation, the 0.127 mev threshold proved desirable as the upper limit was adjusted to 0.420 mev. In this case the widest discriminator interval showed a relatively small (0.9 pcf) error. A 0.170 mev threshold showed that extreme limitation had to be placed on the upper limit. A broad discriminator interval, in this case, produced approximately six times the chemical error created at the threshold interval between 0.170 and 0.215 mev. Although the discriminator interval is relatively narrow (.045 mev) the chemical error was extremely small (0.5 pcf).

The experiments have shown that the threshold energy is a vital factor in chemical composition error control. A cesium gage threshold between 0.127 mev and 0.170 mev provides minimal chemical error with proper selection of the upper discriminator energy, at 10 or 11-inch source-detector separation. The amount of error reduction tends to lessen as source-detector separation is increased from 10 to 11 inches. The best cobalt gage threshold energy was approximately 0.141 mev. Therefore, it seems logical to assume that a threshold energy between 0.13 mev and 0.17 mev, independent of the gamma source being used, would be appropriate.

To conclude this discussion on the 10 mc cesium gage, one must evaluate the three basic gage parameters, and how each relates to the others. It has been established that the 11-inch source-detector separation provided a greater sensitivity ratio than the 10-inch. It was also found that a broader discriminator interval at the 10-inch separation yields less chemical composition error than the 11-inch separation. The experiments also confirmed the assumption that count rates decline with greater separation.

The most significant discovery concerns the discriminator threshold energy. Threshold energies between 0.13 mev and 0.17 mev seem to minimize chemical composition error. These favorable threshold energies appear to be independent of either the cesium or cobalt source.

Judgment is an essential factor in selection of the order of importance placed on gage parameters. Presently, it is felt that chemical composition should be the prime consideration, as this form of error is not inherent in the gage, but rather a function of the soil medium being tested. This error can be controlled and minimized by proper setting of the detector discriminator. Secondly, experiments have shown the cesium "backscatter" gage can meet or exceed the sensitivity ratio requirements now achieved by "transmission" techniques. Thus, the experimental cesium "backscatter" configuration has equalled or exceeded its "transmission" counterpart, hereto been recognized as the most reliable nuclear density gage technique.

The relatively small difference in sensitivity ratios recorded for 10- and 11-inch separations signifies only minor consequences from a calibration curve standpoint. Both separations provided sensitivity ratios greater than 1.9. The count rates interpolated from the calibration curves at 140 pcf density are within or in excess of the 10,000 cpm statistical boundary required by present "backscatter" gage specifications. The 10-inch separation, however, will provide a satisfactory count rate and less chemical error than the 11-inch.

Therefore, it may be concluded from limited test results, that the 10 mc cesium "backscatter" gage should be operated with 10-inch separation, 0.65-inch source collimation, 0.25-inch detector collimation, and discriminator interval set between 0.127 mev and 0.420 mev. A 4-inch minimum thickness of lead shielding must be provided between the 10 mc cesium source and the sodium-iodide scintillation crystal.

These data from the cesium and cobalt density gages tested have enabled tentative selection of gamma source and gage configurations to be used in the prototype nuclear density gage. Final selection will depend on many factors related to field use and evaluation. The cesium and cobalt gages each possess desirable parameters under laboratory conditions. The cesium and cobalt gages embody comparable backscatter parameter specifications, therefore an appropriate gamma source was selected on the basis of discrimination width and shielding requirements. Cesium requires a narrower discriminator interval to maintain a minimum chemical composition error than the cobalt gage. Monitoring a narrow interval might possibly be advantageous when considering the wide range of field soils, as compared to the limited chemical effects displayed by the silicon and calcium standards used by this department. As cobalt requires a greater degree of shielding, the cesium gage seems most desirable. Therefore, under laboratory conditions the cesium gage with 10 mc of Cesium-137 was selected for the prototype.

This investigation has shown that both the cesium and cobalt backscatter gages can be manipulated to meet or exceed our present specifications for a "transmission" gage. It is thus established that the "backscatter" technique can be adopted as an accurate and reliable test method, equivalent to the "transmission" method, now used as a standard field testing method.

This investigation has indicated that a review of present density gage specifications is needed to re-evaluate and redefine acceptance criteria for portable nuclear gage performance. Determinations concerning acceptable limits for each gage parameter can realistically be made only after field test data from the prototype gage have been analyzed. The order of priority given to each gage parameter must also be defined. This research has revealed that the improvement of one gage parameter will usually degrade one or more of the other gage parameters. Therefore, some specification should be provided to place each gage parameter in proper perspective.

PROTOTYPE NUCLEAR MOISTURE-DENSITY GAGE

These experimental findings have culminated in the assembly of an apparatus for determining moisture and density by the nuclear "backscatter" gage technique. This prototype "backscatter" gage was designed and constructed primarily to field evaluate the gage improvements developed in the laboratory.

The prototype gage, referred to as the "Autoprobe", is not restricted to size and weight requirements specified for the portable gages now being used by the California Department of Transportation. The Department's present design concept is to provide a completely automated vehicle unit. This unit will allow the gage operator to: position the Autoprobe over a field test site; lower the gage to the test material; seat the gage on the test surface; record moisture and density readings; retract the autoprobe from the test site; and move to another site, without need for any manual or cumbersome gage preparations. The autoprobe operator will control the entire test procedure from within the vehicle unit. All mechanical and electronic monitoring controls are arranged and installed in the vehicle cab, adjacent to the autoprobe operator. The Autoprobe and vehicle are depicted in Photos 1 through 5.

The Autoprobe and vehicle were designed to adapt to normal field test sites, such as embankment fills and subgrades upon which minimal or no site preparation is required. A device similar to a universal joint enables the Autoprobe to be seated on horizontal as well as inclined planes.

The Autoprobe's versatile design and flexibility will permit changes in gage components and "backscatter" gage geometry (source-detector separation). Thus the gage can be modified for field conditions.

The support vehicle, for the Autoprobe is a 3/4 ton, 4-wheel drive pickup truck. The Autoprobe is mounted and housed behind the rear axle with a hydraulic ram system that lowers and retracts the gage. An air conditioning unit was installed in the truck cab to ensure proper performance of the electronic equipment during summer construction periods.

All electronic components mounted within the truck are modular units conforming to dimensions recommended by the Atomic Energy Commission. A list of general specifications are included later in this section. The most important of these pertains to temperature limitations. Long-term instrument drift, system noise level, and count rate variations should reflect "state-of-the-art" standards.

Other factors considered in the Autoprobe design were vibration, shock, dust, and heat dissipation. Most electronic components within the gage should be capable of sustaining vibration and shock during transit movement. The Autoprobe housing together with its rubber-mounted guide device will prevent serious shock and reduce vibrations to within tolerable limits. Dust intrusion will be controlled by appropriate seals and atmospheric condensation by desiccators. Heat dissipation is controlled by a heat reflecting and insulated housing mounted over the Autoprobe and hydraulic system. Should this housing prove unsatisfactory, a forced air cooling system connected to the vehicle air conditioning may be feasible.

The gage has the capacity to house varied detectors and radio-isotopes. Lead shielding can be adjusted to satisfy radiological health standards. Either scintillation or gas tube type moisture detectors can be easily interchanged, and electronic detector components can be contained inside the Autoprobe. No provisions have been included in the gage design to accommodate Geiger-Mueller detectors. A 2 inch x 2 inch sodium-iodide scintillation detector will be used exclusively for gamma detection. It is anticipated

that the performance of the scintillation crystal will be satisfactory. However, its replacement with a Geiger-Mueller type detector would require disassembly and modification of the Autoprobe. A single-channel analyzer has been included to provide energy discrimination capabilities for the scintillation detector.

As mentioned previously, a 3.5 inch high radioisotope housing will permit adequate depth for changing collimation heights. Detector collimation will be available to similar depths. Adjustments can be made with the Autoprobe to vary the source-detector separation. The Autoprobe was assembled in two parts, with sliding channel and fasteners on the longitudinal sides to facilitate adjustment. The bottom plate of the Autoprobe, which contacts the test surface, acts as a source-detector filter. Therefore, the bottom was made removable so various metals and thicknesses could be substituted if required.

The fabrication and assembly of the Autoprobe housing, hydraulic system, and control devices were accomplished by the Department's laboratory and shop personnel. Preliminary laboratory testing of the Autoprobe was conducted on the Department's series of density standards and the optimum calibration curve and electronic settings were chosen before installing the Autoprobe in the vehicle.

A trial program of field testing and gage evaluation was conducted at various highway construction sites. Subjects of the tests included embankment fills, subgrades, subbases, cement treated base, lime stabilized base, concrete pavement, and asphalt pavement. A wide range of soil types and surface textures were tested to evaluate the Autoprobe error involved by varied soil and texture conditions. Similar procedures were performed with a portable gage on the Autoprobe test sites. Both "backscatter" and "transmission" tests were conducted with the portable gage. The resulting Autoprobe and portable gage data were then subjected to satistical analysis to determine the relative performances of the two gages. This analysis is presented in the following sections. Should the Autoprobe prove to be successful and superior, recommendations for adopting and up-dating present nuclear gage specification will be set forth.

To summarize the discussion of the vehicle-Autoprobe unit, emphasis has been placed on designing a nuclear moisture-density gage which will be functional as well as being versatile from a modification standpoint. Unforeseen difficulties will inevitably arise during the field evaluation, which we hope can be overcome by the Autoprobe's flexible design. Finally, our goal is to apply our findings as new "state-of-the-art" criteria for nuclear gages.

Present Autoprobe Specifications

1. Duplex Source: 10 mc Cesium 137 Gamma Source
   33 mc Americium 241-Beryllium Neutron Source

2. Duplex Source Collimation: 0.75 inches to center of source

3. Second Neutron Source: 50 mc Americium 241-Beryllium

4. Second Neutron Source Collimation: 0.75 inches to center of source

5. Gamma Detector: 2 inch x 2 inch Sodium-Iodide Scintillation Crystal with RCA 6342A photomultiplier tube and preamplifier

6. Gamma detector Collimation: 0.5 inches to bottom of crystal

7. Gamma Source-Detector Separation: 10.0 inches center to center

8. Thermal Neutron Detector: 1 1/2 inch x 3 mm Lithium-Iodide Scintillation cyrstal with RCA 6342A photomultiplier tube and preamplifier

9. Thermal Neutron Detector Collimation: 0.375 inches to bottom of crystal

10. Neutron Source-Detector Separation:

    a. Duplex Source - 3.68 inches center to center
    b. 50 mc Source - 2.50 inches center to center

11. Gamma Discriminator Setting: 0.12 mev to 0.55 mev

12. Neutron Discriminator Setting: Undetermined but can be set experimentally

13. Moisture-Density Count Period: 40 seconds

14. A minimum of four inches of lead shielding between Gamma Source and Detector

15. Gage Bottom Thickness: 0.0625 inch Stainless Steel

16. Source and Detector Bottom Protrusions: 0.3125 inches

<u>Present Autoprobe Performance Specifications</u>

1. Backscatter Density Gage Sensitivity: 1.88

2. Average Density Gage Error Due to Chemical Composition: 1.0 pcf over a density range of 100 to 160 pounds per cubic foot.

3. Backscatter Moisture Gage Sensitivity: 2.84

4. Average Moisture Gage Error due to Chemical Composition: not greater than 1.1 pcf over a range of 100 to 160 lbs. per cubic foot.

5. Average Density Gage Error due to 0.2 inch Air-Gap: not to exceed 6.6 pcf

6. Average Moisture Gage Error due to 0.2 inch Air-Gap: not to exceed 0.8 pcf

7. Standard (Magnesium and Polyethylene) Density Block Count Rate: 1,680 counts per second

8. Standard (Magnesium-Polyethylene) Moisture Block Count Rate: 405 counts per second.

Field Density Test Procedure

A commercial transmission-backscatter gage was selected for use with the Autoprobe during the field trials. The commercial gage served as a means of comparing indicated densities and relative gage performance.

The Autoprobe and commercial transmission-backscatter gages were density-calibrated in the laboratory, using the three calcareous and three silicious density standards fabricated by this Department. The count rate data obtained from each density standard are then related to a chosen count rate density standard that accompanies the gage during field operations. The Autoprobe derives its standard count rate from a magnesium density standard; and the commercial gage count is obtained on the gage storage container which serves as a count rate standard. Both count standards are used periodically during gage operations to verify or adjust gage performance.

A count ratio is calculated by dividing the density measurement count rate by the standard count rate. Thus, the relationship between count ratio and gage indicated density is established. A computer program was developed to calculate and tabulate a

count ratio for each 0.2 pcf change in density. The program ratios provide a density calibration over a range from 90 pcf to 170 pcf. The tabulation, or computer output, is employed by the gage operator to determine the gage indicated density.

The Autoprobe probe assembly was fastened to the vehicle's hydraulic lift which positions the gage on the test surface. The power supply and electronic monitoring system were located in cab of the vehicle. Prior to the field evaluation, a density calibration check was made to determine possible performance deficiencies caused by the vehicle. As no significant change in the density calibration was noted, the mobile unit was qualified for field operations.

Presently, the transmission mode is considered to be the most accurate and reliable nuclear density test method. The transmission technique, which requires insertion of the gamma source into the test material, has proven to be less sensitive to surface effects and more sensitive to density changes. It also monitors a larger volume of compacted materials, due to gage configuration. The use of the eight-inch transmission mode as a standard field testing procedure (in effect since April 1972) is described by California Test Method 231. Therefore, both the Autoprobe and the commercial backscatter gage will be compared to the transmission gage.

Preliminary field trials sought to substantiate the optimum gage parameters incorporated in the Autoprobe, and determine the degree of equality between the transmission gage and the Autoprobe. If equality is established by the field tests, the improved backscatter performance, exemplified by the Autoprobe, can be proposed as an alternative nuclear test method. A major advantage of the backscatter method is the non-destructive nature of the test. The transmission method requires a shaft, perpendicular to the test site surface. This could disturb the surrounding in situ state of the test material. Shafts in cohesionless

materials are frequently difficult to form and subject to cave-in. Dense materials, such as aggregate soils, also impose problems; drilling or coring is often required, and much time can be expended in preparing the transmission shaft. If the improved backscatter gage proves to be acceptable, the Autoprobe could conceivably supplant the transmission gage.

The variety of highway embankment and pavement structural section materials tested during the initial field trials covered a wide range. The nuclear gages were used on seven different materials and soil types, some of which were combinations of two or more soil types.

The test site selection and spacing of the nuclear density gage measurements were random to the extent that they were generally spaced 30 feet longitudinally and staggered about 12 feet transversely. The number of test sites, for any given test material was limited to a consecutive sequence of four sites. Efforts were made to visually select typical segments of the compacted material. The Autoprobe and commercial gage were operated simultaneously on adjacent test sites. A 30-foot longitudinal separation was assumed sufficient to eliminate any interaction between the gages that might influence the detector count rate.

Two test surface conditions were imposed on the backscatter gages. Initially, the gage was placed on the in situ test site, with no preparation of the existing contact area. This is referred to as the "unprepared" surface condition. If the contact area was visually found not to provide a good seating contact with the test material a thin layer of test material fines passing the No. 20 sieve was placed uniformly on the in situ surface before obtaining another series of count rates. This surface condition is called the "prepared" condition.

Transmission gage count rates were obtained following the completion of all backscatter measurements. The body of the transmission gage was placed on an unprepared surface and the gamma source rod inserted in the shaft with care. Care was taken to ensure proper contact between the rod and shaft surface closest to the gage detector.

Four one minute counts were obtained from the commercial gage in the unprepared and/or prepared backscatter modes and transmission mode. Four 40-second counts were obtained from the Autoprobe under unprepared and/or prepared conditions. Conversion of the gage count rate to an indicated density was accomplished by determining the count ratio, as earlier defined; then interpolating the corresponding density from the gage's computer ratio-density tabulation. The four test sites provided a sample of 16 density measurements from each gage and surface condition. The sample mean density ($\bar{x}$) and sample standard deviation (s) were calculated and tabulated for the analysis portion of the field data.

BACKSCATTER GAGE-TEST SURFACE CONTACT AREA

Following analysis of the initial Autoprobe field test data, and discussion with the Autoprobe operators, it was decided that some alterations were required in the Autoprobe to accommodate the wide variety of test surface conditions encountered in the field. As the gage bottom area is relatively large compared to the area of the source collimator and detector collimator openings, small ridges or valleys on the tested surfaces can prevent intimate contact between the two gage components and the test material.

Proper seating of gages on non-uniform surfaces has presented problems to operators using the backscatter technique in the past. Portable gage operators have prepared the test surface by adding a thin layer of native materials to fill irregularities and voids of the contact area. The native materials were first sieved through a No. 4 screen, then spread evenly over the surface and lightly compacted into place. This layer provided a level plane for gage seating. Such method, however, introduced a number of variables which significantly influenced gage measurements. For example, the thickness of layer and degree of compaction was dependent solely upon the judgment of the individual gage operator. The preparation of each test site could result in wide density value variations. Currently available backscatter gages are extremely sensitive to the condition of the surface of the test material. An over-thick layer of sieved material would induce a reduction in measured density, due to the difference in compactive effort. On the other hand, a deficient layer may result in an air gap beneath the source and detector. As gamma rays would migrate from the source to the detector via the air gap the measured density would again indicate a lower value. The nuclear test method approved by this department has excluded the backscatter technique because of the adverse influence of these test surface effects.

The investigators approach to resolving, or mitigating, the backscatter seating problem involved reducing the contact area required. That is to say, they sought to enhance intimate contact of the gamma source collimator and detector with the test material through eliminating, or at least minimizing the balance of the gage bottom area. Intuitively it was reasoned that reduction of the contact area would reduce the probability of air gaps, and concomitantly, reduce the need for surface preparation.

An innovative feature of the Autoprobe, felt to be improvement over the conventional commercial backscatter gage, is the reduced bottom surface area of the gage contacting the material to be tested. Rather than being flat, as with most gages, the Autoprobe bottom has 0.3125-inch thick protrusions directly beneath the gamma detector and the gamma source, 4.625 inches square. The advantage of the small contact areas, as provided on the Autoprobe, is that surface irregularities such as small rocks, crowns, depressions and bumps can be straddled and effective seating simplified. This reduces the amount of density-sensitive gamma emissions streaming along the bottom of the gage to the detector (see Figure 57). Such protrusions, or pads, have been employed on early model commercial gages.

A series of laboratory trials was conducted to determine how the protrusions would affect the density gage sensitivity, chemical composition error, and count rate performance of the Autoprobe. This approach attempted to compare these gage parameters before and after the protrusion pads were installed beneath the gamma source and sodium-iodide scintillation detector. The "before" or initial contact pads were 4.625 inches square stainless steel plates, which protruded 0.0625 inches from the gage bottom. The protrusions to be examined placed the source and detector shields 0.3125 inches below the gage bottom,

and employed the same stainless steel plates mentioned above. The new pad arrangement did not change the basic source-detector collimations. Unfortunately, two gage modifications were being examined simultaneously. The combined influences of source collimator shape and protrusion pad thickness were recorded in the experiments. The detector collimation was unchanged; however, the source collimator was lowered slightly, due to the collimator design. Our experimental hypothesis was to verify that the increased pad thickness will not reduce the backscatter gage performance of the Autoprobe.

The six density standards employed in other phases of this research were used to obtain calibration curves for each of the two gage conditions. In order to simulate the poorest possible seating condition likely to be encountered in the field, the entire gage body was elevated above the surface of the standards with small brass plates under each corner of the gage bottom. This introduced air gaps beneath the source and detector of 0.0625 and 0.197 inch thickness, respectively. In another experiment, aluminum plates were placed in the air gap between the source and detector pads while the gage was seated on the surface of the standards to determine the amount of gamma migration through the air-gap.

The changes in protrusion pad thickness and source collimator cavity shape resulted in marked differences in density gage sensitivity, chemical composition effects and error, due to backscatter gage seating or air-gap. It was indicated that the two modifications reduced gage sensitivity by 3.5 percent, when gage calibration curves from the "before" and "after" modification were compared. This decline was noted when the gage was properly seated on the standards, (flush condition). Compared with the calibration curves for the 0.197-inch air-gap condition, the modifications were responsible for a 7.7 percent decline. These results were discouraging; however, the change recorded for the

chemical composition error was rewarding. The chemical composition error resulting from the modifications did not exceed 2.5 pcf, for both the flush and air-gap conditions. The error increased by approximately 0.5 pcf due to the air-gap. With the gage in the premodified state, chemical error increased from 3.0 pcf, under the flush condition, to 5.25 pcf due to the 0.197-inch air-gap condition. The calibration curves obtained by the experiments are shown on Figure 58.

Comparison of the gage calibration curves indicates that the average error of the calibration line, due to the air-gap was reduced by approximately 27 percent, or 3 pcf. The value of the protrusions and source collimator is therefore a priority selection between gage sensitivity, and the chemical composition-calibration line errors caused by air-gaps frequently encountered in the field. In view of the wide variation in field conditions, it was the opinion of the researchers that the sacrifice in the gage sensitivity was outweighed by the progress made towards ensuring a reduction of error magnitude when an air-gap condition is encountered.

The reduction in sensitivity is probably attributable in greater part to the streaming of gamma emissions in the air-gap between the source and detector when the gage is placed in the flush condition, as shown on Figure 57. When lead sheets were inserted into the air-gap space (to determine the gamma counts originating from this area) approximately 1,000 counts were recorded during a 40-second count period. Evidently the protrusion height is detrimental to gage sensitivity, as mentioned earlier. Perhaps the air-gap counts resulted from the aluminum spacers employed to increase the pad depth. Holes were machined in the spacers to allow the source and detector housing to maintain the collimation heights relative to the test surface. Since the source and detector housings drop below the main portion of the primary shielding within the gage body, the amount of lead surrounding the source and detector, in the area of the protrusions, is restricted to

the housing thickness only. Due to the size of the source cavity and detector diameter, the housing thickness is insufficient to absorb all of the gamma emissions penetrating their walls.

The aluminum spacers will be replaced with tungsten spacers in the near future. Hopefully, the high density tungsten will resolve the problem of sensitivity loss, while maintaining the favorable results related to air-gap and chemical error.

ANALYSIS OF FIELD DATA

The density data gathered during the Autoprobe field trials were evaluated statistically to test the assumption that the Autoprobe is superior to a commercial backscatter density gage. Several comparisons were made between the Autoprobe and a commercial gage selected for the field trials. The commercial gage employed was a relatively new product of an established gage manufacturer.

The performances of three nuclear density gages were statistically compared under the assumption that the data from each gage conformed to its normal distribution characteristics. The commercial gage was operated in the transmission configuration to provide the data standards used for the statistical analysis. Transmission gage performance is presently accepted as the most accurate and reliable nuclear gage density method. Several reasons, stated by this Department, justify the adoption of the transmission method. The same commercial gage was also used in the backscatter configuration, under two field conditions. To determine how irregular test surfaces beneath the backscatter gage influence gage performance, a density was first obtained without disturbing the surface texture. Secondly, a layer of the fine-grained test soil was placed on the irregular surface to create a smooth, uniform contact surface for the backscatter gage. These two test conditions, used with both the commercial and Autoprobe backscatter gage, will be referred to in the discussion as the unprepared and prepared test conditions.

The entire analysis was made to determine how the Autoprobe density measurements compared with measurements obtained from the commercial transmission-backscatter gage. The mean density ($\bar{x}$) and standard deviation (s) obtained by each gage were calculated using a normal distribution procedure. A graphical presentation of the calculated values provided an efficient means of evaluating

and comparing the performance of each gage. Figure 59 shows the assumed normal distribution curves of the gage indicated densities obtained from a silty-sand embankment material. The ordinate represents the percent probability that the gage-indicated density will be a particular value. To begin the analysis, the density distribution curve for the transmission gage is drawn and ± one standard deviation located. The area under the curve between ± one standard deviation assumes that 68.26 percent of all transmission gage measurement will be within these limits. The density distributions of the Autoprobe and commercial backscatter gage are then compared to the probability that their indicated density will be within the limits set by the transmission gage. Thus, the backscatter gage possessing the greatest probability of indicating the same density as the transmission gage is considered to be the better gage.

With this criterion established, Figure 59 shows that the Autoprobe has a much greater probability of indicating the transmission gage density than the commercial gage. In this case, the Autoprobe probability is between 18 and 24 percent compared to 2 and 5 percent for the commercial backscatter gage. Surface preparation increased the probability and moved the Autoprobes mean indicated density toward the transmission value. The commercial gage did not respond in the same manner. Although the mean density was moved favorably, the probability decreased by 3 percent, which was primarily due to the smaller standard deviation on the prepared surface. A similar analysis was applied to each individual material tested in the field.

A complete review of all the distribution curves for all test materials indicate that the Autoprobe is not equivalent to the performance of the transmission gage. The analysis, however, did verify the advantages of the backscatter gage improvements built into the Autoprobe. All the mean densities and standard

deviations are summarized on Table 18 and the percent probability of coincident measurements between gages are shown on Table 19. The data provided by these tables, together with coincident probability, indicate that the Autoprobe's performance is superior to the commercial backscatter gage. The Autoprobe appears less sensitive to test surface irregularities than the commercial gage; this is probably the primary factor in Autoprobe superiority.

Preparation of the backscatter gage test surface has a definite effect on gage performance. Both backscatter gages appear to be sensitive to surface affects. Surface preparation decreased the differences in the measured mean density and standard deviation between both backscatter gages and the 8-inch transmission gage. These reductions were approximately 27 and 58 percent, respectively. The commercial backscatter gage, however, showed an extreme change in differences due to surface preparation. This segment of the analysis permits the conclusion that the Autoprobe without surface preparation is nearly equivalent to the commercial backscatter gage with prepared surface.

The third segment of the analysis examined the relationship between the indicated density distributions of the backscatter gages and transmission gage. The values were derived from averaging the probabilities obtained from all test material distribution curves. This analysis compared the probability that each backscatter gage will yield a density within $\pm$ one standard deviation of the mean transmission gage density. As stated previously, the probabilities attained by the backscatter gages on the various materials tested are available on Table 19. In general, the average probability for both backscatter gages were not exceptionally high; however, the probabilities did, in some cases, exceed 80 percent. Average Autoprobe probabilities, as listed in Table 20, ranged from 33 to 36 percent for unprepared

and prepared surfaces, respectively. The commercial backscatter gage indicated a range between 11 and 20 percent for the same surface conditions. Therefore, Autoprobe displayed a 16 to 22 percent improvement in backscatter gage probability, which represents nearly double the backscatter probability of producing the same density as the transmission gage. In reference to the test surface preparation effects, an average 7 percent elevation of the probability was noted.

These analyses also included an attempt to classify backscatter performance based on soil or construction material type tested for in situ density. Each soil was classified according to grain size, which also relates to the unprepared surface conditions experienced by the backscatter gages.

Gravel and aggregate, typical of most subbase materials, are classified as rough and irregular surfaces. Sands, silts, and a foundary slag are defined as materials with loose, irregular, or smooth surfaces. Rolled surfaces, such as Asphalt Concrete (AC), Cement Treated Base (CTB), and the clay soils, in addition to the borate soils are considered as smooth surfaced materials. The portland cement concrete (PCC) pavement encountered was classified separately, due to the uniformity of the road surface texture. The broomed-finish, longitudinal to the travelled way, provided an excellent surface for comparing textural influences.

Analogous to surface texture classification, the in situ materials were classified according to matrix particle size. In most instances, surface texture is dependent on particle size. The exception in this approach was noted for asphalt concrete surfaces. The asphalt matrix, being a crushed and rounded aggregate with the bituminous binder, presented a smooth uniform test surface for the backscatter gage.

The materials or soil types were grouped according to particle size. Five types were established and gage performance trends noted by comparing the absolute difference between mean density and standard deviation or spread in gage measurements. The backscatter gages are compared with the transmission gage and core sample data.

The results of the particle size analysis are listed in Table 21. A significant change occurred in the differences between gage standard deviations of the commercial and Autoprobe backscatter gages. These results indicate that the detection of random radiation scattered between the test surface-gage interface are effectively impaired by test surface preparation prior to taking gage measurements. Reference to the standard deviation differences associated with the backscatter-transmission and core data leads to a similar conclusion.

The influence of test surface preparation on the mean density differences was also apparent. The differences recorded between the backscatter gages did not vary substantially from the unprepared surface data, which implies that the same degree of influence was experienced by both backscatter gages.

The comparison between the transmission and backscatter differences also demonstrates how surface texture influences gage performance. The absolute differences of mean density and standard deviation between the commercial and transmission gage were significantly reduced by surface preparation. Differences noted between the Autoprobe and transmission gage were not as pronounced, but surface preparation did produce small reductions. It was obvious that the Autoprobe possesses superior qualities which tend to make it less sensitive to surface produced errors.

The calculated differences listed in Table 21 were used to test the data for visible trends. A series of regression lines were computed and the best regression equation chosen to represent the data trend. According to the results obtained by computer program, the relationship between the mean density and standard deviation differences and soil type, as presented by Table 21, was not confirmed conclusively. A consistency, however, was noted between the parameter differences. Equations derived from the standard deviation differences all indicate a best fit regression having the form $Y = A + B/X$, where Y signifies the difference between two gage deviations, and X represents the soil type. The index of determination, for the regression lines of the standard deviation differences, averaged 0.33, which is very poor. All the regression fits for the differences in mean density resembled a straight line equation of the form $Y = A + BX$, and possessed an average determination index of 0.62. Therefore, it seems that the density differences do indicate some influence due to the soil type divisions assumed. The regression plots of the computer output are shown on Figure 60 and Figure 61.

One soil type, however, seems to produce a sizeable difference due to a factor other than the test surface conditions. The distinct differences recorded between the backscatter gages and the transmission parameters showed relatively high values for materials with fine particle size and relatively smooth surfaces. Due to the absence of additional evidence, the hypothesis for this occurrence is probably chemical in nature. Cations bound to the clay lattice are the possible cause for these high differences.

The most noticeable differences between transmission and backscatter densities did occur on the borate soil. The differences ranged from 19 to 24 pcf and 2 to 13 pcf relative to the 8-inch and 4-inch transmission depths, respectively. These differentials

seemed significant since they occurred on smooth soil surfaces, which should have reduced most surface effects. The borate content is assumed to be responsible for most gage errors. The test results revealed that the count rates increased and produced the differences mentioned above.

A spectrum of the energies within our discriminator limits was not obtained during the density measurements, thus it was not determined which detected energies were responsible for the count rate increases. Conclusive evidence pointing to borate influence was not confirmed by field or laboratory tests. Some reasonable doubt can be attributed to the physical characteristic of the soil. The soil appeared to be light and powdery, beneath a thin surface crust probably produced by desiccation. At increasing depths below the surface, a higher degree of compaction was apparent. This fact seems to be verified by the 4-inch and 8-inch transmission measurements. Therefore, the borate influence could not be separately defined, even though theoretical reasoning warrants its existance.

In summating this discussion of Table 21, it appears that test surface quality is a major factor governing the benefits of improved backscatter gage construction. The contact area between the backscatter gage and the test material can conceivably erase most traces of backscatter improvement. It is obvious that this area of research will require further investigation.

REFERENCES

1. Transportation Research Board, "Results of the 1973 Questionnaire on Highway Applications to Nuclear Techniques", Highway Research Circular No. 154, July 1974.

2. Picker X-Ray Corporation, "Radioisotope Training Manual, Part I-Theory" Nuclear Division 1960.

3. U. S. Department of Health, Education, and Welfare, Public Health Service, "Radioassay Procedures For Environmental Samples", National Center for Radiological Health, Rockville, Maryland, January 1967.

4. U. S. Department of Health, Education, and Welfare, Public Health Service, "Radiological Health Handbook" Consumer Protection and Environmental Health Service, Rockville, Maryland, January 1970.

5. U. S. Department of Commerce, "Measurement of Neutron Flux and Spectra for Physical and Biological Applications" National Bureau of Standards, Handbook 72, January 1960.

6. Picker X-Ray Corporation, "Radioisotope Training Manual, Part III-Neutron Experiments" Nuclear Division 1963.

7. Troxler Electronics Laboratory, Inc., "Instruction Manual, Depth Moisture Gauge and Surface Moisture Gauge", Raleigh, North Carolina.

8. U. S. Department of Commerce, "X-Ray Attenuation Coefficients From 10Kev to 100Mev", National Bureau of Standards.

9. Reuter-Stokes, "Neutron Proportional Counters for Neutron Physics Experiments, Neutron Monitoring, Industrial Gaging" Cleveland, Ohio.

From Radioassay Procedures For Environmental Samples. Ref# 3

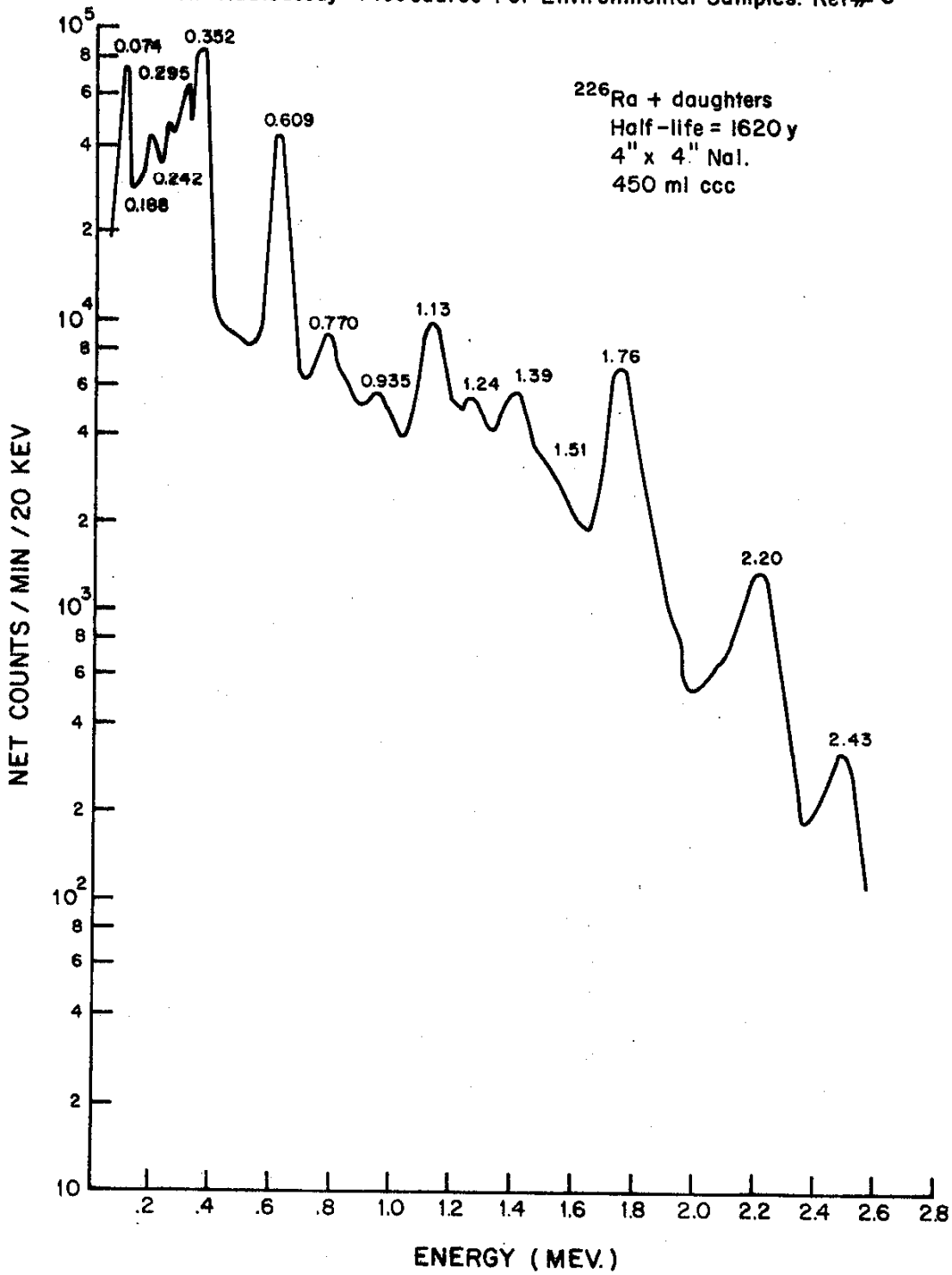

GAMMA SPECTRUM OF ^{226}Ra AND DAUGHTERS -450 ml

Figure 1

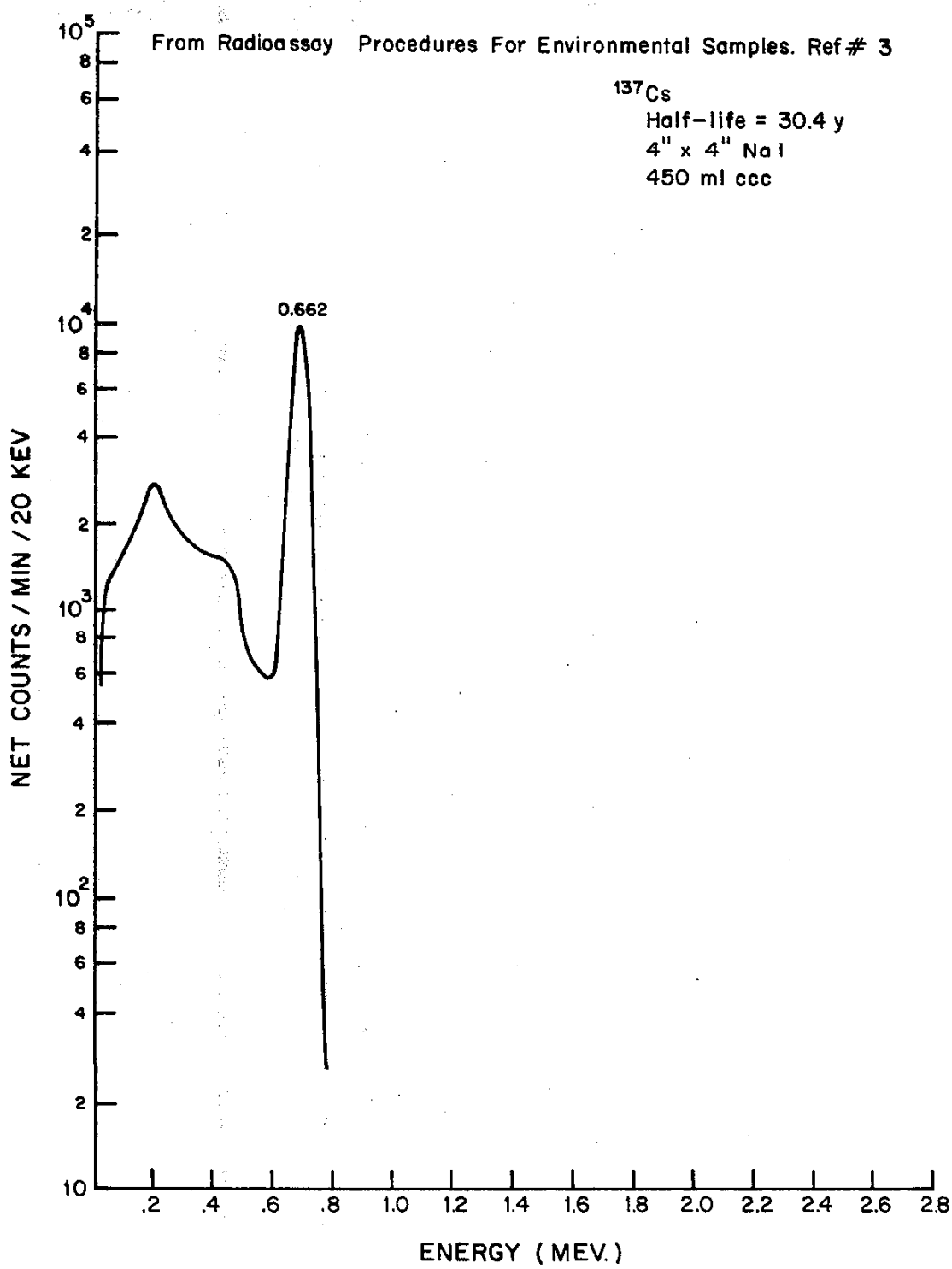

GAMMA SPECTRUM OF ^{137}Cs - 450 ml

Figure 2

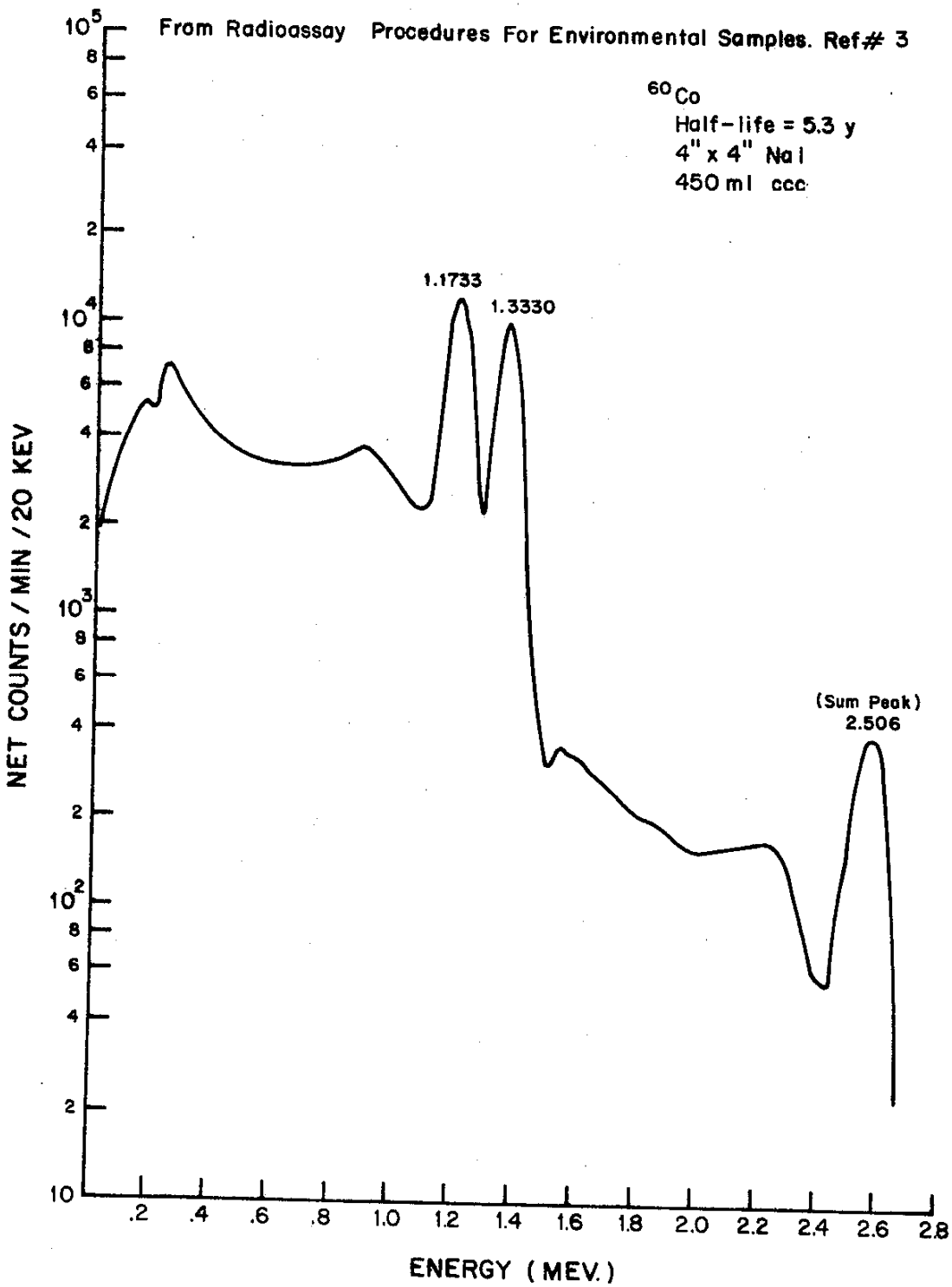

GAMMA SPECTRUM OF ^{60}Co – 450 ml

Figure 3

DETERMINATION OF CHEMICAL COMPOSITION ERROR MAGNITUDE FROM DENSITY CALIBRATION CURVE

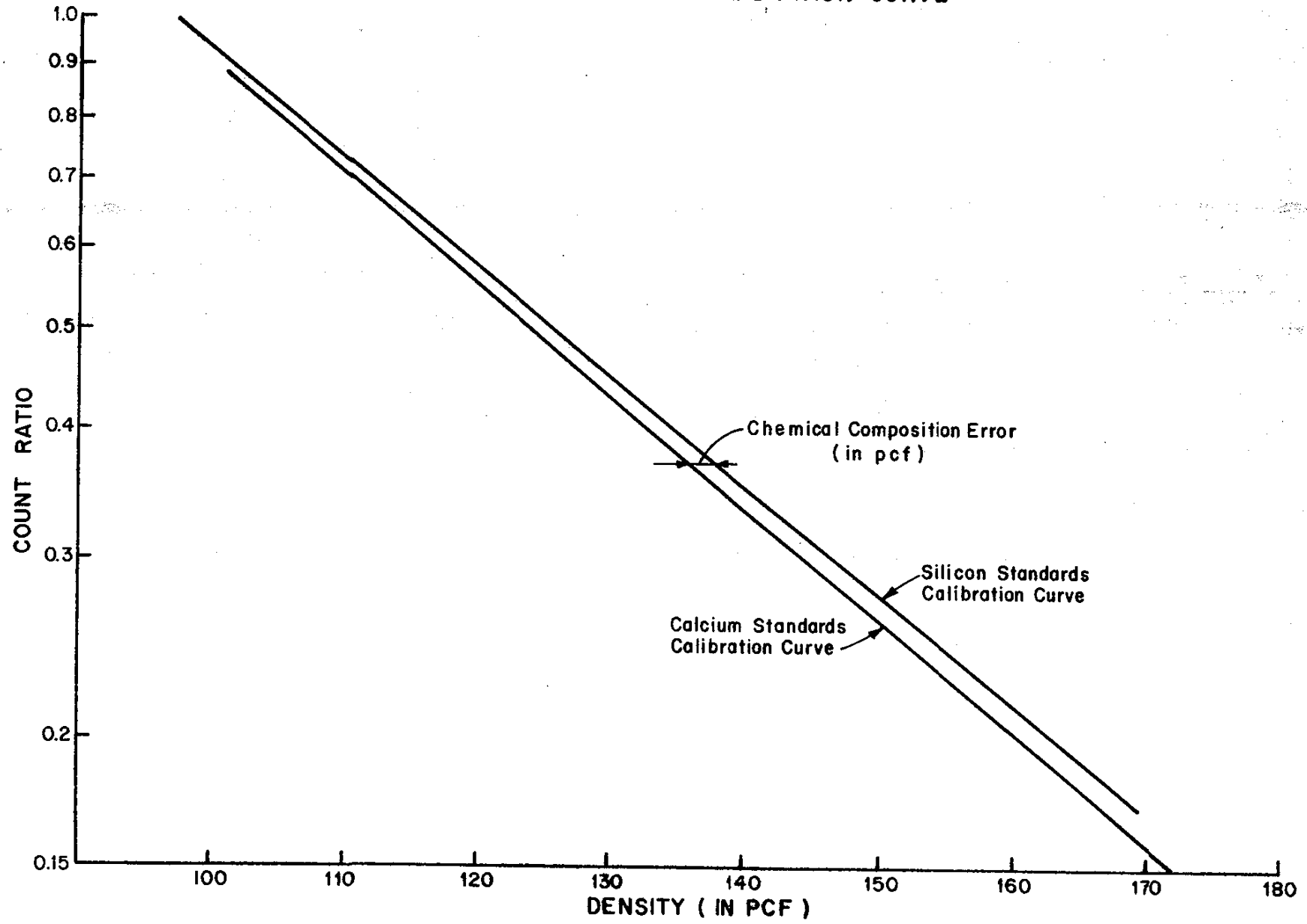

Figure 4

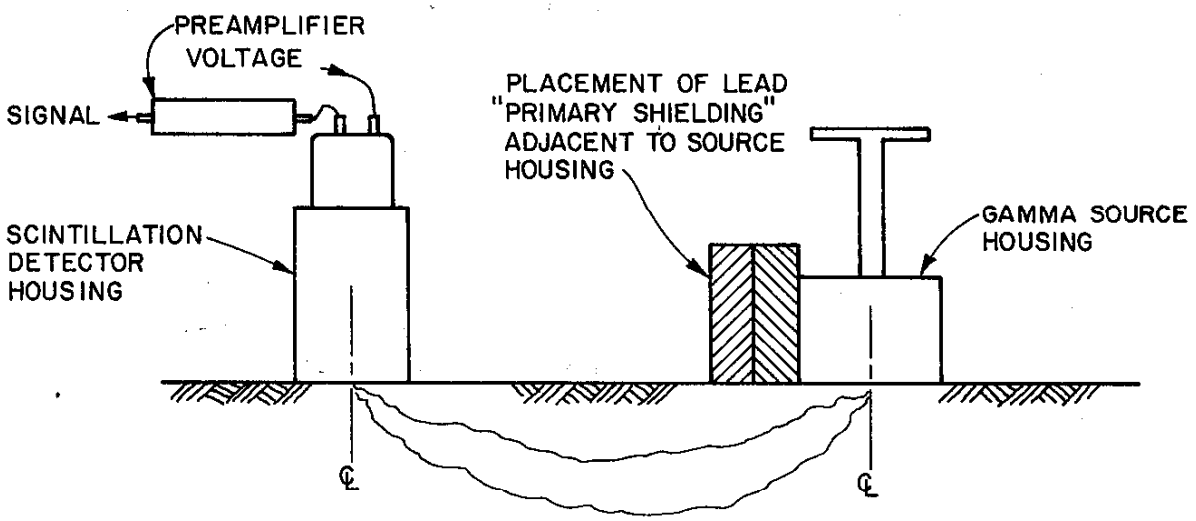

BACKSCATTER APPARATUS

Figure 5

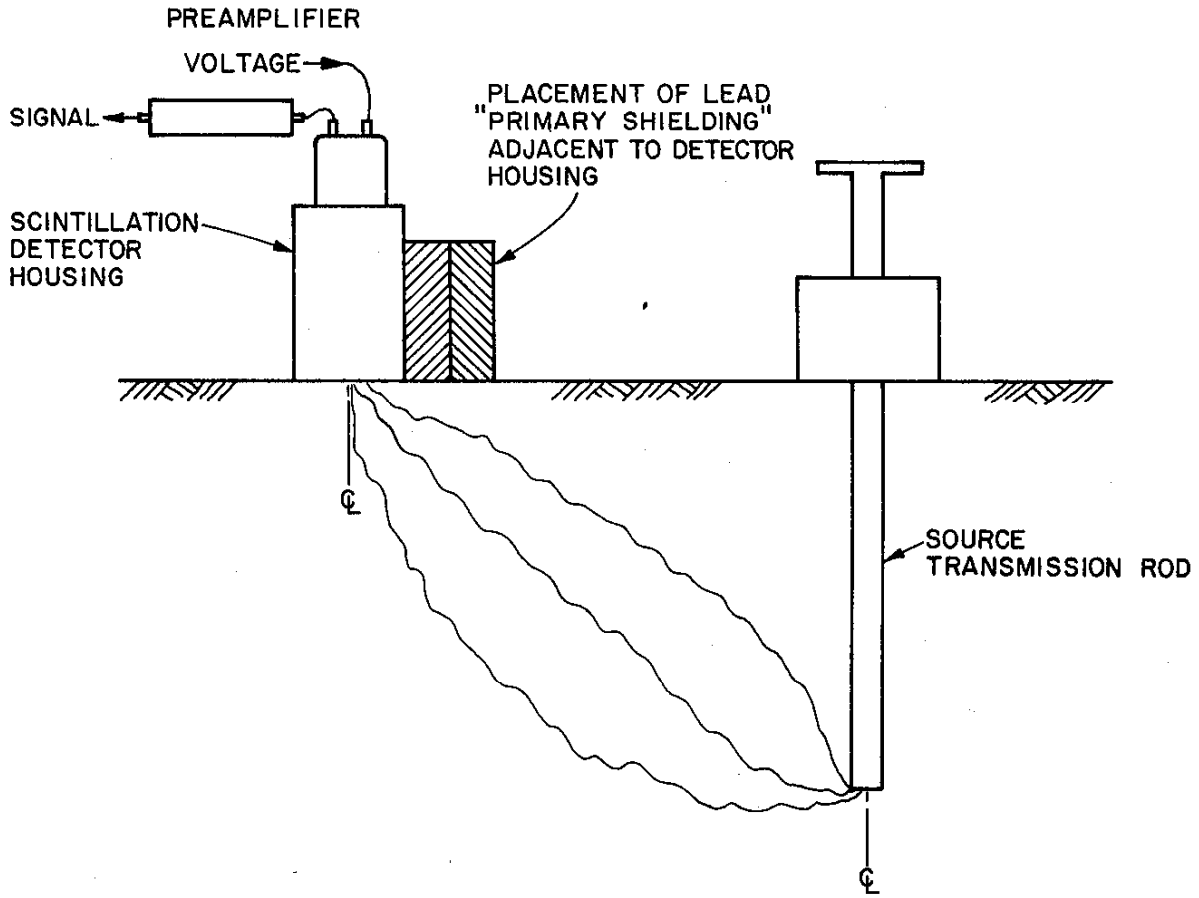

TRANSMISSION APPARATUS

Figure 6

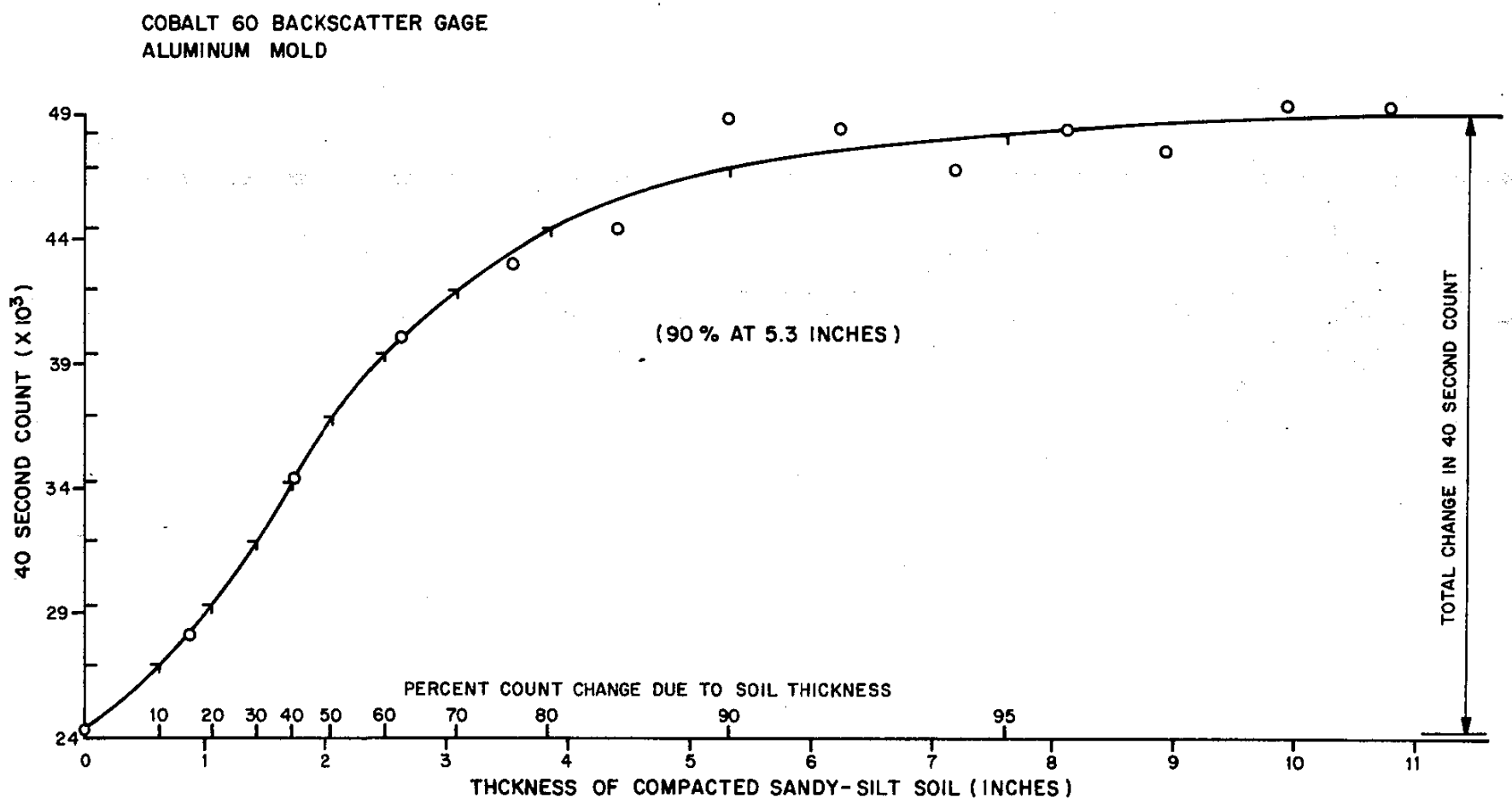

DEPTH OF INFLUENCE OF COBALT EMISSION PENETRATION
IN A SANDY-SILT STANDARD

Figure 7

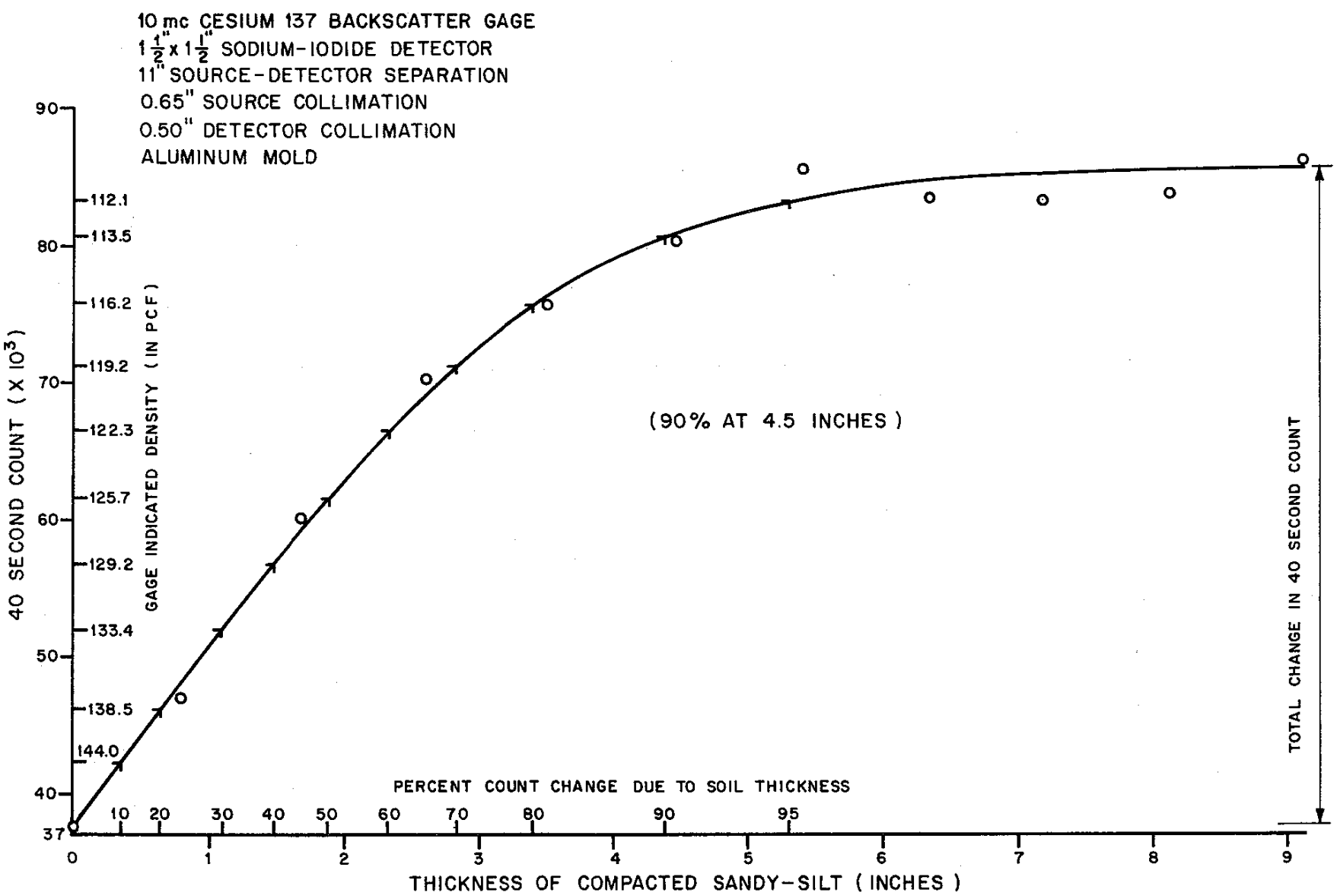

DEPTH OF INFLUENCE OF CESIUM EMISSION PENETRATION
IN A SANDY-SILT STANDARD

Figure 8

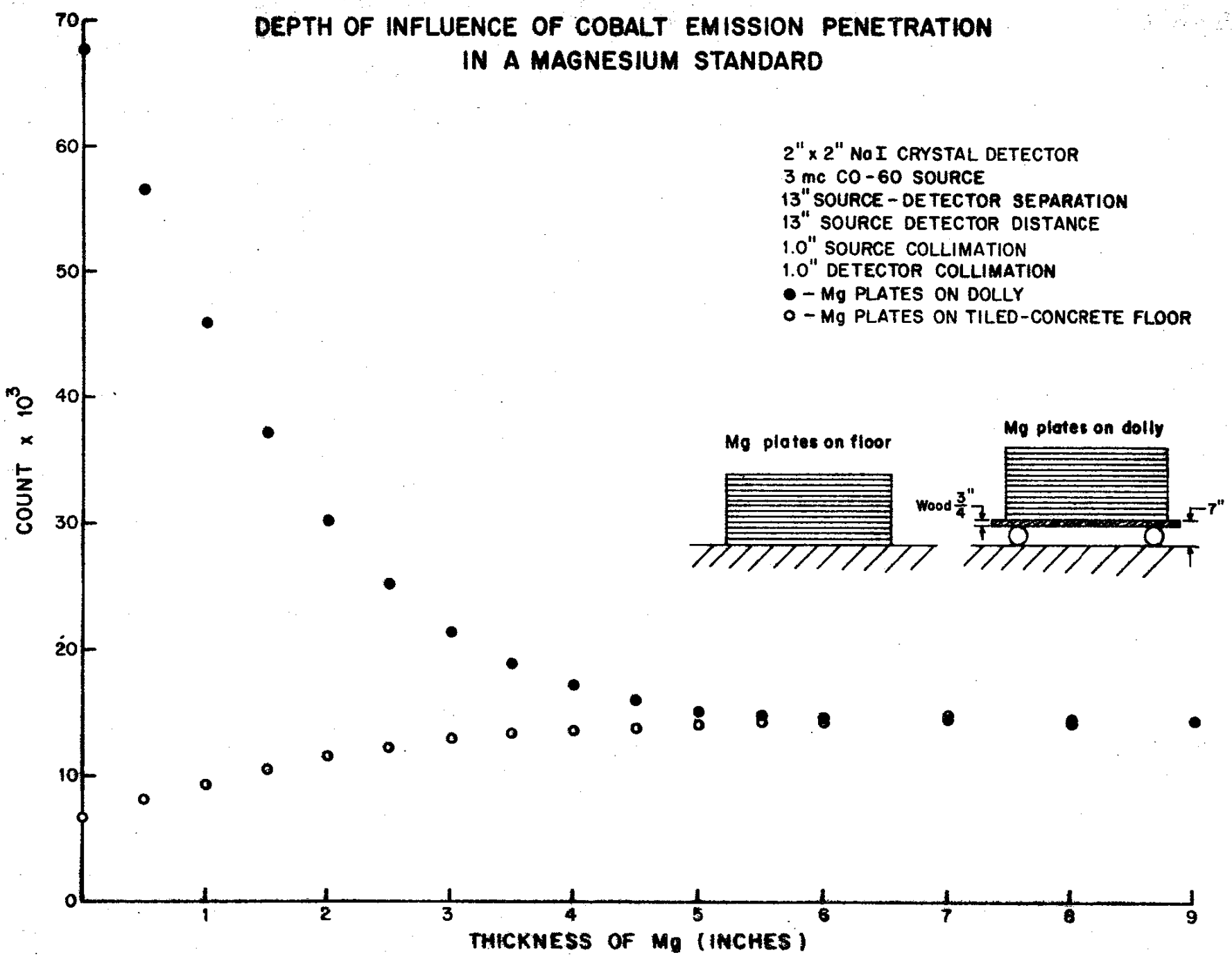
DEPTH OF INFLUENCE OF COBALT EMISSION PENETRATION
IN A MAGNESIUM STANDARD
2" x 2" NaI CRYSTAL DETECTOR
3 mc CO-60 SOURCE
13" SOURCE-DETECTOR SEPARATION
13" SOURCE DETECTOR DISTANCE
1.0" SOURCE COLLIMATION
1.0" DETECTOR COLLIMATION
● - Mg PLATES ON DOLLY
○ - Mg PLATES ON TILED-CONCRETE FLOOR
Mg plates on floor
Mg plates on dolly
Wood 3/4"
7"
COUNT x 10^3
0
10
20
30
40
50
60
70
1
2
3
4
5
6
7
8
9
THICKNESS OF Mg (INCHES)

Figure 9

DEPTH OF INFLUENCE OF CESIUM EMISSION PENETRATION IN A MAGNESIUM STANDARD

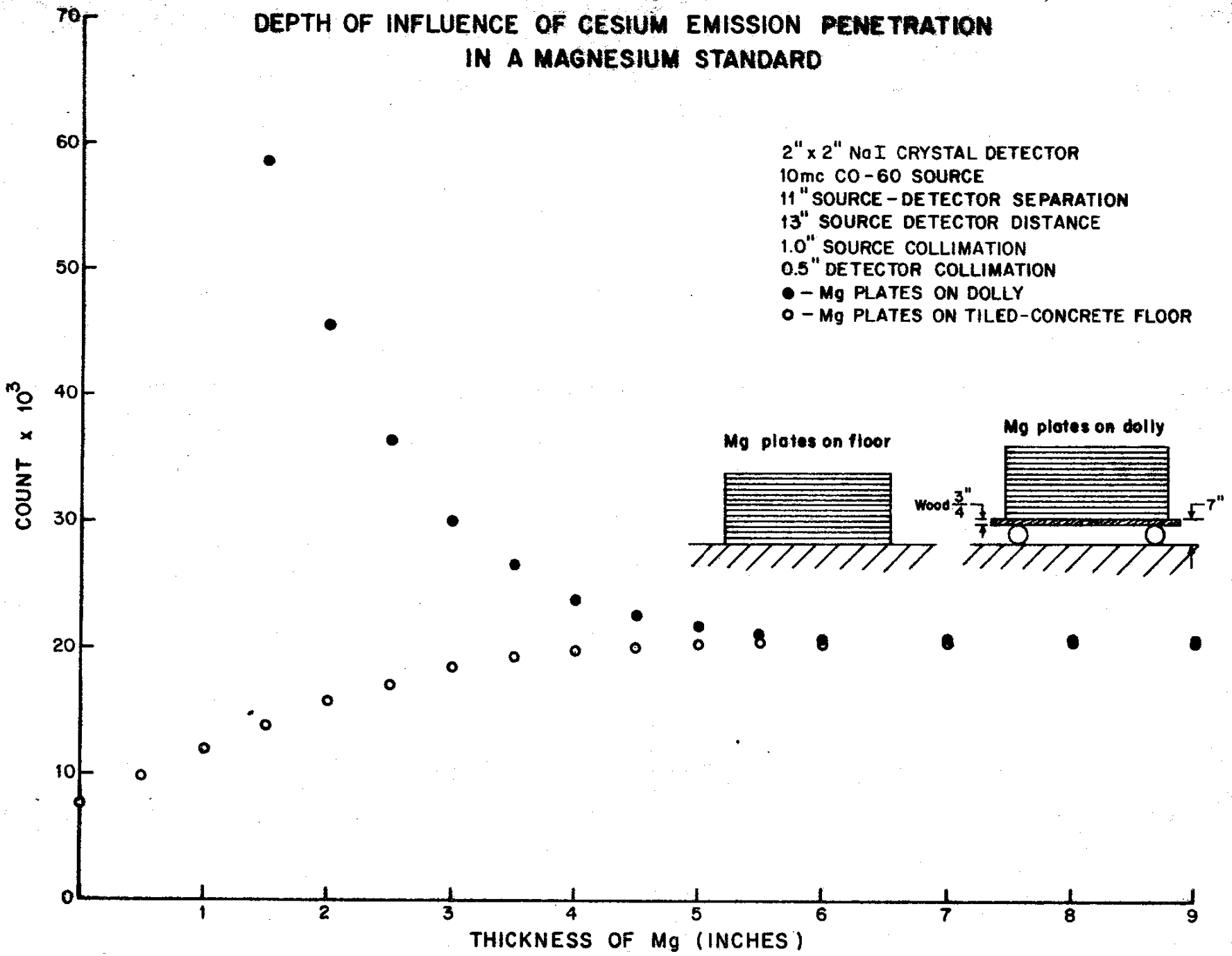

Figure 10

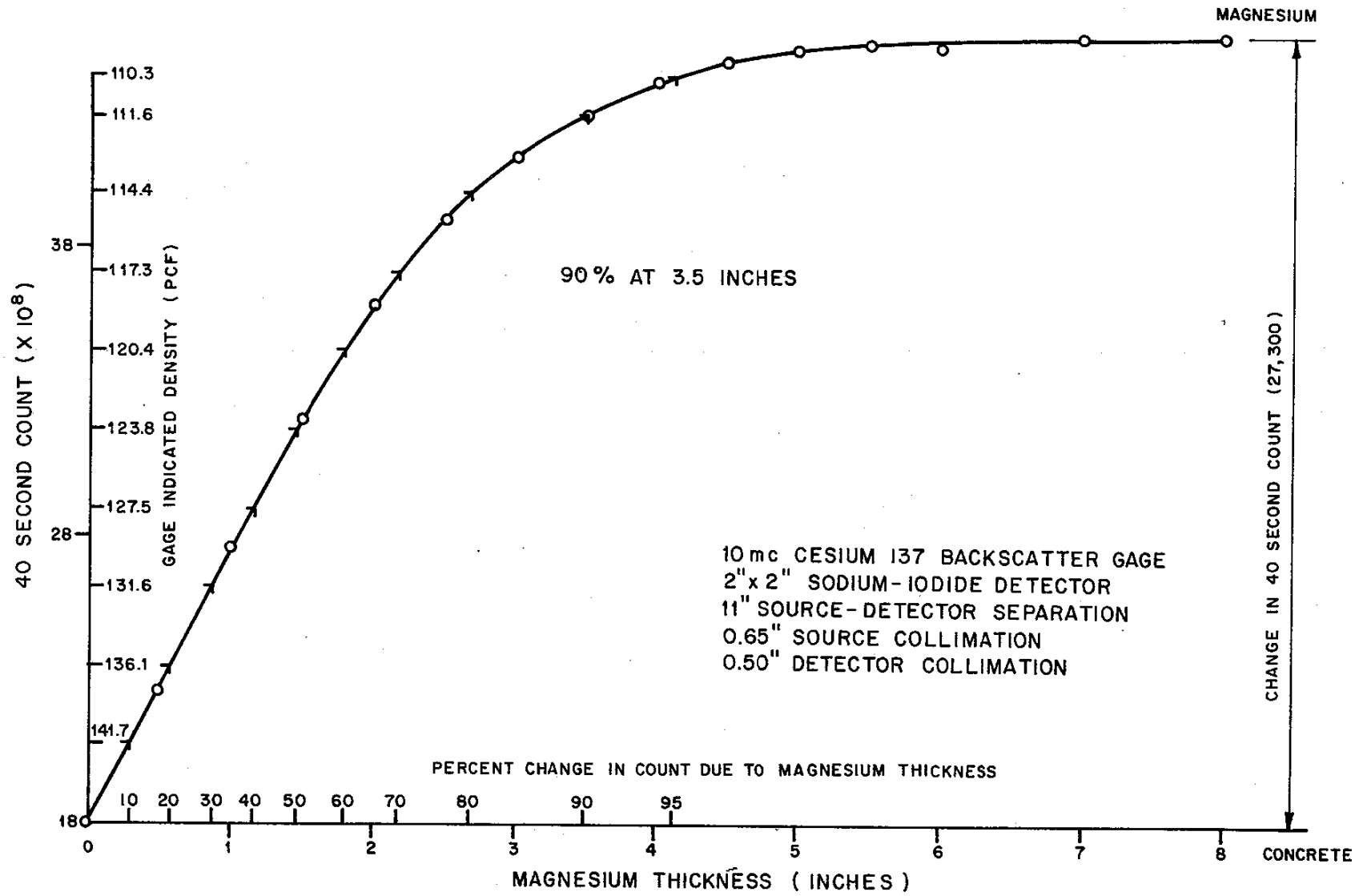

DEPTH OF INFLUENCE OF COBALT EMISSION PENETRATION IN A MAGNESIUM STANDARD VS GAGE INDICATED DENSITY

Figure 11

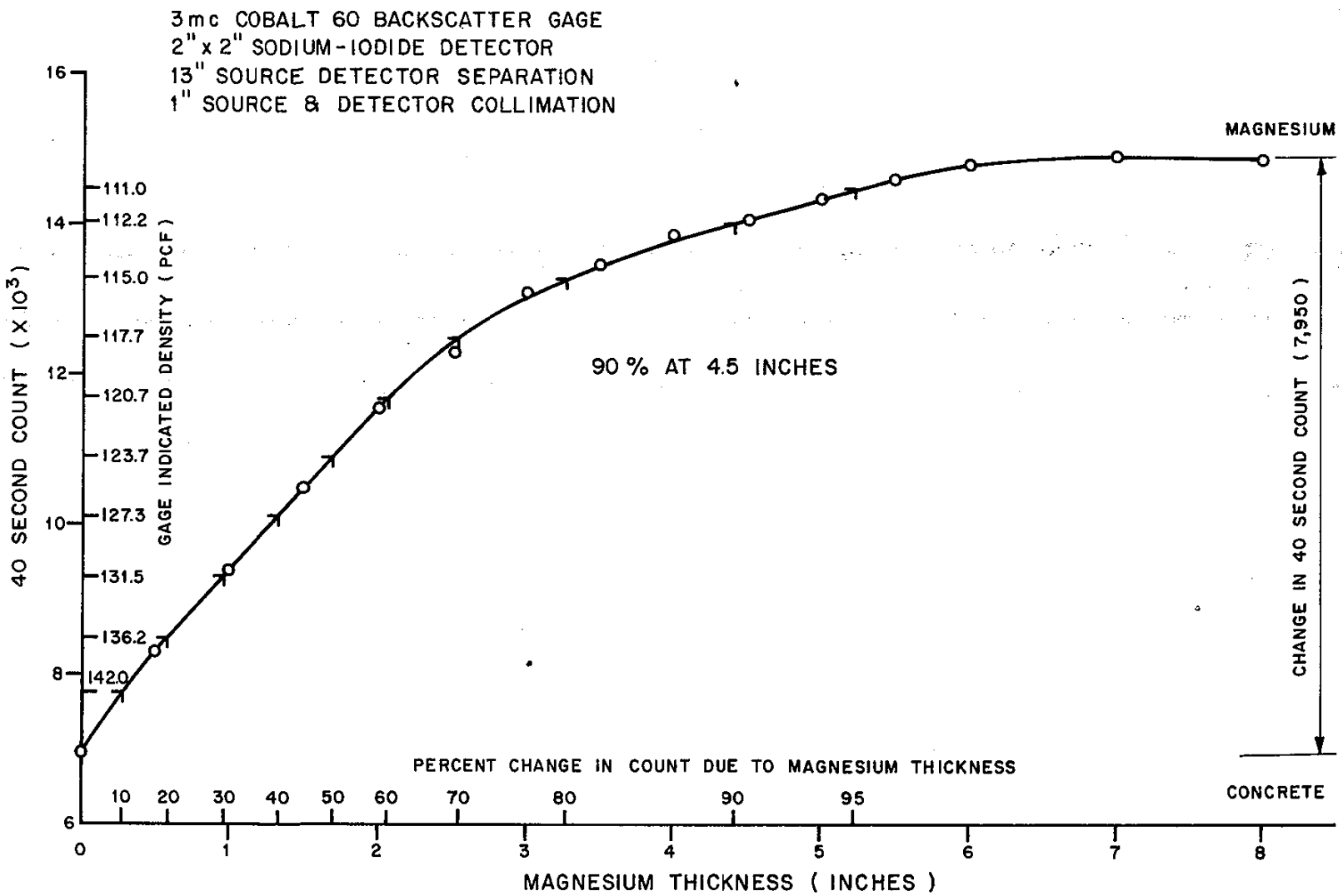

DEPTH OF INFLUENCE OF CESIUM EMISSION PENETRATION IN A MAGNESIUM STANDARD VS GAGE INDICATED DENSITY

Figure 12

CALIBRATION CURVE FOR THE EXPERIMENTAL CESIUM 137 BACKSCATTER GAGE

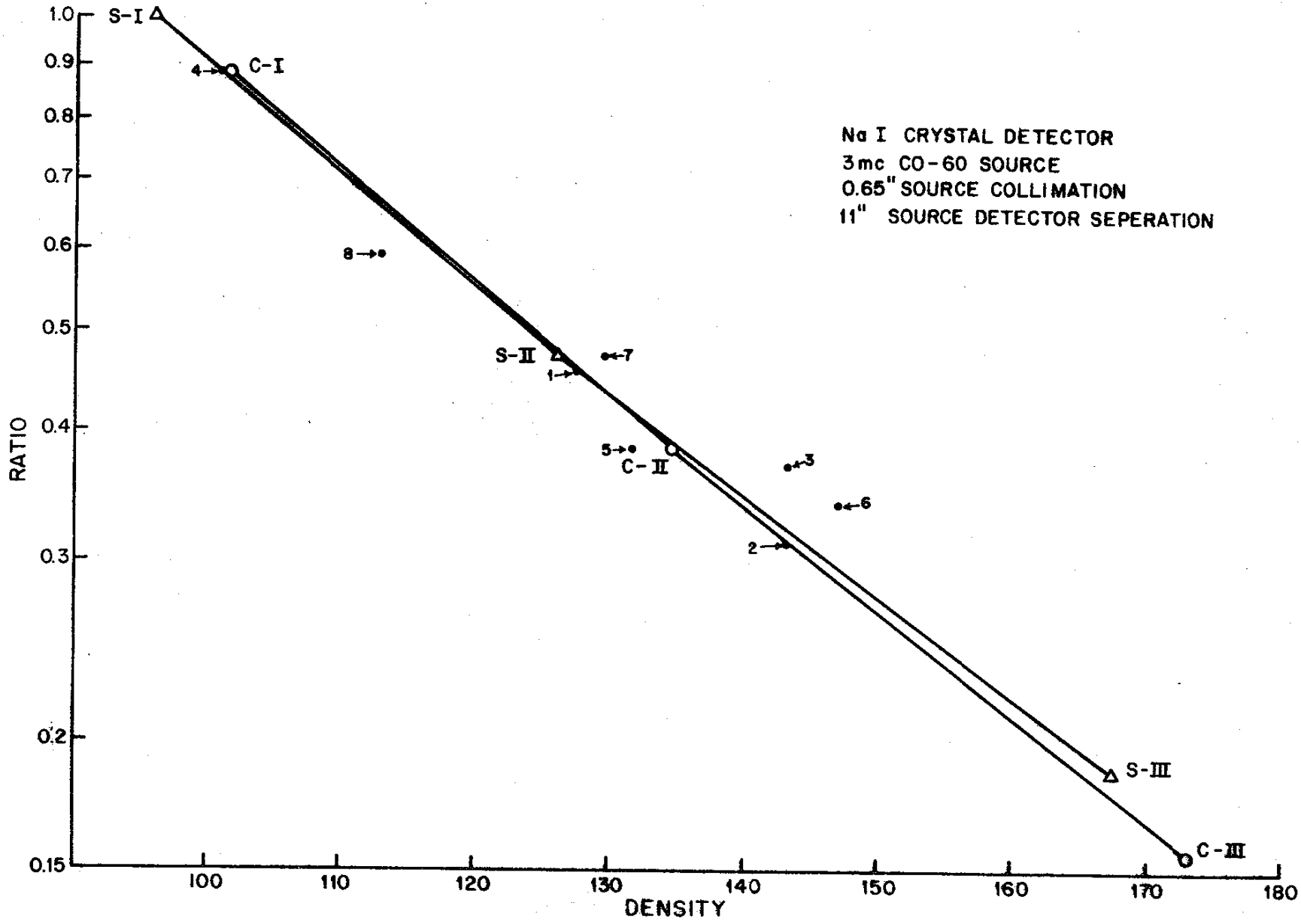

Figure 13

CALIBRATION CURVE FOR THE EXPERIMENTAL COBALT 60
BACKSCATTER GAGE

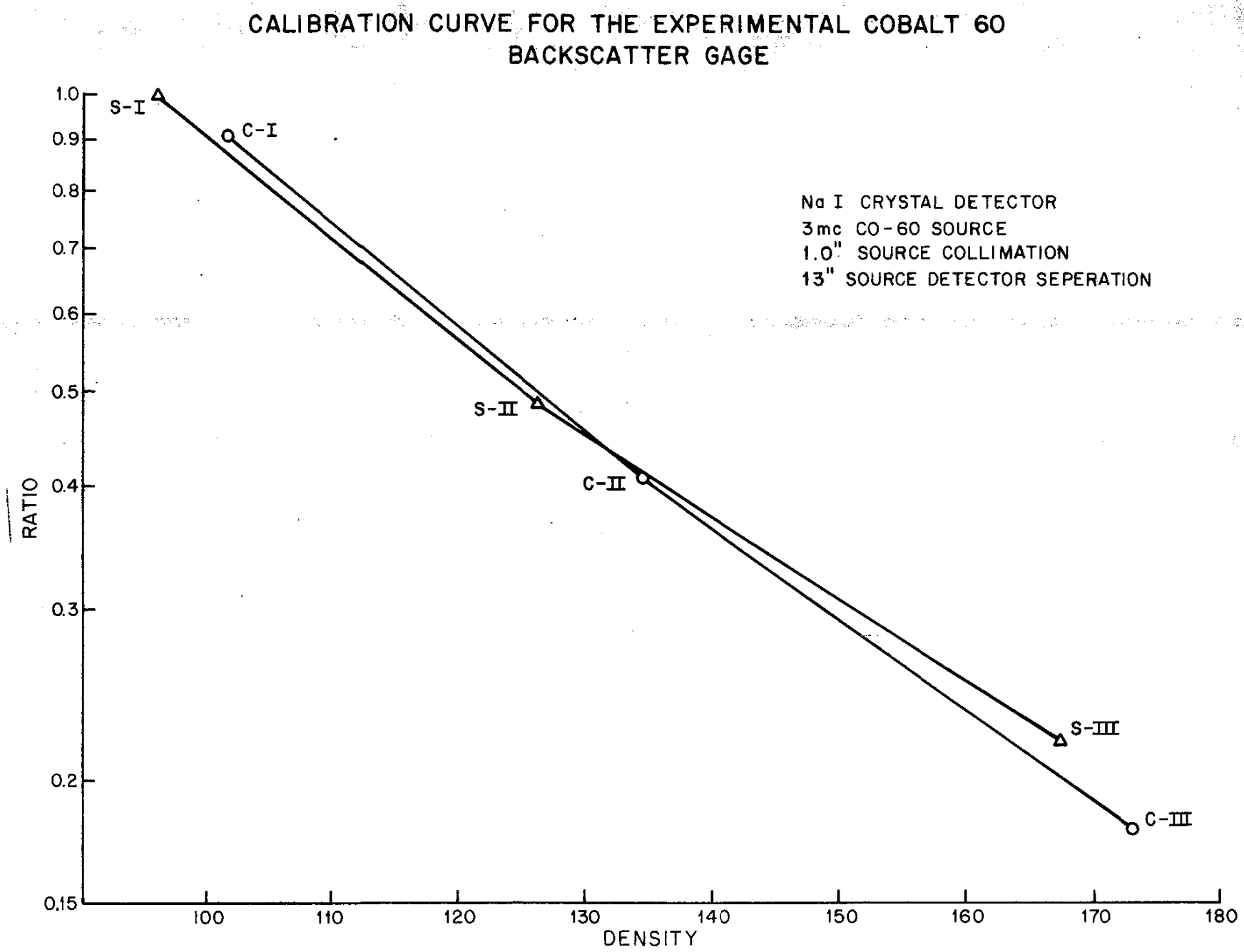

Figure 14

CALIBRATION CURVE FOR THE EXPERIMENTAL COBALT 60 BACKSCATTER GAGE

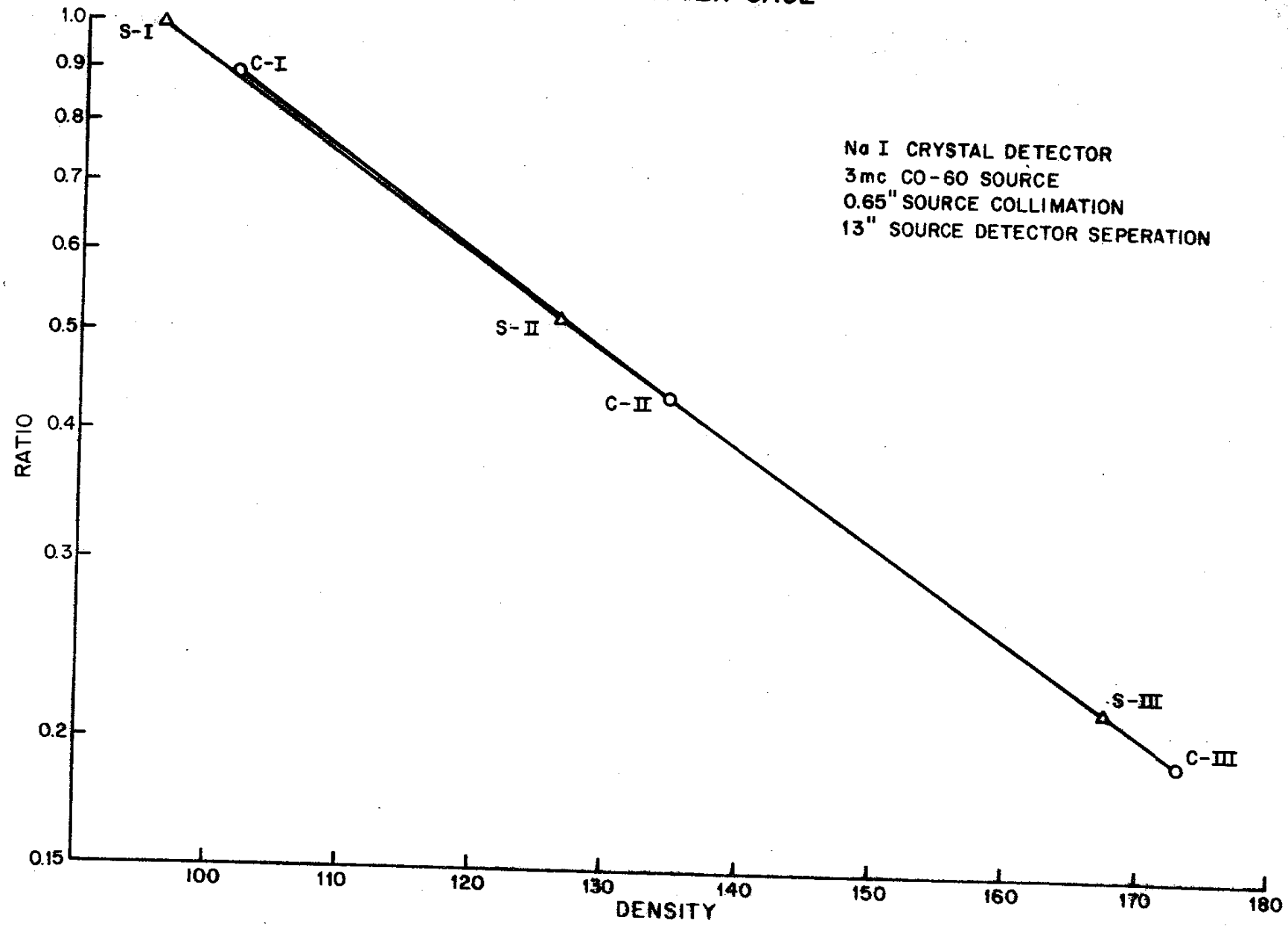

Figure 15

NEUTRON SPECTRUM FROM A BF_3 PROPORTIONAL COUNTER

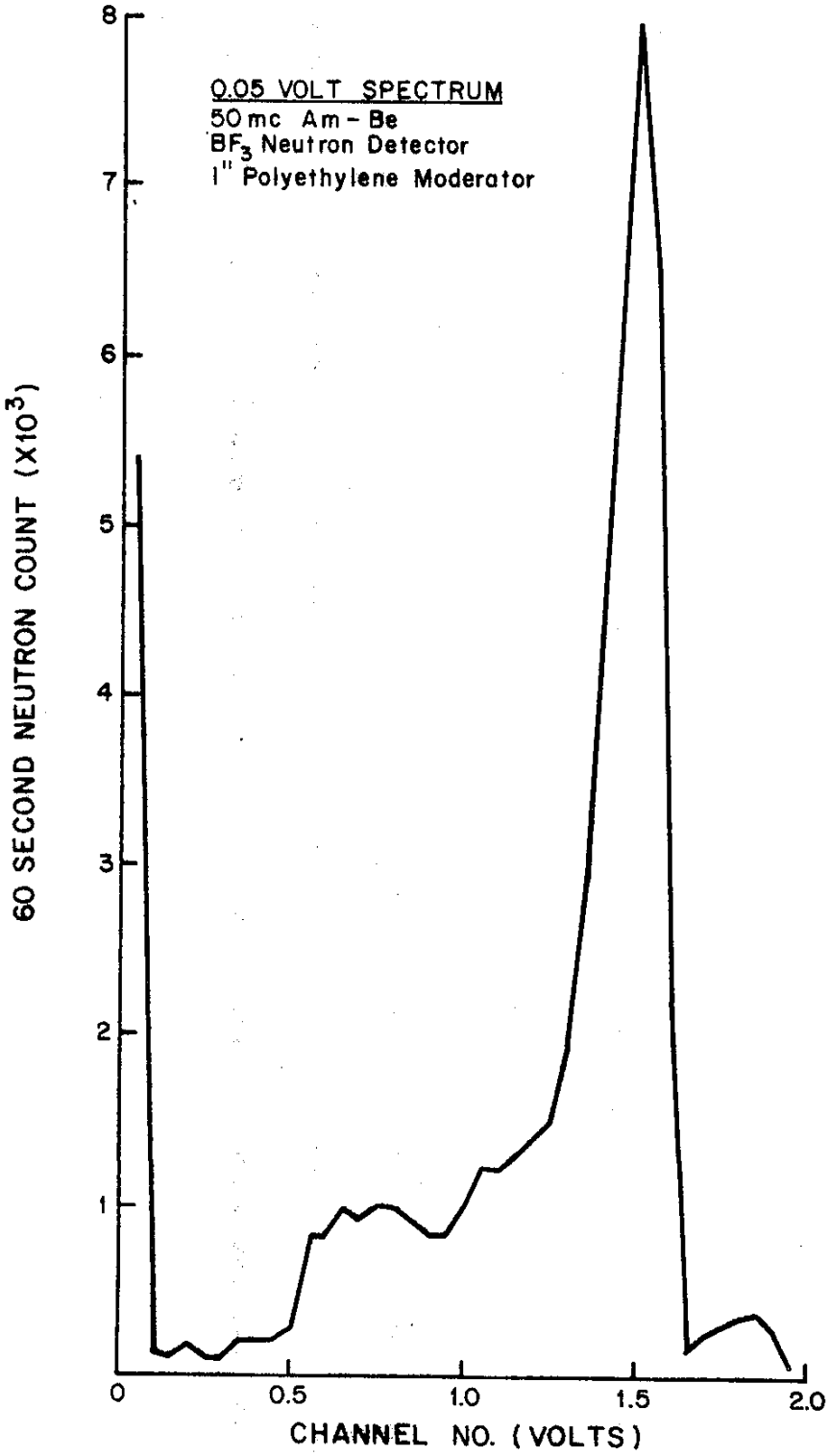

Figure 16

NEUTRON SPECTRUM FROM A He-3 PROPORTIONAL COUNTER

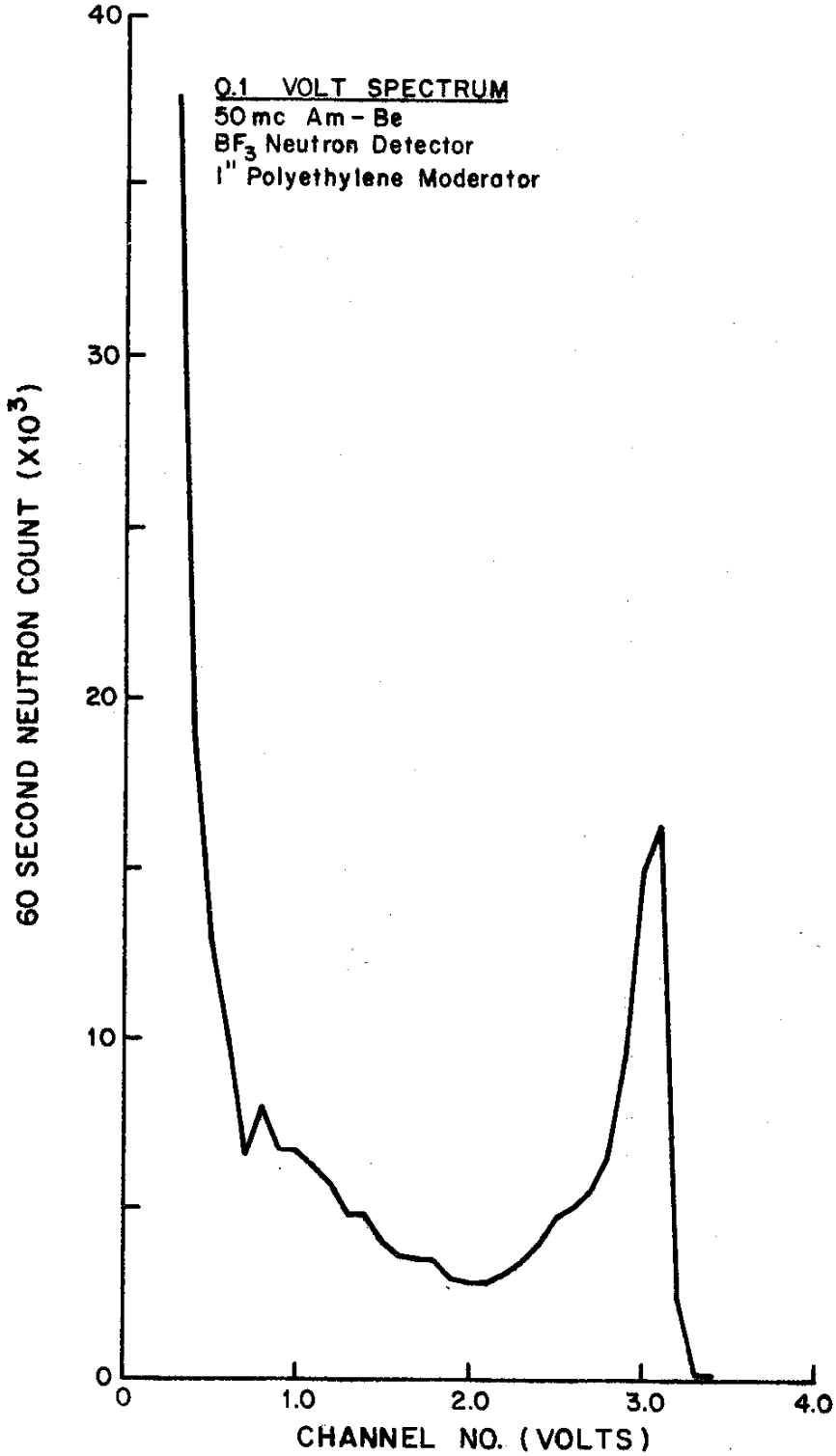

Figure 17

REDUCTION OF NEUTRON ABSORPTION EFFECTS OBTAINED BY BORON TRIFLORIDE (BF_3) DETECTOR DISCRIMINATION

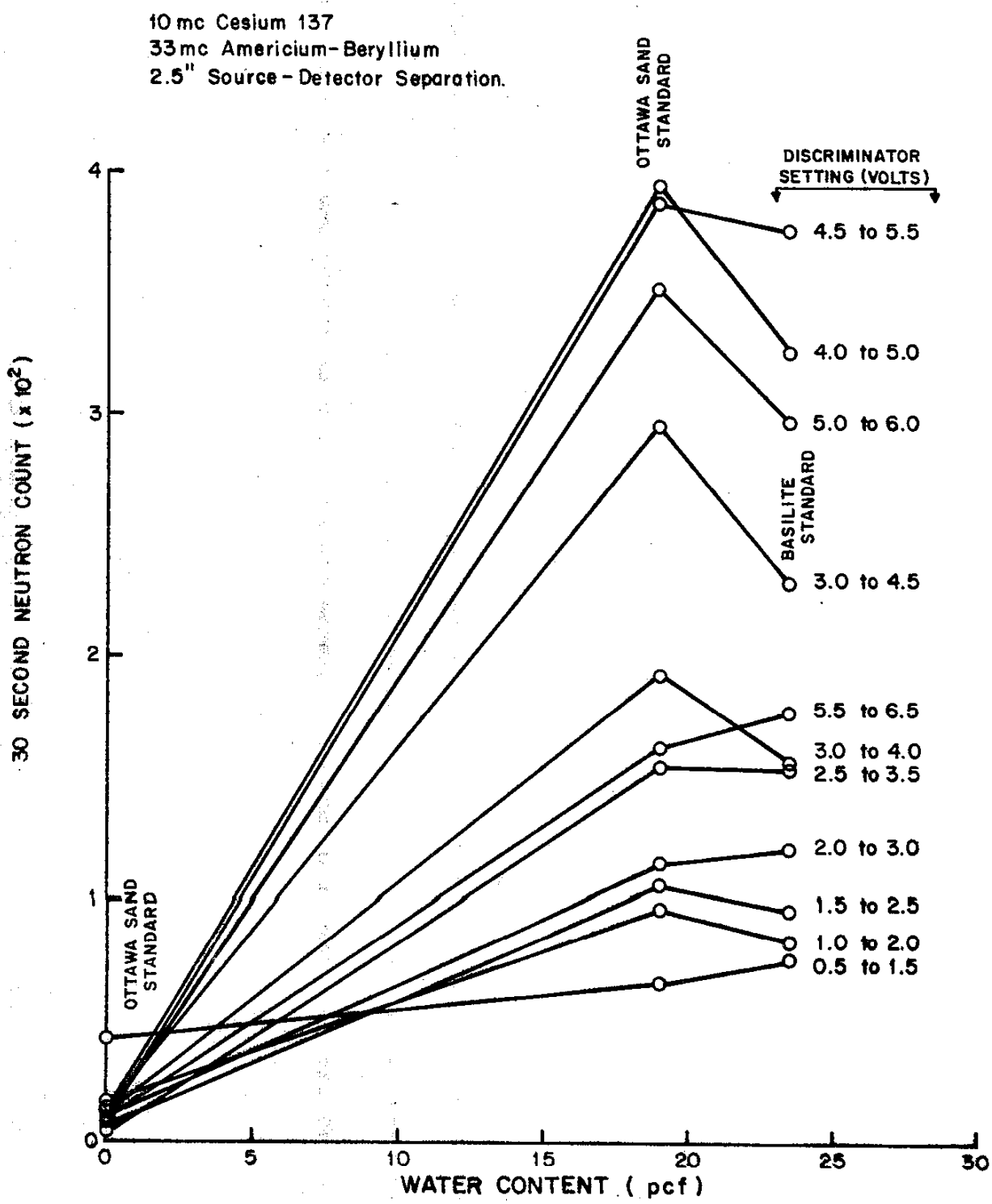

Figure 18

REDUCTION OF NEUTRON ABSORPTION EFFECTS OBTAINED BY HELIUM (He-3) DETECTOR DISCRIMINATION

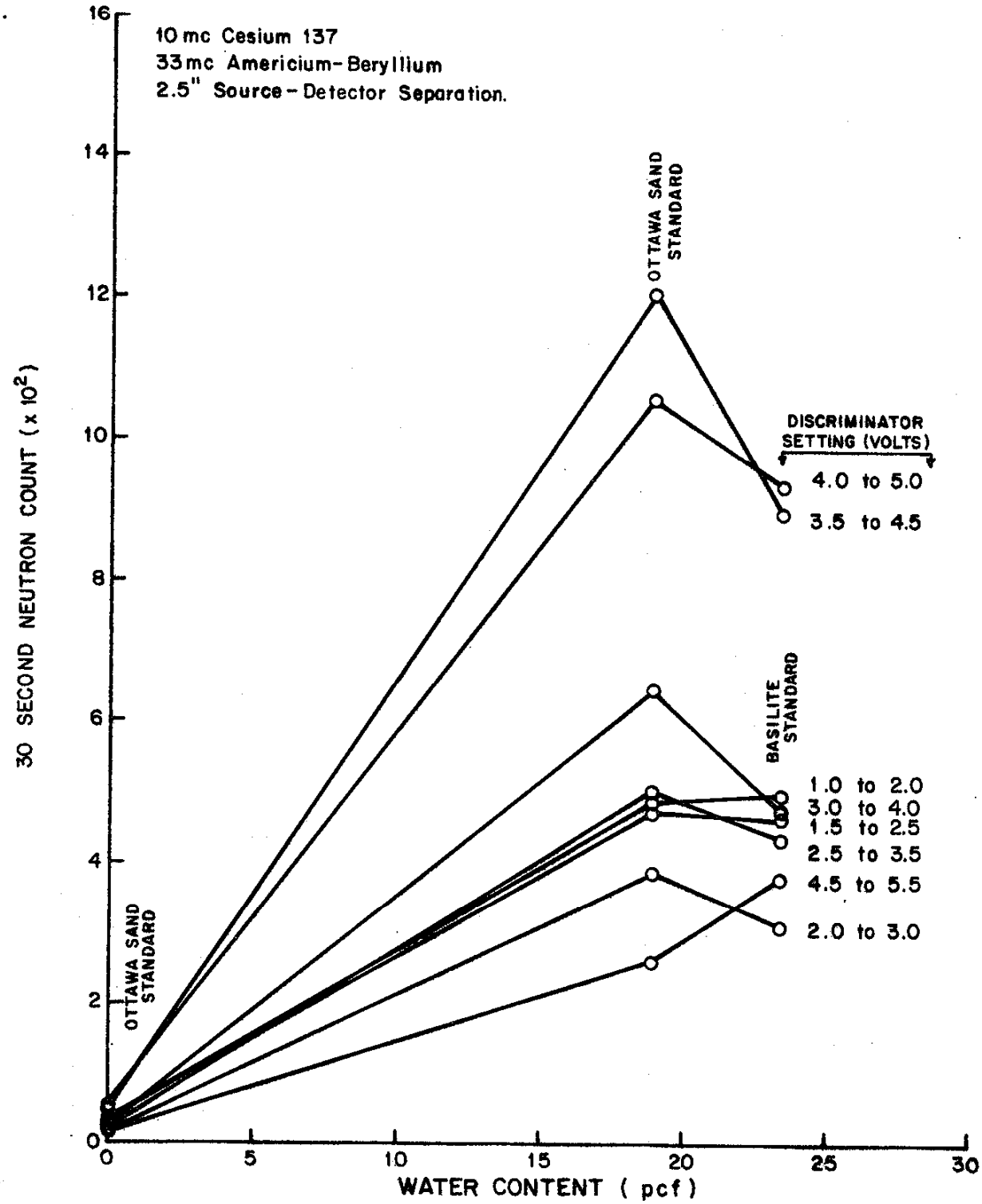

Figure 19

REDUCTION OF NEUTRON ABSORPTION EFFECTS OBTAINED BY LITHIUM-IODIDE DETECTOR DISCRIMINATION

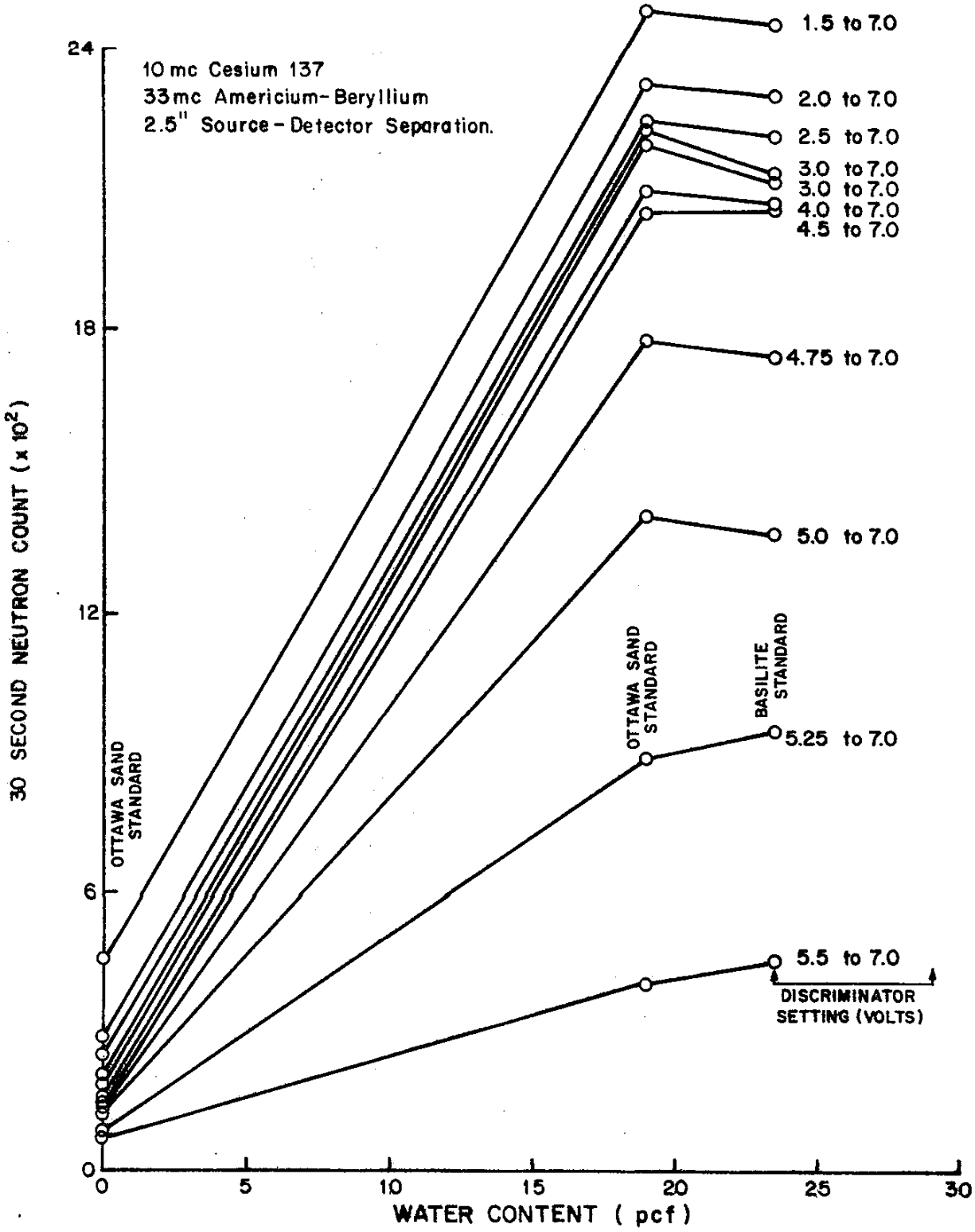

Figure 20

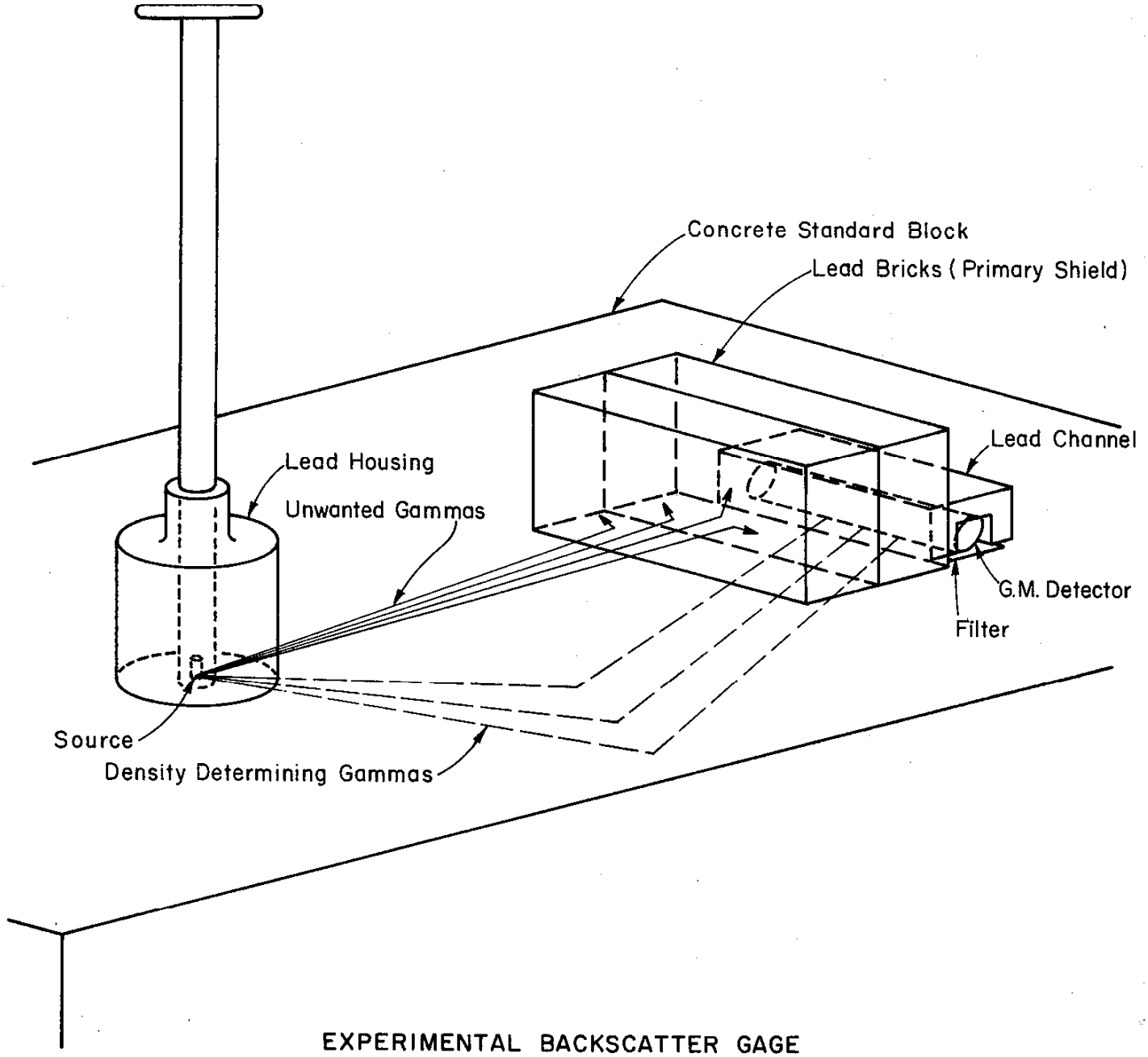

EXPERIMENTAL BACKSCATTER GAGE
EMPLOYING A GEIGER-MUELLER DETECTOR

Figure 21

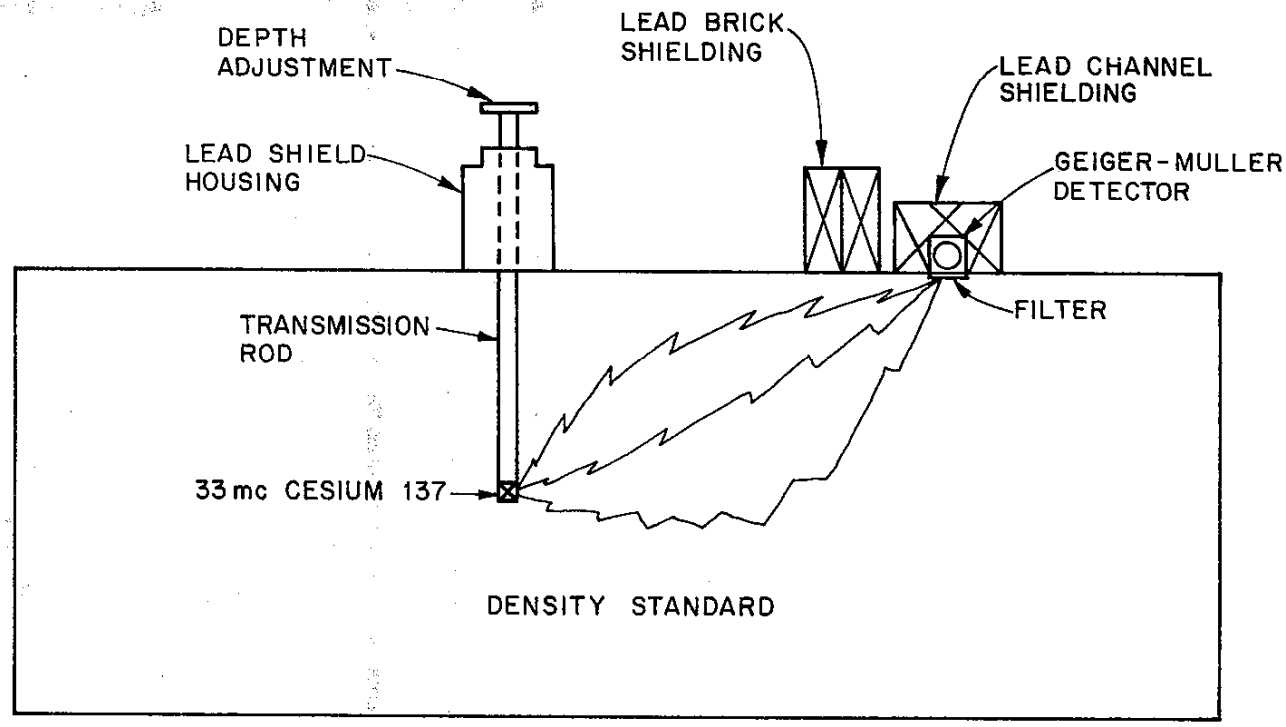

EXPERIMENTAL TRANSMISSION GAGE
EMPLOYING A GEIGER-MUELLER DETECTOR

Figure 22

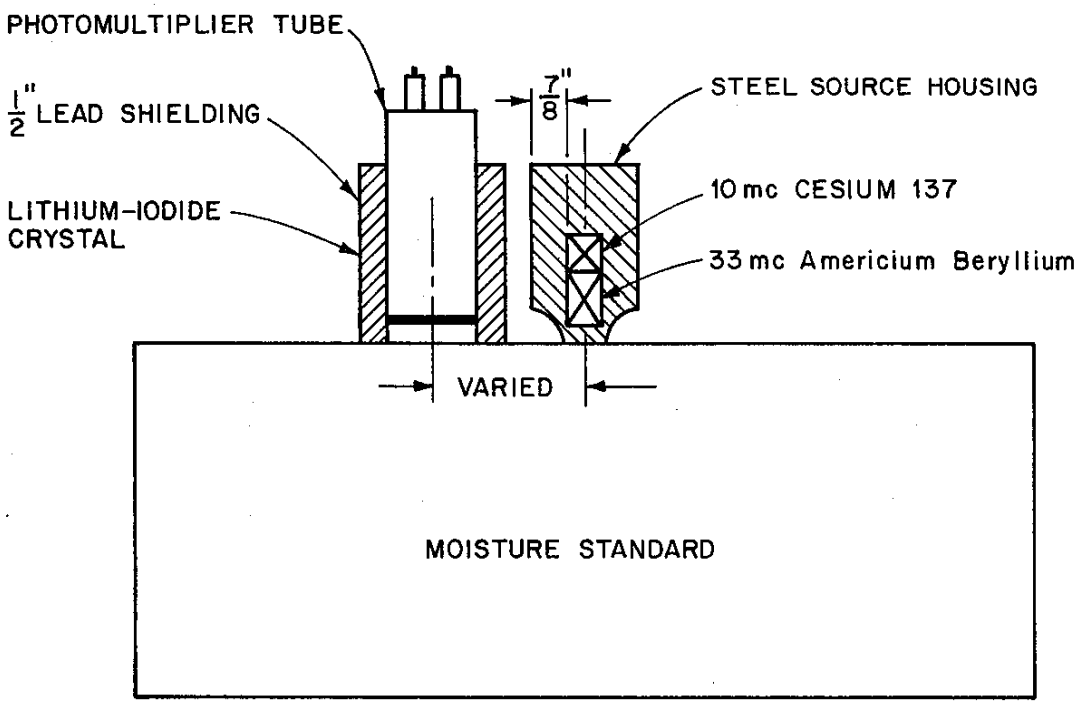

EXPERIMENTAL BACKSCATTER MOISTURE GAGE
EMPLOYING A LITHIUM-IODIDE SCINTILLATION DETECTOR

Figure 23

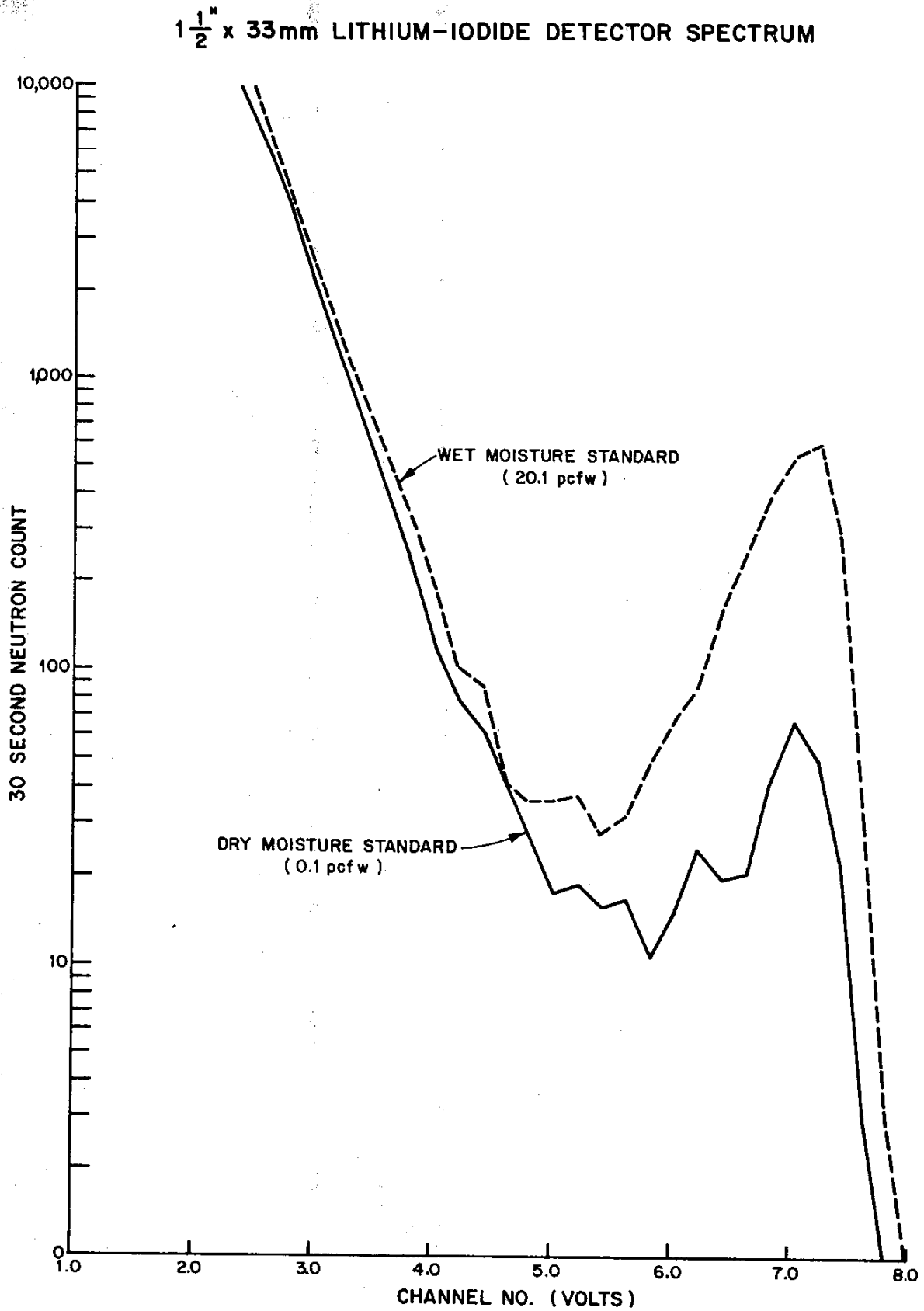
1 1/2" x 33mm LITHIUM-IODIDE DETECTOR SPECTRUM
10,000
1,000
100
10
0
30 SECOND NEUTRON COUNT
WET MOISTURE STANDARD
(20.1 pcfw)
DRY MOISTURE STANDARD
(0.1 pcfw)
1.0
2.0
3.0
4.0
5.0
6.0
7.0
8.0
CHANNEL NO. (VOLTS)

Figure 24

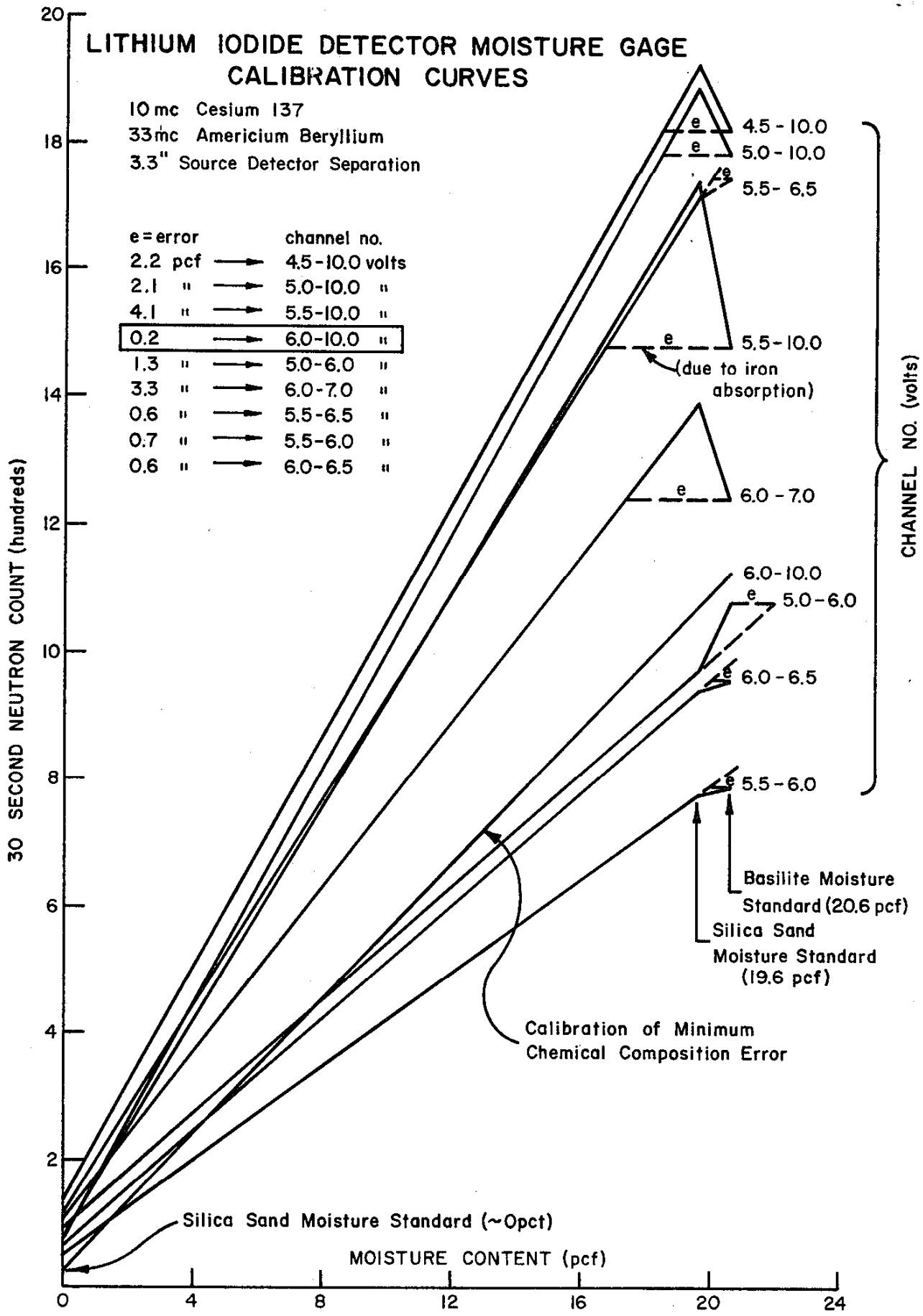
LITHIUM IODIDE DETECTOR MOISTURE GAGE
CALIBRATION CURVES
10 mc Cesium 137
33 mc Americium Beryllium
3.3" Source Detector Separation
e = error
channel no.
2.2 pcf → 4.5-10.0 volts
2.1 " → 5.0-10.0 "
4.1 " → 5.5-10.0 "
0.2 → 6.0-10.0 "
1.3 " → 5.0-6.0 "
3.3 " → 6.0-7.0 "
0.6 " → 5.5-6.5 "
0.7 " → 5.5-6.0 "
0.6 " → 6.0-6.5 "
4.5 - 10.0
5.0 - 10.0
5.5 - 6.5
5.5 - 10.0
(due to iron absorption)
6.0 - 7.0
6.0 - 10.0
5.0 - 6.0
6.0 - 6.5
5.5 - 6.0
CHANNEL NO. (volts)
Basilite Moisture Standard (20.6 pcf)
Silica Sand Moisture Standard (19.6 pcf)
Calibration of Minimum Chemical Composition Error
Silica Sand Moisture Standard (~0pct)
30 SECOND NEUTRON COUNT (hundreds)
MOISTURE CONTENT (pcf)
0
4
8
12
16
20
24
2
4
6
8
10
12
14
16
18
20

Figure 25

BORON TRIFLORIDE DETECTOR MOISTURE GAGE CALIBRATION CURVES

10 mc Cesium 137, 33 mc Americium Beryllium
2.5" Source Detector Separation

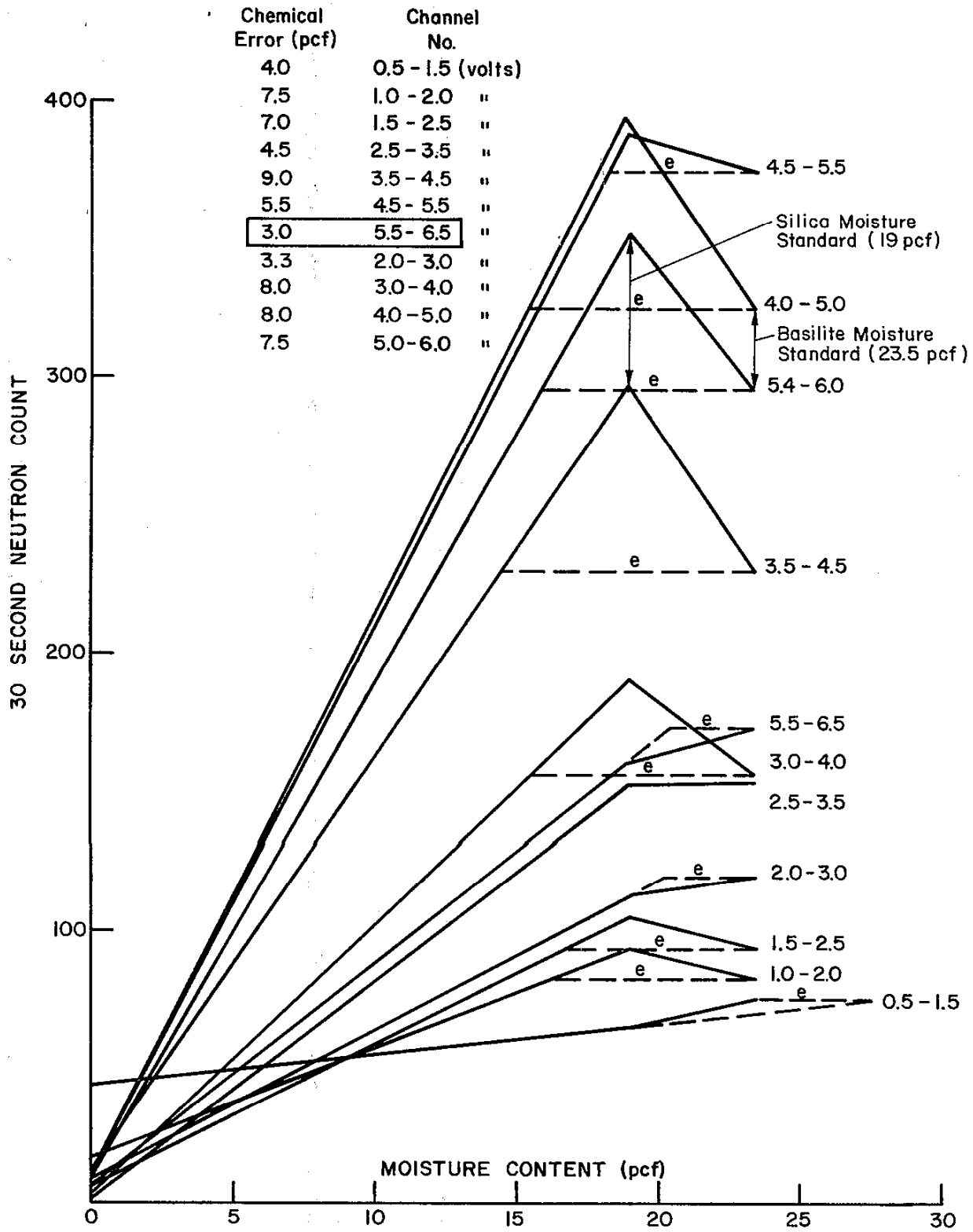

Figure 26

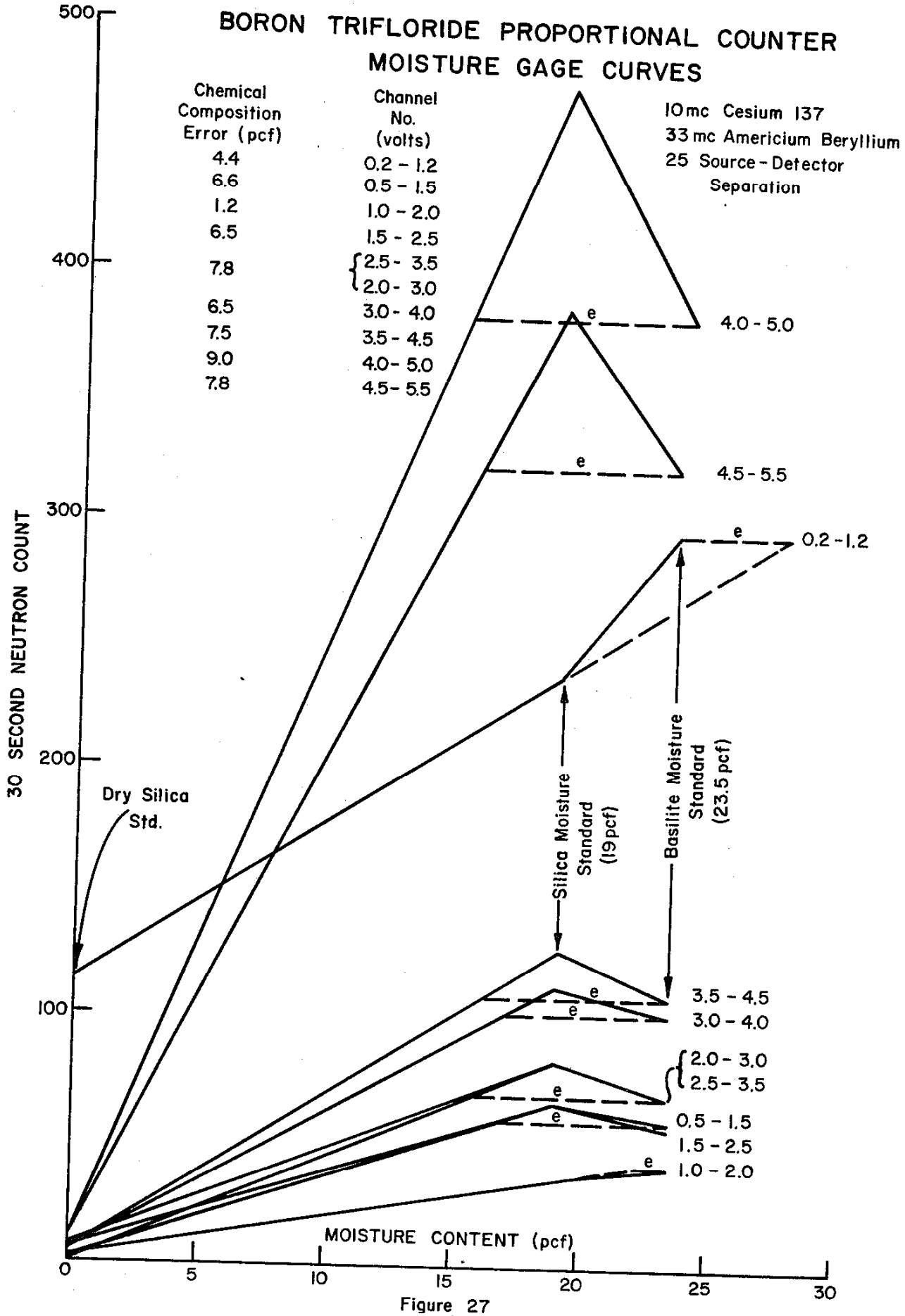
BORON TRIFLORIDE PROPORTIONAL COUNTER
MOISTURE GAGE CURVES
Chemical Composition Error (pcf)
4.4
6.6
1.2
6.5
7.8
6.5
7.5
9.0
7.8
Channel No. (volts)
0.2 - 1.2
0.5 - 1.5
1.0 - 2.0
1.5 - 2.5
2.5 - 3.5
2.0 - 3.0
3.0 - 4.0
3.5 - 4.5
4.0 - 5.0
4.5 - 5.5
10 mc Cesium 137
33 mc Americium Beryllium
25 Source - Detector Separation
4.0 - 5.0
4.5 - 5.5
0.2 - 1.2
3.5 - 4.5
3.0 - 4.0
2.0 - 3.0
2.5 - 3.5
0.5 - 1.5
1.5 - 2.5
1.0 - 2.0
e
Dry Silica Std.
Silica Moisture Standard (19 pcf)
Basilite Moisture Standard (23.5 pcf)
30 SECOND NEUTRON COUNT
500
400
300
200
100
0
MOISTURE CONTENT (pcf)
5
10
15
20
25
30

Figure 27

8 INCH HELIUM 3 PROPORTIONAL COUNTER MOISTURE GAGE CALIBRATION CURVES

10 mc Cesium 137
33 mc Americium Beryllium
2.5 inch Source - Detector Separation

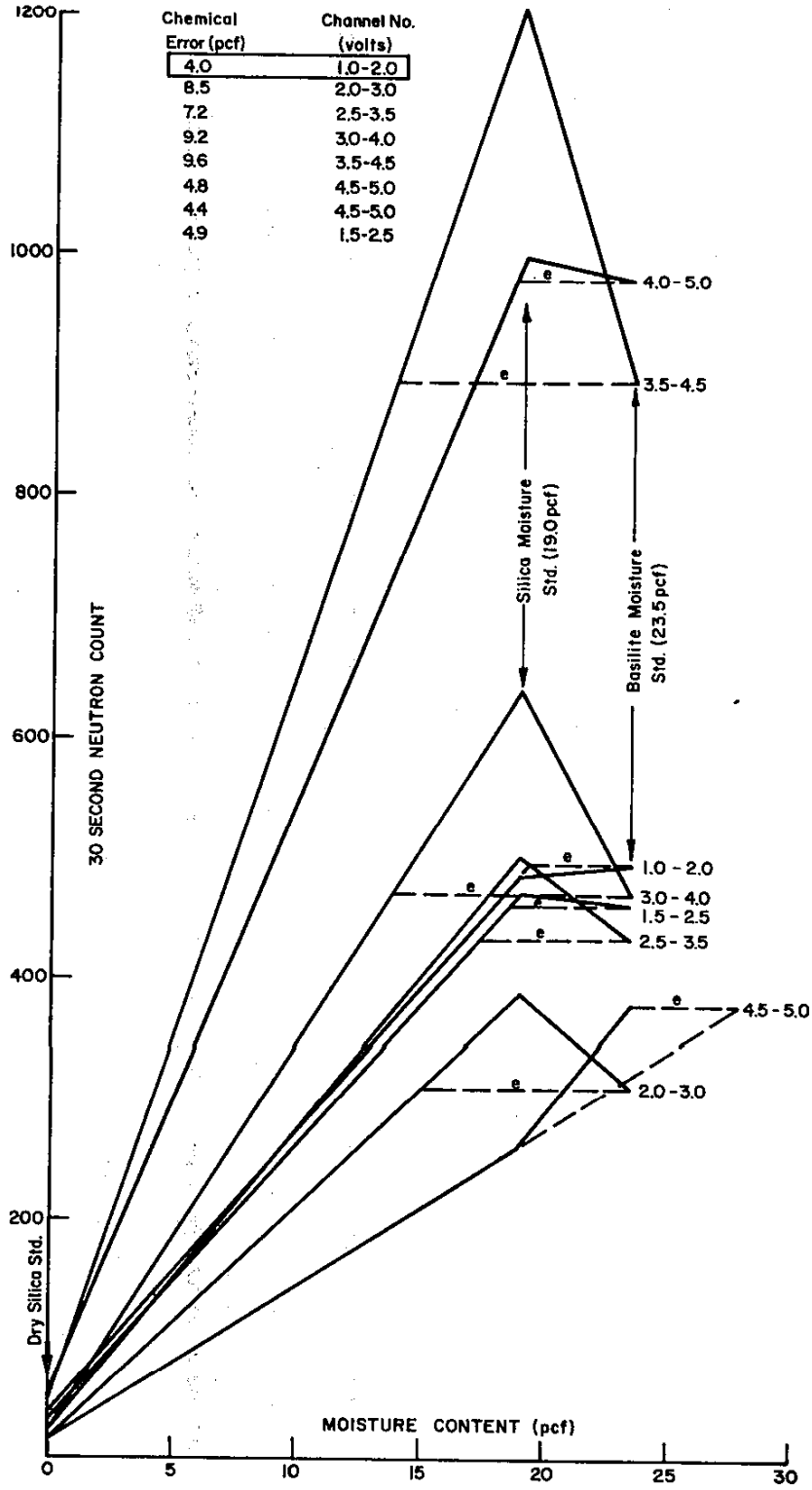

Figure 28

COMPARISON OF THERMAL NEUTRON DETECTORS BY MOISTURE GAGE CALIBRATION CURVES

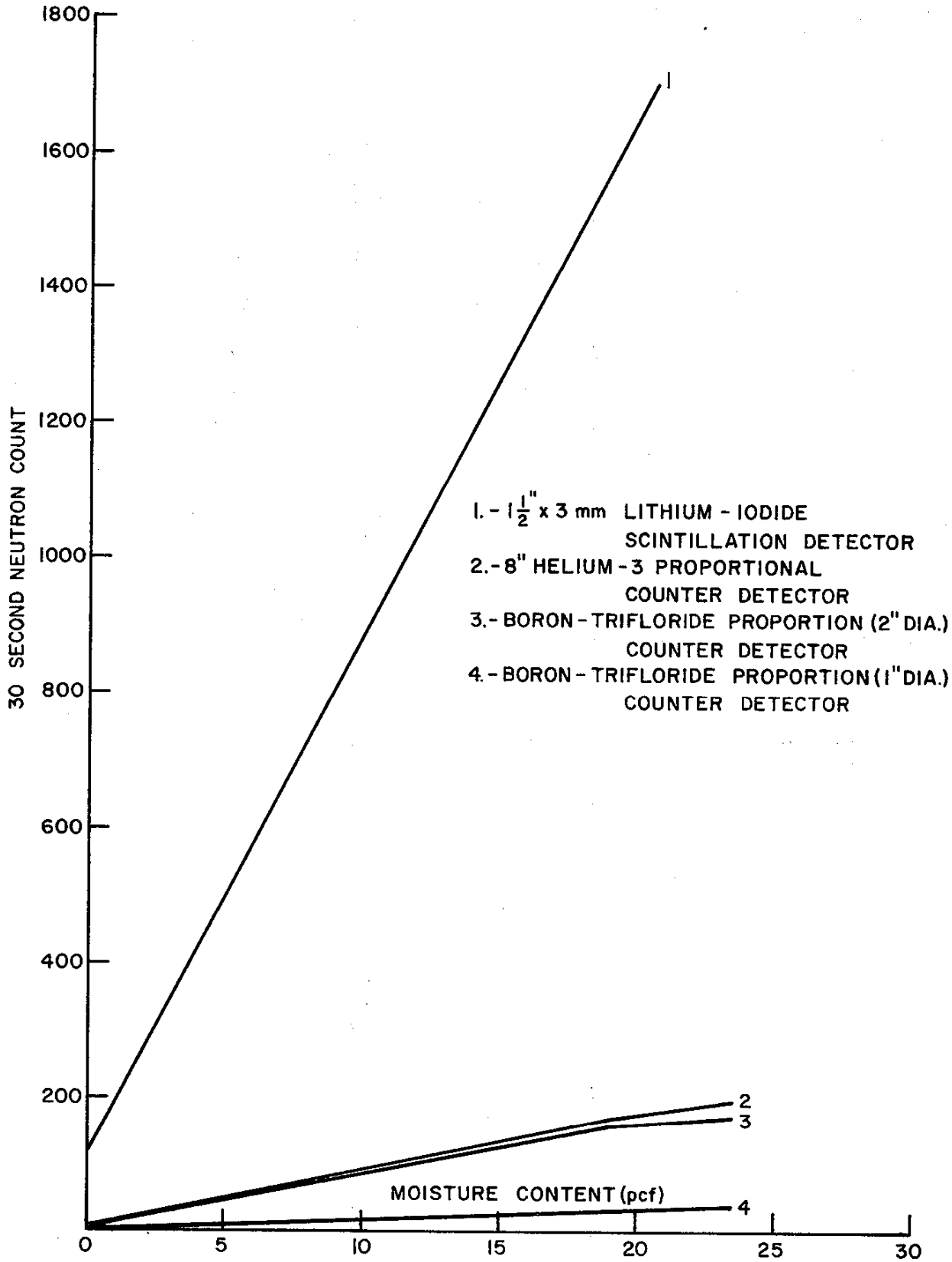

Figure 29

HELIUM (He_3) DETECTOR COUNT RATE PLATEAU INTERVALS OBTAINED BY APPLIED DETECTOR VOLTAGE AND AMPLIFICATION VARIATON

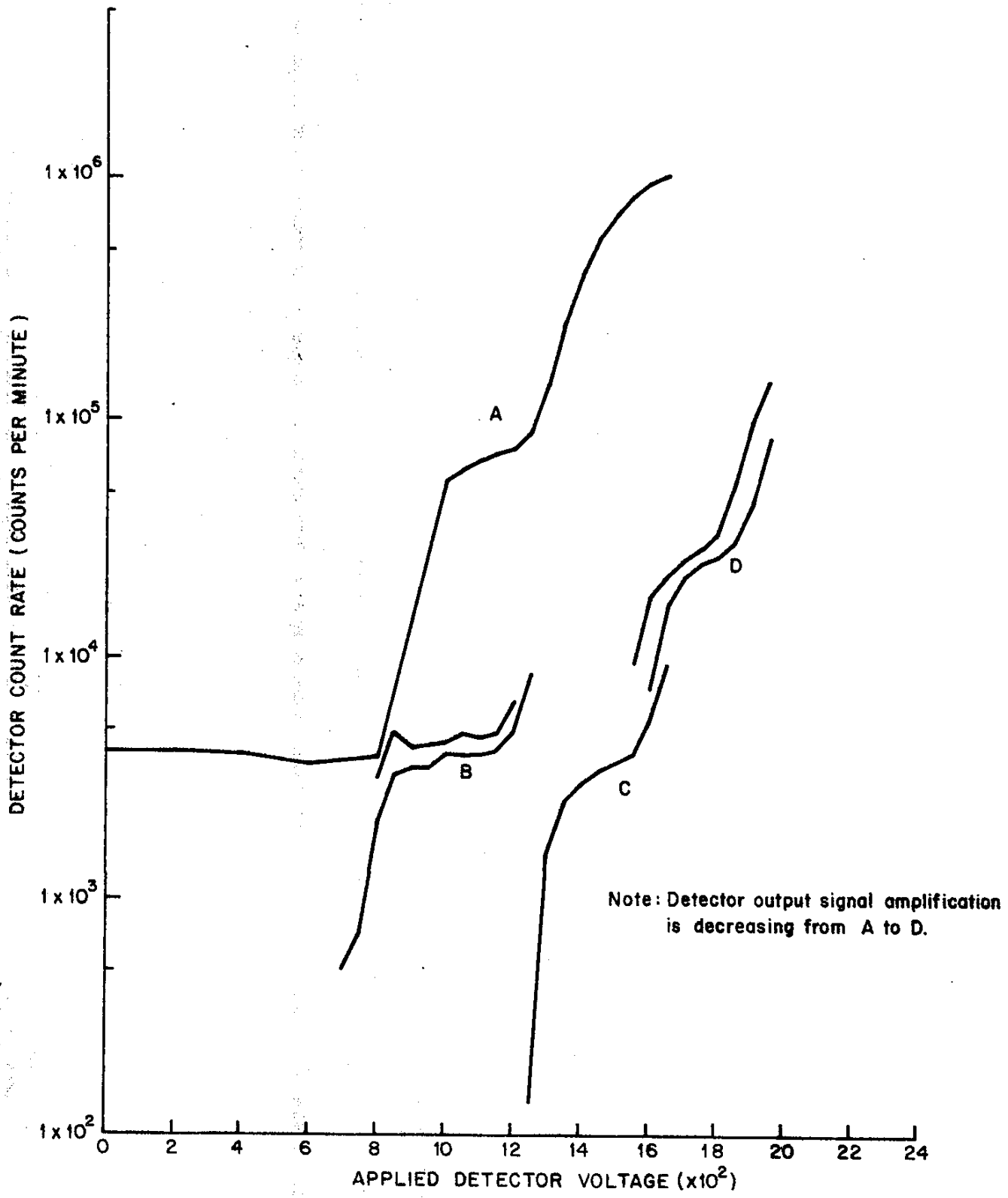

Figure 30

TWO INCH DIAMETER BORON TRIFLORIDE DETECTOR COUNT RATE PLATEAU INTERVALS OBTAINED BY APPLIED DETECTOR VOLTAGE AND AMPLIFICATION VARIATON

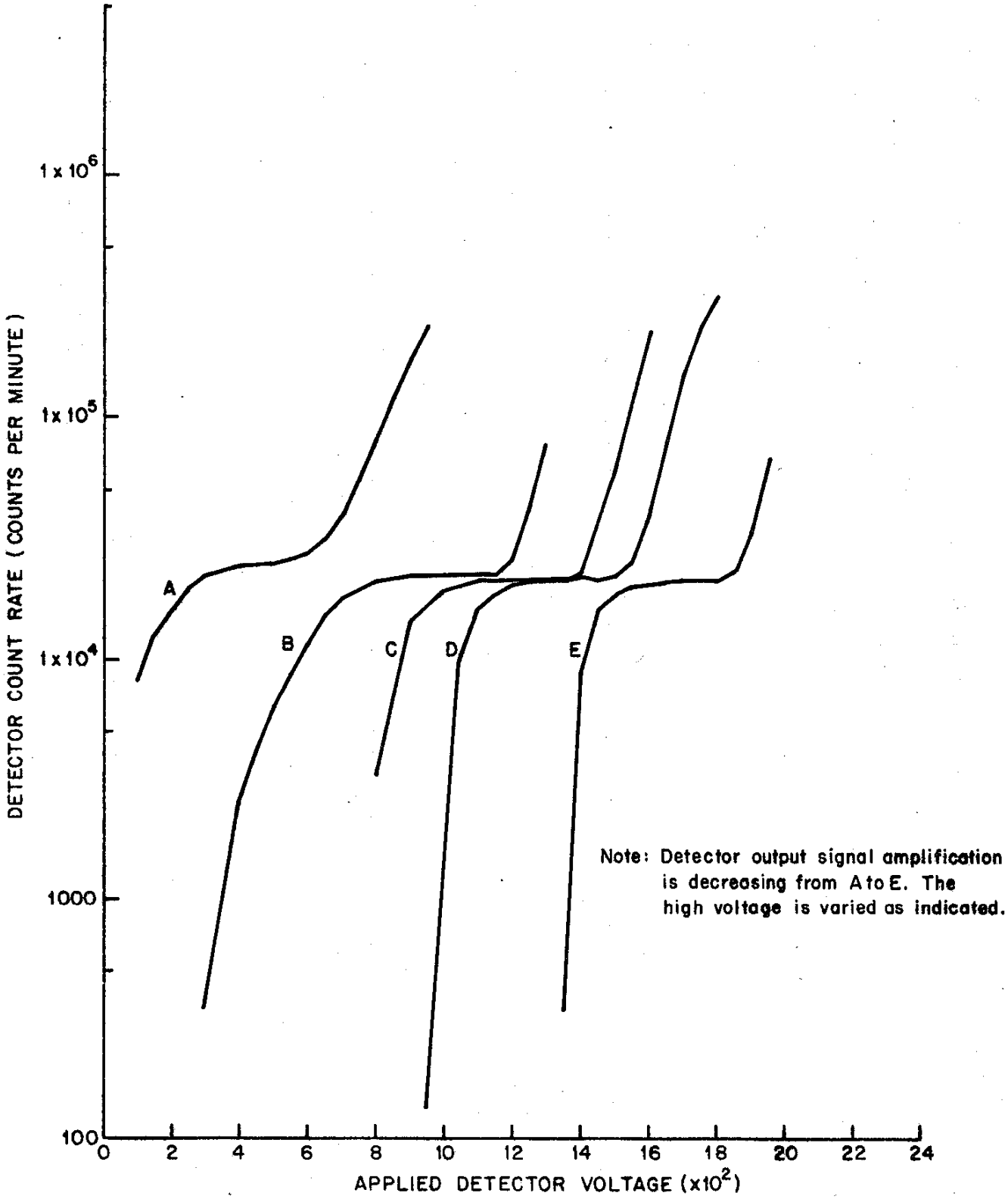

Figure 31

ONE INCH DIAMETER BORON TRIFLORIDE DETECTOR COUNT RATE PLATEAU INTERVALS
OBTAINED BY APPLIED DETECTOR VOLTAGE
AND AMPLIFICATION VARIATON

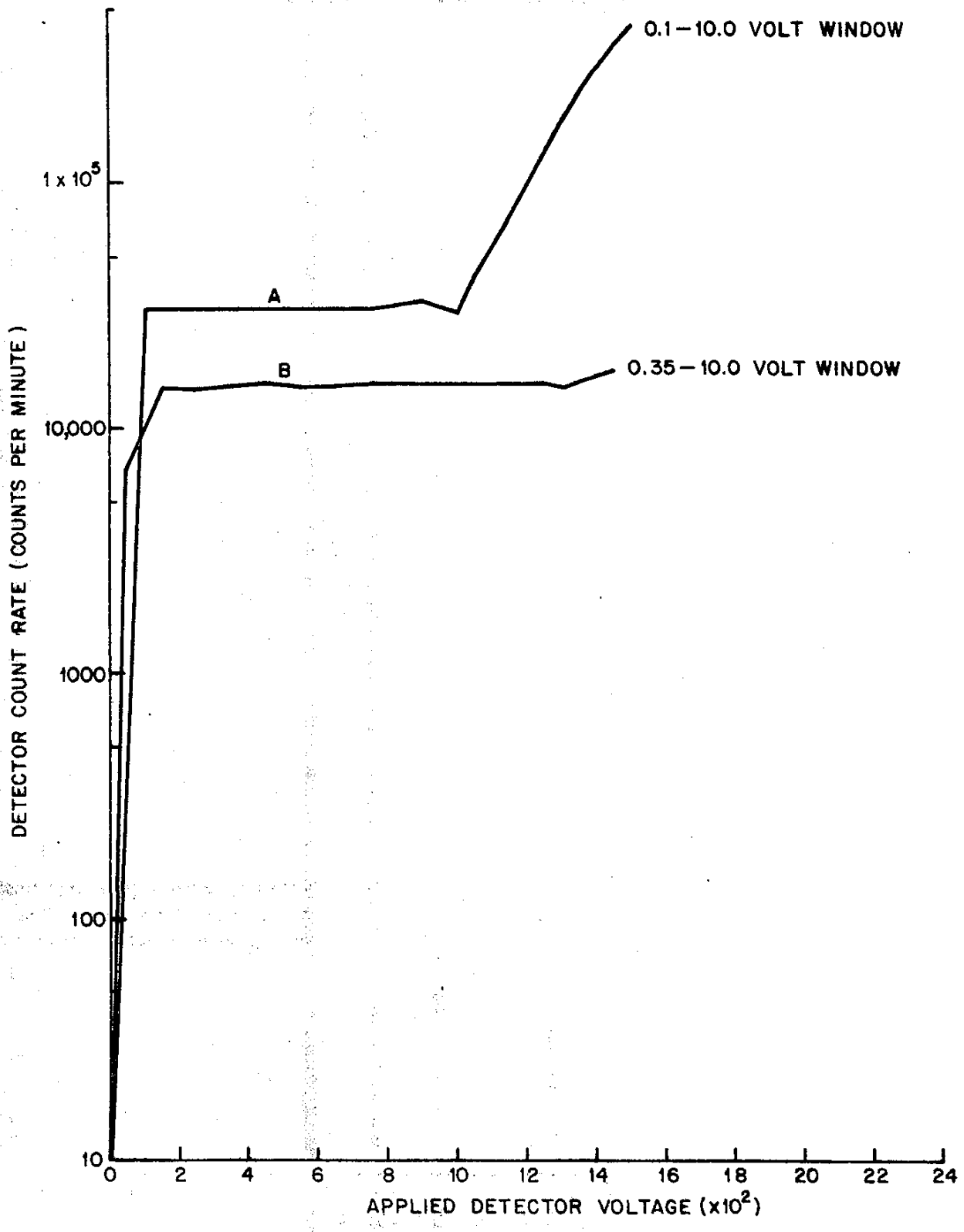

Figure 32

HELIUM (He-3) DETECTOR COUNT RATE VARIATIONS DUE TO OPERATING TEMPERATURE INFLUENCES

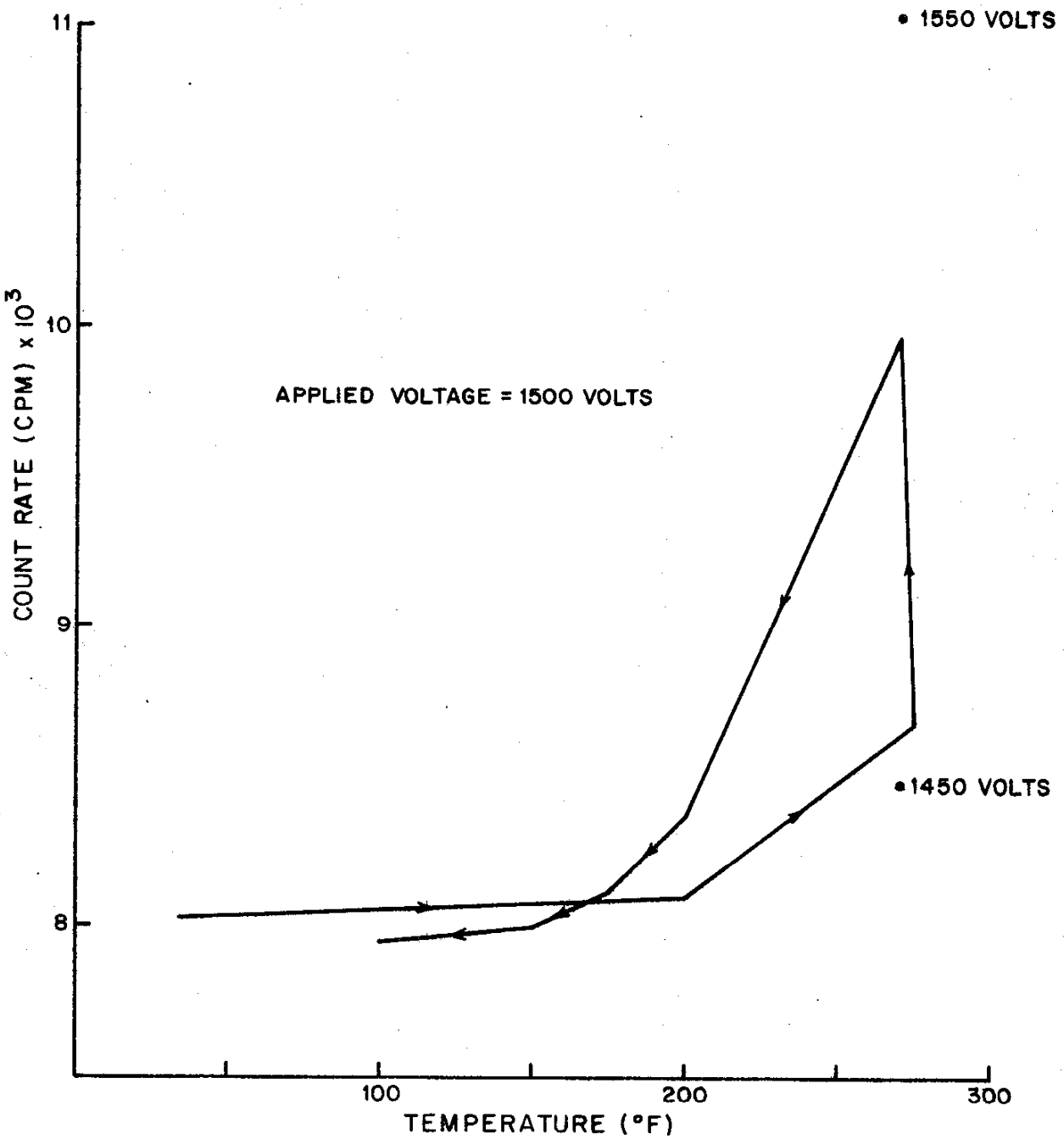

Figure 33

TWO INCH DIAMETER BORON TRIFLORIDE DETECTOR COUNT RATE VARIATION DUE TO OPERATING TEMPERATURE INFLUENCES

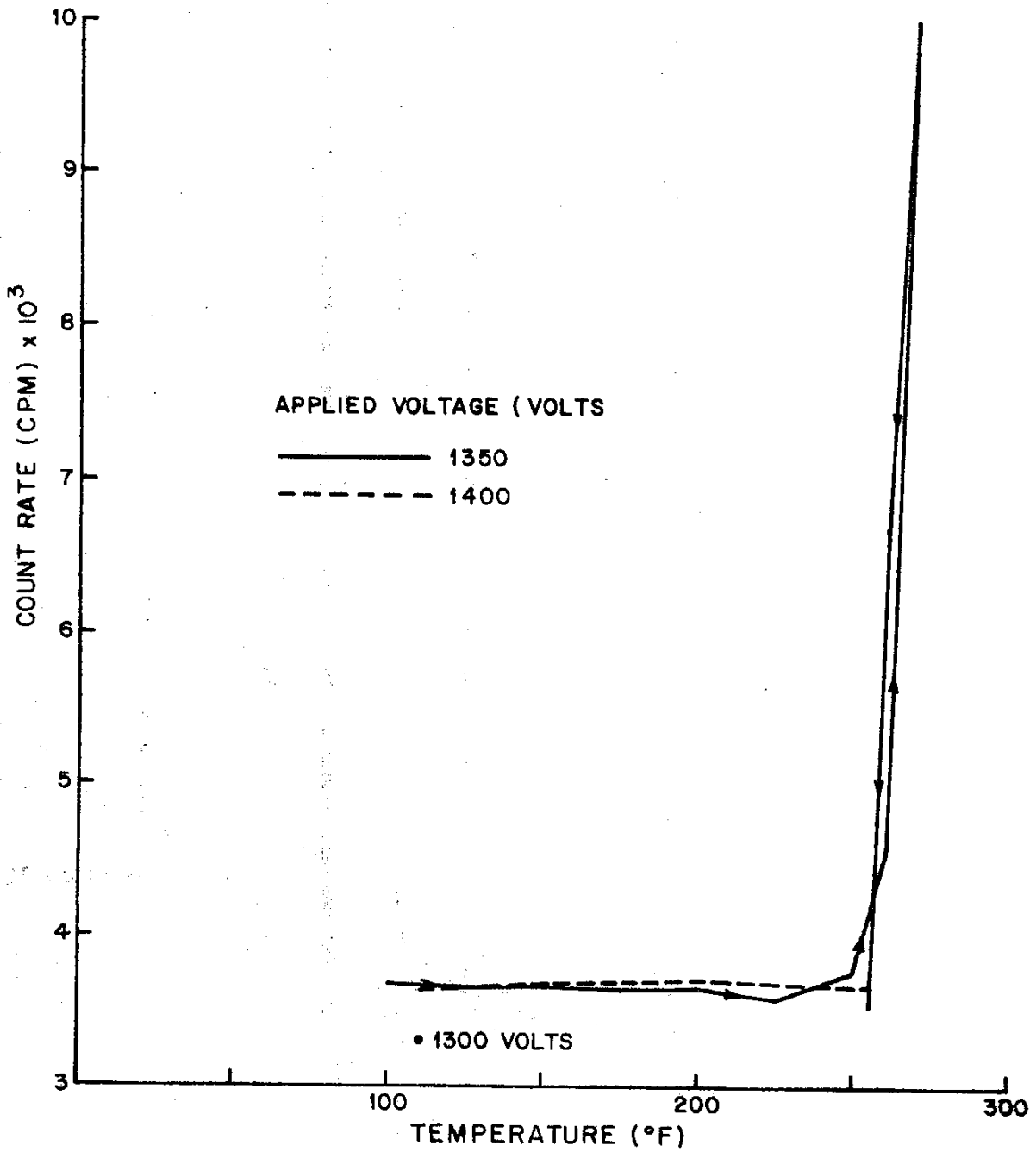

Figure 34

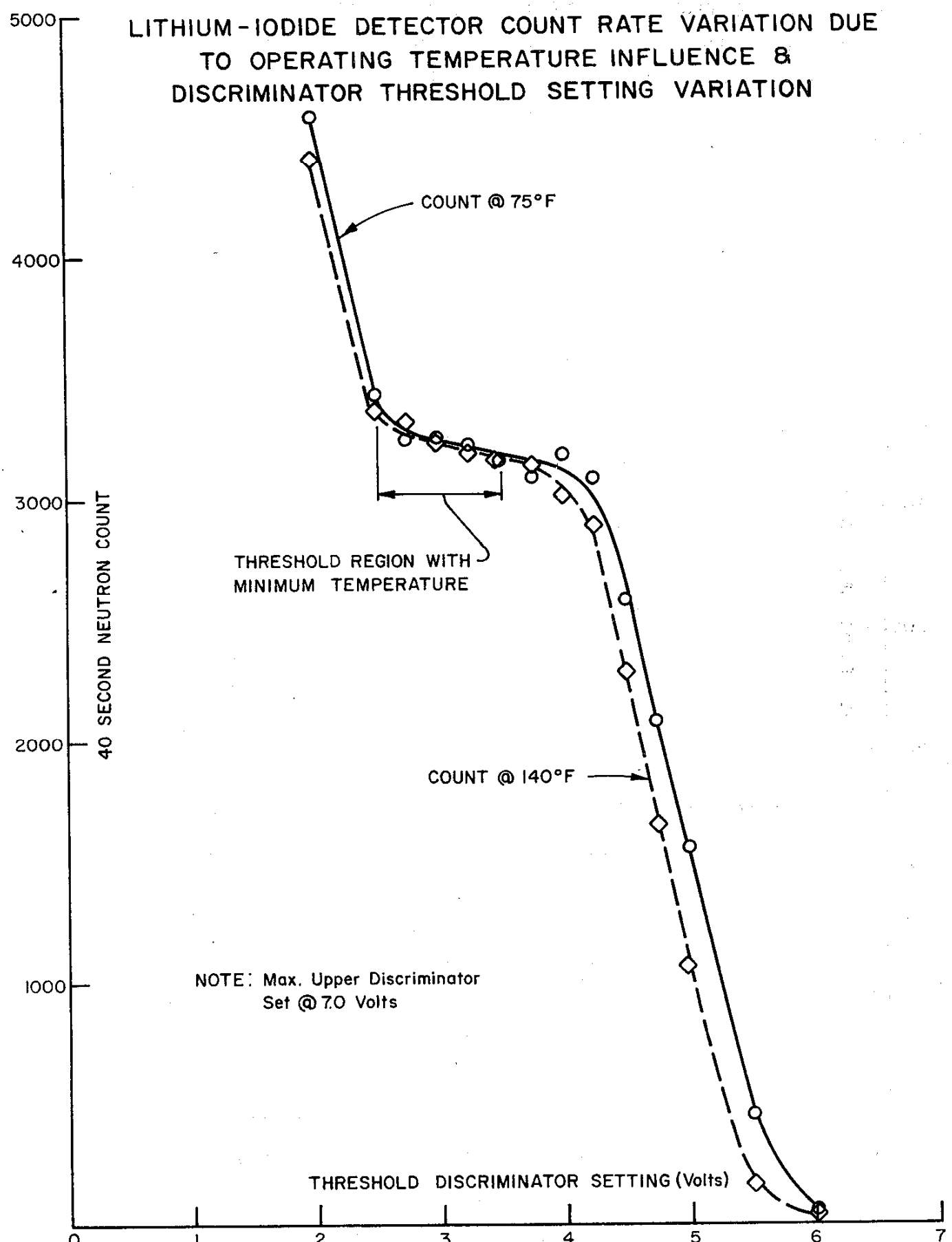
LITHIUM-IODIDE DETECTOR COUNT RATE VARIATION DUE TO OPERATING TEMPERATURE INFLUENCE & DISCRIMINATOR THRESHOLD SETTING VARIATION
COUNT @ 75°F
THRESHOLD REGION WITH MINIMUM TEMPERATURE
COUNT @ 140°F
NOTE: Max. Upper Discriminator Set @ 7.0 Volts
40 SECOND NEUTRON COUNT
5000
4000
3000
2000
1000
THRESHOLD DISCRIMINATOR SETTING (Volts)
0
1
2
3
4
5
6
7

Figure 35

LITHIUM - IODIDE DETECTOR COUNT RATE VARIATION DUE TO TEMPERATURE VARIATION AND DISCRIMINATOR INTERVAL

NOTE: DISCRIMINATOR INTERVAL = 0.5 VOLTS

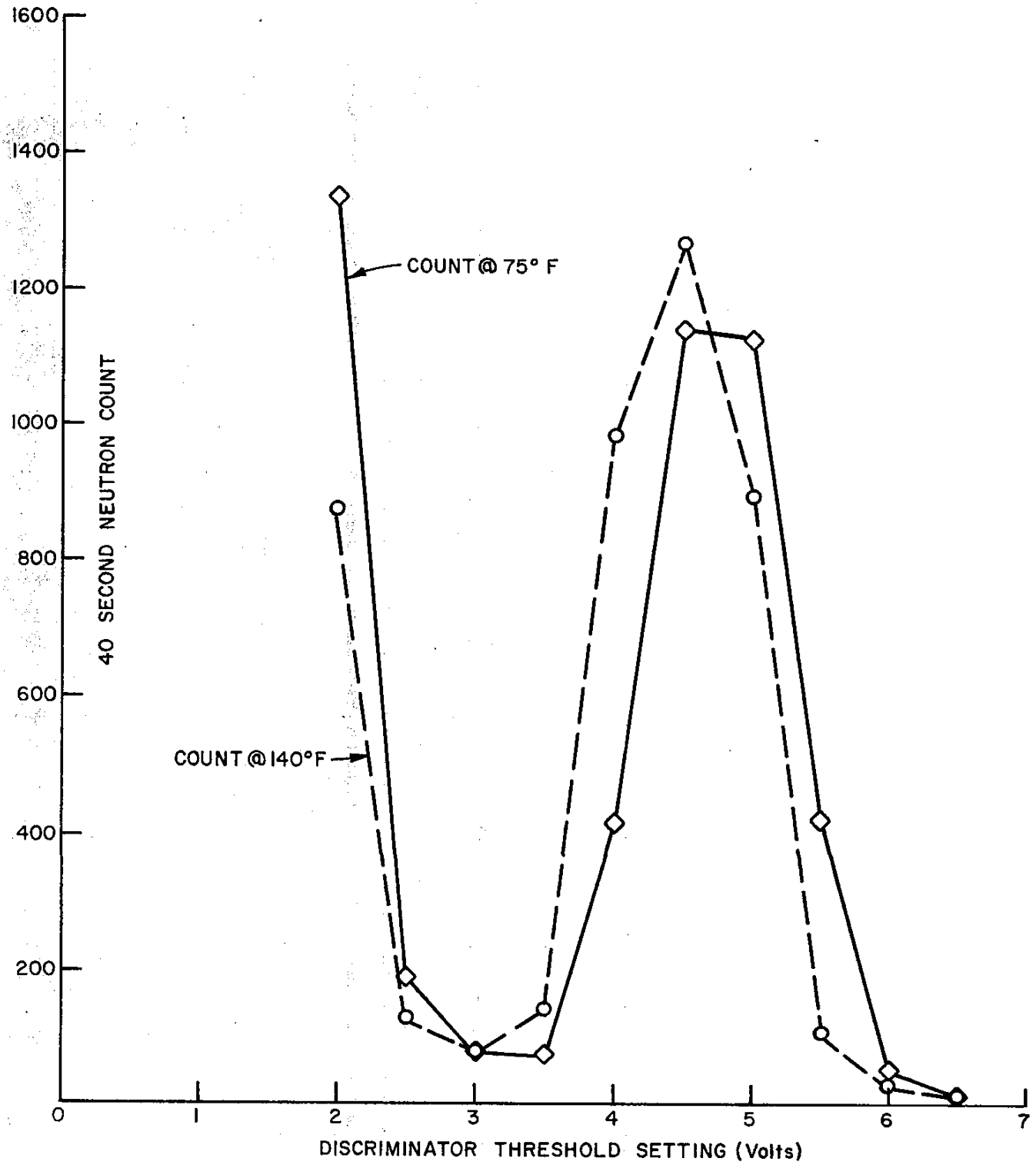

Figure 36

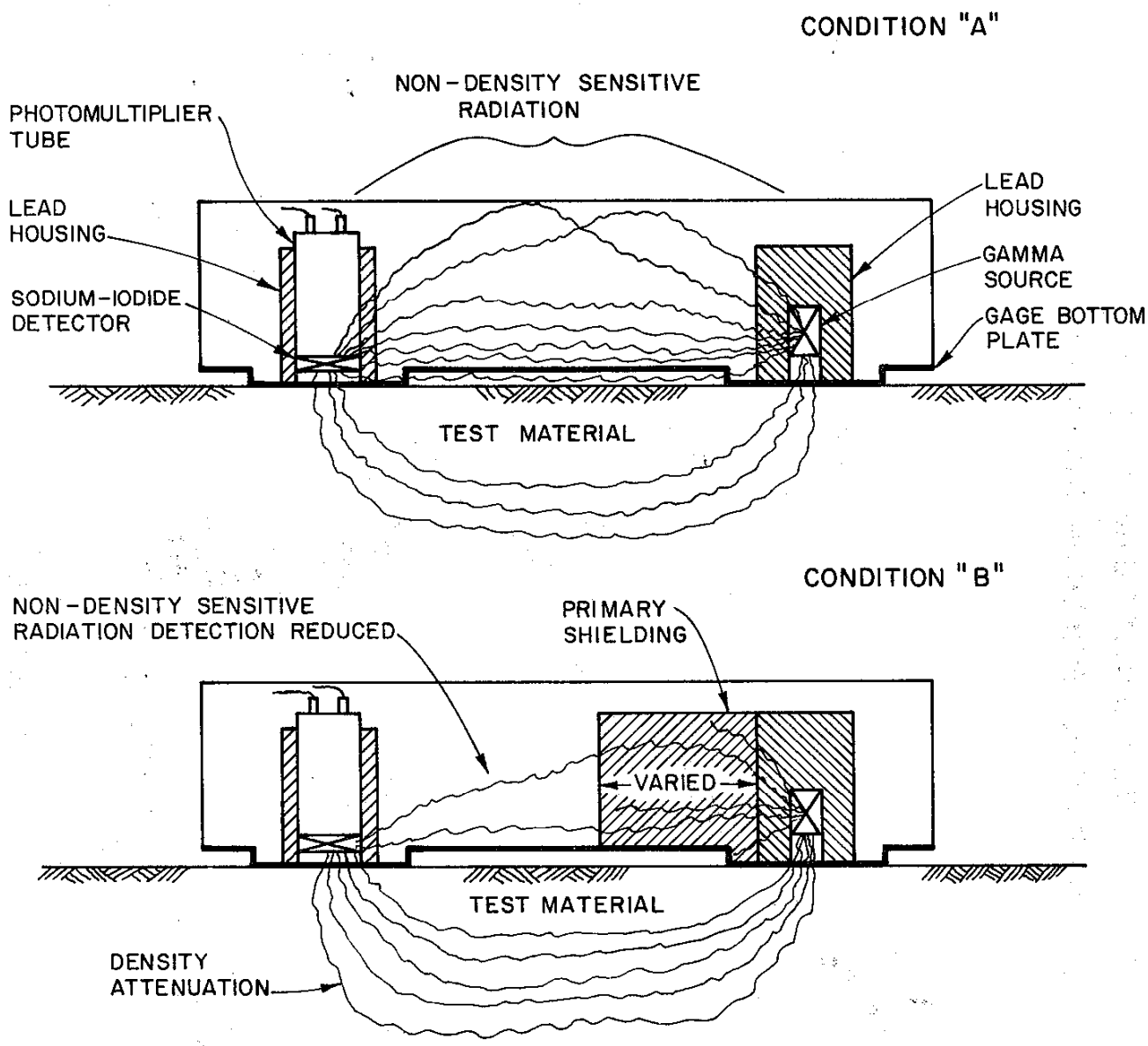

BACKSCATTER DENSITY GAGE PRIMARY SHIELDING

Figure 37

VARIATION OF BACKSCATTER DENSITY GAGE CALIBRATION CURVE DUE TO PRIMARY SHIELDING THICKNESS

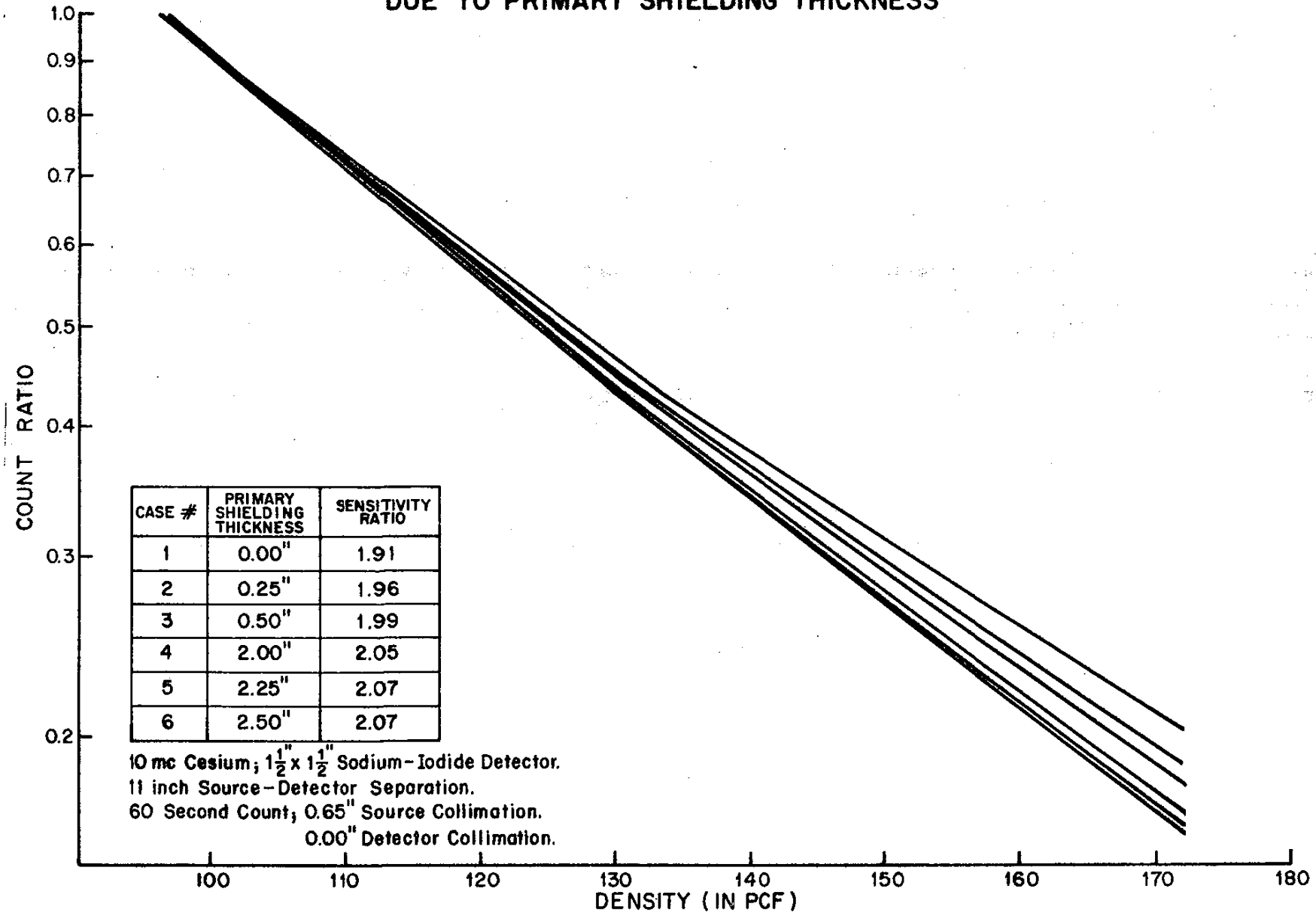

CASE #	PRIMARY SHIELDING THICKNESS	SENSITIVITY RATIO
1	0.00"	1.91
2	0.25"	1.96
3	0.50"	1.99
4	2.00"	2.05
5	2.25"	2.07
6	2.50"	2.07

10 mc Cesium; $1\frac{1}{2}$" x $1\frac{1}{2}$" Sodium-Iodide Detector.
11 inch Source-Detector Separation.
60 Second Count; 0.65" Source Collimation.
0.00" Detector Collimation.

Figure 38

OBSERVED DENSITY STANDARD COUNT RATE CHANGE DUE TO PRIMARY SHIELDING THICKNESS

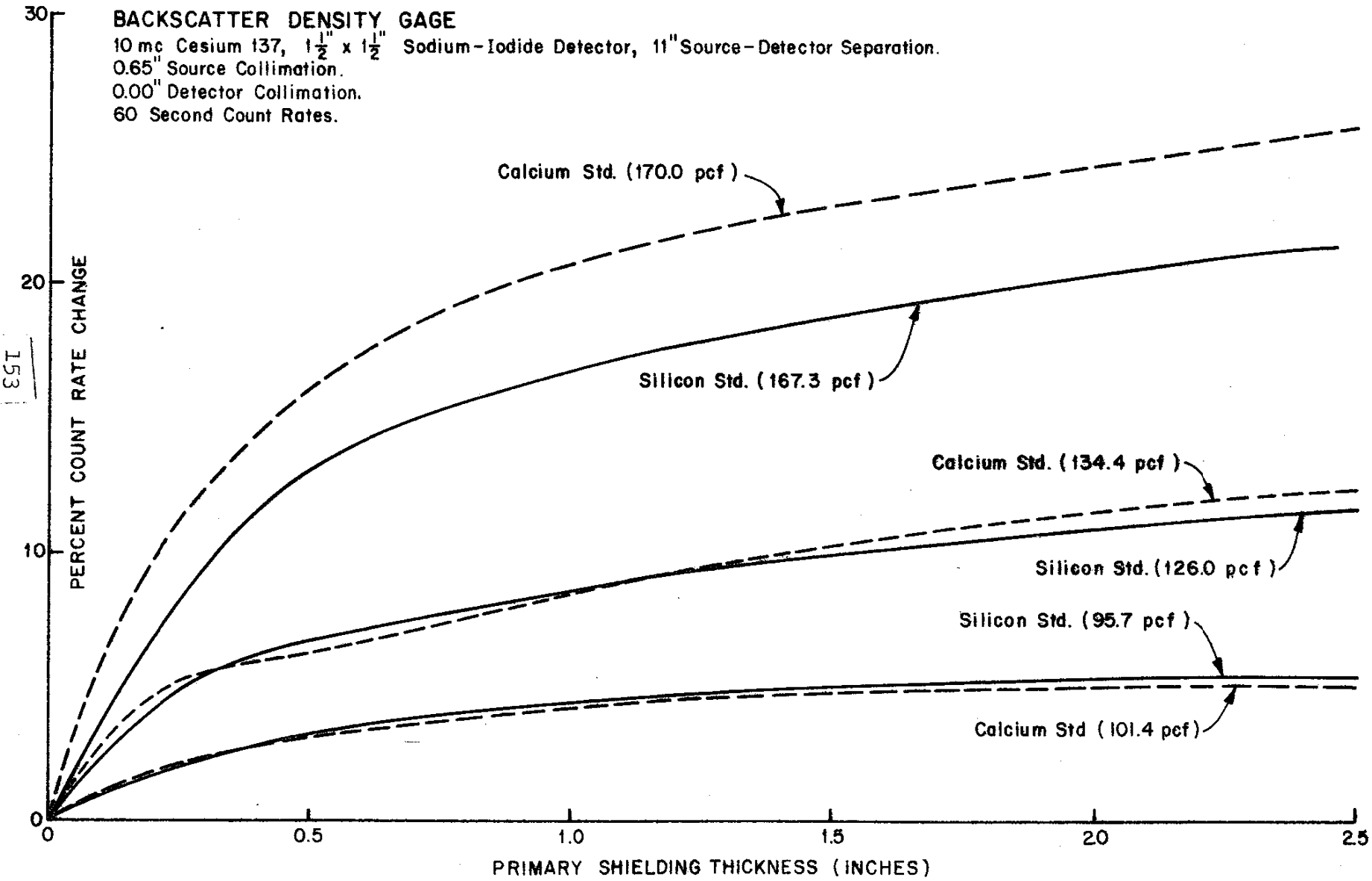

Figure 39

AVERAGE PERCENT COUNT RATE REDUCTION DUE TO PRIMARY SHIELDING RECORDED ON THE CALIFORNIA DENSITY CALIBRATION STANDARDS

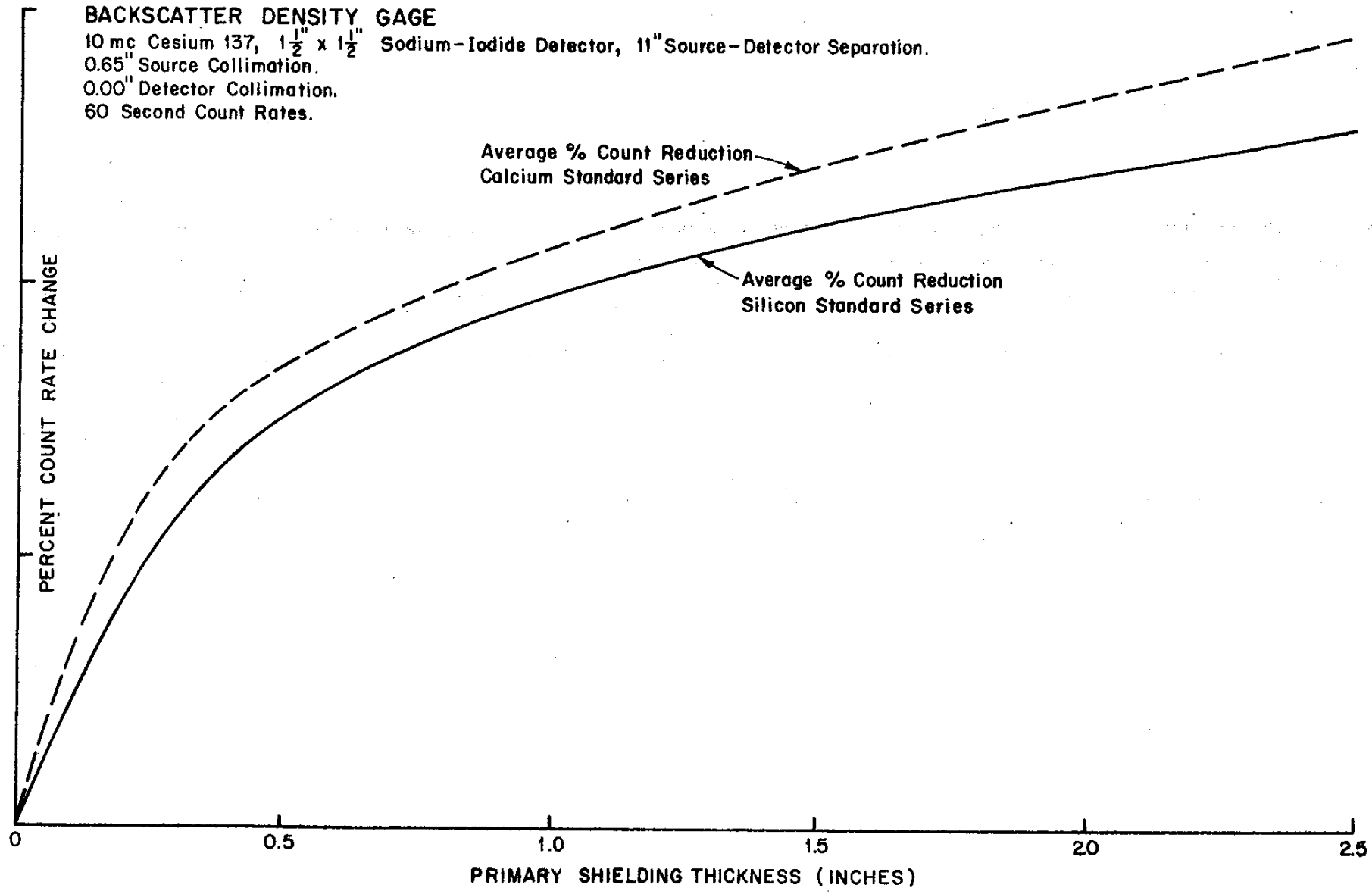

Figure 40

BACKSCATTER DENSITY GAGE CHEMICAL COMPOSITION ERROR
DUE TO PRIMARY SHIELDING THICKNESS

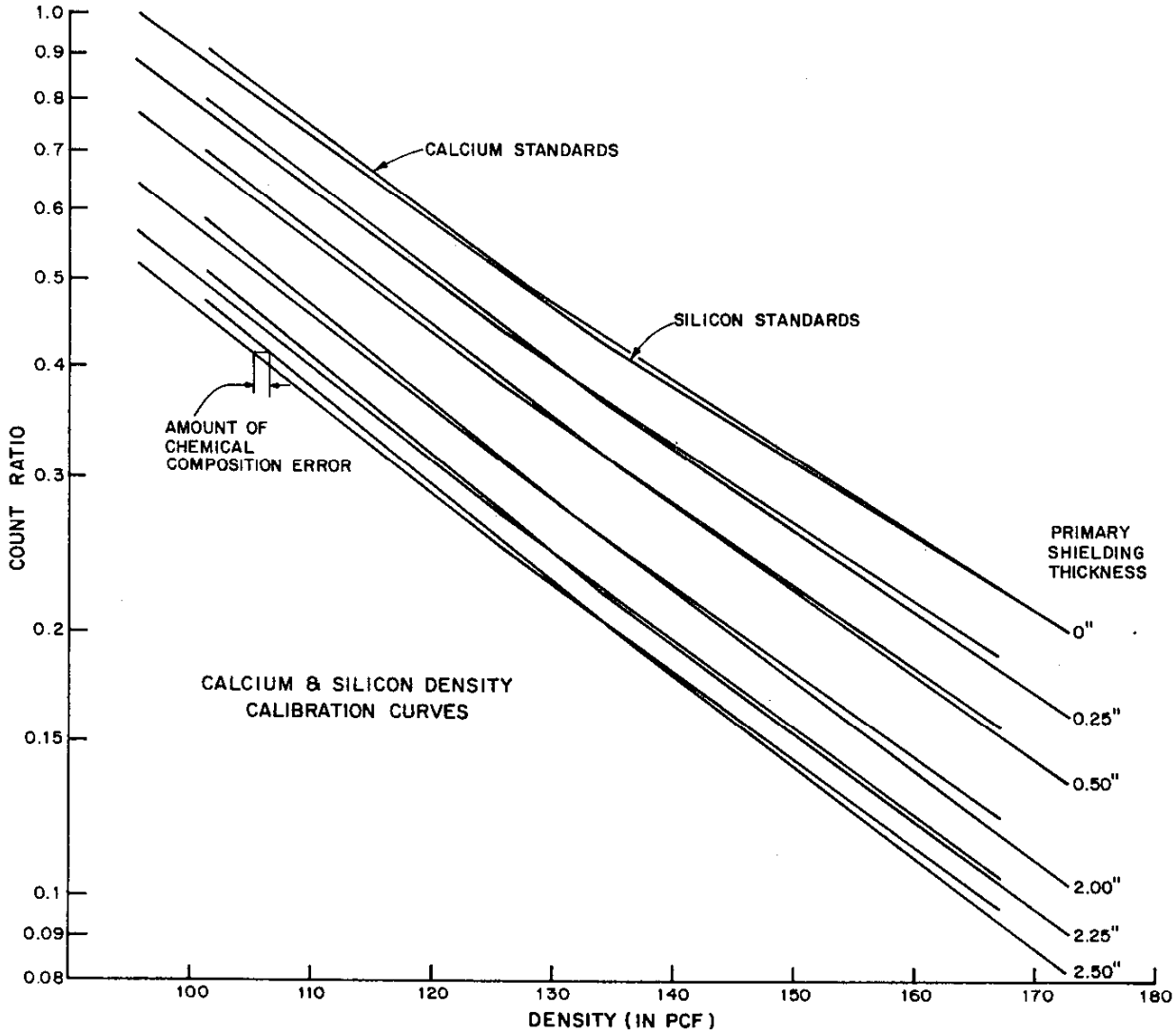

Figure 41

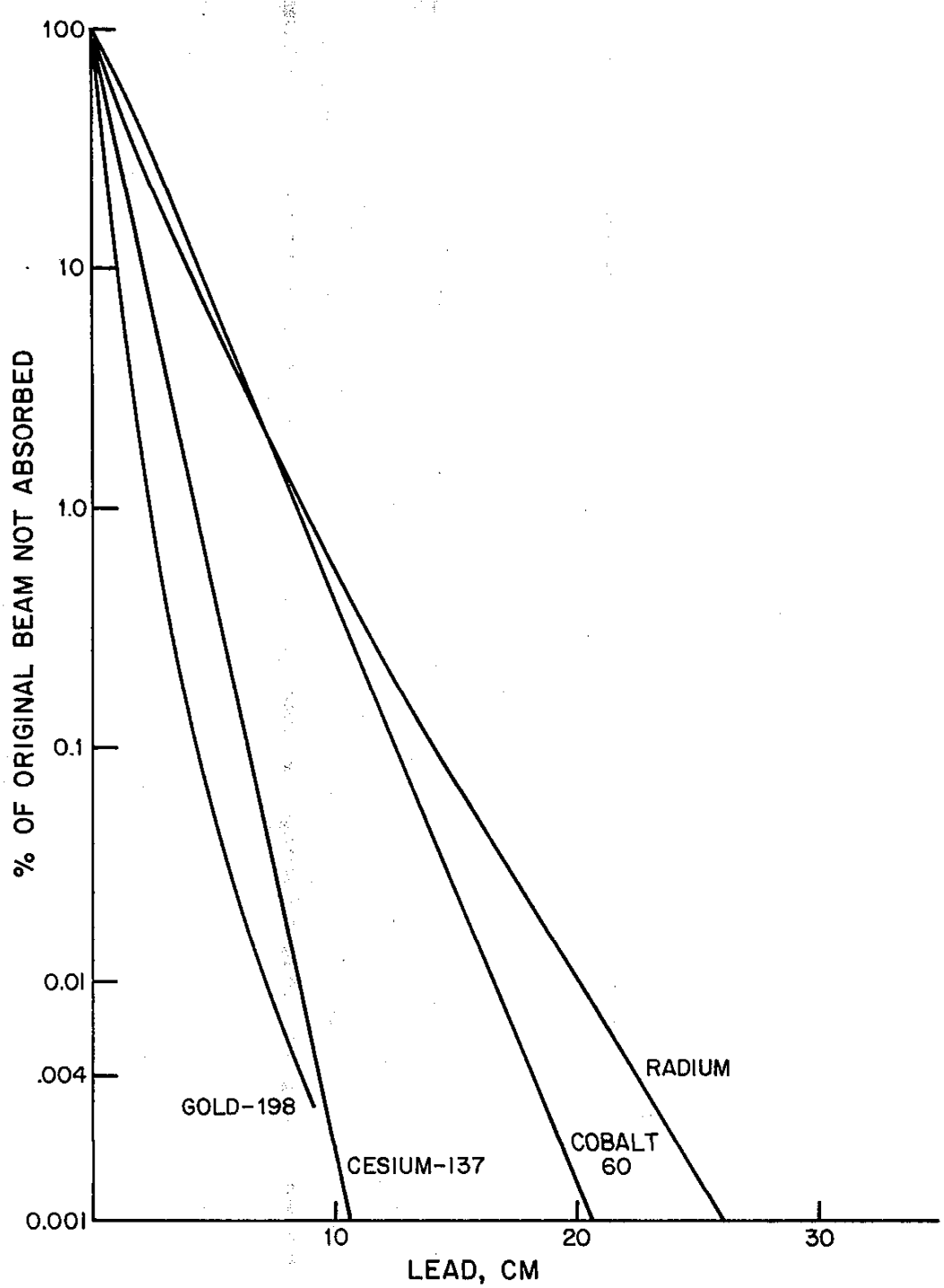

GAMMA RAY ABSORPTION USING LEAD

Figure 42

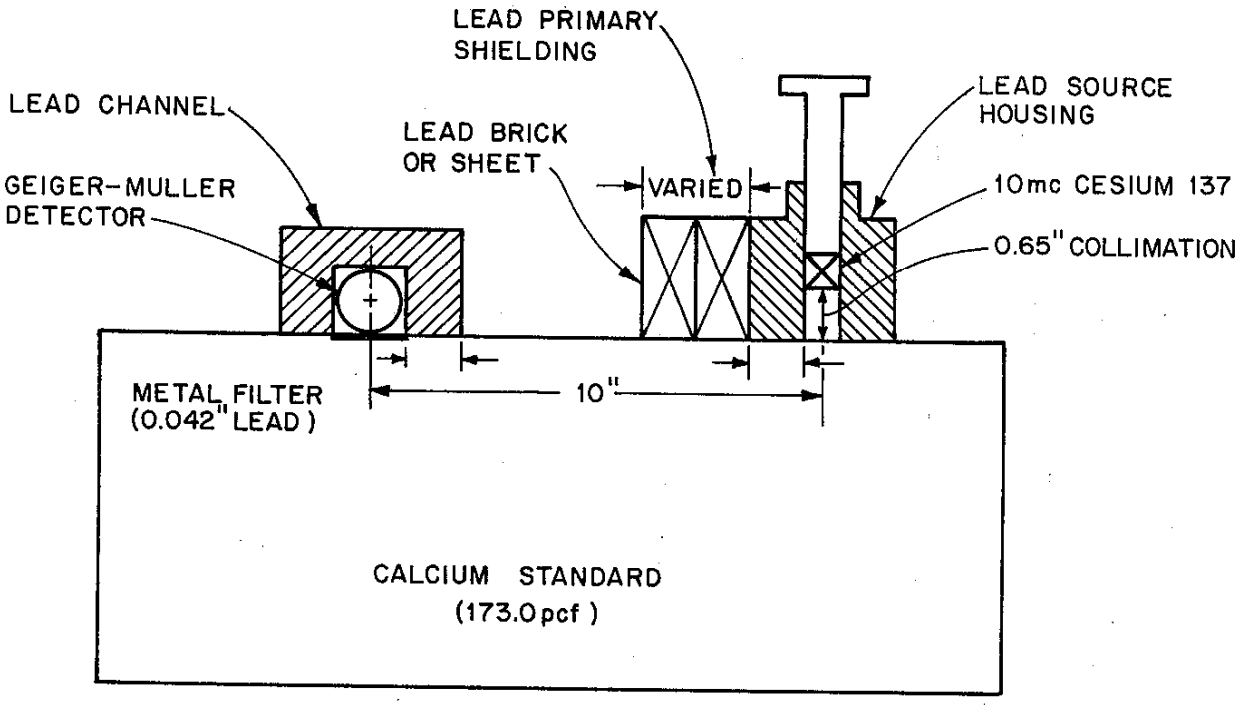

GEIGER-MUELLER BACKSCATTER DENSITY GAGE
PRIMARY SHIELDING TEST APPARATUS

Figure 43

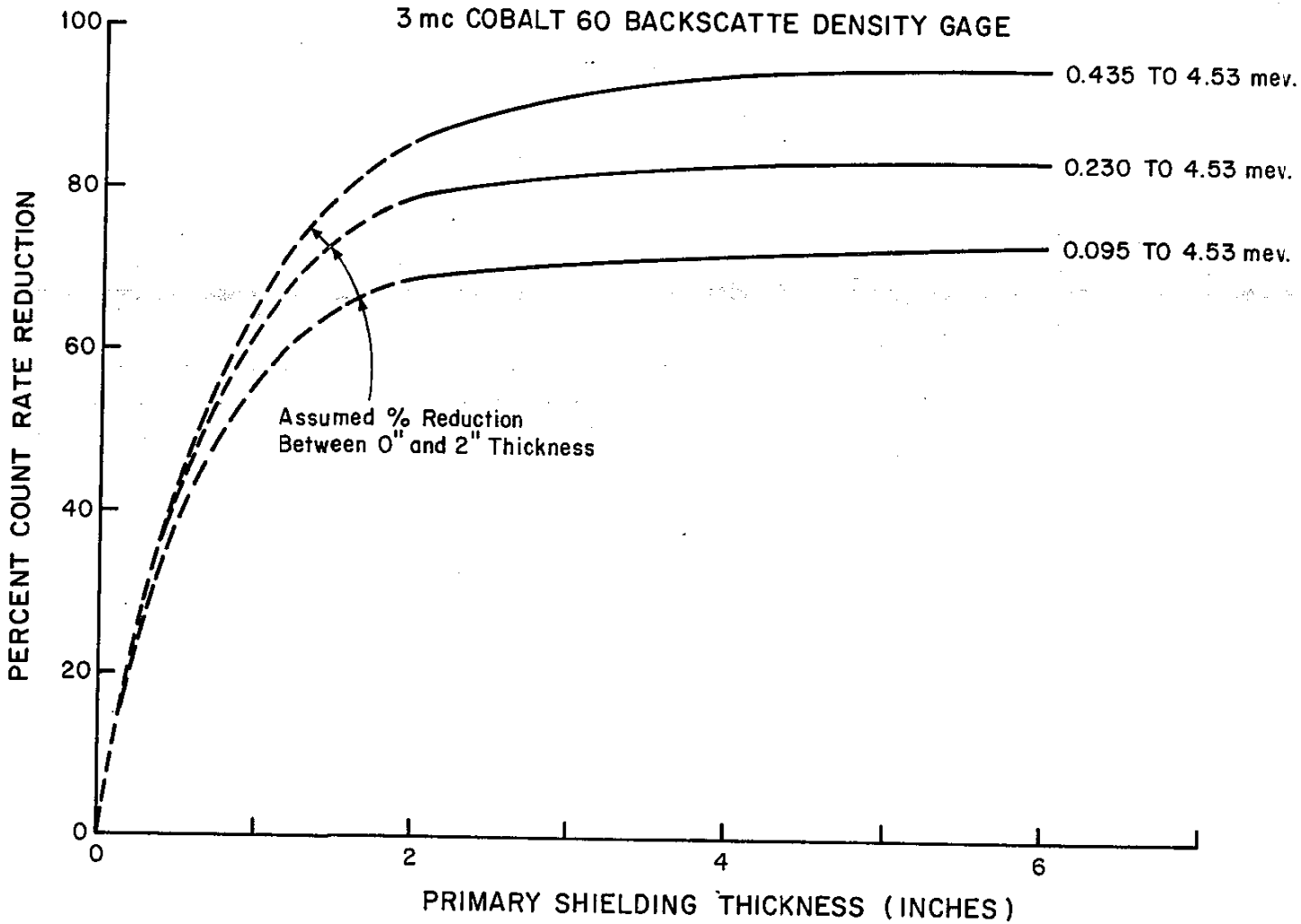

OBSERVED PERCENT COUNT RATE REDUCTION
DUE TO PRIMARY SHIELDING THICKNESS AND DETECTED GAMMA ENERGIES

Figure 44

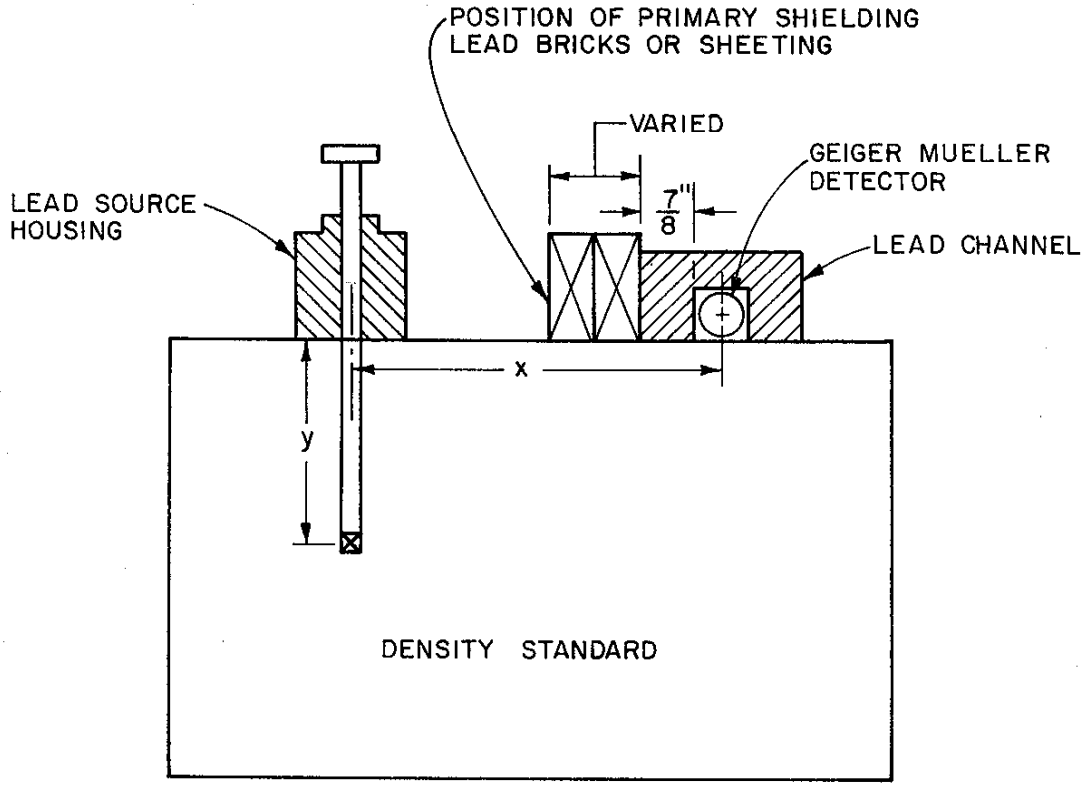

TRANSMISSION GAGE TEST APPARATUS TO DETERMINE PRIMARY SHIELDING INFLUENCE ON COUNT RATE

Figure 45

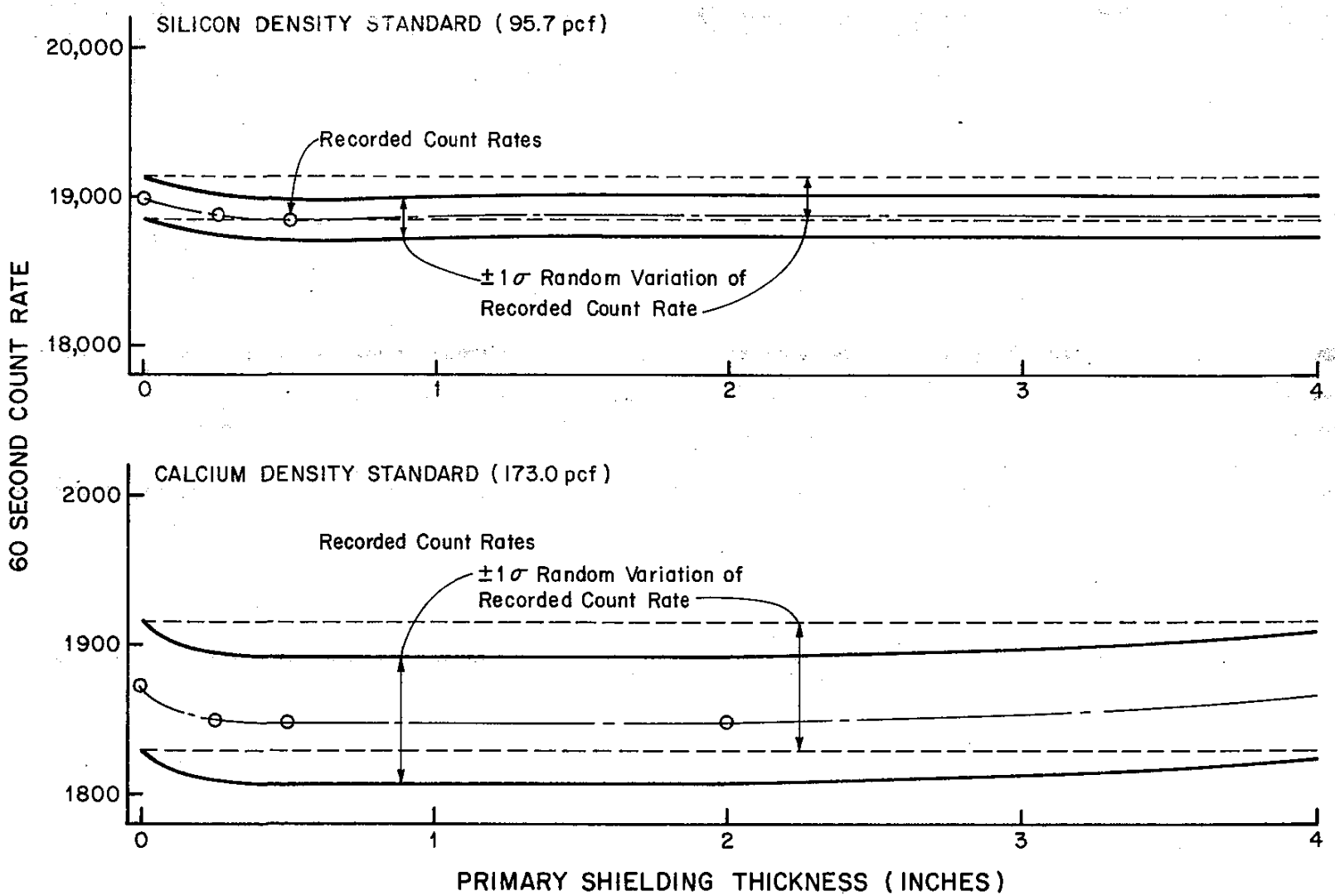

PRIMARY SHIELDING INFLUENCE ON TRANSMISSION GAGE COUNT RATE

Figure 46

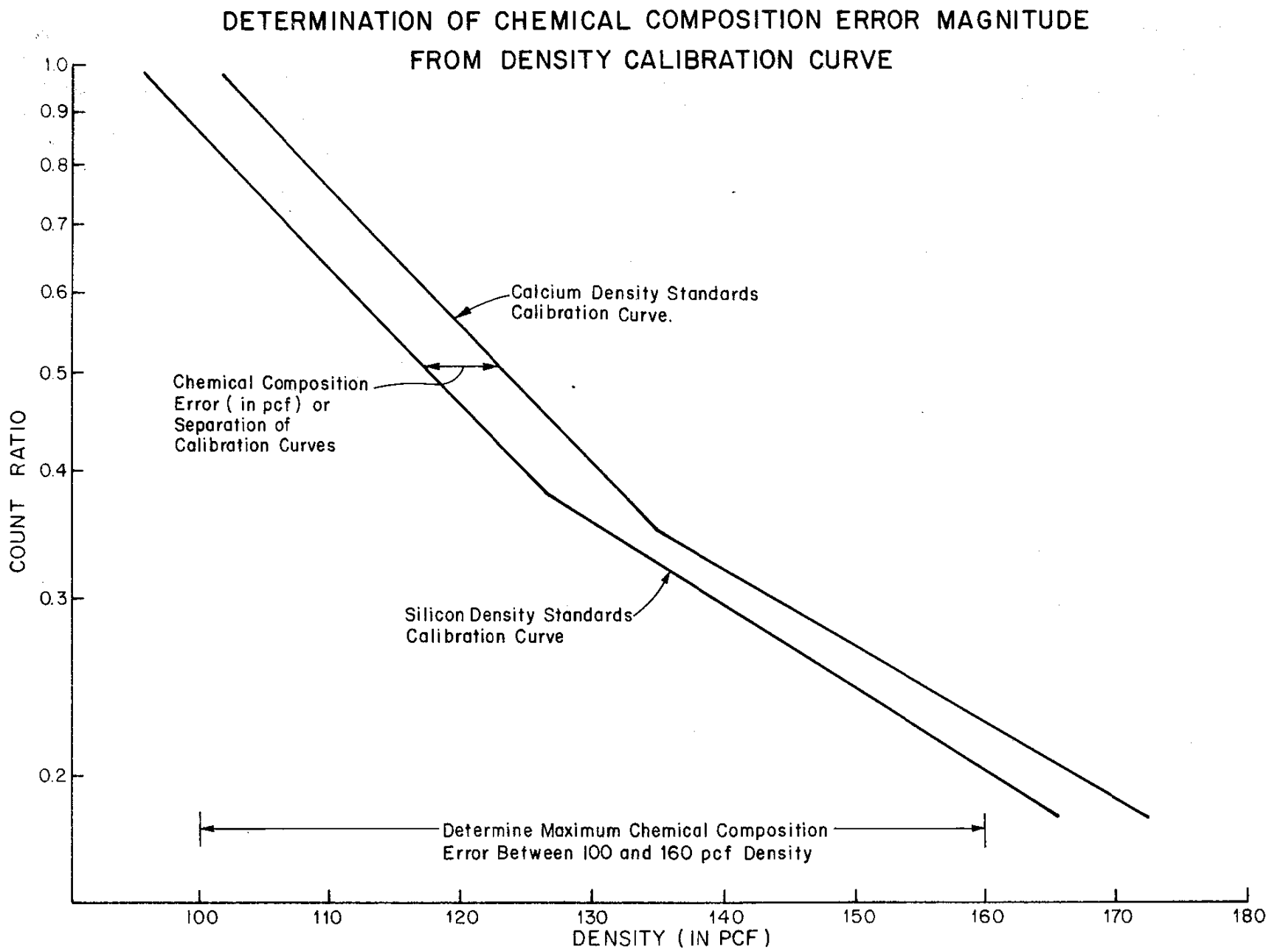
DETERMINATION OF CHEMICAL COMPOSITION ERROR MAGNITUDE
FROM DENSITY CALIBRATION CURVE
COUNT RATIO
1.0
0.9
0.8
0.7
0.6
0.5
0.4
0.3
0.2
Calcium Density Standards
Calibration Curve.
Chemical Composition
Error (in pcf) or
Separation of
Calibration Curves
Silicon Density Standards
Calibration Curve
Determine Maximum Chemical Composition
Error Between 100 and 160 pcf Density
100
110
120
130
140
150
160
170
180
DENSITY (IN PCF)

Figure 47

THE EFFECT OF NEUTRON ENERGY DISCRIMINATION ON MOISTURE GAGE CHEMICAL COMPOSITION ERROR

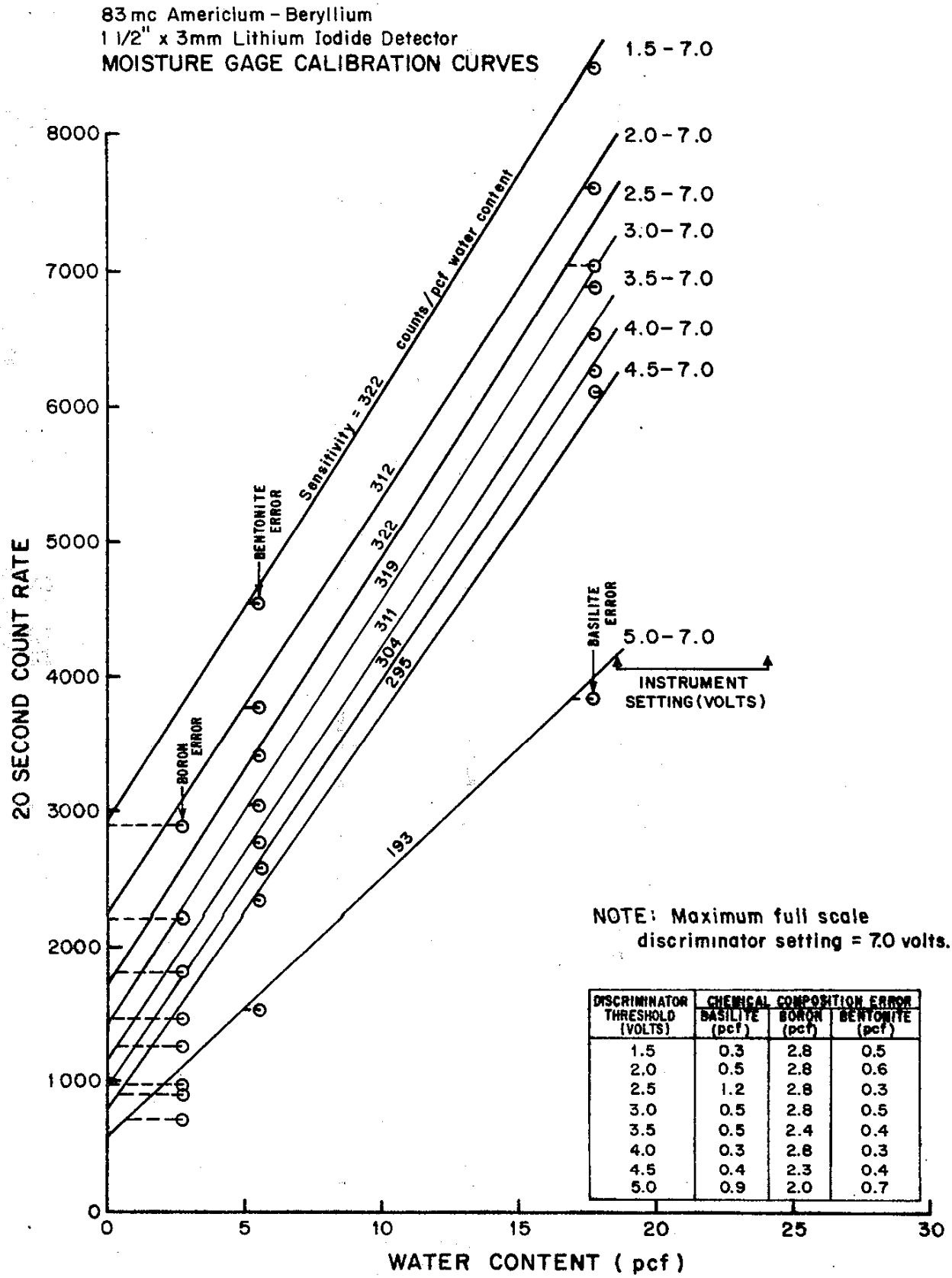

NOTE: Maximum full scale discriminator setting = 7.0 volts.

DISCRIMINATOR THRESHOLD (VOLTS)	CHEMICAL COMPOSITION ERROR		
	BASILITE (pcf)	BORON (pcf)	BENTONITE (pcf)
1.5	0.3	2.8	0.5
2.0	0.5	2.8	0.6
2.5	1.2	2.8	0.3
3.0	0.5	2.8	0.5
3.5	0.5	2.4	0.4
4.0	0.3	2.8	0.3
4.5	0.4	2.3	0.4
5.0	0.9	2.0	0.7

Figure 48

EFFECTIVENESS OF 0.01" CADMIUM-DISCRIMINATOR ON MOISTURE GAGE CHEMICAL COMPOSITION ERROR

83 mc Americium - Beryllium
1 1/2" x 3mm Lithium Iodide Detector
MOISTURE GAGE CALIBRATION CURVES

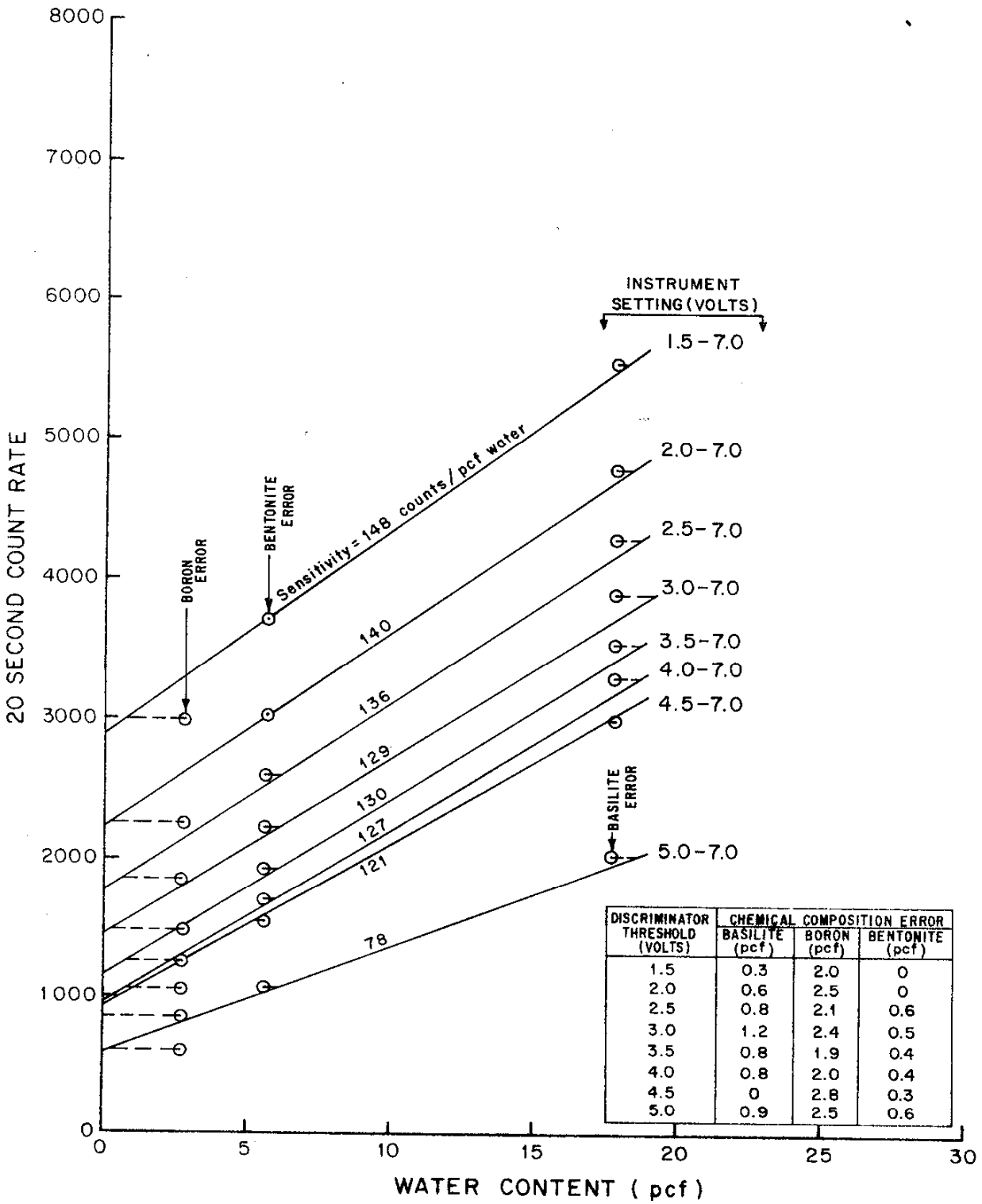

DISCRIMINATOR THRESHOLD (VOLTS)	CHEMICAL COMPOSITION ERROR		
	BASILITE (pcf)	BORON (pcf)	BENTONITE (pcf)
1.5	0.3	2.0	0
2.0	0.6	2.5	0
2.5	0.8	2.1	0.6
3.0	1.2	2.4	0.5
3.5	0.8	1.9	0.4
4.0	0.8	2.0	0.4
4.5	0	2.8	0.3
5.0	0.9	2.5	0.6

Figure 49

EFFECTIVENESS OF 0.2188" POLYETHYLENE-FILTER DISCRIMINATOR ON MOISTURE GAGE CHEMICAL COMPOSITION ERROR

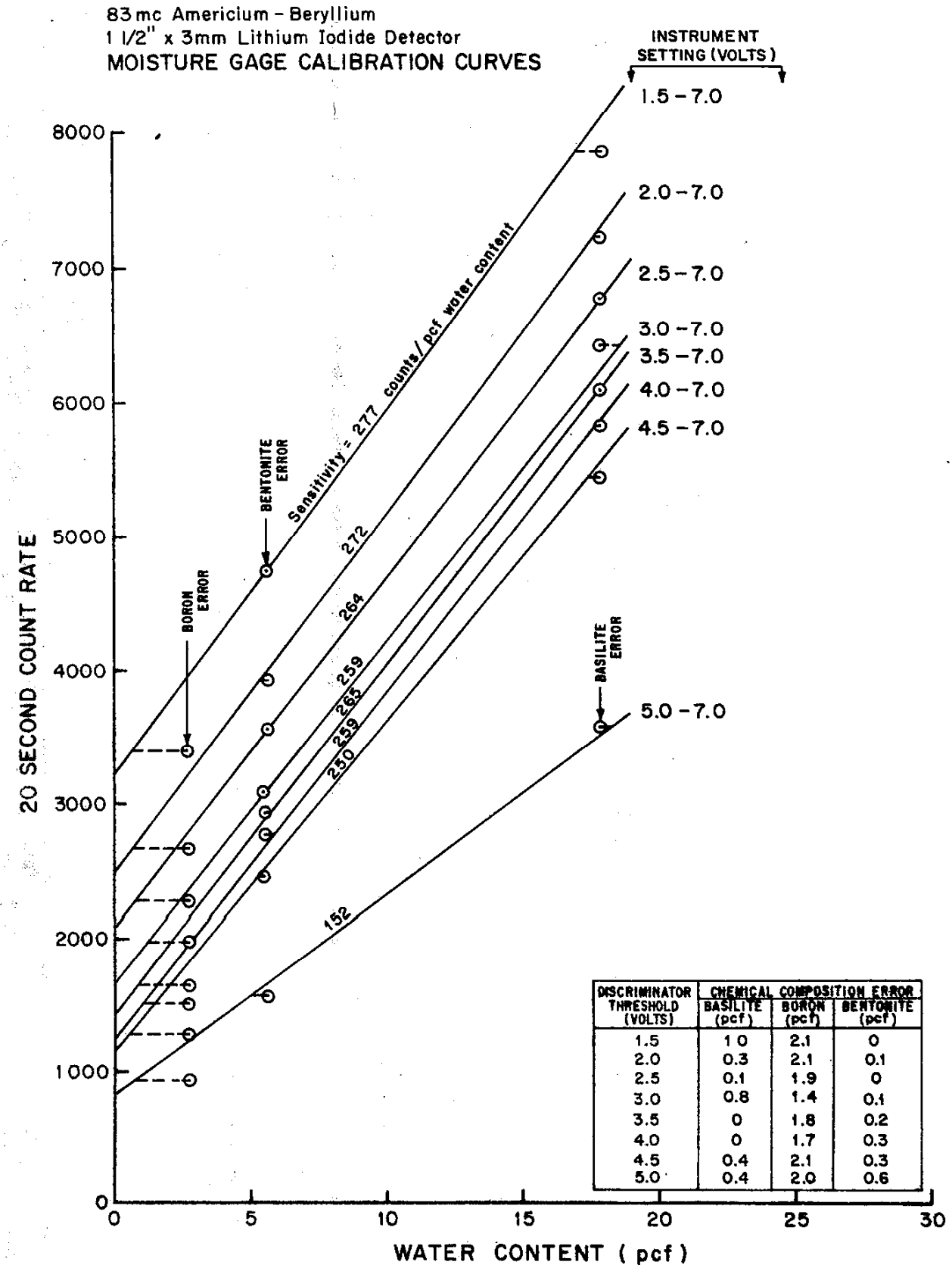

DISCRIMINATOR THRESHOLD (VOLTS)	CHEMICAL COMPOSITION ERROR		
	BASILITE (pcf)	BORON (pcf)	BENTONITE (pcf)
1.5	1 0	2.1	0
2.0	0.3	2.1	0.1
2.5	0.1	1.9	0
3.0	0.8	1.4	0.1
3.5	0	1.8	0.2
4.0	0	1.7	0.3
4.5	0.4	2.1	0.3
5.0	0.4	2.0	0.6

Figure 50

EFFECTIVENESS OF 0.01" CADMIUM & 0.2188" POLYETHYLENE DISCRIMINATOR ON MOISTURE GAGE CHEMICAL COMPOSITION ERROR

83 mc Americium - Beryllium
1 1/2" x 3mm Lithium Iodide Detector
MOISTURE GAGE CALIBRATION CURVES

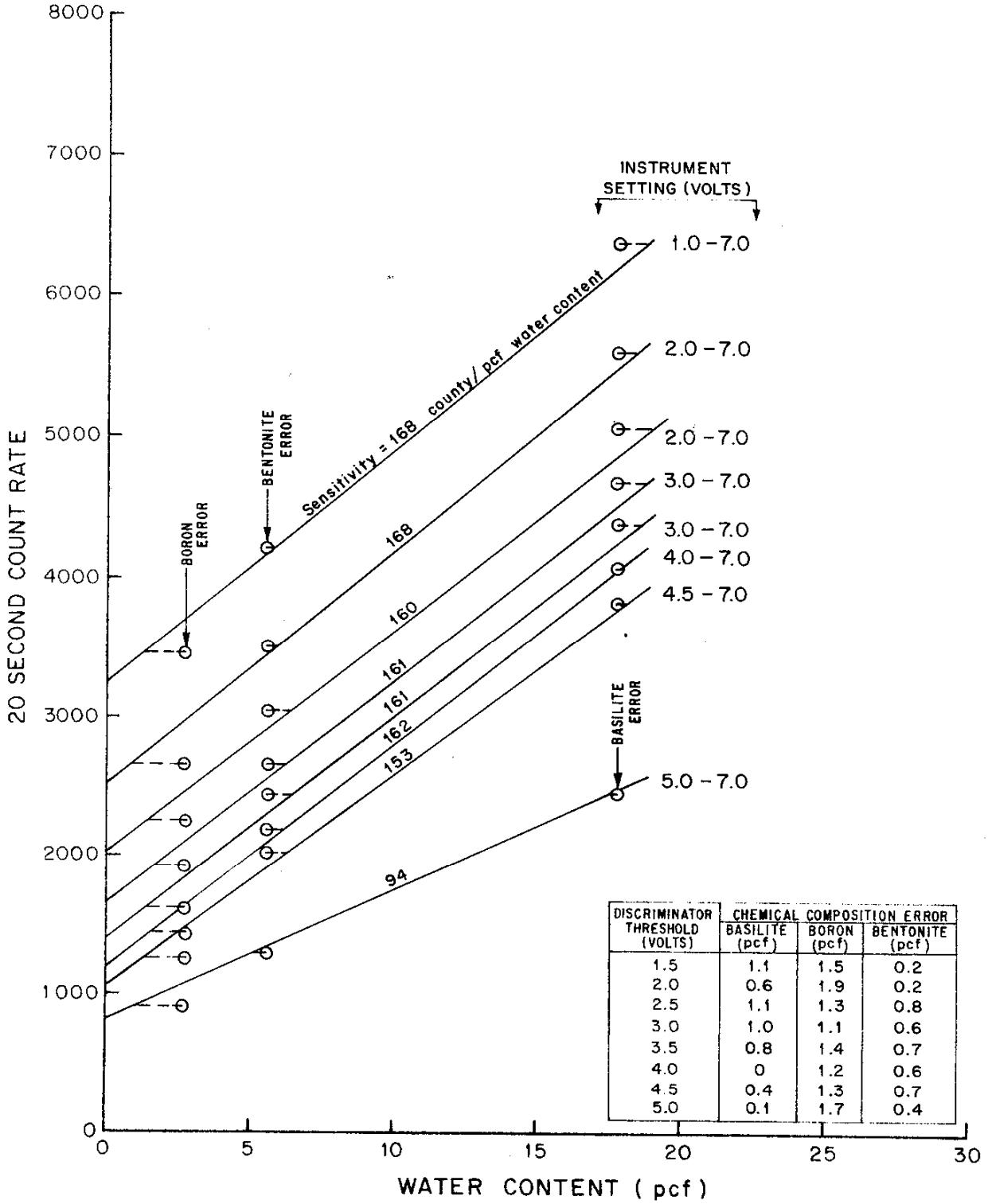

DISCRIMINATOR THRESHOLD (VOLTS)	CHEMICAL COMPOSITION ERROR		
	BASILITE (pcf)	BORON (pcf)	BENTONITE (pcf)
1.5	1.1	1.5	0.2
2.0	0.6	1.9	0.2
2.5	1.1	1.3	0.8
3.0	1.0	1.1	0.6
3.5	0.8	1.4	0.7
4.0	0	1.2	0.6
4.5	0.4	1.3	0.7
5.0	0.1	1.7	0.4

Figure 51

OPTIMUM OBSERVED CALIBRATION CURVE FOR A COBALT 60 BACKSCATTER GAGE

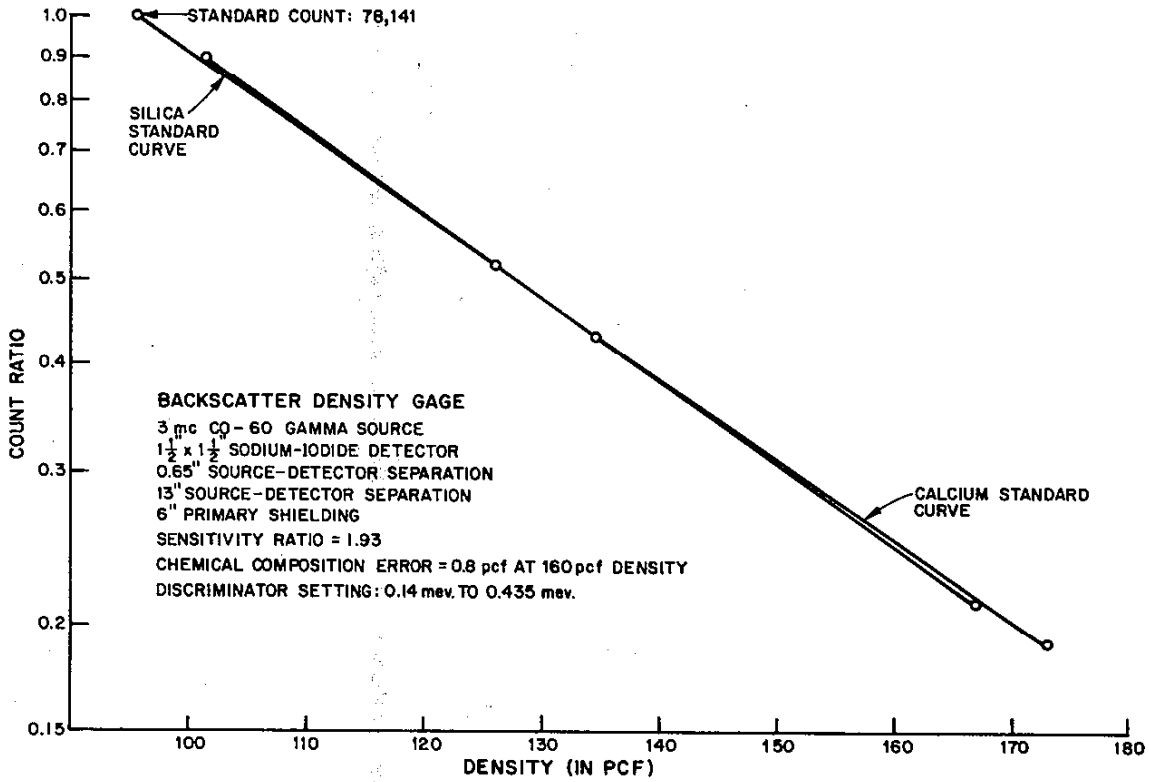

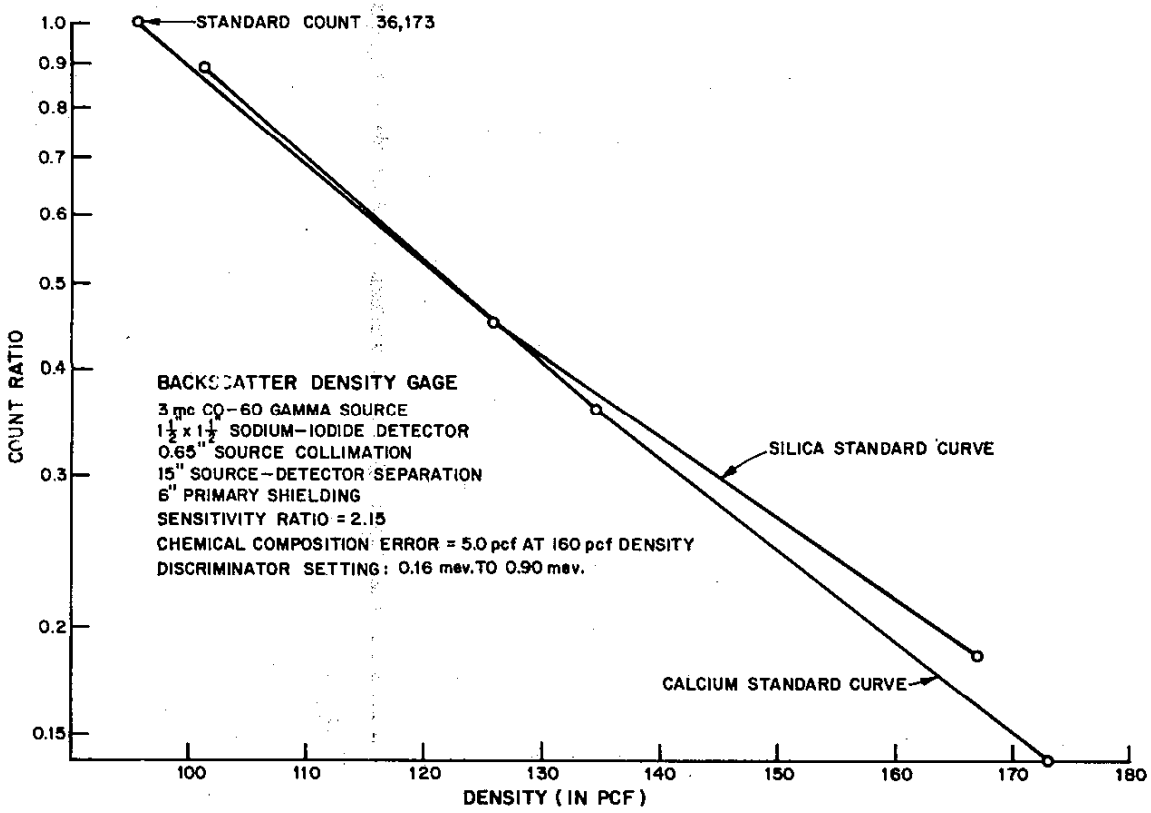

Figure 52

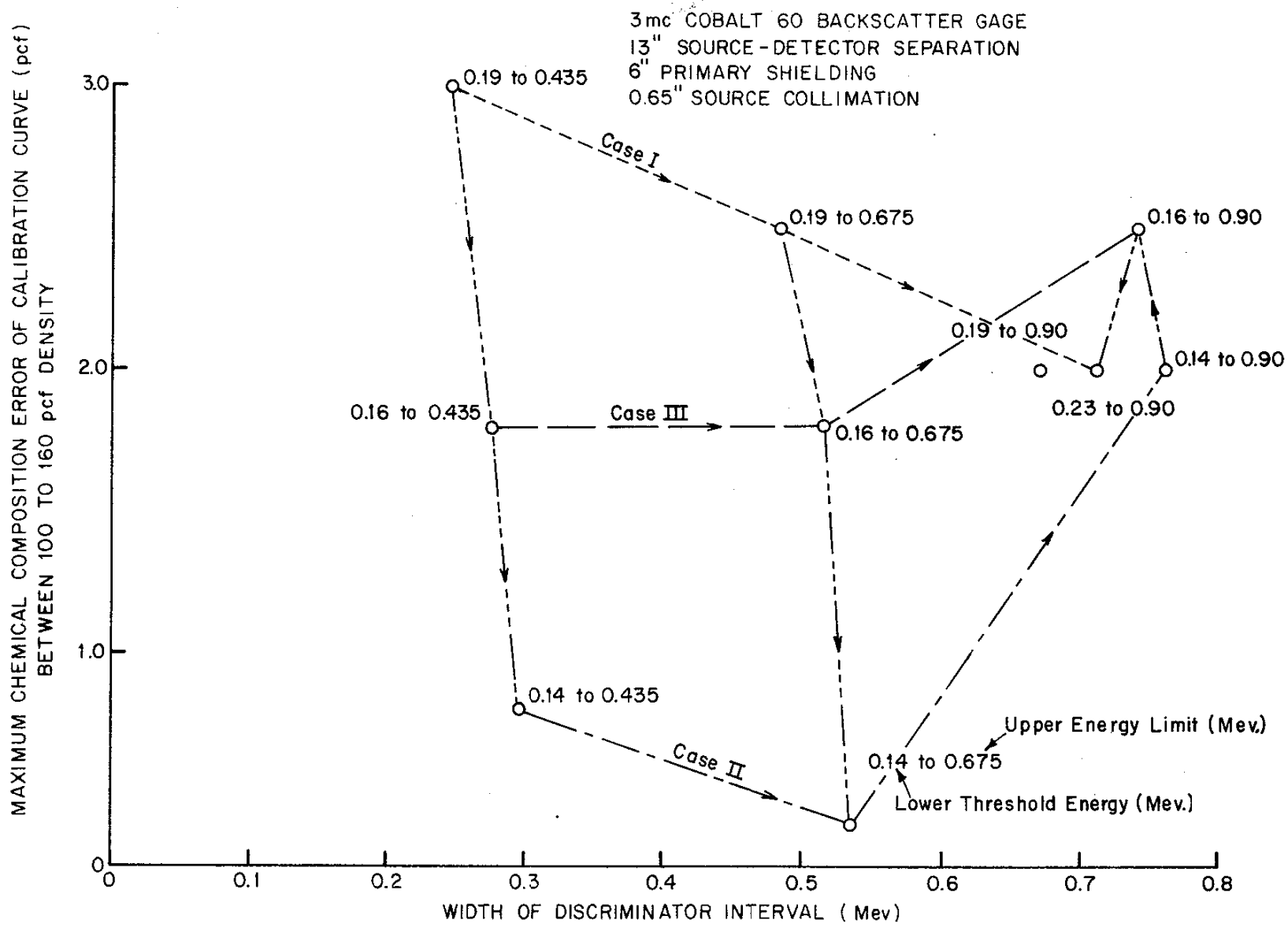

Note: Arrow denotes increasing discriminator interval.

THE VARIATION OF CHEMICAL COMPOSITION ERROR DUE TO DISCRIMINATOR SELECTION

Figure 53

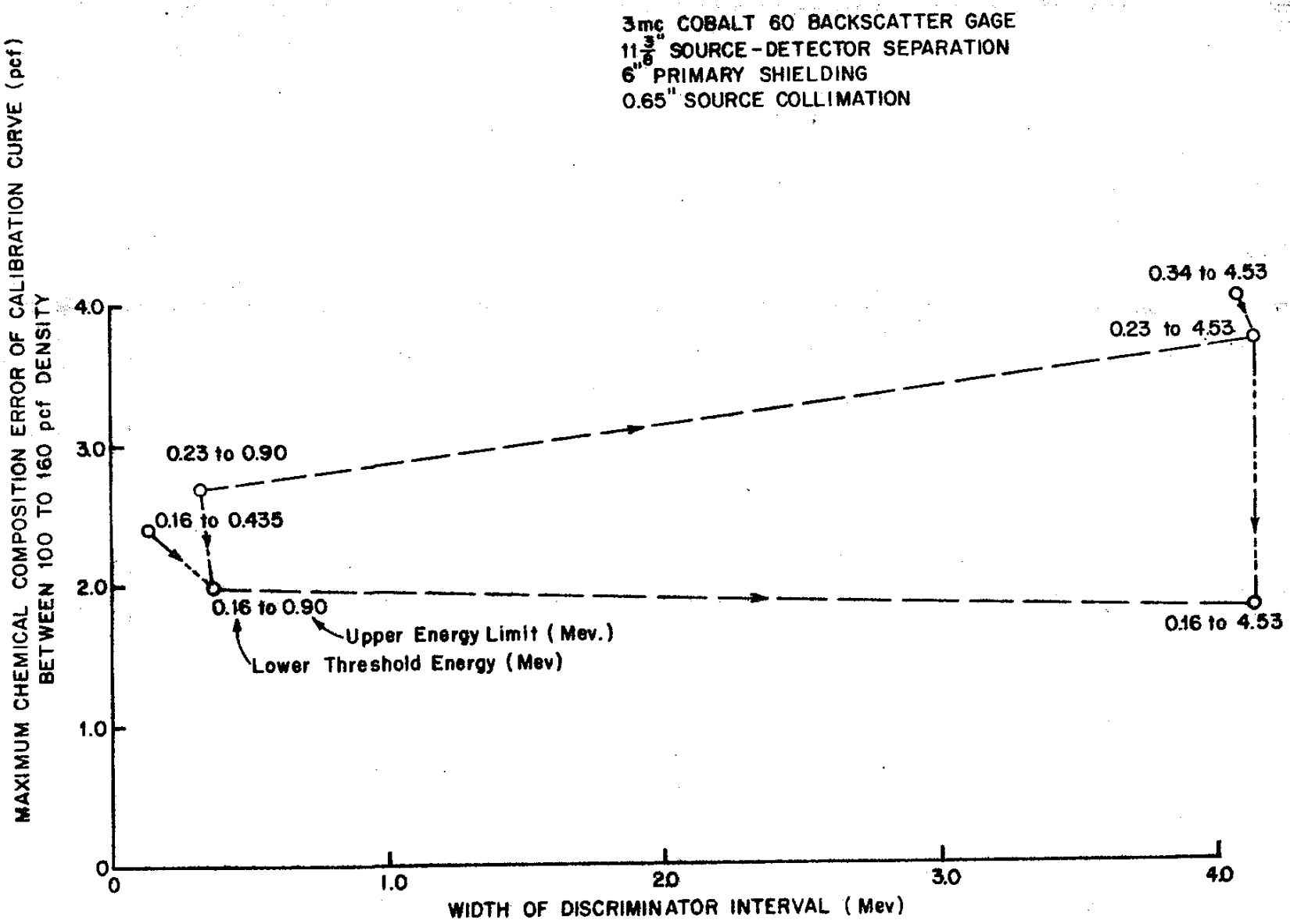

Note: Arrow denotes increasing discriminator interval.

THE VARIATION OF CHEMICAL COMPOSITION ERROR DUE TO DISCRIMINATOR SELECTION

Figure 54

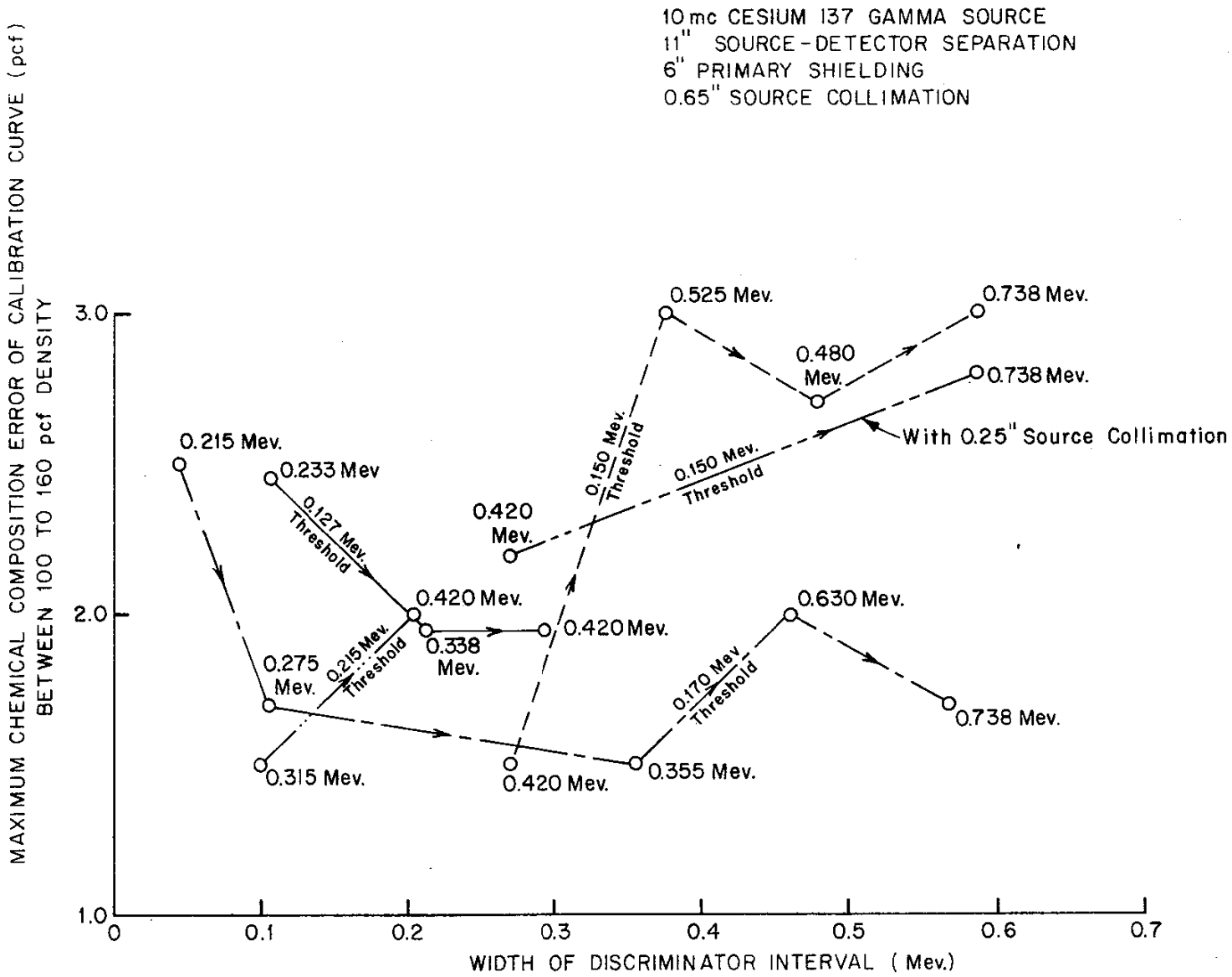

Note: Arrow denotes increasing discriminator interval.

THE VARIATION OF CHEMICAL COMPOSITION ERROR DUE TO DISCRIMINATOR SELECTION

Figure 55

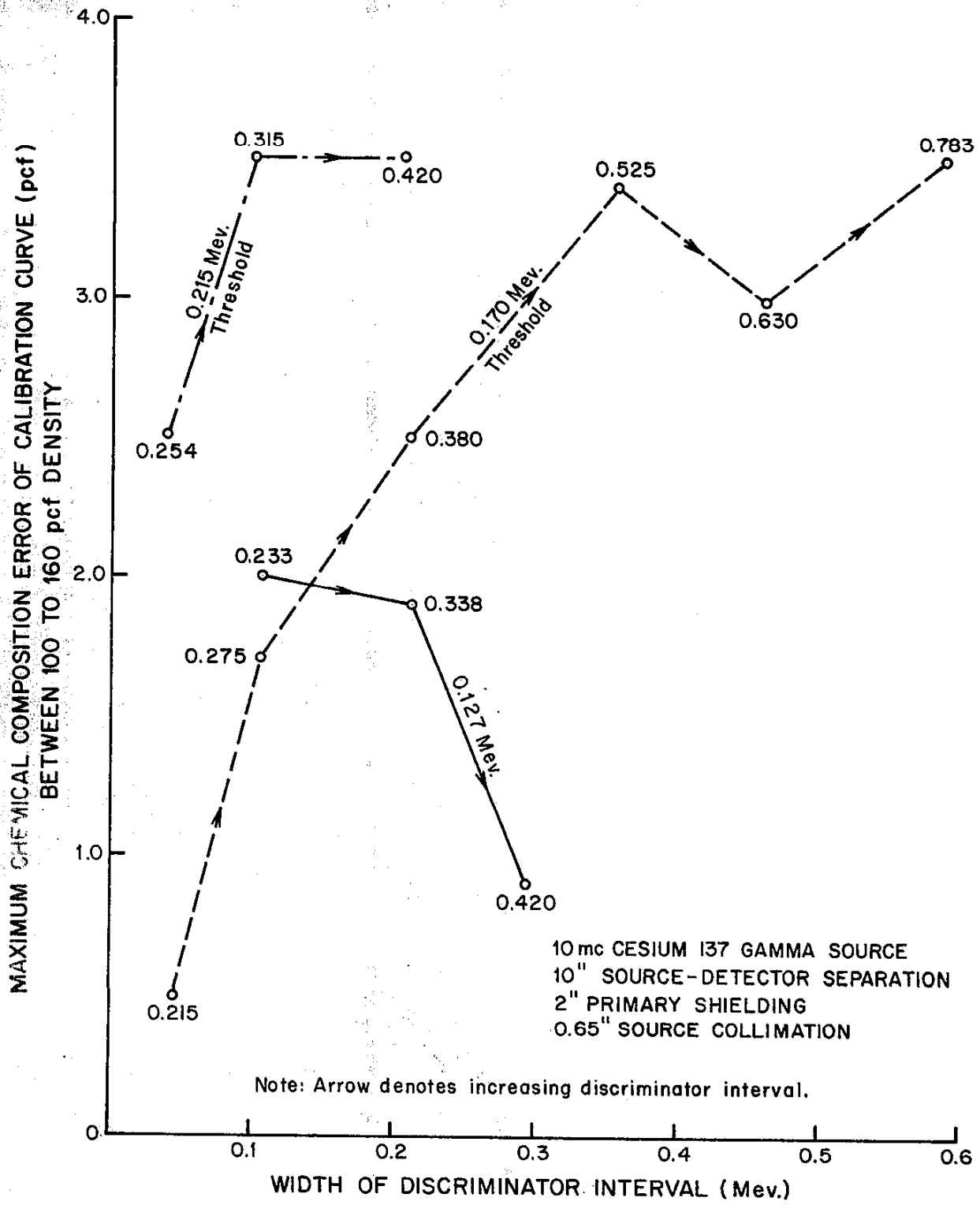

THE VARIATION OF CHEMICAL COMPOSITION ERROR DUE TO DISCRIMINATOR SELECTION

Figure 56

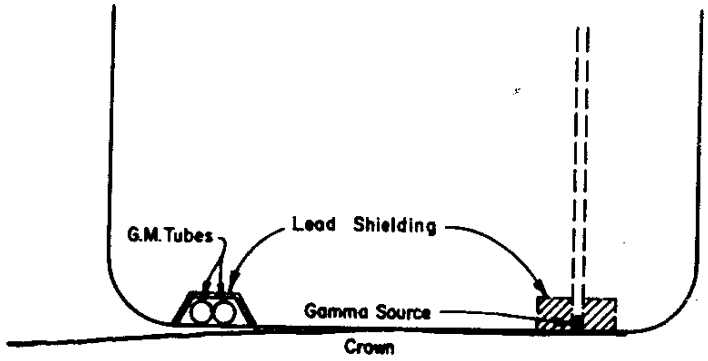

COMMERIAL GAGE

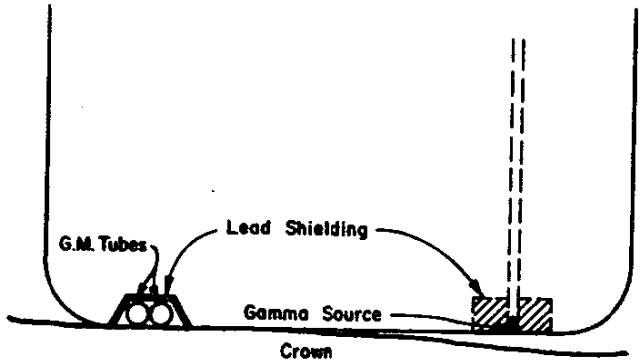

COMMERIAL GAGE

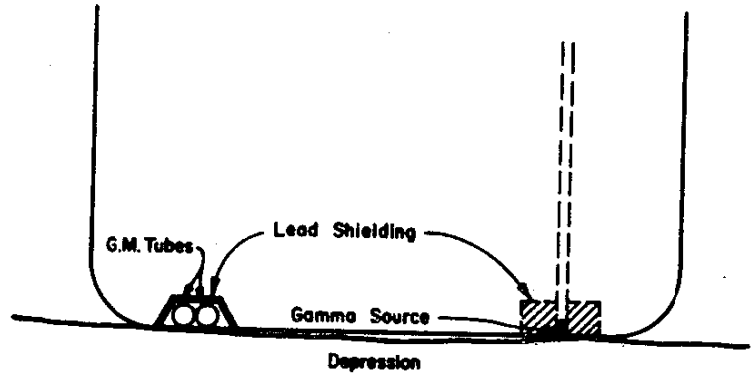

COMMERIAL GAGE

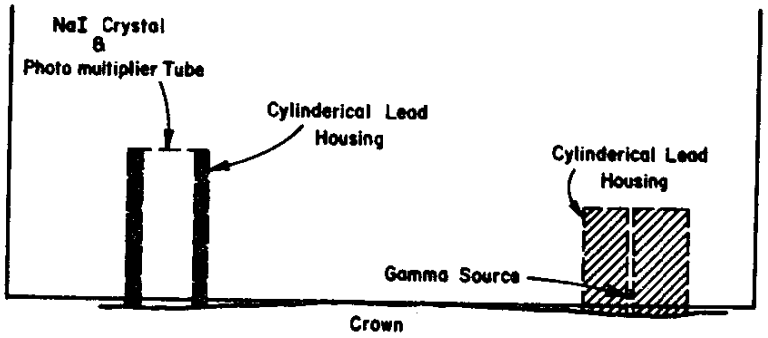

AUTO PROBE GAGE

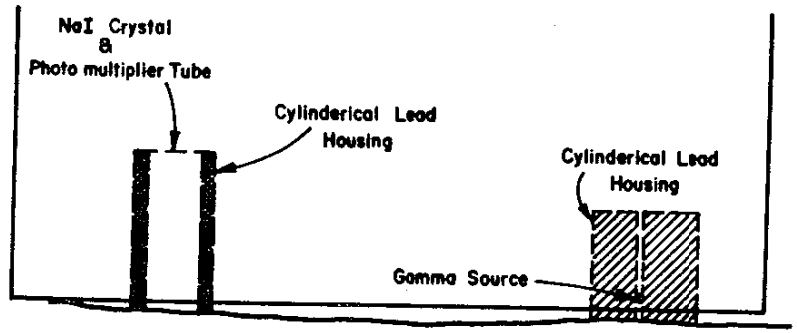

AUTO PROBE GAGE

SOURCES OF AIR-GAP ERROR

CALIBRATION CURVES RESULTING FROM CHANGES IN SOURCE COLLIMATOR CAVITY SHAPE & PROTRUSION PAD THICKNESS

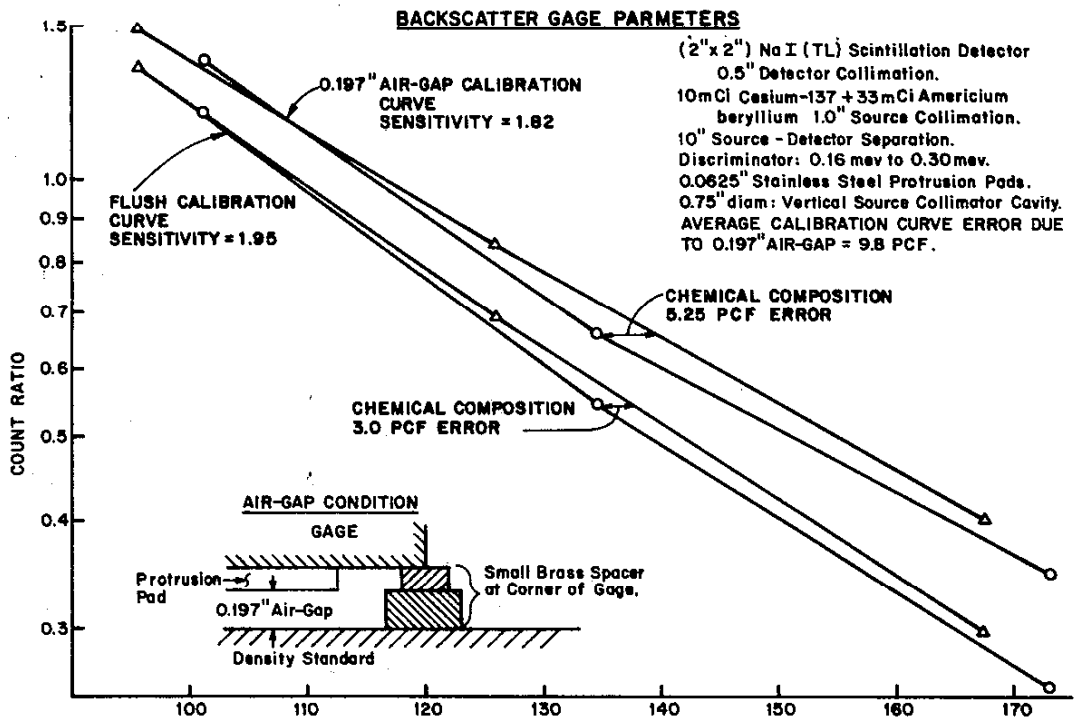

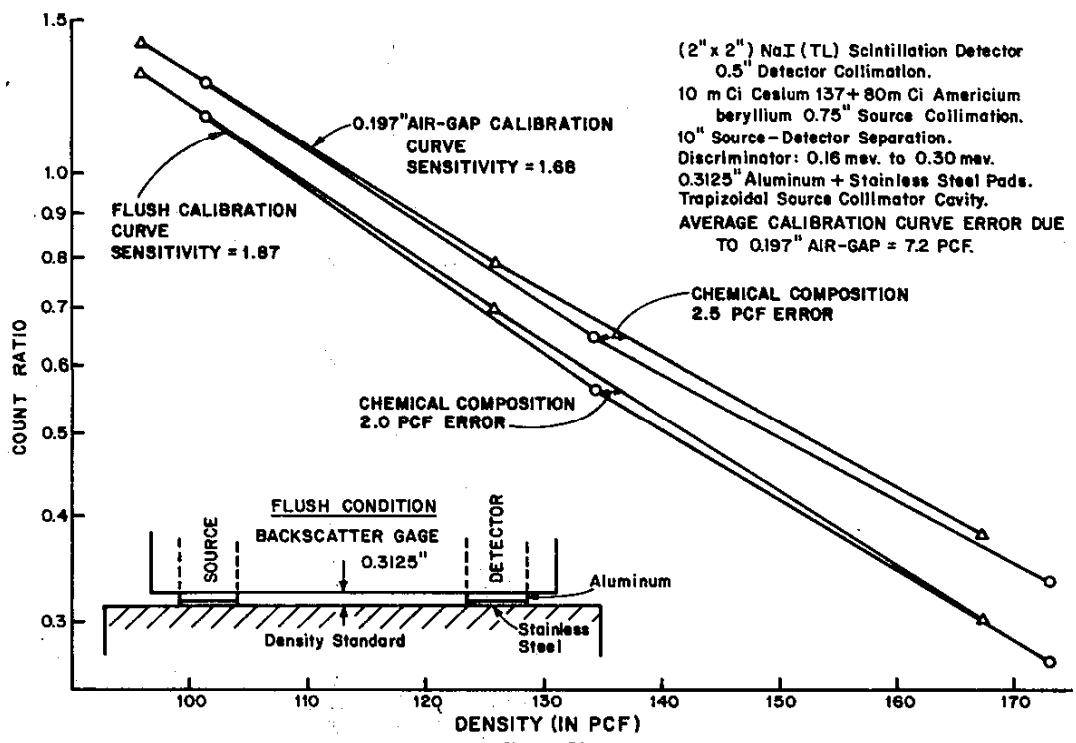

Figure 58

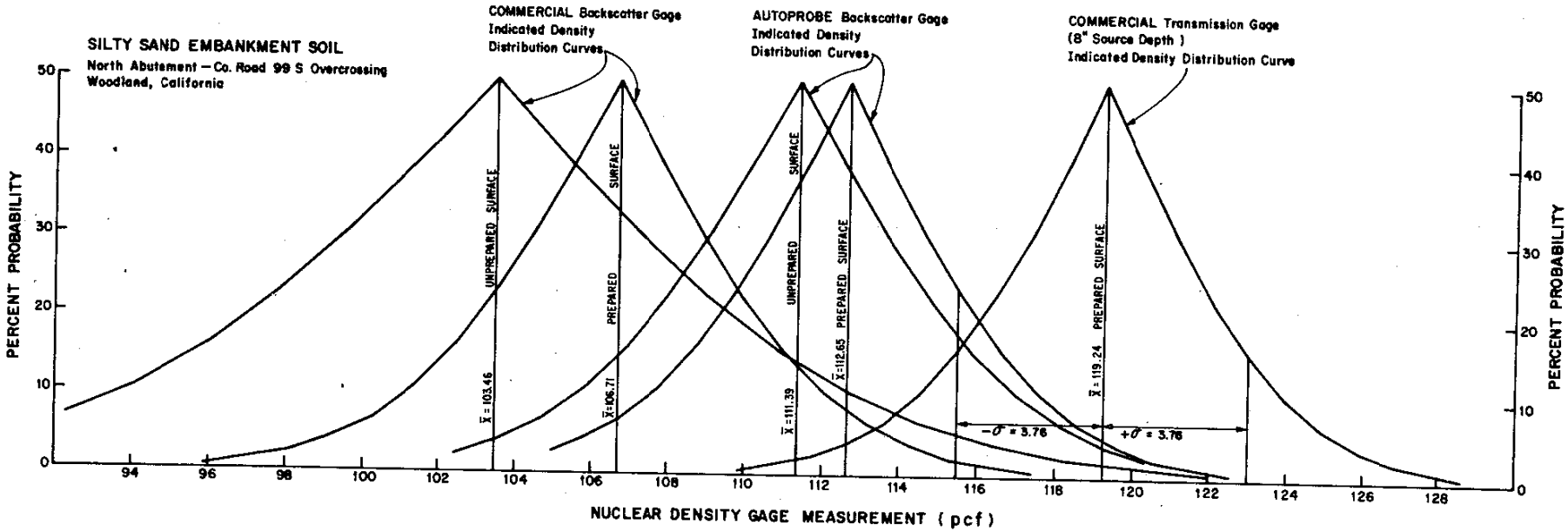

COMPARISON OF NUCLEAR DENSITY GAGE MEASUREMENT STATISTICS

Figure 59

REGRESSION ANALYSES OF ABSOLUTE DIFFERENCE BETWEEN STANDARD DEVIATIONS OF THE COMMERCIAL AND AUTOPROBE BACKSCATTER GAGES WITH TRANSMISSION GAGE AND CORE SAMPLES RELATIVE TO SOIL TYPE GROUPING

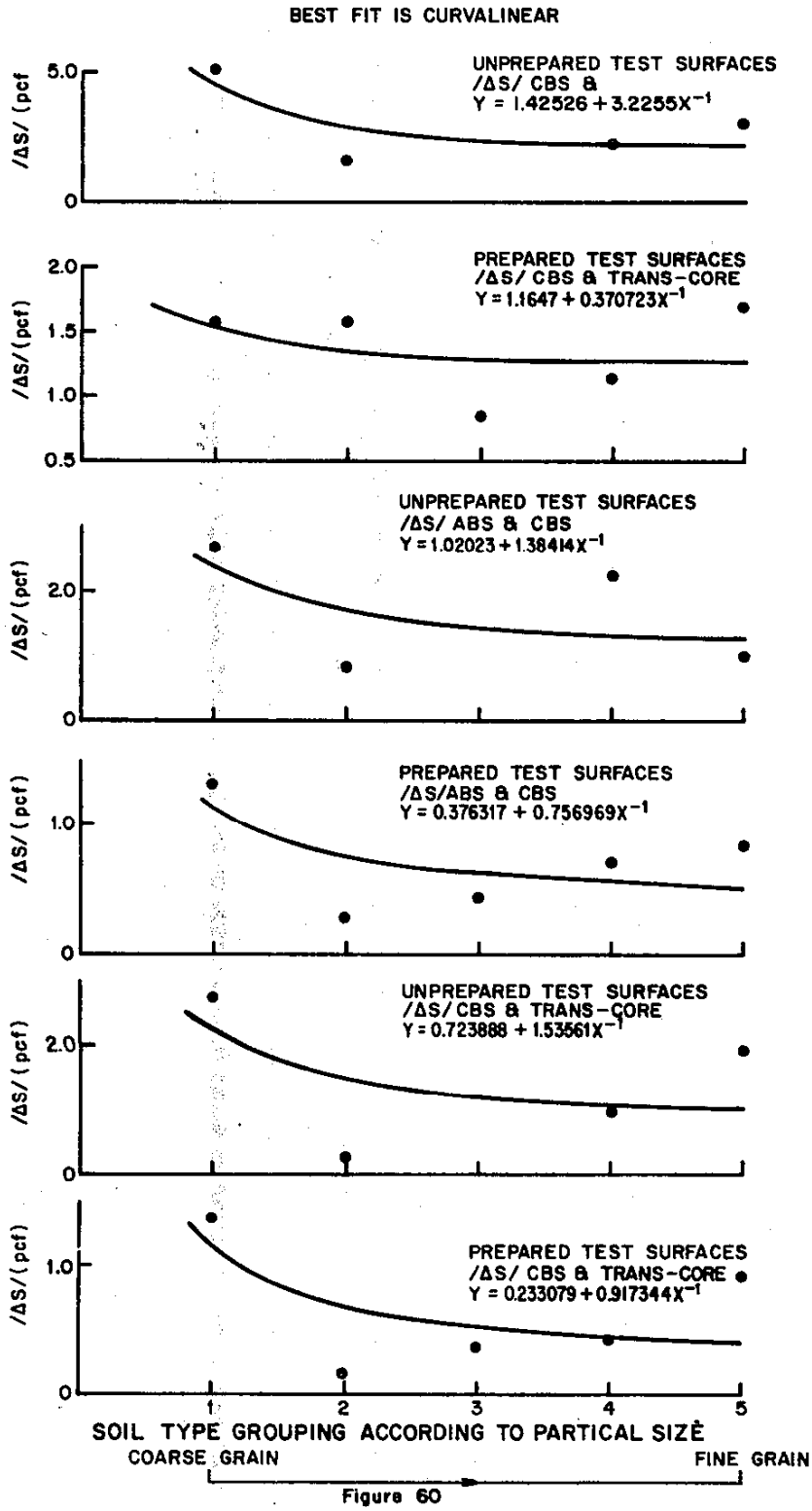

Figure 60

REGRESSION ANALYSES OF ABSOLUTE DIFFERENCE BETWEEN MEAN INDICATED DENSITY OF THE COMMERCIAL AND AUTOPROBE BACKSCATTER GAGE WITH TRANSMISSION GAGE AND CORE SAMPLES RELATIVE TO SOIL TYPE GROUPING

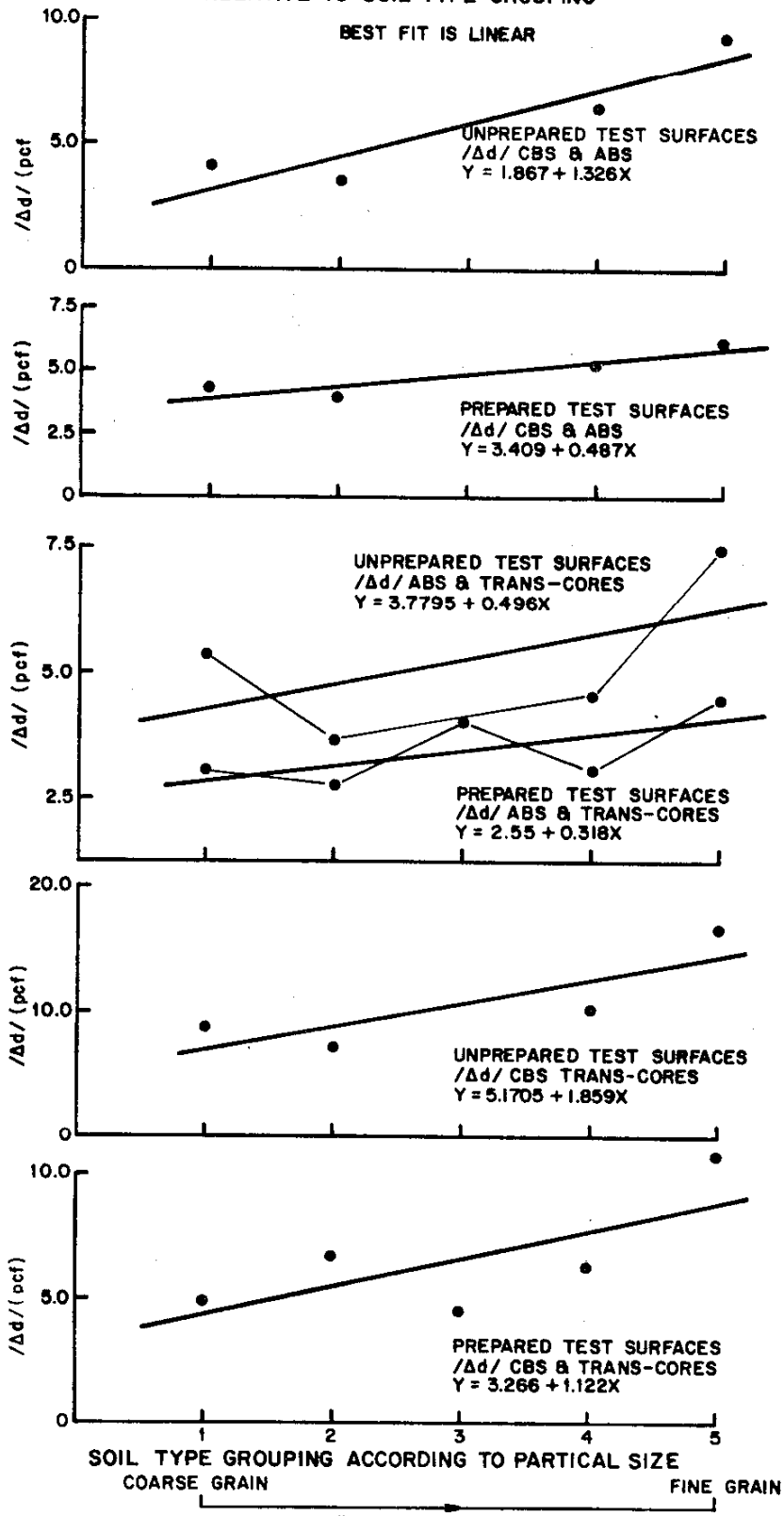

Figure 61

TABLE 1

BACKSCATTER GAGE AIR-GAP ERROR
OBTAINED BY LABORATORY EXPERIMENTS

Air-Gap Condition	Air-Gap Error (in pcf) for: 0 Inch Detector Collimation, 0.25 Inch Source Collimation, Standard Density Block						Average Air-Gap Error (in pcf)
	C-I	C-II	C-III	S-I	S-II	S-III	
1	1.5	1.2	3.0	1.0	0.6	2.0	1.5
2	0.3	0.5	2.2	0.3	0.8	3.0	1.2
3	1.0	0.5	0.7	0.9	0.8	0.2	0.7
4	2.2	3.0	6.0	1.8	3.0	4.8	3.4

Air-Gap Condition	Air-Gap Error (in pcf) for: 0 Inch Detector Collimation, 0.65 Inch Source Collimation, Standard Density Block						Average Air-Gap Error (in pcf)
	C-I	C-II	C-III	S-I	S-II	S-III	
1	0.4	0.5	0.7	0.2	1.0	0.8	0.6
2	0.2	0.6	0.6	0.2	0.4	2.2	0.7
3	0.1	0.0	0.7	0.1	1.0	1.2	0.5
4	1.5	1.8	6.7	1.7	1.9	4.0	2.9

Air-Gap Condition	Air-Gap Error (in pcf) for: 0.25 Inch Detector Collimation, 0.65 Inch Source Collimation, Standard Density Block						Average Air-Gap Error (in pcf)
	C-I	C-II	C-III	S-I	S-II	S-III	
1	0.8	0.3	1.7	0.2	0.4	0.7	0.7
2	0.1	0.7	1.8	0.2	0.2	3.7	1.1
3	0.3	0.7	1.8	0.6	0.7	0.7	0.8
4	1.2	2.2	3.6	1.0	1.7	3.7	2.2

Air-Gap Condition	Gage Configuration
1	Air-Gap Between Source Collimator and Test Surface
2	Air- Gap Between Primary Shielding and Test Surface
3	Air-Gap Between Gamma Detector and Test Surface
4	Air-Gap Between Entire Backscatter Gage & Test Surface

TABLE 2

MANUFACTURER'S GAMMA DETECTOR SPECIFICATIONS

GEIGER MUELLER DETECTOR NO.:		I	II	III
Diameter	(in.)	5/8	NOT AVAILABLE	5/8
Overall Length	(in.)	7-3/8		5-1/2
Active Length	(in.)	5-3/4		3-1/4
Operating Voltage	(volts)	900 or 700		800
Recovery Time	(sec)	100		150
Plateau Length	(volts)	150		200
Plateau Slope	(volts)	8%		8%
Wall Thickness	(in.)	0.009		0.01
Operating Temperature	(^{o}c)	-55 to +100		-40 to +175

GAMMA DETECTOR NO.:	IV
Scintillation Material	Sodium-Iodine (Thallium Activated)
Dimensions	1-1/2" Diameter 1-1/2" Thick
Wave Length of Maximum Light Emission, (A^{o})	4100
Decay Constant	0.25 seconds
Material Density	3.67 gm/cc
Relative Pulse Height*	210

*With 10 sec. anode time constant (Robert Swank-"Annual Review of Nuclear Science", Vol. 4 (1954)

TABLE 3

SUMMARY OF DETECTOR TEST RESULTS OBTAINED IN THE BACKSCATTER GAGE CONFIGURATION

Gamma Detector	Source-Detector Separation	Filter Type & Thickness	Primary Shielding Thickness	Approximate Range of 60 Second Count	Chemical Composition Error (pcf)	Sensitivity Ratio
G. M.-I	6.5"	none	2" Lead	2000 - 1000	15.0	1.43
		0.026" Lead		700 - 500	7.5	1.38
		0.042" Lead		400 - 300	5.5	1.32
	10"	none	4" Lead		11.5	1.84
		0.0045" Lead		180 - 100	12.0	1.97
		0.026" Lead			23.0	*
		0.042" Lead			25.0	*
G. M.-II	9"	none	4" Lead	9000 - 4500	3.0	1.76
		0.0045" Lead		7000 - 3500	4.5	1.78
		0.0135" Lead		5700 - 2500	4.5	1.78
		0.018" Lead		5000 - 2500	2.5	1.70
		0.0225" Lead		4500 - 2500	1.5	1.71
		0.026" Lead		3000 - 1500	2.5	1.75
		0.042 " Lead		1700 - 900	3.5	1.70
		0.033 " Brass		7000 - 3500	2.5	1.75
		0.0045" Lead		6000 - 3000	2.4	1.75
		0.033 " Brass		"	"	"
		0.033 " Brass		5000 - 2500	3.0	1.75
		0.0135" Lead		"	"	"
G. M.-II	10"	none	4" Lead	6000 - 2500	8.5	1.85
		0.0045" Lead		5000 - 2500	5.0	1.89
		0.0135" Lead		4000- 2000	5.0	1.88
		0.026 " Lead		2000 - 950	3.5	1.91
		0.042 " Lead		1100 - 500	6.7	1.91
		0.033 " Brass		5000 - 2000	3.5	1.92
		0.0045" Lead		4400 - 2000	2.5	1.88
		0.033 " Brass		"	"	"
		0.0135" Lead		3500 - 1500	2.5	1.90
		0.033 " Brass		"	"	"
		0.026 " Lead		2000 - 900	4.5	1.90
		0.008 " Poly-ethylene		"	"	"
G. M.-III	9"	none	4" Lead	10000 - 5100	8.5	1.71
		0.0135" Lead		6000 - 3000	5.5	1.75
		0.0225" Lead		4800 - 2000	8.0	1.79
		0.042 " Lead		1600 - 800	1.8	1.82

* Due to the extreme composition effect it was not possible to determine this sensitivity ratio.

TABLE 4

SUMMARY OF DETECTOR TEST RESULTS OBTAINED IN THE TRANSMISSION GAGE CONFIGURATION

Gamma Detector	Source-Detector Separation & Source Depth	Filter Type & Thickness	Primary Shielding Thickness	Approximate Range of 60 Second Count	Chemical Composition Error (pcf)	Sensitivity Ratio
G. M.-III	10" x 10"	none	4" Lead	14000 - 5500	6.0	2.28
		0.0045" Lead		12000 - 4500	5.0	2.33
		0.0135" Lead		10000 - 3500	4.0	2.35
		0.026 " Lead		6400 - 2200	4.5	2.49
		0.042 " Lead		4700 - 1500	2.5	2.63
		0.0555" Lead		4300 - 1400	2.3	2.63
		0.068 " Lead		3700 - 1200	1.8	2.72
		0.085 " Lead		3100 - 1000	2.3	2.73
		0.111 " Lead		2500 - 800	2.5	2.80
	12" x 10"	0.042 " Lead		2600 - 700	2.5	3.23
		0.0555" Lead		2300 - 600	1.0	3.20
		0.068 " Lead		2100 - 500	2.5	3.33
	12" x 12"	0.042 " Lead		1700 - 300	6.0	3.68
		0.0555" Lead		1300 - 300	6.0	3.64
		0.068 " Lead		1200 - 200	5.2	3.63

TABLE 5

SUMMARY OF SODIUM-IODINE SCINTILLATION DETECTOR TEST RESULTS IN THE BACKSCATTER & TRANSMISSION CONFIGURATION

Test Configuration & Discriminator Settings	Source-Detector Separation & Source Depth	Filter Type & Thickness	Primary Shielding Thickness	Approximate Range of 60 Second Count	Chemical Composition Error (pcf)	Sensitivity Ratio
Backscatter (0.15 to 0.42) Mev	11"	none	2" Lead	80000 - 34000	1.6	2.10
Backscatter (0.15 to 0.275) Mev				67000 - 30000	1.6	2.00
Backscatter (0.15 to 0.42) Mev			none	85000 - 41000	1.5	1.88
Backscatter (0.15 to 0.275) Mev				64000 - 27000	2.2	1.94
Transmission (0.42 to 2.1) Mev	12" x 6"	none	none	57000 - 22000	1.5	2.44
Transmission (0.42 to 2.1) Mev	12" x 12"			25000 - 6500	2.5	3.21

TABLE 6

PROPORTIONAL COUNTER (NEUTRON DETECTOR) SPECIFICATIONS

Neutron Detector Type	BF_3 Gas	B-10 Lined	He-3 Gas
Diameter (in)	1	1	1
Sensitive Length (in)	8-1/8	4	6
Wall Thickness (in)	0.032	0.032	0.020
Enrichment (Baron $_{10}$)	96%	92%	-
Operating Voltage at Mid-Plateau (volts)	900	1600	1200
Plateau Length (volts)	1200	200	400
Plateau Slope (%/100 volts)	1	0.1	1
Max. Temperature (^{o}C)	150	200	150
Gas Fill Pressure (Atmos.)	0.527	0.329	2.0
Neutron Sensitivity cps per n/sq.cm. per sec.	4.0	1	8

TABLE 7

LITHIUM-IODIDE SCINTILLATION DETECTOR SPECIFICATIONS

Scintillation Material	Lithium-Iodide (Europium Activated)
Dimensions	38 mm (1-1/2 inch) diameter 3 mm thickness
Wavelength of maximum Light Emission (A^{o})	4400
Decay Constant (sec.)	1.4
Density (gm/cc)	4.06
Relative Pulse Height*	74

*With 10 sec. anode time constant (Robert Swank - "Annual Review of Nuclear Science", Vol. 4 (1954)

TABLE 8

GAMMA EVENTS RECORDED BY PROPORTIONAL NEUTRON DETECTORS
(100mc CESIUM GAMMA SOURCE)
AT 3 INCHES

Discriminator Interval (Channel Voltage)	Detector		
	He-3 Gas	BF_3 Gas	B-10 Lined
0.05 - 10.0	-	189,800	75,500
0.1 - 10.0	3,715,400	-	100
0.15 - 10.0	-	-	-
0.20 - 10.0	1,305,900	-	-
0.50 - 10.0	16,700	-	-
0.70 - 10.0	600	-	-
1.0 - 10.0	14	-	-
1.3 - 10.0	4	-	-
GAMMA EVENTS RECORDED BY PROPORTIONAL NEUTRON DETECTORS (10mc CESIUM GAMMA SOURCE) AT 18 INCHES			
0.05 - 10.0	-	-	424,600
0.10 - 10.0	-	-	6,500
0.15 - 10.0	-	-	80
0.20 - 10.0	4,199,000	-	12
0.50 - 10.0	128,000	-	-
0.75 - 10.0	-	-	-
1.00 - 10.0	150	-	-

TABLE 9

SUMMARY OF PROPORTIONAL COUNTER TEST RESULTS

Neutron Detector No.	BF_3 Gas	B-10 Lined	He-10 Gas
Gamma to Neutron Pulse Height Ratio	1:30	1:20	1:10
Count Rate (C.P.M.)	796	1,685	4,808
Plateau Length (volts)	1,150	250	200
Heat Sensitivity (^{o}F)	300	250	200
Chemical Sensitivity (pcf)	5.75+	5.75+	0.7
Plateau Slope (counts/volt)	0.65	2.0	75.0
Operating Voltage	725	1,025	1,450

TABLE 10

VARIATION OF PERCENT CHEMICAL COMPOSITION ERROR IN THE CALIBRATION CURVE DUE TO PRIMARY SHIELDING THICKNESS PLACED IN THE BACKSCATTER DENSITY GAGE

Primary Shielding Thickness (in inches)	Percent of Calibration Curve with Chemical Composition Error		Maximum Chemical Composition Error (pcf)
	1 pcf or More	1 pcf or Less	
0.00	15.3	84.8	1.5
0.25	54.4	45.6	2.0
0.50	42.1	57.9	1.5
2.00	64.0	36.0	2.5
2.25	17.2	82.8	1.5
2.50	50.8	49.2	2.0

TABLE 11

PRIMARY SHIELDING EFFECT ON COUNT RATE

Primary Shielding Thickness (in inches)	Average Percent Count Rate Reduction (10 mc Cesium Backscatter Gage Apparatus)	
	Sodium-Iodide Detector 1-1/2" x 1-1/2"	Single Geiger-Mueller Detector w/ and w/o 0.042" Lead Filter
0.25	5.6	40.0
0.50	8.0	-
2.00	12.9	76.0
2.25	13.3	-
2.50	13.7	-
4.00	-	79.0

TABLE 12

SUMMARY OF CHEMICAL COMPOSITION ERROR AND GEIGER-MUELLER DETECTOR SENSITIVITY DUE TO BACKSCATTER GAGE CONFIGURATION

Detector Type	Source-Detector Separation (in inches)	Filter	Thickness (in inches)	Maximum Chemical Composition Error (pcf) Bet. 100/160	Sensitivity Ratio	Primary Shielding Thickness (in inches)
Halogen Quenched	6.25	Lead	0.0045	5.0	1.32	4
" "	"	"	0.026	7.0	1.37	4
" "	"	None	0	15.0	1.44	4
" "	10	None	0	11.0	1.91	4
" "	10	Lead	0.0045	11.5	1.85	4
" "	10	"	0.026	25	1.89	4
" "	10	"	0.042	25	1.57	4
Tantalum Lined	9	None	0	3.0	1.74	4
" "	"	Lead	0.0045	4.5	1.78	4
" "	"	"	0.0135	4.5	1.78	4
" "	"	"	0.018	3.0	1.72	4
" "	"	"	0.0225	2.0	1.73	4
" "	"	"	0.026	2.5	1.75	4
" "	"	Brass	0.033	3.0	1.75	4
		Brass	0.033	2.5	1.75	4
" "	"	Lead	0.0045			
		Brass	0.033	3.0	1.75	4
" "	"	Lead	0.0135			
		Lead	0.042	3.5	1.70	4
Tantalum Lined	10	None	0	8.0	1.85	4
" "	"	Lead	0.0045	4.5	1.89	4
" "	"	"	0.0135	5.0	1.89	4
" "	"	"	0.026	4.0	1.91	4
" "	"	"	0.042	7.0	1.91	4
" "	"	Brass	0.033	3.5	1.92	4
		Brass	0.033	2.0	1.88	4
		Lead	0.0045			
		Brass	0.033	2.5	1.90	4
		Lead	0.0135			
Platinum Lined	9	None	0	8.0	1.77	4
" "	"	Lead	0.0135	5.5	1.62	4
" "	"	"	0.0225	4.5	1.80	4
" "	"	"	0.042	2.0	1.86	4

TABLE 13

THE EFFECTS OF ELECTRONIC ENERGY DISCRIMINATION ON CHEMICAL COMPOSITION ERROR AND SENSITIVITY RESPONSE RATIO IN THE BACKSCATTER MODE (1-1/2" x 1-1/2" SODIUM-IODIDE SCINTILLATION DETECTOR)

Energy Discrimination Interval (in Mev.)	Source-Detector Separation 10"		Source-Detector Separation 11"	
	Maximum Chemical Composition Error (pcf) Bet. 100/160	Sensitivity Ratio	Maximum Chemical Composition Error (pcf) Bet. 100/160	Sensitivity Ratio
0.127 - 0.170	4.5	1.97	-	2.11
0.127 - 0.233	2.0	1.96	2.5	2.12
0.127 - 0.338	2.0	1.94	2.0	2.09
0.127 - 0.420	1.0	1.93	2.0	2.07
0.170 - 0.215	0.5	1.94	2.5	2.12
0.170 - 0.275	1.5	1.92	2.5	2.08
0.170 - 0.380	2.5	1.89	3.0	2.04
0.170 - 0.525	-	-	1.5	2.03
0.170 - 0.630	3.0	1.90	2.0	2.00
0.170 - 0.738	3.25	1.90	1.5	2.01
0.215 - 0.254	2.5	1.94	-	-
0.215 - 0.315	3.0	1.89	1.5	2.03
0.215 - 0.420	3.5	1.84	-	-

TABLE 14

THE EFFECTS OF ENERGY DISCRIMINATION ON CHEMICAL ERROR IN THE TRANSMISSION MODE

Detector Type G. M.	Horizontal Source Detector Separation	Vertical Source Depth (inches)	Filter Material	Filter Thickness (in inches)	Maximum Chemical Composition Error (pcf) Bet. 100/160	Sensitivity Ratio	Primary Shielding Thickness (in inches)
Detector 1:							
Platinum Lined	10	10	Lead	0.042	2.5	2.63	2
" "	"	"	"	0.0555	2.0	2.63	"
" "	"	"	"	0.0680	1.0	2.72	"
" "	"	"	"	0.085	3.0	2.73	"
" "	"	"	"	0.111	2.5	2.79	"
" "	12	"	"	0.042	2.5	3.23	"
" "	"	"	"	0.0555	1.0	3.24	"
" "	"	"	"	0.068	2.5	3.33	"
" "	"	12	"	0.042	6.0	3.68	"
" "	"	"	"	0.0555	5.5	3.64	"
" "	"	"	"	0.068	5.0	3.63	"
Detector 2:							
Platinum Lined	10	10	None	0	6.0	2.29	2
" "	"	"	Lead	0.0045	5.5	2.33	"
" "	"	"	"	0.0135	4.0	2.35	"
" "	"	"	"	.026	4.5	2.49	2

THE EFFECTS OF ENERGY DISCRIMINATION ON CHEMICAL COMPOSITION ERROR IN THE TRANSMISSION (1-1/2" x 1-1/2" SODIUM-IODIDE SCINTILLATION DETECTOR AND CESIUM 137 SOURCE) MODE

Energy Discrimination Interval (in Mev.)	Source-Detector Separation 6" Source Depth 6"		Source-Detector Separation 12" Source Depth 6"	
	Maximum Chemical Composition Error (pcf) Bet. 100/160	Sensitivity Ratio	Maximum Chemical Composition Error (pcf) Bet. 100/160	Sensitivity Ratio
0.045 - 2.09	8.0	1.48	5.5	2.39
0.105 - 1.04	2.5	1.49	3.0	2.36
0.215 - 1.04	3.0	1.52	1.5	2.33
0.420 - 1.04	3.5	1.62	1.0	2.41
0.630 - 1.04	2.0	2.70	3.0	2.67

TABLE 15

ENERGY DISCRIMINATION EFFECTS ON MOISTURE GAGE CHEMICAL COMPOSITION ERROR AND SENSITIVITY

Initial Electronic Discriminator Set for: 3.5 Volts to 7.0 Volts

Filter Conditions	Chemical Basilite pcf	Composition Bentonite pcf	Error Boron pcf	Sensitivity in Counts/lb per cf
No Filters	0.3	0.4	2.4	311
0.01 inch Cadmium	0.8	0.4	1.9	130
0.21875 inch Polyethylene	0.0	0.2	1.8	265
0.43750 inches of Polyethylene	1.0	0.3	1.5	238
0.01 inch Cadmium w/ 0.21875 inch Polyethylene	0.8	0.7	1.4	160
0.01 inch Cadmium w/ 0.43750 inch Polyethylene	0.1	1.2	0.9	178

83mc Americium 241-Beryllium Neutron Source = 50mc @ 2.50" separation & 33mc @ 3.68" separation

1-1/2" x 3mm Lithium-Iodide Scintillation Detector

TABLE 16

COBALT 60 BACKSCATTER GAGE CONFIGURATIONS WHICH EXCEED 1.90 SENSITIVITY RATIO

Discriminator Setting (Mev)	Source-Detector Separation (inches)	Sensitivity Ratio	Gamma Source Collimation (inches)	Chemical Composition Error (pcf)	1 Minute Count From Calibration Curve at 140 pcf (approximate)
0.14 - 0.435	13	1.93	0.65	0.8	29,850
0.14 - 0.675	↓	1.90	↓	0.4	34,800
0.14 - 0.90		1.90		2.0	35,372
0.16 - 0.435		1.94		1.5	26,200
0.16 - 0.675		1.93		1.8	29,000
0.16 - 0.90		1.99	1.0	3.5	13,600
0.19 - 0.435		1.91	0.65	3.0	22,200
0.23 - 0.90		1.93	1.0	3.5	8,100
0.16 - 0.90	14	1.97	0.65	9.0	17,000
0.16 - 0.90	15	2.21	1.0	9.5	6,100
0.16 - 0.90	↓	2.15	0.65	5.0	11,700
0.23 - 0.90		2.06	0.65	5.5	7,700
0.23 - 0.90		2.12	1.0	11.5	3,750

Backscatter Gage Apparatus Constants:
(1) 6 inch Primary Shielding
(2) 1-1/2" x 1-1/2" Sodium-Iodide Scintillation Detector
(3) 3 millicurie Cobalt 60 Gamma Source

TABLE 17

CESIUM 137 BACKSCATTER GAGE CONFIGURATIONS WHICH EXCEED 1.90 SENSITIVITY RATIO

Discriminator Setting (Mev)	Source-Detector Separation (inches)	Sensitivity Ratio	Gamma Source Collimation (inches)	Chemical Composition Error (pcf)	1 Minute Count From Calibration Curve at 140 pcf (approximate)
0.127 - 0.233	11	2.12	0.65	2.4	27,900
0.127 - 0.338		2.09		1.9	38,700
0.127 - 0.420		2.07		1.9	40,600
0.150 - 0.420		2.03		1.5	22,800
0.150 - 0.525		2.02		3.0	34,900
0.150 - 0.630		2.01		2.7	34,800
0.150 - 0.738		2.02		3.0	34,700
0.170 - 0.215		2.12		2.5	10,400
0.170 - 0.275		2.08		1.7	20,500
0.170 - 0.525		2.03		1.5	28,100
0.170 - 0.630		2.00		2.0	28,200
0.170 - 0.738		2.01		1.7	28,500
0.215 - 0.315		2.03		1.5	13,800
0.215 - 0.420		1.98		2.0	16,900
0.150 - 0.420		1.90	0.35	2.4	91,600*
0.150 - 0.738		1.82		2.1	100,500*
0.150 - 0.420		1.97	0.25	2.2	104,200
0.150 - 0.738		1.98		2.8	108,400
0.127 - 0.233	10	1.96	0.65	2.0	47,100
0.127 - 0.338		1.94		1.9	64,500
0.127 - 0.420		1.93		0.9	68,700
0.170 - 0.215		1.94		0.5	17,400
0.170 - 0.275		1.92		1.7	34,200
0.170 - 0.380		1.89		2.5	44,600
0.170 - 0.525		1.91		3.4	47,300
0.170 - 0.630		1.90		3.0	47,700
0.170 - 0.738		1.90		3.5	47,800
0.215 - 0.254		1.94		2.5	12,600
0.215 - 0.315		1.89		3.5	23,000
0.215 - 0.420		1.84		3.5	28,500

Backscatter Gage Apparatus Constants:
(1) 2" Primary Shielding (Lead)
(2) 1-1/2" x 1-1/2" Sodium-Iodide Scintillation Detector
(3) 10 millicurie Cesium 137 Gamma Source

*Recorded Count Rate Without 2" Primary Shielding

TABLE 18

MEAN DENSITY OF GAGE MEASUREMENTS (pcf)

Materials Tested	Backscatter Gage				Transmission Gage	
	Commercial		Autoprobe		Source Depth	
	Unprepared	Prepared	Unprepared	Prepared	8 Inches	4 Inches
Silty-Sandy Gravel	-	113.5	113.5	119.5	121.6	119.3
Gravelly Sand	-	118.2	121.2	122.4	126.9	124.9
-#30 Sand	-	115.0	115.5	117.3	113.9	-
Silty Sand	-	103.8	-	109.8	114.0	-
Silty Sand	103.5	106.7	111.4	112.7	119.2	-
Fine Silty Sand	106.0	106.0	105.0	112.3	110.1	-
Fine Sandy Silt	105.6	109.5	115.9	116.7	115.6	-
Silt	122.3	123.0	128.8	128.9	133.2	-
Aggregate Base	132.1	138.5	134.2	140.9	138.6	-
Aggregate Base	136.0	140.7	139.4	141.2	140.5	-
Aggregate Base	132.8	137.8	137.4	139.2	138.8	-
-3" Subbase	104.6	106.4	107.6	115.9	109.3	-
Gravel & Cobbles w/ Clay-Silt Binder	105.2	116.9	112.7	121.2	127.9	-
Cement Treated Base	-	129.2		134.9	136.4	136.8
Silty Clay	97.0	102.3	106.3	107.6	113.7	-
Silty Clay	-	112.8	-	116.2	119.9	-
Gravelly Clay	-	117.3	-	120.6	121.7	-
Alkali Clay	-	98.2	-	105.9	105.8	105.1
Iron Slag	-	116.0	107.6	115.6	-	116.0
Borate Soil	-	76.4	-	87.1	99.5	89.3
Asphalt Concrete	-	145.0	-	145.5	149.5 Core Density	
Concrete Pavement	143.9	144.8	148.4	149.3	149.7 Core Density	
Concrete Pavement	141.4	141.4	144.5	145.5	149.7 Core Density	
Concrete Pavement	142.1	142.7	145.1	146.0	149.7 Core Density	
STANDARD DEVIATION OF DENSITY MEASUREMENTS (pcf)						
Silty-Sandy Gravel	-	3.95	6.03	2.89	5.76	5.61
Gravelly Sand	-	10.0	10.6	11.0	12.8	13.3
-#30 Sand	-	0.55	1.29	1.15	1.02	-
Silty Sand	-	5.35	-	4.00	3.08	-
Silty Sand	7.39	4.29	4.48	3.95	3.76	-
Fine Silty Sand	3.87	3.33	1.51	3.53	4.32	-
Fine Sandy Silt	7.18	5.67	4.96	5.05	4.73	-
Silt	5.72	4.22	4.22	4.21	3.59	-
Aggregate Base	2.93	1.95	5.00	2.07	1.58	-
Aggregate Base	4.43	2.79	4.09	3.03	1.59	-
Aggregate Base	12.65	7.65	3.77	3.55	2.45	-
-3" Subbase	6.13	2.28	4.32	2.84	2.69	-
Gravel & Cobbles w/ Clay-Silt Binder	11.2	3.80	11.5	6.7	3.70	-
Cement Treated Base	-	3.35	-	2.71	2.87	2.64
Silty Clay	4.65	3.94	3.63	2.51	1.70	-
Silty Clay	-	2.37	-	1.56	0.87	-
Gravelly Clay	-	1.37	-	1.12	1.89	-
Alkali Clay	-	3.50	-	2.65	0.95	2.52
Iron Slag	-	2.40	1.74	0.53	-	0.56
Borate Soil	-	3.38		2.51	1.88	2.42
Asphalt Concrete	-	1.56		1.12	0.75 Core	
Concrete Pavement	2.30	3.18	0.64	1.01	0.90 Core	
Concrete Pavement	4.22	2.41	0.88	0.70	0.90 Core	
Concrete Pavement	0.97	1.76	0.41	0.72	0.90 Core	

Backscatter Gage Apparatus Constants:
(1) 2" Primary Shielding (Lead)
(2) 1-1/2" x 1-1/2" Sodium-Iodide Scintillation Detector
(3) 10 millicurie Cesium 137 Gamma Source

Note: Recorded Count Rate Without 2" Primary Shielding

TABLE 19

PERCENT PROBABILITY OF COINCIDENT DENSITY MEASUREMENTS BETWEEN THE BACKSCATTER AND TRANSMISSION GAGES

	Backscatter Gage							
	Commercial				Autoprobe			
	Unprepared		Prepared		Unprepared		Prepared	
Transmission Source-Depth	8"	4"	8"	4"	8"	4"	8"	4"
Materials Tested								
Silty-Sandy Gravel	-	-	28.5	47.0	33.3	44.9	89.4	97.3
Gravelly Sand	-	-	64.2	72.1	73.0	76.2	75.1	78.3
-#30 Sand	-	-	44.6	-	29.8	-	2.3	-
Silty Sand	-	-	8.9	-		-	38.4	-
Silty Sand	5.4	-	2.0	-	18.0	-	23.8	-
Fine Silty Sand	52.0	-	52.0	-	30.9	-	68.9	-
Fine Sandy Silt	2.0	-	9.6	-	65.5	-	61.3	-
Silt	10.2	-	5.8	-	39.5	-	39.6	-
Aggregate Base	4.5	-	57.6	-	16.4	-	34.5	-
Aggregate Base	15.5	-	42.9	-	29.0	-	38.8	-
Aggregate Base	13.5	-	24.9	-	45.1	-	50.6	-
-3" Subbase	6.2	-	8.6	-	27.0	-	0.0	-
Gravel & Cobbles	3.6	-	1.4	-	10.6	-	20.1	-
w/ Clay-Silt Binder	-	-		-	-	-	-	-
Cement Treated Base	-	-	10.0	6.8	-	-	64.6	59.2
Silty Clay	0.0	-	0.8	-	5.1	-	4.0	-
Silty Clay	-	-	0.5	-	-	-	3.6	-
Gravelly Clay	-	-	3.50	-	-	-	86.2	-
Alkali Clay	-	-	2.0	10.0	-	-	27.8	64.2
Iron Slag	-	-		19.0	-	-	0.0	58.2
Borate Soil	-	-	0.0	0.0	-	-	0.0	48.7
Asphalt Concrete			0.0				0.8	
Concrete Pavement	2.0		7.0		22.7		59.2	
Concrete Pavement	4.2		0.0		0.0		0.0	
Concrete Pavement	0.0		0.0		0.0		0.0	

Backscatter Gage Apparatus Constants:
(1) 2" Primary Shielding (Lead)
(2) 1-1/2" x 1-1/2" Sodium-Iodide Scintillation Detector
(3) 10 millicurie Cesium 137 Gamma Source

Note: [1]Recorded Count Rate Without 2" Primary Shielding

TABLE 20

AVERAGE ABSOLUTE DIFFERENCE BETWEEN NUCLEAR DENSITY MEASUREMENTS

	Commercial & Autoprobe Backscatter Gage		Commercial Backscatter & 8" Transmission Gage		Autoprobe Backscatter & 8" Transmission Gage	
	Unprepared	Prepared	Unprepared	Prepared	Unprepared	Prepared
Mean Densities (pcf)	5.32	4.62	10.17	7.25	4.94	3.68
Standard Deviation (pcf)	2.23	0.99	3.67	1.37	1.98	0.99

AVERAGE PERCENT PROBABILITY OF IDENTICAL NUCLEAR DENSITY MEASUREMENTS

	Commercial Backscatter w/ 8" Transmission Gage		Autoprobe Backscatter w/ 8" Transmission Gage	
	Unprepared	Prepared	Unprepared	Prepared
% Probability of Identical Density Measurement	11.39	20.43	32.56	36.45

TABLE 21

AVERAGE ABSOLUTE DIFFERENCE (LBS.) BETWEEN NUCLEAR DENSITY MEASUREMENTS BASED ON MATERIAL OR SOIL TYPE

Material or Soil Type		Commercial & Autoprobe Backscatter Gage		Commercial Backscatter & 8" Transmission Gage		Autoprobe Backscatter & 8" Transmission Gage		GRAIN SIZE
		Unprepared	Prepared	Unprepared	Prepared	Unprepared	Prepared	
Gravel, Cobbles Aggregates with Fines I	Δd	4.12	4.25	8.88	4.90	5.37	3.10	Course
	Δs	2.68	1.33	5.07	1.55	2.73	1.38	
Portland Cement Concrete Pavement (Textured Surface) II				Commercial Backscatter & Core Samples		Autoprobe Backscatter & Core Samples		
	Δd	3.53	3.97	7.23	6.73	3.70	2.77	
	Δs	0.83	0.29	1.60	1.55	0.26	0.16	
Asphalt Concrete Pavement (Smooth Surface) III				Commercial Backscatter & Core Samples		Autoprobe Backscatter & Core Samples		
	Δd	-	0.50	-	4.50	-	4.00	
	Δs	-	0.44	-	0.81	-	0.37	
Sands Silts Slag IV				Commercial Backscatter & 8" Transmission Gage		Autoprobe Backscatter & 8" Transmission Gage		
	Δd	6.43	5.18	10.18	6.31	4.60	3.15	
	Δs	2.25	0.71	2.17	1.10	0.97	0.43	
Clays Borate V				Commercial Backscatter & 8" Transmission Gage		Autoprobe Backscatter & 8" Transmission Gage		
	Δd	9.30*	6.08	16.70*	10.72	7.40*	4.50	
	Δs	1.02*	0.84	2.95*	1.66	1.93*	0.92	

Δd Average Absolute Difference in Mean Density

Δs Average Absolute Difference in Standard Deviation

*The Occurance of the Large Differences Between Gages is Probably Due to Soil Mineral Composition.

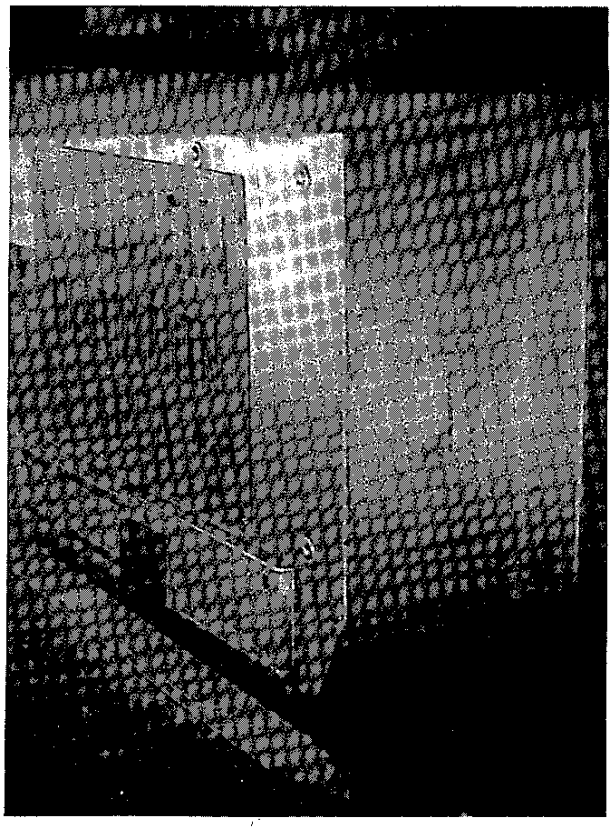

PHOTO 1 - AUTOPROBE IN CONTACT WITH SOIL

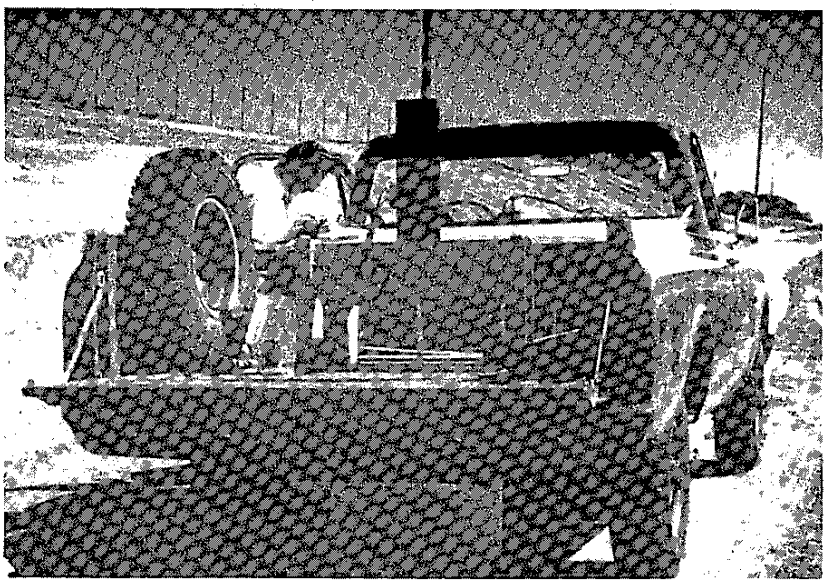

PHOTO 2 - FIELD TEST:

CLAYEY, SILTY SAND WITH AGGREGATE

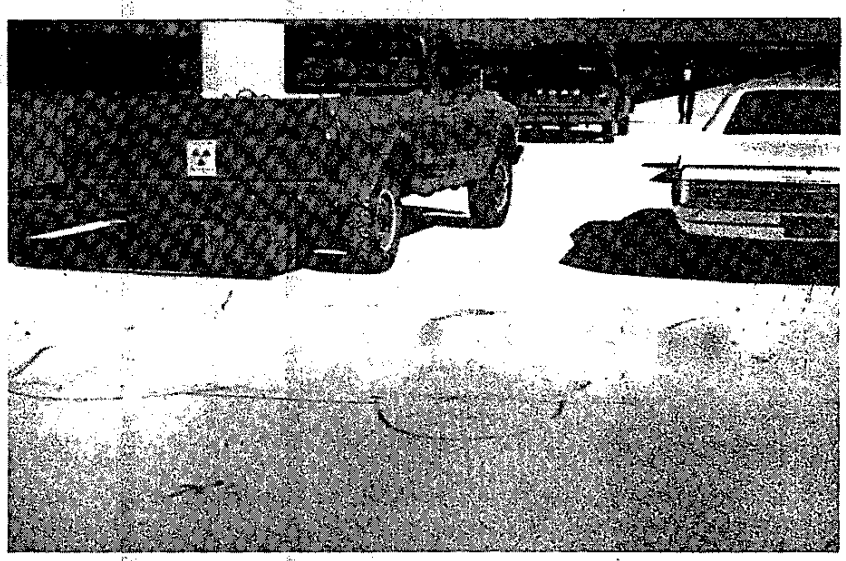

PHOTO 3 - FIELD TEST: PORTLAND CEMENT CONCRETE PAVEMENT

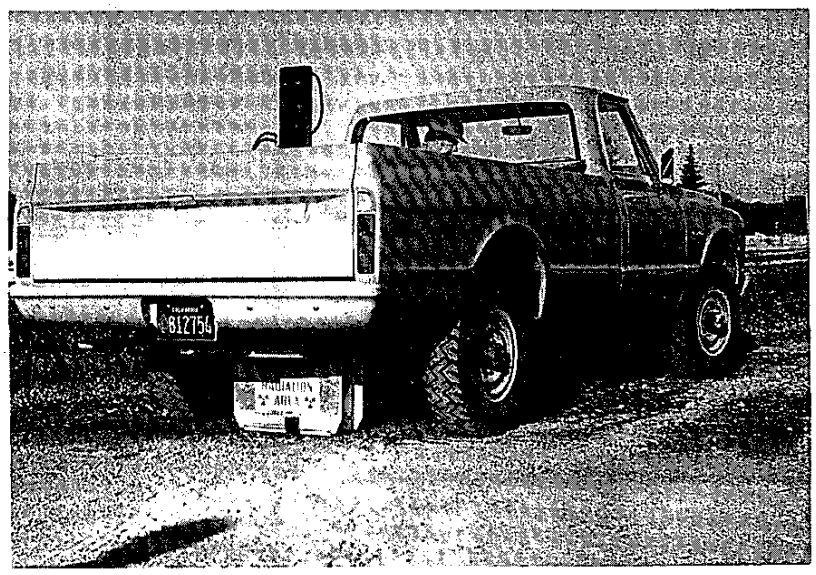

PHOTO 4 - FIELD TEST: SILTY SAND AND AGGREGATE SUBBASE

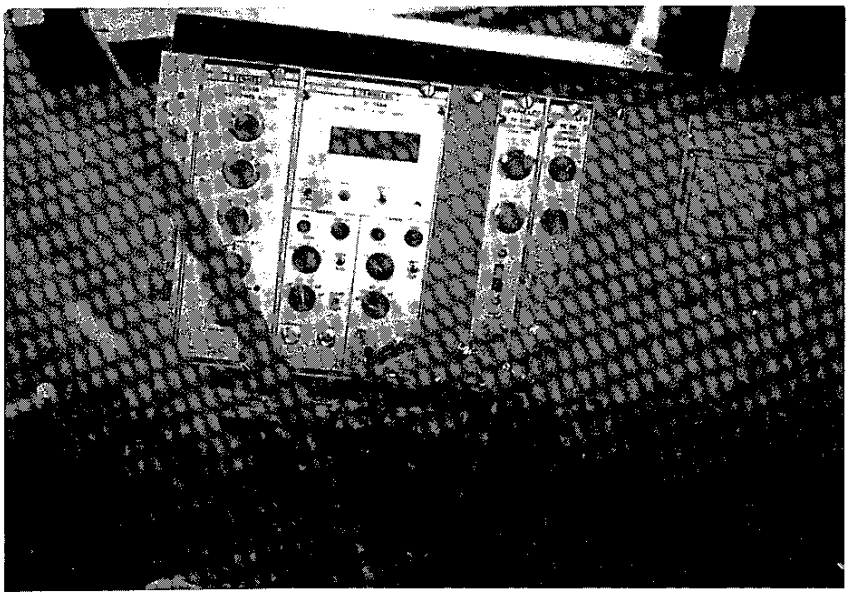

PHOTO 5 - ELECTRONIC INSTRUMENT MODULE

APPENDIX A

California Department of Transportation
Specifications for Nuclear Density-Moisture Gage

SPECIFICATIONS FOR NUCLEAR DENSITY-MOISTURE GAGE

September 1973

I. GENERAL

The portable nuclear density-moisture surface gage shall be suitable for determining density and moisture of soils, aggregates, treated bases, and the density of asphalt pavements. It shall be capable of determining density in two operating modes. These modes shall be direct transmission of gamma radiation, and backscatter of gamma radiation. The gage shall determine moisture by detecting backscattered thermalized neutrons.

The gage shall be a single unit, self-contained and consist of a radioactive source, radiation detectors, power supplies, counting circuits, timing circuits, data display, and related electronic components.

The gage shall be dustproof, moisture proof, shock resistant, and electronically stable. The gage shall operate reliably, accurately, and with negligible drift, in all three operating modes, over an ambient temperature range of 32°F to 145°F and with the probe on, or in, material whose internal and surface temperature will range between 32°F and 300°F.

The radioactive source shall be in the transmission rod and the radiation detector(s) in the case.

The gage shall weigh not more than forty (40) pounds and have outside dimensions not to exceed seventeen (17) inches in length, ten (10) inches in width and twenty-two (22) inches in height.

All above specified dimensions apply to the gages with any appurtenant lid or cover in place and closed. The dimensions include the carrying handle and any exterior tube positioning brackets with the tubes in place.

All electronic circuitry, radiation detectors and batteries shall be so arranged as to be easily removable from the case without removing, unshielding, or in any way disturbing the source.

All electronic circuitry shall be of solid state, mechanically sound, modular construction. The circuitry shall be mounted on G-10 epoxy glass plug-in circuit boards. The manufacturer shall provide sufficient "burn-in" time for electronic subassemblies to assure himself that premature failure or change

in electrical characteristics of a component is only a remote possibility. The length of "burn-in" time shall conform to current instrumentation industry practice and in no case shall be less than fifty (50) hours total.

An exterior service access opening shall be provided in the gage case to permit the use of an external test meter to check the output of the primary voltage supplies while the circuitry is in operation. High voltage adjustment controls to obtain plateau curves for the gamma and neutron detectors shall be adjustable by means of the service access opening. The intent is that the external test meter connection facilities, and the high voltage adjustment controls will be affixed to the electronic circuitry chassis in such a way as to be removable from the case as part of the chassis for bench testing and adjustment, as well as to be reachable through the access opening for field testing and adjustment without removal of the electronic chassis from the case. A dust and moisture proof cover plate to be provided for the service access opening shall be secured in place by means of machine screws rather than sheet metal screws.

Exception to the external test meter connection facilities may be taken, provided the manufacturer supplies a suitable extender board as a part of the gage purchase price. The use of such a board shall be evaluated, on an actual gage, by the purchaser to determine whether or not the exception will be allowed. A bidder may also take exception to the provision of high voltage adjustment controls provided the detectors meet the requirements set forth in Section II of these specifications.

Design of the probe, scaler, and control panel shall reflect consideration of the human operator and the manner in which he functions as the user of the gage.

II. GAGE SYSTEM

The radioactive source, to be placed in the ground for operation in the direct transmission mode shall be contained in a transmission rod either 5/8 $\pm$ 1/64 inch in outside diameter or 3/4 $\pm$ 1/64 inch in outside diameter. The tube shall be made of non-corrosive material having a minimum hardness of 60 as rated on the Rockwell B scale. The tube shall be strong enough to resist bending in normal hard usage and the outside surface shall be smooth and true. Permanent markings, referenced to the center of a radioactive source within the rod, shall be provided on the outside surface of the rod (or guide rod) at one (1) inch intervals to denote, from two (2) to eight (8) inches, the depth, below ground, of the transmission readings.

Any gamma detector used in the gage shall be of the halogen quenched, platinum cathode, Geiger-Mueller type. The operational response curve of any gamma detector used in the gage shall exhibit a well defined plateau with respect to applied voltage when used on a density standard weighing between 100 and 140 lbs. per cu. ft. The plateau shall have a minimum length of two hundred and fifty (250) volts and shall have a slope of five (5) percent, or less, per one hundred (100) volt change. The slope percentage shall be based on the following relationship:

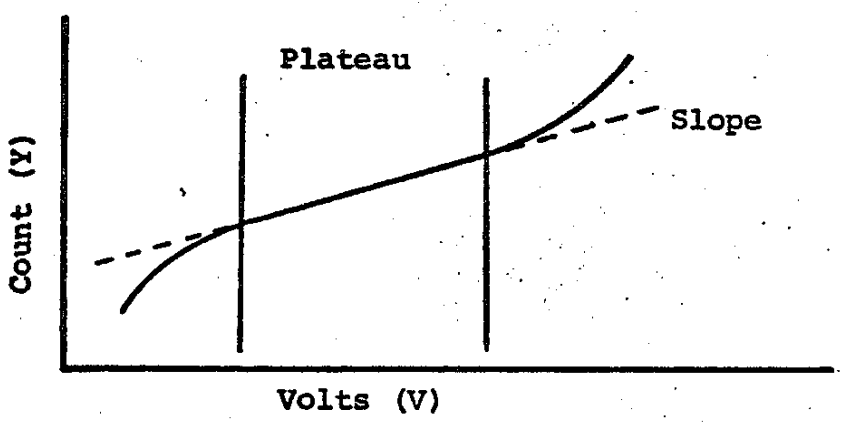

$$\text{Slope} = \frac{Y_2 - Y_1}{\left(\frac{Y_2+Y_1}{2}\right)\ (V_2-V_1)}\ (10^4) = \%/100 \text{ volts}$$

Y = Counts
V = Volts

The operating voltage, for the gamma detector, shall be set by the manufacturer at a point in the plateau about one-third (1/3) of the length of the plateau from the lower end. In the event the manufacturer elects to provide a fixed high voltage supply, rather than the specified variable supply, he shall provide a certificate stating that the detector characteristics, during the life of the detector, will not change the plateau to the extent that a change in operating voltage would be required. Additionally, in this case, he shall provide normally priced supply of replacement detectors with plateau ranges which essentially duplicate that of the original detector, for a minimum 5-year period subsequent to the date of delivery of the gage.

Except as provided below, a separate high voltage plateau adjustment shall be provided for each radiation detector. The intent is that each detector should operate within its plateau voltage.

Exception to a separate adjustment will be allowed if the manufacturer will certify that his detectors are of such standard manufacture that required operating voltage for replacement detectors will not change significantly for a 5-year period. The intent is that tube replacement can be made, and optimum performance obtained, without modification of the unit. Recalibration with tube replacement is satisfactory.

The detector(s) shall be easy to remove from the gage case and any detector(s) shall be connected to other circuitry by means of male and female connectors at the base of the detector.

A guide for the transmission rod shall be provided to hold the rod so that the long axis of the rod coincides with a plumb line when the gage is placed on a level surface. The guide shall be sturdy and shall provide positive mechanical indexing for the rod at all marked depths. The guide shall be so designed, that once the rod is indexed, the source-detector geometry cannot be altered by rocking or sliding of the rod with respect to the guide. When the source rod is in the 8-inch transmission position, a 20-pound force applied perpendicular to the end of the rod in one direction, then applied at 180° in the opposite direction shall not cause more than .125 inch differential movement. The gage will be held rigidly in place during this test.

A satisfactory method shall be provided for visually indexing the rod with respect to rotation, about its long axis, within the guide. Positive mechanical indexing shall also be provided for the rod when the backscatter mode is used. Also, design of the rod and the bracket shall be such that soiling of the rod resulting from normal usage neither causes sticking nor necessitates frequent cleaning. One hundred (100) tests will be performed in the 8-inch direct transmission mode in any soil type (at any moisture) used for highway construction and no excessive sticking of the rod shall occur. The transmission rod will not be wiped by the operator during these tests. A self cleaning unit shall be a part of the gage. In addition, the bracket shall be easy to clean and shall protect both ends of the inserted portion of the transmission rod from mechanical damage or contamination with soil or asphalt. In the event that a guide for the rod for the backscatter mode is built into, rather than affixed to, the case, it shall be in the form of a sheath which is easily cleaned and whose opening does not communicate, in any way, with the interior of the gage case.

The isotopes in the radioactive source shall consist of between eight (8) to ten (10) millicuries of Cesium^{137} and fifty (50) millicuries of Americium^{241} Beryllium. The source shall be doubly encapsulated in stainless steel, and shall be so contained in the gage system case that it may readily be exposed while taking readings and contained within shielding when not in use. The source shall be positively positioned and secured within the transmission rod and designed so that no movement of the rod (source) occurs about its longitudinal axis. The operation and design of the source-shielding complex shall be such that emitted radiation, with the source in any exposed position, does not vary from one time to another. The radiation levels shall not exceed 10 mrem/hr at a distance of 6 inches from the top and sides of the gage while in the normal backscatter operating position on the surface of compacted soil weighing 150 pounds per cubic foot. The gamma and neutron radiation levels shall not exceed 50 mrem/hr at a distance of 6 inches from the bottom of the gage while in the safe or shielded position.

The gage shall be equipped with a keyed locking device to prevent accidental unshielding of the source.

In the event that the handle used for carrying the probe also serves to unshield the source, the handle shall be designed so as to not only be stable while carrying, but also to prevent accidental unshielding of the source.

The detector for thermalized neutrons for moisture determination shall be a Boron Triflouride tube(s).

III. POWER SOURCES

The gage shall be capable of operation from its own self-contained power pack, and 115 $\pm$ 10 volt, 60 Hz alternating current. The self-contained power pack shall be composed of nickel-cadmium batteries. These batteries shall be sealed and leakproof. The batteries used in the power pack shall have sufficient ampere-hour capacity, based on a ten (10) hour discharge rate to properly operate the gage as discussed below.

The gage shall be equipped with a charging circuit capable of recharging the power pack at a rate equal to the battery manufacturer's recommendations. The charging circuit shall operate whenever the gage is connected to the 115 $\pm$ 10 volt, 60 Hz alternating current and shall be so designed as to automatically prevent overcharging the internal power pack. The combination of current drain and battery capacity shall be such that, beginning with a full charge, the gage can be operated continuously

for 400 count-read cycles spaced over 16 hours; and the power pack can then be brought back to full charge within an 8-hour charge period with the charger operating on a 115 ± 10 volt 60 Hz A.C. supply. A count-read cycle, for the purposes of this paragraph, shall consist of a one (1) minute count followed by a five (5) second display period.

The gage shall have a device to automatically turn off the gage when the battery drops to below a satisfactory operating level. Individual batteries in a pack, may be soldered together, but a battery pack consisting of two or more batteries shall have plug in leads to facilitate easy replacement in the field.

The battery condition shall be visually indicated on the scaler control panel. It may be a go no-go indicator and shall be operated by a switch. A continuous indicator so long as the gage is turned on is acceptable.

All voltage supplies shall be highly regulated and shall produce sufficient power to satisfy all demands of the gage. All high voltage supplies, regardless of the basic power source used and with the gage in operation, shall supply, at any setting of the high voltage adjustment controls, a voltage which will remain constant, with respect to time, within ± 1/2 percent between 32 to 145 F.

The gage shall be equipped with an automatic electronic timer. The frequency base for the timer shall be either a crystal or a tuning fork oscillator. The timer shall be preset to sixty (60) seconds ± one (1) second and that time interval shall be repeatable within ± 0.03 second over operating temperature ranges specified in Section I. A check circuit shall be provided to verify timer accuracy and counting function. It shall be selectable by means of a switch and shall count pulses or multiples thereof from some standard frequency base such as a crystal, tuning fork oscillator, or 60 Hz A.C. The check function shall provide not less than 3600 pulses per minute.

The gage shall be capable of counting zero to 99,999 counts per minute. The resolution time shall be two micro-seconds or less. Display of count shall be electronic and shall be made automatically at the end of the counting interval. The display shall continue for some minimum length of time not less than 10 seconds for an in line digital display. If the count is not displayed automatically, a visual signal shall indicate the end of the counting cycle and the display shall be selectable for a period not less than 1-1/2 minutes. Electronic circuitry in the scaler shall be refined such that spurious counts are not generated. Count shall

be displayed to, at least, the nearest ten (10) counts. Units shall be counted but need not be displayed provided that accuracy requirements, stated elsewhere in these specifications, are met.

IV. PERFORMANCE CRITERIA

Each gage must satisfy the performance criteria listed below when tested in the manner prescribed by these specifications. All references to the capacity of the gages to determine density or moisture are made in terms of a set of calibration density and moisture standards maintained by the California Division of Highways. These calibration blocks are located at the Transportation Laboratory at 5900 Folsom Boulevard, Sacramento, California. The term, "Reference calibration curve," will mean a calibration curve established using these standards.

The reference moisture and density calibration curves will be established by taking at least four one-minute readings on each standard. The mean value of a set of these readings will be used to determine each point on the reference calibration curve. The calibration curves for either transmission or backscatter density will consist of three semi-logarithmic regressions. One regression will represent standards high in calcium, the second will represent standards high in silica and the third will represent an average of all standards. Unless otherwise specified, the third, or average, regression line will be the one used to determine specification compliance. The calibration for moisture will be a linear curve based on data between approximately 0 and 25 pounds of water per cubic foot.

EFFECTS OF DROPPING

The gage will be dropped on its bottom surface from a height of 6 inches on a 1-inch diameter steel ball bearing placed on a concrete floor. The ball bearing is placed randomly so that contact is made on any bottom point of the gage. The gage shall operate correctly after 2 drops in all modes of operation. The average of four one-minute counts shall not deviate more than ± 1 pcf in density and moisture as compared to tests performed before the drops. Tests before and after will be performed on the same standard. There shall be no cracking or distortion of the case.

The gage will also be dropped from a height of 10 inches onto a asphalt concrete surfacing weighing approximately 140 pcf. The same performance criterias stated in the preceding paragraph shall apply.

SENSITIVITY TO VIBRATION

The gage will be fastened securely to a vibrating table for a period of twenty (20) to twenty-four (24) hours. The vibrating table will have a frequency of 12.5 ± 0.1 vibrations per second and an amplitude of 0.1 ± 0.01 inch. The equipment shall operate correctly after this period of vibration in all modes of operation. The average of four one-minute counts shall not deviate more than ± 1 pcf in density and moisture as compared to tests before vibration. Tests before and after will be performed on the same standard.

EFFECT OF MOISTURE

The gage will be placed in a warm (100° to 105°F) dry environment for one or more hours then transferred to a moist room having 100% humidity and a temperature 30°F less than the dry room, for one hour. The gage will be covered to prevent water from dripping directly upon the units. After three dry-moist cycles, the average of four one-minute counts shall not deviate more than ± 1 pcf in density and moisture from tests performed at room temperature (70° to 75°F). Tests shall be performed on the same standard.

EFFECT OF AMBIENT TEMPERATURE

At an ambient temperature of between 60° and 70°F; the average of four one-minute readings in the eight in. transmission position on a density standard of between 120 and 140 lbs per cu ft, and the average of four one-minute readings on a moisture standard of between 10 and 20 lbs per cut ft, will be determined. The gage will then be placed in a heat controlled room or oven at 145° ± 5°F for two (2) hours and the readings repeated. Count ratios will be determined based on a standard count between 60 and 70°F.

These count ratios must not indicate a shift of more than ± 1 lb per cu ft density or moisture from the reading on the same standards at an ambient temperature of between 60° and 70°F, as determined by the reference calibration curves for the gage.

The same tests shall be performed with the gage temperature being lowered from ambient temperature between 60° and 70°F to 35°F ± 3°F. The drop to 35°F shall be performed in a cold box set to 35°F. The same specification of ± 1 lb per cu ft density or moisture will apply at the ambient and 35°F temperature.

EFFECT OF HOT SUBSTRATE

The average of four one-minute readings in the backscatter position will be taken on an aluminum standard with the gage and standard at 60° - 70°F. The standard will then be heated until the internal temperature is 300°F. At this point, the gage will be placed on the standard for 10 minutes and the readings will be repeated as above. The average of these counts must not indicate a shift of more than ± 1 lb per cu ft density from the reading on the same standards at the temperature of between 60° and 70°F, as determined by the reference calibration curves for the gage. The tests at 300°F shall be completed in 15 minutes.

STABILITY WITH TIME

The daily and day-to-day random variation in indicated density of an arbitrary standard of between 120 and 140 lbs per cu ft density, when measured by an average of four one-minute counts in the eight in. transmission position, shall not vary more than ± 0.8 lb per cu ft. The daily and day-to-day random variation in indicated moisture of an arbitrary standard of between 10 and 20 lbs per cu ft moisture when measured by an average of four one-minute counts shall not vary more than ± 0.8 lb per cu ft.

In either moisture or density, a systematic variation or drift greater than that permissible for normal aging of detector tubes shall not be permitted.

EFFECT OF CHEMICAL COMPOSITION

The California Division of Highways has a set of three high silica and a set of three high calcium density calibration standards. A separate reference calibration curve shall be determined for the silica and calcium standards at the eight in. transmission position. These curves will be a semi-logarithmic regression. The spread between the curves shall not be greater than two and one half (2.5) lbs per cu ft when measured at any point between 100 and 160 lbs per cu ft. In the backscatter density mode the spread between these reference calibration curves, for the same range of densities, shall not be greater than two and one half (2.5) lbs per cu ft.

MINIMUM ONE-MINUTE COUNT-DENSITY

When the gage is used in the transmission position at a depth of eight (8) inches there shall be not less than 11,000 counts per minute indicated at a soil density of 140 lbs per cu ft. This shall be a count of the actual detector discharges, and not electronically or otherwise multiplied. When the gage is used in the backscatter position on a similar density standard, it shall have not less than 10,000 counts per minute without multiplication.

MINIMUM ONE-MINUTE MOISTURE COUNT

When the gage is used to determine the water content of a 10 lb per cu ft moisture standard, there shall be a minimum count of not less than 1600 counts per minute. This shall be a count of the actual detector tube discharges and not electronically or otherwise multiplied. There shall be not more than 500 moisture counts per minute when the gage is suspended in air.

PERMISSIBLE VARIATION IN DENSITY DETERMINATION

When determining density in the eight (8) in. transmission position of a standardization block of between 110 and 140 lb per cu ft density, the average of a set of two readings shall constitute a density determination. In a set of ten such density determinations, no more than 3 shall indicate a density variation greater than ± 0.3 lb per cu ft as determined by the reference calibration curve.

When used in the backscatter position, no more than 3 in a set of ten such density determinations shall indicate a density variation greater than ± 0.8 lb per cu ft.

PERMISSIBLE VARIATION IN MOISTURE DETERMINATION

When determining moisture on a standardization block of between 10 and 20 lbs per cu ft moisture, the average of a set of two readings shall constitute a moisture determination. In a set of ten such moisture determinations, not more than 3 shall indicate a moisture variation greater than 0.3 lb per cu ft as determined by the reference calibration curve.

SENSITIVITY RATIO-DENSITY

The count (or count ratio) of the reference density calibration curve for the eight in. transmission position at 110 lbs per cu ft density shall be equal to or greater than 2.0 times the count (or count ratio) at 140 lbs per cu ft density. This ratio shall be equal to or greater than 1.5 when used in the backscatter position.

SENSITIVITY RATIO-MOISTURE

The count (or count ratio)of the reference moisture calibration curve at 20 lb per cu ft moisture shall be greater than 3.0 times the count (or count ratio) at 5 lb per cu ft moisture.

V. ACCESSORIES

A permanent shipping container constructed of metal or wood shall be furnished for the gage. When wood is used it shall be 1/2" thickness grade AB exterior plywood with all joints glued and with glued interior corner chamfer strips. Shock absorbing mounting for the gage shall be provided within the container. Exterior corners shall be protected by metal corners. The container lid shall be hinged and provided with locking hasps accepting 3/8" shank padlocks and a folding chest handle equal to Stanley No. 1205K size 3-1/2" shall be attached to the container. All exterior surfaces of the containers shall be protected with two (2) coats of first quality exterior paint or enamel. All containers shall be constructed and labeled to comply with all applicable State and Federal regulations. With the gage in the shipping container, the radiation level must not exceed 10 mrem/hr at any point on the top, sides or bottom surfaces and must not exceed 0.5 mrem/hr at 3 feet from the top, sides or bottom surfaces.

The following accessory items shall be furnished for each gage and included with the respective gage in the shipping container.

1. The gage shall be provided with a single standard to obtain nuclear counts in density and moisture in such a manner that the respective detectors are used in each measurement within the range of normal operation. This standard shall remain stable with time and be so constructed that the source and detector tubes can be repeatedly placed at the same identical position with respect to the surface of the standard.

2. A power cable for battery charging of sufficient cross-section to prevent voltage drop shall be supplied for connection to the 110-130 volt power source. This cable shall have a minimum length of 8 feet. One end shall have the standard 3-prong male plug for connection to standard outlet and the other end shall have a weatherproof connector for connection to the gage.

3. Operation and maintenance manuals in booklet form shall be provided. Operating and troubleshooting procedures for the gage shall be detailed. A block diagram shall be provided for each circuit module, and one block diagram shall show the intermodular relationships. Complete schematic diagrams for all circuitry shall be provided. The schematics shall include wave form diagrams sufficient to analyze performance. the wave form diagrams shall show wave shape and list nominal amplitude and pulse width. All components in the schematics shall be identified and referenced to a complete parts list. The parts list shall show at least two sources

for commercial components or parts, except standard hardware items. Exception to the two sources can be taken for specialized parts fabricated in the manufacturer's plant or by other vendors for the manufacturer.

4. The vendor shall designate by name, address, telephone number and air freight shipping point, the service facility to which the gage and/or components thereof are to be shipped for repairs, replacements or servicing required during the warranty period. This information may appear in the operation or maintenance manual, in separate shipping instructions, or on a plate attached to the shipping container.

5. Wipe test results, as specified by the State and/or Federal regulating agencies, shall be provided for the radioactive source in each gage.

6. Copies of any calibration curves worked up by the manufacturer during the course of his gage preparation and testing shall be provided. It is not intended that the vendor submit complete calibration curves for the gages since this will be done by the purchaser.

VI. DELIVERY, SERVICE AND WARRANTY

The vendor shall be responsible for delivery of the gages to the customer's dock at 5900 Folsom Boulevard, Sacramento, California. The manufacturer shall staff and maintain permanent facilities within the State of California. These facilities shall provide complete maintenance and repair services for the nuclear gages purchased as a result of his successful bid.

Each complete gage and each component thereof including cables, cable connecting devices and batteries shall be warranted for a period of one (1) year from the date of the acceptance of the gage by the State of California. If a gage fails to function properly during the warranty period the manufacturer shall assume full liability for restoring the complete gage including connecting cables, cable connectors and batteries to proper working order without cost to the State of California. The manufacturer shall assume all transportation charges and incidental expenses involved in the shipment of gages and/or components under warranty from a shipping point selected by the State of California to the service facility designated by the manufacturer and the return of the shipped items to the point of origin. Transportation shall be via air freight whenever feasible. The total time lapse that a gage and/or components reach and leave the manufacturer's facility shall not exceed eight (8) calendar days. The warranty shall be voided by

physical damage, modification, alteration, abuse or misuse of a gage beyond normal service usage in field and laboratory applications outlined in appropriate test methods and procedures of the State of California.

VII. VENDOR'S BID PROPOSAL

Schematic drawings of the gage are to be submitted with the bid. These drawings must show the arrangement of the components, the size of the case, the source strength, the model number, the size and type detectors used, and the estimated radiation level six inches from all sides and the bottom of the case. Prototype gages may be submitted for inspection and the vendor may use the State's calibration blocks for checking compliance with specification. Other pertinent information concerning the gage shall also be presented by the bidder. All data will remain confidential and will be used to determine if the bid is acceptable to the State. The acceptance of the design portrayed in the drawings and data submitted for bid purposes will not relieve the manufacturer of the full responsibility for furnishing a gage which shall meet these specifications and all requirements of the California Department of Public Health, California Administrative Code, Title 17 and all other pertinent rules, regulations, or orders in effect in California. The manufacturer shall also assume all responsibility for obtaining approval for the use of the gage(s) in California.

In the event that the California Division of Highways might wish to purchase complete sets of plug-in circuit boards or modules for gage maintenance, the vendor shall supply, in his bid proposal, a price list for all the modules in the gage he proposes to supply. These module prices will not be a consideration in bid evaluation.